

(NASA-CR-144316) DEVELOPMENT OF A SOLID  
PROPELLANT VISCOELASTIC DYNAMIC MODEL FINAL  
REPORT (FITZGERALD (J. E.) AND ASSOCIATES)  
221 P HC \$7.75 CSCL 211

N76-25433

CSCL 21I

UNCLAS  
42157

G3/28

# DEVELOPMENT OF A SOLID PROPELLANT VISCOELASTIC DYNAMIC MODEL

by

W. L. Hufford and J. E. Fitzgerald

April 1976

## **FINAL REPORT**

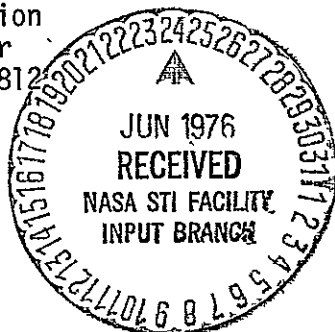
Prepared under Contract No. NAS 8-31342

by

J. E. Fitzgerald & Associates  
2809 Woodland Park Drive (NE)  
Atlanta, Georgia 30345

for

National Aeronautics & Space Administration  
George C. Marshall Space Flight Center  
Marshall Space Flight Center, Alabama 35812



DEVELOPMENT OF A SOLID PROPELLANT  
VISCOELASTIC DYNAMIC MODEL

by

W. L. Hufferd and J. E. Fitzgerald

April 1976

FINAL REPORT

Prepared under Contract No. NAS 8-31342

by

J. E. Fitzgerald & Associates  
2809 Woodland Park Drive (NE)  
Atlanta, Georgia 30345

for

National Aeronautics & Space Administration  
George C. Marshall Space Flight Center  
Marshall Space Flight Center, Alabama 35812

## PREFACE

This report discusses work performed under NASA Contract NAS-8-31342 for the George C. Marshall Space Flight Center, Marshall Space Flight Center, Alabama 35812. The cognizant technical officer was Mr. Frank Bugg.

No new technology was developed during the course of the program.

PRECEDING PAGE BLANK NOT FILMED

DEVELOPMENT OF A SOLID PROPELLANT  
VISCOELASTIC DYNAMIC MODEL

by

W. L. Hufford and J. E. Fitzgerald  
J. E. Fitzgerald & Associates

ABSTRACT

The results of a one year study to develop a dynamic response model for the Space Shuttle Solid Rocket Motor (SRM) propellant is presented. An extensive literature survey was conducted, from which it was concluded that the only significant variables affecting the dynamic response of the SRM propellant are temperature and frequency. Based on this study, and experimental data on propellants related to the SRM propellant, a dynamic constitutive model was developed in the form of a simple power law with temperature incorporated in the form of a modified power law.

A computer program was generated which performs a least-squares curve-fit of laboratory data to determine the model parameters and calculates dynamic moduli at any desired temperature and frequency.

Additional studies investigated dynamic scaling laws and the extent of coupling between the SRM propellant and motor cases. It was found, in agreement with other investigations, that the propellant provides all of the mass and damping characteristics whereas the case provides all of the stiffness. In view of this result, the usual direct geometric dynamic scaling laws are valid for the SRM even though the propellant is a viscoelastic material with strong frequency dependent properties.

TABLE OF CONTENTS

Preface . . . . .	i
Abstract . . . . .	iii
Nomenclature . . . . .	ix
I. INTRODUCTION . . . . .	1
II. SUMMARY OF ACCOMPLISHMENTS . . . . .	3
2.1 Task A - Identification of Pertinent Variables Affecting Dynamic Response. . . . .	3
2.2 Task B - Development of Dynamic Response Model. . . . .	4
2.3 Task C - Coupling, Scaling and Computer Code Development . . . . .	6
2.3.1 Coupling Between SRM Propellants and Motor Case . . . . .	6
2.3.2 Scaling Laws . . . . .	6
2.3.3 Computer Code Development. . . . .	7
2.4 New Technology . . . . .	8
III. VIBRATION OF SOLID ROCKET MOTORS . . . . .	9
3.1 General Discussion . . . . .	9
3.2 Structural Analysis Procedures . . . . .	12
3.2.1 Gross Dynamic Behavior . . . . .	13
3.2.2 Local Dynamic Behavior . . . . .	14
3.3 Vibration Analyses of the Shuttle SRM . . . . .	21
3.4 Complex Eigenvalue Approach to Solving Viscoelastic Vibration Problems . . . . .	26
IV. VARIABLES AFFECTING PROPELLANT DYNAMIC RESPONSE PROPERTIES . . . . .	32
4.1 Time-Temperature-Frequency Response . . . . .	32
4.1.1 Isothermal Response. . . . .	33
4.1.2 Time-Temperature Superposition . . . . .	39
4.2 Humidity Effects. . . . .	40

4.3	Strain Level Effects . . . . .	43
4.3.1	General Discussion of Strain Level Effects on Propellant Response. . . . .	44
4.3.2	Second Order Deformation Effects in Simple Shearing and Torsion Tests . . . . .	46
4.3.3	Experimental Data on the Effects of Strain on Propellant Dynamic Response Properties' . . . . .	56
4.4	Pressure Effects . . . . .	73
4.5	Aging Effects . . . . .	75
4.5.1	General Discussion of Aging of Solid Propellants . . . . .	76
4.6	Epoxy/Curative Ratio Effects . . . . .	82
4.6.1	General Discussion of Epoxy/Curative Ratio Effects . . . . .	82
4.7	Internal Heat Generation . . . . .	83
4.8	Damage Effects . . . . .	84
V.	DEVELOPMENT OF THE SRM PROPELLANT DYNAMIC RESPONSE MODEL . . . . .	89
5.1	Rationale For Selection of the Response Model. .	90
5.2	Verification of The Dynamic Response Model . .	96
5.3	Computer Program For The Dynamic Response Model. . . . .	99
VI.	DYNAMIC SCALING AND COUPLING BETWEEN MOTOR CASE AND SRM PROPELLANT. . . . .	102
6.1	Dynamic Scaling Laws for Space Shuttle SRM . . .	102
6.1.1	Longitudinal Shear Vibration. . . . .	104
6.1.2	Axial Vibration of A Composite Rod. . . . .	106
6.1.3	Beam Bending Vibration. . . . .	109
6.1.4	Torsional Vibrations. . . . .	112
6.1.5	Lateral Vibration of A Star Point . . . . .	113
6.1.6	Summary of Scaling Laws . . . . .	114
6.2	Coupling Between The SRM Propellant and Motor Case . . . . .	115

VII	CONCLUSIONS AND RECOMMENDATIONS. . . . .	117
7.1	Conclusions . . . . .	117
7.2	Recommendations . . . . .	118
VIII	REFERENCES . . . . .	120
APPENDIX A - LITERATURE SURVEY		A-1
APPENDIX B - COMPUTER PROGRAM FOR SRM PROPELLANT DYNAMIC RESPONSE		B-1
APPENDIX C - COMPUTER PROGRAM CARD DECK		C-1

### LIST OF FIGURES

#### Figure

1	Simple Shear Geometry	47
2	Simple Shear Stress State	47
3	Double Lap Chevron Shear Test Specimen	51
4	Absolute Tensile Modulus vs. Amplitude for Sinusoidal Strain at 0.5 Hertz,	51
5	Unconfined Shear Test, Stress Field	55
6	Real Part of Shear Modulus for Various Transverse Compressions	55
7	Thermomechanical Response, Constant Strain Amplitude Excitation, Adiabatic Boundary Conditions, PBAA Propellant	85
8	Thermomechanical Response, Constant Strain Amplitude Excitation, Isothermal Boundary Conditions, PBAA Propellant	85
9	Thermomechanical Response, Inertial Loading, Adiabatic Boundary Conditions, PBAA Propellant	86
10	Thermomechanical Response, Inertial Loading, Isothermal Boundary Conditions, PBAA Propellant	86
11	Dynamic Heating, Isothermal Boundary Conditions, PBAA Propellant	87
12	Master Stress Relaxation Modulus Versus Temperature Reduced Time	92
13	Master Dynamic Modulus Versus Temperature Reduced Frequency	93
14	Time-Temperature Shift Factor Versus Temperature	97
15	Dynamic Shear Modulus Versus Temperature Reduced Frequency for TP-H1123 and H-13 Propellant	98

16	Longitudinal Shear Vibration	104
17	Circular Frequency Coefficient	104
18	Axial Vibration Model	109
19	Star Point Model	113

## LIST OF TABLES

**Table**

I	Results for The First Natural Frequency Response of First IBM Dynamic Analysis of Shuttle SRM	24
IIa	Dynamic Tension Test Results at a Frequency of 3.5 Hz	58
IIb	Dynamic Tension Test Results at a Frequency of 11 Hz	59
IIc	Dynamic Tension Test Results at a Frequency of 35 Hz	60
IId	Dynamic Tension Test Results at a Frequency of 110 Hz	61
IIIa	Dynamic Shear Test Results at a Frequency of 3.5 Hz	62
IIIb	Dynamic Shear Test Results at a Frequency of 11 Hz	63
IIIc	Dynamic Shear Test Results at a Frequency of 35 Hz	64
IID	Dynamic Shear Test Results at a Frequency of 110 Hz	65
IV	Dynamic Shear Modulus of Live TP-H 1123 Propellant Test Data for Various Dynamic Displacements	67
V	Dynamic Shear Moduli of H-13 Inert Propellant Test Data for Various Dynamic Displacements	69
VI	Dynamic Shear Moduli of TP-H1123 Live Propellant as Affected by Various Static Displacements	71
VII	Dynamic Shear Moduli of H-13 Inert Propellant as Affected by Various Static Displacements	72
VIII	Dynamic Shear Moduli of TP-H1123 Live Propellant as Affected by Pressure	74
IX	Model Parameters	99
X	Comparison of Predicted and Measured Dynamic Modulus	100
XI	End Condition Parameter	110

## NOMENCLATURE

$a_T$	= time-temperature shift function
$a$	= propellant grain inner radius
$A$	= cross-sectional area
$A_n$	= end-fixity parameter
$b$	= propellant grain outer radius
$c$	= specific heat capacity
$c$	= motor case outer radius
$C_1, C_2$	= Mooney-Rivlin constants
$e$	= small strain tensor
$E$	= tensile modulus
$E^*$	= complex tensile modulus
$E_0$	= coefficient in power-law representation of dynamic modulus
$E_l$	= coefficient in power-law representation of relaxation modulus
$E_e$	= Long-time equilibrium relaxation modulus
$E_g$	= short-time glassy relaxation modulus
$E_k$	= coefficients in the Prony series representation of the relaxation modulus
$E_{rel}$	= relaxation modulus
$g$	= acceleration of gravity
$G$	= shear modulus
$G^*$	= complex shear modulus

$H(t)$  = Heaviside unit step function  
 $I$  = area moment of inertia  
 $I_1, I_2$  = first and second invariants of deformation tensor  
 $k$  = scale factor or shearing deformation constant  
 $K$  = bulk modulus  
 $K^*$  = complex bulk modulus  
 $[K]$  = stiffness matrix  
 $L$  = propellant grain length  
 $m$  = exponent in temperature shift-factor representation  
 $[M]$  = mass matrix  
 $n$  = acceleration in g's  
 $n$  = exponent in power-law representation of dynamic modulus  
 $P$  = hydrostatic pressure  
 $\{r\}$  = nodal point displacement vector  
 $[R]$  = nodal point force vector  
 $\dot{R}$  = strain rate in constant strain rate test  
 $t$  = case thickness or stress tensor  
 $T$  = temperature  
 $T_a$  = experimentally determined constant in temperature shift-factor representation  
 $T_g$  = glass transition temperature  
 $T_s$  =  $T_g + 50^\circ\text{C}$   
 $T_R$  = reference temperature  
 $W$  = strain energy

$\epsilon$  = dilatation or uniaxial strain  
 $\epsilon^*$  = complex strain amplitude  
 $\delta$  = loss tangent  
 $\delta_B$  = loss tangent in bulk  
 $\delta_E$  = loss tangent in extension  
 $\delta_G$  = loss tangent in shear  
 $\delta(t)$  = Dirac delta function  
 $\beta$  =  $1/\delta$   
 $\frac{d\theta}{dt}$  = temperature use rate  
 $\rho$  = density  
 $\tau_0$  = characteristic time  
 $\tau_k$  = time constant in Prony series representation of relaxation modulus  
 $\sigma$  = uniaxial (or shear) stress  
 $\sigma^*$  = complex stress amplitude  
 $\nu$  = Poisson's ratio  
 $\omega$  = frequency  
 $\Omega_n$  = circular frequency coefficient  
 $\zeta$  = structural damping coefficient

Superscripts:

$m$  = model parameter  
 $'$  = prime = real part of complex quantity  
 $''$  = double prime = imaginary part of complex quantity

Subscripts:

c = case property

p = propellant property

## DEVELOPMENT OF A SOLID PROPELLANT VISCOELASTIC DYNAMIC MODEL

### I. INTRODUCTION

The overall objective of the work reported herein was the development of a physically realistic dynamic viscoelastic response model for the Space Shuttle Solid Rocket Motor (SRM) propellant. Specific tasks included:

TASK A: Literature survey to identify and delineate all pertinent variables which affect the dynamic viscoelastic response of the SRM propellant.

TASK B: Develop a dynamic viscoelastic response model for the shuttle SRM propellant including the effects of all variables found in TASK A to significantly influence the propellant dynamic viscoelastic response.

TASK C: (1) Demonstrate coupling between the SRM propellant and the motor case.  
(2) Demonstrate scaling laws and give extrapolation limits.

- (3) Document and furnish the SRM propellant dynamic viscoelastic response model in the form of a computer program compatible with the MSFC UNIVAC 1108 computer.

All objectives have been met. The following sections describe the investigations leading to the development of the dynamic response model for the SRM propellant discussed in Section V.

The studies related to TASK C are presented in Section VI.

The literature survey compiled under TASK A and presented as a special report [1]\* has been updated and is included as Appendix A.

Appendix B includes a listing and documentation, including examples, for the computer program for the DYNAMIC VISCOELASTIC response model (DYNVIS). A card deck for the computer code has been submitted to the Marshall Space Flight Center as Appendix C to this report.

All propellant data used in the development of the dynamic constitutive model and its validation were obtained from published reports of experimental studies conducted by Thiokol/Wasatch Division [2] and at the University of Utah [3]. The University tests were conducted on UTI-610 propellant, an inert PBAN propellant used in dynamic model tests of the SRM at the NASA/Langley facility. The Thiokol tests were conducted on live and inert propellant with characteristics similar to the shuttle SRM propellant.

---

\* Numbers in square brackets refer to references listed at the end of the main body of the report.

## II. SUMMARY OF ACCOMPLISHMENTS

All requirements and objectives of the program have been met.

An oral presentation with viewgraphs was made at The George C. Marshall Space Flight Center on 24 April 1976 to the Technical Monitor, Mr. Frank Bugg and to personnel of Brown Engineering Company, led by Mr. Malcolm Tagg. Suggestions and comments arising from that presentation have been included.

### 2.1 TASK A - IDENTIFICATION OF PERTINENT VARIABLES AFFECTING DYNAMIC RESPONSE

The literature survey was completed and published as Special Report No. 1 in August 1975. This report, updated, and included here as Appendix A, lists pertinent references and includes a critical review or abstract of each article.

The primary source was the extensive Solid Rocket Structural Integrity Library developed originally under contract to Edwards Air Force Base by the Firestone Flight Sciences Laboratory of California Institute of Technology, and later taken over and maintained by the College of Engineering, University of Utah. This library includes not only open literature sources, but extensive holdings of pertinent governmental laboratory reports and industry technical reports which normally receive only limited distribution.

This source was supplemented and updated by personal acquisitions of more recent reports with special emphasis on the NASA/Langley 1/8-scale

dynamic model tests and Thiokol/Wasatch reports and data on the SRM propellant physical properties.

The variables selected for examination were:

Temperature

Humidity

Frequency

Pressure

Strain Level (both static prestrain and dynamic strain)

Aging

Epoxy/Curative Ratio

Internal Heat Generation

Damage Effects

## 2.2 TASK B - DEVELOPMENT OF DYNAMIC RESPONSE MODEL

Based on measured propellant dynamic response over the anticipated frequency and temperature range of interest to the Shuttle SRM, a power law of the form

$$E = E_0 (\omega_a T)^n \quad (1)$$

was selected for representation of the real (storage) and imaginary (loss) components of the propellant tensile or shear modulus. In Equation (1),  $E_0$  represents the baseline modulus at a temperature-reduced frequency,  $\omega_a T$ , of 1 Hz; that is at a frequency of 1 Hz at a given reference temperature  $T_R$ . The exponent  $n$  represents the slope of the  $\log_{10}$ (modulus)

versus  $\log_{10}(a_T)$  curve and  $a_T$  is the time-temperature shift factor.\*

The variables found to have a potentially significant influence on the SRM propellant dynamic response consisted of:

- A. TEMPERATURE, accounted for through the use of the time-temperature shift factor  $a_T$  (see Section 4.1).
- B. FREQUENCY, accounted for as shown in Equation (1) (see Section 4.1).
- C. HUMIDITY may be accounted for through moisture-time-temperature superposition; however, the nature and moisture diffusivity of the shuttle SRM is such as to render humidity effects negligible (see Section 4.2).
- D. PRESSURE, over the range of bulk strain levels in the shuttle SRM pressure effects are statistically insignificant (see Section 4.4).
- E. STRAIN LEVEL, including static prestrain and dynamic imposed strain, is insignificant (see Section 4.3).
- F. AGING effects, for motors over six months old, are accounted for by direct testing of aged propellant samples. The counter-balancing effects of oxidative cross-linking and/or continued post-cure reactions versus hydrolytic chain scission produce negligible effects for motors less than six months old (see Section 4.5).

---

\*All logarithms referred to herein and in figures are taken to the base 10.

- G. EPOXY/CURATIVE RATIO is the usual quantity which is adjusted, as a quality control measure, based on the functionality of the pre-polymer to maintain moduli within specified limits. Thus, its effect is not included in the model (see Section 4.6).
- H. INTERNAL HEAT GENERATION is negligible for the duration and level of dynamic strains encountered in the shuttle SRM (see Section 4.7).
- I. DAMAGE effects are concluded to be negligible for the range of static and dynamic strain levels and histories encountered in the shuttle SRM (see Section 4.8).

## 2.3 TASK C - COUPLING, SCALING AND COMPUTER CODE DEVELOPMENT

### 2.3.1 Coupling Between SRM Propellants and Motor Case

Based on simplified assumptions and analyses, it is concluded that, similar to other solid rocket motors, the SRM propellant provides the mass and damping characteristics and no stiffness; whereas the case provides the stiffness and has negligible contribution to the mass or damping characteristics under vibratory loading. Analyses in support of these conclusions are presented in Section 6.2.

### 2.3.2 Scaling Laws

Again, based on simplified assumptions and analyses, which are nevertheless representative of more detailed analysis results, it is concluded

that simple straight geometric scaling can be used to predict the prototype SRM response based on scaled dynamic model tests even with the strong frequency and temperature dependence of the SRM propellant.

Details of these analyses are presented in Section 6.1.

### 2.3.3 Computer Code Development

Based on the results of the above tasks a computer code has been developed in standard ANSI Fortran IV which will perform a least-squares curve-fit of master modulus versus temperature-reduced frequency test data to determine the parameters  $E_0$  and  $n$  in Equation (1), and/or predict the dynamic modulus as a function of temperature and frequency, given  $E_0$  and  $n$ .

The computer code is applicable to the real and imaginary parts of the tensile or shear modulus and can predict response of any of these modulus components at different frequencies and temperatures. If both real and imaginary components of the modulus are input, then the loss tangent defined by

$$\tan\delta = \frac{E''}{E'} \quad \text{or} \quad \frac{G''}{G'} \quad (2)$$

is also calculated.

Output of the computer program has been formatted in SI units; however, scaling from British to SI units is such that the inner logic of the code permits either system of units to be used.

A listing and documentation for the computer code, including examples of its use, are included as Appendix B to this report. A card deck for the computer program has been submitted to the Marshall Space Flight Center, care of Mr. Frank Bugg, as Appendix C, under a separate cover.

## 2.4 NEW TECHNOLOGY

No new technology was developed during this program, inasmuch as the purpose was the integration and utilization of proven technology in the development of the SRM propellant dynamic response model.

### III. VIBRATION OF SOLID ROCKET MOTORS

General surveys of vibration effects on solid rocket motors have been presented by IBM [4], Hufferd and Fitzgerald [5], Fitzgerald and Hufferd [6], Achenbach [7], and Baltrukonis [8]. An extensive bibliography, including abstracts, was prepared during the course of this research [1] and is presented as Appendix A to this report. This section presents an overview of the problems associated with vibration of solid rocket motors, structural analysis procedures, specific results of dynamic analyses of the shuttle SRM, and a discussion of the complex eigenvalue approach for solving viscoelastic vibration problems.

#### 3.1 GENERAL DISCUSSION

Compared to other structures, solid propellant rocket motors possess rather unique structural features. Whereas the mass of the propellant is very large compared to the mass of the thin-walled case, the propellant is generally compliant and contributes little to the stiffness of the composite structure, affecting the gross dynamic behavior of the motor mainly through its mass. Furthermore, since propellants are viscoelastic materials, the propellant provides considerable damping to the system. Consequently, transient effects attenuate very quickly and steady-state oscillations require a high energy input since a large amount of energy is dissipated.

Energy dissipation can give rise to serious secondary effects due to the characteristically strong temperature dependence of propellant mechanical properties. A continuing energy input may give rise to substantial increases

in temperature with subsequent deleterious effects on propellant response. Moreover, in rocket motor vibrations, energy is coupled into the propellant grain from the vibrating case by the inertial reaction of the mass of the propellant grain to the accelerating case. Disregarding inertia and material property degradation, large temperature increases are encountered whenever the applied stress or strain exceeds a certain critical value. The combination of temperature-dependent properties and inertia leads to the possibility of temperature and displacement jump instabilities which are similar to the phenomena observed in a nonlinear spring-mass system in which the spring softens with increasing displacement.

In considering the vibration response of solid rocket motors, two propellant physical property parameters are of particular significance. These are the log-log slope of the reduced relaxation modulus in the time-temperature region of interest (slope of the curve log modulus versus log reduced time) and the slope of the log shift factor,  $a_T$ , versus the temperature range of interest. The amplification factor at resonance (with or without jump instability effects) which, along with the acceleration level, determines the peak strains imposed on the propellant is a function of the relaxation modulus slope only. As this slope decreases (i. e., as the propellant becomes more elastic and less viscoelastic) damping decreases and the propellant strain amplitude at resonance increases. Conversely, as the slope increases, corresponding to an increase in viscous response, the strains at resonance decrease and the resonance broadens. With all other factors equal, a propellant with a large slope would be subjected to smaller deformations at resonance.

The slope of the shift factor versus temperature curve is a measure of the temperature sensitivity of the viscoelastic properties of a propellant.

Since the mechanical property temperature sensitivity along with inertial loading conditions produces the nonlinear jump instability effect, it follows that for otherwise identical conditions, the jump in stability effect will be most predominant for propellants which have a large shift factor versus temperature slope.

The thermomechanical coupling problem has been studied for rods under longitudinal vibrations [9], slabs under lateral vibrations [10] and cylinders under axial shear vibrations [11]. Additional studies have investigated the influence of temperature-dependent properties and thermo-mechanical coupling on propagating discontinuities [11 - 16]. For a shear mode of vibration, for example, these investigations have shown that the rate of mechanical dissipation, and hence heat generation, is proportional to the square of the magnitude of the shear strain (or stress). This result leads to the observation that heat generation is greatest in areas of high local stresses or strains such as occur at a star valley or a case-grain termination point. Maximum dissipation also occurs at the natural frequency of the system, although significant temperature rises have been observed at frequencies equal to about one-half the natural frequency.

Results have also shown that an increase in slab thickness (i.e., grain web thickness) will increase the steady state temperature, assuming that strain is unchanged. The equilibrium temperature is linear in frequency and loss modulus, and a quadratic function of the slab thickness and the strain [4,5]. Disregarding the temperature dependence of the loss modulus, doubling the slab thickness (grain web thickness) results in a fourfold increase in the steady-state temperature.

The above discussion has been concerned only with what might be called "reversible" thermomechanical effects resulting from the propellant thermoviscoelastic properties and cyclic loading conditions. "Irreversible" effects which include fracture, degradation or decomposition effects and autoignition which can be the result of the combined high temperature and cyclic strain conditions of the vibration environment have not been accounted for. These phenomena, are, of course, also of paramount importance; however, the establishment of a failure criterion for the thermal-vibration environment is a difficult task. Experience has shown that for the conditions usually encountered in solid rocket motor vibration, fracture or severe degradation will usually precede and prevent temperature rises to levels at which autoignition will occur. Propellant susceptibility to fracture under prescribed vibration conditions is a significant factor in practical situations, however, and is found to vary significantly from propellant to propellant as well as for various transient loading conditions.

The problems of physical or chemical degradation for the combined thermomechanical environment is undoubtedly the most difficult and least understood of the failure mechanisms known to be significant for vibration of solid propellant. Degradation of CTPB propellant under sustained vibration has been shown by Tormey and Britton [17]. Degradation of other composite propellant formulations has also been shown [12, 13, 15, 16].

### 3.2 STRUCTURAL ANALYSIS PROCEDURES

Depending on the particular loading conditions it is often sufficient to study only the gross dynamic behavior of a solid rocket motor, whereas

other loading conditions require consideration of local dynamic behavior.

### 3.2.1 Gross Dynamic Behavior

The analysis of gross dynamic behavior can be carried out by employing a simple model which describes the lowest flexural and longitudinal modes only. The dynamic analysis of such a simple model is straightforward and is discussed in many textbooks, see for example [18]. The one difficulty is the selection of the appropriate mass and stiffness parameters of the simple model. Generally the bending and longitudinal stiffnesses of the propellant grain are neglected relative to the casing stiffness, but the mass of the propellant is taken into account. For gross dynamic behavior such a simple model is adequate for engineering purposes, as shown by Gottenberg [19], who has reported on an experimental investigation of steady-state transverse vibrations of a long steel cylindrical tube containing an inert propellant with a circular perforation. Many bending modes were detected, and the lowest mode was compared with the predictions of a simple beam theory as described above. The comparisons were satisfactory. Difficulties were encountered in detecting modes other than bending modes, but one axisymmetric longitudinal mode and a few breathing modes were identified. For a full scale four-stage solid propellant research vehicle, analytical and experimental results on the frequencies and mode shapes of the three lowest modes were compared by Leadbetter, et al. [20]. In the experiments the fuel mass was simulated by weights. Good agreement for the three mode shapes and the lowest natural frequency was observed.

From the above investigations it has been found that the maximum amplitude ratio of the response to the excitation and the phase angle by which the response lags the excitation are simply related to the loss tangent of the propellant for the lowest longitudinal and flexural modes of vibration. A slightly more complicated expression results for lateral vibration of the case-grain interface with a higher amplification factor because of the strong influence of the case stiffness. A typical value of the loss tangent of composite solid propellants is about 0.5 [5,6]. This value gives use to an amplification factor between 2 and 2.25 [5,6]. The log-log slope of the relaxation modulus curve typically ranges between 0.1 and 0.3 for propellants [5,6].

### 3.2.2 Local Dynamic Behavior

To study local dynamic behavior it is necessary to consider a much more complicated mathematical model in which the grain is represented by a deformable viscoelastic continuum. The analysis of such a model also provides guidelines to select in a more rational manner stiffness and inertia parameters for the simple models which are used for gross dynamic behavior. To make the model tractable to analytical treatment, several idealizations are normally made to deal with the complex geometry of the port, the end conditions and the intricate material behavior of the propellant. As an initial model one might consider an infinitely long composite cylinder with a rigid outer layer and a very compliant, linearly elastic core with a circular port. The early analytical work on the dynamics of solid propellant rockets was generally concerned with this rather crude model. This initial work, which was reviewed by Baltrukonis [8], has

now been superseded by studies which include the effects of an elastic casing by considering a composite cylinder of two concentric layers both of which are infinitely long (see, e.g., [7]). Since the outer layer, which represents the motor casing, is usually thin relative to its mean radius, shell theory may be used in describing its behavior. Not much progress has been achieved in recent years in dealing with problems resulting from the complicated internal perforations, and the state of affairs with regard to analytical solutions is largely still as reported by Baltrukonis [8]. The internal passages in the grain are usually three dimensional in character with shapes dictated by considerations of internal ballistics. For an infinitely long rigidly encased elastic cylinder with a star-shaped port some information on natural frequencies of axial shear vibrations has been obtained by employing conformal mapping techniques. The problem of end conditions has been more successfully attacked recently and a few studies are available dealing with models of finite length [3].

The complications stemming from the viscoelastic behavior of the propellant are conceptually not difficult to overcome if the material behavior is essentially linear [5-7].

A major reason for the decline, in the last ten years, in the further development of analytical vibration models has been the development of finite element models for the steady state vibration of solid propellant rocket motors [21-25].

The finite element models lead to definition of a stiffness matrix, a mass matrix and a damping coefficient matrix for the discretized system.

Lumped-mass and consistent-mass methods are used for defining the mass distribution. The lumped-mass method concentrates the element masses in a manner that maintains the location of the center of mass of the structure, whereas, in the consistent-mass approach the mass is represented as it is actually distributed in the structure. In practice, better agreement has been obtained using the lumped-mass approach. This approach requires a large number of coordinate points for accurate analysis of systems with primarily distributed masses; however, the mass matrix for the entire structural assemblage is diagonal and positive definite, thereby reducing computation times. On the other hand, the consistent-mass approach requires excessive computational effort to obtain a desired degree of accuracy.

Damping matrices can be derived analogous to those used for the mass and stiffness matrices of appropriate internal damping characteristics. Propellant damping is accounted for using the dynamic complex representation of material properties.

In dynamic problems, Hamilton's variational principle is frequently used to derive Lagrange's equations of motion for the discrete system. In the absence of damping the system of equations to be solved has the form

$$[M] \{ \ddot{r}(t) \} + [K] \{ r(t) \} = \{ R(t) \} \quad (3)$$

where the mass matrix  $[M]$  is composed of the element masses,  $\{R(t)\}$  represents the vector of nodal point forces at time  $t$ , and  $\{r(t)\}$  represents the vector of nodal point displacements at time  $t$ . The natural frequencies

of the system are obtained by taking the nodal point force vector  $R(t)$  to be the null-vector.

For damped systems it is necessary to employ modal damping to obtain solutions for the damped structure. Several methods are available for introducing damping for a propellant grain. An effective damping coefficient,  $[C_{\text{eff}}]$  may be defined by

$$[C_{\text{eff}}] = \frac{[K'']}{\omega} \quad (4)$$

where  $[K'']$  represents the imaginary part of the complex stiffness matrix. Some structural codes, such as NASTRAN, employ a structural damping coefficient,  $\zeta$ , defined by

$$\zeta = \frac{G''}{2G'} = \frac{1}{2} \tan \delta_G \quad (5)$$

where  $G''$  and  $G'$  are, respectively, the imaginary and real part of the complex shear modulus.

More directly, steady state dynamic viscoelastic analyses may be obtained from the corresponding elastic counterpart, employing the viscoelastic-elastic correspondence principle; in which all elastic material constants are replaced by their corresponding viscoelastic counterpart expressed as frequency dependent complex numbers, i.e.,

$$E \rightarrow E^*(i\omega) = E'(\omega) + iE''(\omega)$$

$$G \rightarrow G^*(i\omega) = G'(\omega) + iG''(\omega)$$

$$K \rightarrow K^*(i\omega) = K'(\omega) + iK''(\omega)$$

$$v \rightarrow v^*(i\omega) = v'(\omega) + iv''(\omega)$$

where  $K$  denotes the bulk modulus and  $\nu$  represents Poisson's ratio. Lame's relations still hold among the complex moduli in the frequency plane so that

$$\nu^*(i\omega) = \frac{1}{2} - \frac{E^*(i\omega)}{6K^*(i\omega)} \quad (5)$$

An elastic material is represented in this notation by a complex modulus with a real part which is constant with frequency and imaginary part which is zero for all frequencies. The common assumption of a constant, elastic bulk modulus implies that the dynamic Poisson's ratio will contain a nonzero imaginary part as discussed in Section 3.4. Equation (3), for the natural frequencies of vibration, then takes the form

$$[-\omega^2 M + K' + iK''] \{r^*\} = 0 \quad (6)$$

or

$$\begin{bmatrix} -\omega^2 M + K', & K'' \\ - & - & - & - & - & - \\ K'', & \omega^2 M - K' \end{bmatrix} \begin{Bmatrix} r' \\ - \\ r'' \end{Bmatrix} = \begin{Bmatrix} 0 \\ - \\ 0 \end{Bmatrix} \quad (7)$$

The above replacement leads to a system of equations with twice as many unknowns as the corresponding elastic problem; however, the solutions may be obtained in a manner analogous to the static case. Obvious simplifications are noted if the problem is handled throughout in complex arithmetic.

Two general techniques are employed for solving the equations of motion for vibration loading. The first consists of direct step-by-step integration of the simultaneous differential equations. The response history is divided into a sequence of time increments of equal length and the equations of motion are formulated on an incremental basis. The motion computed during each time increment is added to the conditions at the beginning of the increment to obtain the conditions at the end. Thus, the response is evaluated step-by-step through the desired time range, starting with any given initial condition. In a nonlinear system the stiffness may be changing as the structure responds, but it is normally assumed that it remains constant during each time increment; provided that these increments are made short enough. The acceleration is assumed to vary linearly during the time increment, which leads to expressions for the change in acceleration (and velocity) in terms of the initial conditions and the change of displacement.

The incremental equations of motion are solved by standard static analysis methods; for example, Gauss elimination.

In the second method of solving the equations of motion, the equations are first decoupled by transforming to normal (mode shape) coordinates which are solved independently mode by mode, and the modal results superposed to obtain the total response. In this method, known as mode superposition, the displacement vector is expressed as a linear combination of mode shapes. Substitution of this expression into the equations of motion results in a single uncoupled equation for the  $n^{\text{th}}$  mode of the system. The solutions of each modal response equation are obtained by any convenient

procedure. For arbitrary loading histories, the Duhamel integral provides an efficient solution. Once the time history for the generalized coordinate of all significant modes has been obtained, the modal displacements are obtained by superposition.

The mode superposition method is advantageous if the essential dynamic response of the structure is contained in the first few mode shapes. This will be the case if the applied load can be approximated reasonably well by inertia force patterns associated with the first few modes, and if the frequency content of the input is largely represented by the corresponding lowest frequencies. In cases where the applied load distribution is extremely complex or the time variation contains significant high frequency components, it is necessary to include many modes of vibration to obtain adequate accuracy by mode superposition. In this case, the step-by-step direct integration may be more efficient. Direct integration must be employed in any case if the structural response is nonlinear due to either material or geometric effects.

The response to transient loading is most readily obtained by first obtaining the response to a unit impulse by mode superposition or direct integration and then using the Duhamel convolution integral for the prescribed loading. Random vibration is handled in a similar manner by integrating the power spectral density curve describing how the excitation energy is distributed over the frequency range to obtain an rms value for the excitation level.

### 3.3 VIBRATION ANALYSES OF THE SHUTTLE SRM

Several vibration analyses of the space shuttle SRM have been conducted by IBM [4,26] and Thiokol/Wasatch Division [2]. Additional one-eighth scale dynamic model tests have been conducted by the NASA/Langley facility with the experimental results presented in a preliminary report [27]. Analyses of the one-eighth scale models has been carried out by Grumman Aerospace Corporation [28]. Some of the results of these investigations are summarized herein for later comparative purposes in Sections 6.1 and 6.2 related to scaling of frequency response data and coupling between the motor case and the propellant grain. The results also indicate that reasonably good agreement is obtained from simplified analyses of dynamic response with more sophisticated NASTRAN analyses and experimental results.

IBM [4] conducted simplified and NASTRAN analysis for, among other things, longitudinal through the thickness shear vibrations. They also investigated the effects of moduli and grain length. The properties shown below, representative of the shuttle SRM, were used in their analysis for longitudinal shear vibrations:<sup>\*</sup>

$$a = 20 \text{ inches}$$

$$b = 70 \text{ inches}$$

$$\rho_p = 0.064 \text{ lb/in}^3$$

$$v_p = 0.495$$

---

\*Where data has been taken from other sources in which the data was originally presented in British Engineering units, we have not converted such data to SI units to avoid introducing additional errors of translation.

They assumed the outer boundary to be rigidly clamped. In addition, based on information received from United Technology Corporation (now known as United Technologies Chemical Systems Division, UTCSD), two different expressions were used for representation of the dynamic complex shear modulus, depending upon strain level. For low strains the representation

$$G' = 2800 \omega^{220}$$

was used in their simplified analysis, and

$$G = 6244 (1 + 0.384i)$$

was used in their NASTRAN complex eigenvalue analysis. A value of  $G = 6244$  was used in a NASTRAN real eigenvalue analysis.

At high strains, the corresponding representations were

$$G' = 900 \omega^{145}$$

and

$$G = 1365 (1 + .245i)$$

The simplified analyses were carried out using the expression

$$\omega_n = \frac{\Omega_n}{2} \sqrt{\frac{G'}{\rho b^2}} g \quad (8)$$

where  $\Omega_n$  is a circular frequency coefficient which depends on the ratio

a/b, as discussed in Section 6.1. Table I presents the results for the first natural frequency using Equation (8) and a NASTRAN real and complex eigenvalue analysis, including the effects of length as determined from the NASTRAN analysis.

IBM subsequently conducted a more complete NASTRAN analysis of longitudinal shear vibration including coupling with the case [26] and forced vibrations. These analyses treated several geometries which included more realistic representations of propellant grain configuration with forward and aft skirts, nose cone and nozzle attached. A constant shear modulus of 1333 psi and a loss tangent of 0.246 were used in all analyses. The results indicated several longitudinal modes below 50 Hz with the first in the neighborhood of 15 Hz with a maximum shear strain of 0.95%.

The NASA/Langley Research Center has conducted dynamic tests of one-eighth scale models of the shuttle SRM and mated external tank model. Three propellant grain configurations were manufactured by UTCSD using inert UTI-610 propellant which has the same binder-fuel-curable components as UTP-3001 propellant used in the TITAN III-C with inert sodium chloride and inert ammonium sulphate substituted for the live oxidizer, ammonium perchlorate. All had 0.1875 inch thick aluminum shells and were 19.5 inches in diameter and 147.32 inches long. The propellant length was approximately 145.4 inches. The propellant grain inner diameters were varied to represent lift-off, mid-burn and end-of-burn configurations.

The preliminary model test at NASA/Langley [27] for the lift-off configuration indicated the first bending mode at 54.1 Hz, the first torsional mode at 135.3 Hz and the first longitudinal mode at 149.7 Hz.

TABLE I  
 RESULTS FOR THE FIRST NATURAL FREQUENCY RESPONSE  
 OF FIRST IBM DYNAMIC ANALYSIS  
 OF SHUTTLE SRM [4]

	<u>Low Strains</u>	<u>High Strains</u>
Equation (8)	38.1 Hz	17.9 Hz
Real Modulus	38.2 Hz	~ 17.9 Hz
Complex Modulus	38.8 Hz	18.0 Hz
L = 100 inches	37.0 Hz	17.3 Hz
L = 150 inches	37.7 Hz	17.6 Hz
L = 300 inches	38.2 Hz	17.9 Hz

Grumman [28] has also conducted dynamic analyses of the SRM models tested at the NASA/Langley facility using NASTRAN. They used a constant modulus of elasticity of  $E = 25,000$  psi ( $G = 8333$  psi) and a loss tangent of 0.52 based on material property data supplied by UTCSD.\*

The results of Grumman's NASTRAN analysis for the lift-off configuration gave the first bending mode at 56.2 Hz (compared to 58.4 Hz for simple beam theory), 168.3 Hz for the first torsional mode (compared to 161 for simple beam theory) and 196 Hz for the first longitudinal mode (compared to 180 for simple beam theory).

Part of the reason for the discrepancy between Grumman's analyses and the experimental results of NASA/Langley may be attributed to the fact that the material properties used by Grumman are probably unrealistic for the actual test conditions.

The final set of analyses conducted on the shuttle SRM, to be discussed herein, were conducted by Thiokol/Wasatch Division [23] on a model 312 inches long, a grain O,D, of 146 inches and an inner port diameter of 67 inches using properties of TP-H1123 and H-13 (inert TR-H1123) propellant, which are similar to the shuttle SRM propellant. Their results indicated a first longitudinal thickness shear mode at 14.6 Hz with  $G' = 650$  psi for TP-H1123 propellant and 11.4 Hz with  $G' = 380$  psi for H-13 inert propellant at 70°F. The natural frequencies varied from 8.6 Hz at 40°F to 26 Hz at 90°F for the first longitudinal shear mode.

---

\*Subsequent conversations with Dr. Lamar Deverall of UTCSD indicated that the data provided by UTCSD was obtained using a piezo-electric device which results in strain levels of micro-inches/inch. These values are unrealistically high for the shuttle SRM.

### 3.4 COMPLEX EIGENVALUE APPROACH TO SOLVING VISCOELASTIC VIBRATION PROBLEMS

The usual relations developed for dynamic viscoelasticity apply when only one modulus is involved, such as the tensile modulus,  $E'$ ,  $E''$ ; shear modulus,  $G'$ ,  $G''$ ; bulk modulus  $K'$ ,  $K''$ ; or Poisson's ratio,  $\nu'$ ,  $\nu''$ . However, when one more than one modulus is involved, or assumptions are made regarding the bulk response, certain consistency relations are required of the various loss tangents (i.e., damping coefficients),

$$\tan \delta_E = \frac{E''}{E'} \quad (9a)$$

$$\tan \delta_G = \frac{G''}{G'} \quad (9b)$$

$$\tan \delta_K = \frac{K''}{K'} \quad (9c)$$

$$\tan \delta_\nu = \frac{\nu''}{\nu'} \quad — \quad (9d)$$

If the last listed, i.e., Equation (9d), is non-zero, then the lateral contraction is out of phase with respect to the major elongation which is perpendicular to it.

The consistency relations required between the various moduli and their physical consequences are discussed in this section.

In pseudo-linear first order theories of isotropic elasticity and viscoelasticity, Poisson's ratio,  $\nu$ , is defined in terms of Young's modulus,  $E$ , and the shear modulus,  $G$ , through the well known Lamé relation

$$G = \frac{E}{2(1+\nu)} \quad (10)$$

Solving (10) for  $\nu$  yields

$$\nu = \frac{E}{2G} - 1 = \frac{E-2G}{2G} \quad (11)$$

For steady state vibration problems, one often uses the complex eigenvalue approach wherein the moduli,  $E$  and  $G$ , are decomposed into real parts,  $E'$ ,  $G'$  and imaginary parts  $E''$ ,  $G''$ , i.e.,

$$E = E' + iE''; \quad G = G' + iG'' \quad (12)$$

Substituting Equation (12) into Equation (11) and grouping the real and imaginary parts then yields the real and imaginary parts of Poisson's ratio,  $\nu$ ,

$$\nu = \nu' + i\nu'' \quad (13)$$

where

$$\nu' = \frac{G'(E'-2G') + G''(E''-2G)}{2(G'^2 + G''^2)} \quad (14)$$

and

$$\nu'' = \frac{E''G' - E'G''}{2(G'^2 + G''^2)} \quad (15)$$

Defining the loss tangent,  $\tan \delta$ , as the ratio of the imaginary to the real part of a modulus, the loss tangent in extension and the loss tangent in shear can be denoted, respectively, as

$$\tan \delta_E = \frac{E''}{E'} ; \text{ extensional loss tangent} \quad (16a)$$

$$\tan \delta_G = \frac{G''}{G'} ; \text{ shear loss tangent.} \quad (16b)$$

Thus, Equation (15) may be rewritten as

$$v'' = \frac{(\tan \delta_E - \tan \delta_G) E' G'}{2(G'^2 + G''^2)} , \quad (17)$$

In Equation (17), it is seen that the denominator is always a positive real number for materials with shear resistance (as is the product in the numerator),  $E' G'$ . Thus, either  $v''$  is zero or non-zero.

If the loss tangent in extensional tests differs from the loss tangent in simple shear tests, the term in Equation (17)

$$\tan \delta_E - \tan \delta_G \neq 0 \quad (18)$$

and  $v''$  is non-vanishing.

For materials of the above type wherein  $\tan \delta_E \neq \tan \delta_G$ , an extensional steady state vibration test will produce lateral strains out of phase with the longitudinal strains. This will result in an oscillatory

volume change leading to possible damage and subsequent extensional modulus reduction of the material.

If, on the other hand, the loss tangents are found to be equal in extensional tests and simple shear tests, then from Equation (17) we see that the imaginary part of Poisson's ratio vanishes; i.e.,  $\nu'' = 0$ . The experimental result of equal loss tangents means

$$\tan \delta_E = \tan \delta_G = \frac{E''}{E'} = \frac{G''}{G'} \quad (19)$$

which when substituted into Equation (14) after rewriting, is

$$\nu' = \frac{E'G' + E''G''}{2(G'^2 + G''^2)} \sim 1 \quad (20)$$

then yields

$$\nu' = \frac{E' - 2G'}{2G'} \quad (21)$$

Comparing Equation (21) with Equation (11) demonstrates that in the case of equal loss tangents, Poisson's ratio is real, and has the same form as in static elasticity with the real parts of  $E$  and  $G$  being the determining factor.

For incompressibility in the above case, i.e.,  $\nu = \frac{1}{2}$ , the relation between the real parts of  $E$  and  $G$  is given by

$$G' = \frac{E'}{3} \quad \text{if } \nu = \nu' = \frac{1}{2} \quad (22)$$

In conclusion, it must be emphasized that Poisson's ratio can be taken as a real number if and only if the loss tangent in extension tests equals the loss tangent in simple shear at the frequency of interest.

Consider now the bulk modulus relation under hydrostatic pressure,  $P$ . The well known relation is

$$\epsilon = -\frac{3}{E} (1 - 2\nu)P = -\frac{1}{K} P \quad (23)$$

where  $\epsilon = e_1 + e_2 + e_3$ , the dilatation. Writing  $K = K' + iK''$  and substituting into Equation (23) yields after a little algebra with  $\nu$  real,

$$K' = \frac{E'}{3(1-2\nu)} \frac{1 + i \tan \delta_E}{1 + i \tan \delta_K} \quad (24)$$

where  $\tan \delta_K$  is defined as  $k''/k'$ . If the loss tangent in bulk response equals the loss tangent in extension, Equation (24) reduces to

$$K' = \frac{E'}{3(1-2\nu)} \quad (25a)$$

$$K'' = K' \tan \delta_E \quad (25b)$$

Thus, the fact, if observed experimentally, that  $\tan \delta_E = \tan \delta_G$  requires that  $\nu$  be real. This in turn leads to Equation (24) where  $K'$  may differ from the usual elastic relation if the loss tangent in bulk does not equal the loss tangent for extension.

If all three loss tangents are equal, i.e.,

$$\tan \delta_E = \tan \delta_G = \tan \delta_K \quad (26)$$

then

$$E = E'(1 + i \tan \delta_E) \quad (27a)$$

$$G = G'(1 + i \tan \delta_E) \quad (27b)$$

$$K = K'(1 + 2 \tan \delta_E) \quad (27c)$$

$$\nu = \nu' = \frac{E' - 2G}{2G'} \quad (27d)$$

It must be pointed out that the relations given by Equation (27) hold only if Equation (26) holds and  $K$  cannot be taken as a fixed, real number unless  $\tan \delta_E = 0$  when  $\nu$  is real.

The results from References 2 and 3, and the general literature show that, for the space shuttle SRM, under its range of frequencies and strain levels while under pressurization, the decomposition for the moduli used in the model of Section V is valid.

#### IV. VARIABLES AFFECTING PROPELLANT DYNAMIC RESPONSE PROPERTIES

During the course of this investigation pertinent variables which potentially could significantly influence the SRM propellant dynamic response were identified. Due to its viscoelastic nature, time, temperature and frequency were, of course, dominant. Additional variables, identified as noted previously, included:

- A. Humidity Level
- B. Pressure Level
- C. Strain Level
- D. Aging.
- E. Chemical Parameters (epoxy/curative ratio)
- F. Internal Heat Generation
- G. Damage or Permanent Memory Effects

The following subsections discuss the potential influences of these variables on the SRM propellant dynamic response, and where the effects are significant the mechanism for incorporating them into the dynamic model developed in Section V.

##### 4.1 TIME-TEMPERATURE-FREQUENCY RESPONSE

When considering the stress-strain relation of an elastic material, it is evident that for a particular value of stress there is associated a particular value of strain, and regardless of the length of time that the stress acts on the body, or what path was followed in applying it, the

strain remains constant. In viscoelastic materials, on the other hand, when a stress is applied to the body, the strain state depends upon the manner in which the stress is applied; that is, whether the load is applied rapidly or slowly. Thus, the history of loading, as well as the magnitude of the load must be considered in describing the response of a viscoelastic material. In addition, a viscoelastic body will not maintain a constant deformation under a constant stress, regardless of the loading pattern; rather, it will deform or creep with time. Also, if such a body is constrained at constant deformation, the stress necessary to hold it constrained gradually diminishes or relaxes with time.

The stresses and strains at a point in a viscoelastic body may thus be expected to vary with time, or the frequency of loading. And consequently, also with temperature, as will become evident.

The following paragraphs present a general discussion of the procedures for representing the viscoelastic response properties of solid propellants. Additional details and justification of the applicability of the procedures to solid propellants are presented in References 5, 6, 29 and 30. The development herein is in terms of the modulus of the material. Completely analogous results can be obtained employing the creep compliance representation of the response.

#### 4.1.1 Isothermal Response

A convenient representation for the uniaxial (or shear) stress,  $\sigma$ , in a linear viscoelastic material is the so-called integral or relaxation formulation which, for the isothermal case, has the form

$$\sigma(t) = \int_{-\infty}^t E_{\text{rel}}(t-\tau) \frac{d\varepsilon(\tau)}{d\tau} d\tau \quad (28)$$

Where  $E_{\text{rel}}(t-\tau)$  is the relaxation modulus in tension (or shear) and  $\varepsilon(t)$  is the imposed strain history.

The relaxation modulus is defined as the stress decay associated with a step input strain  $\varepsilon_0$ . With  $\varepsilon = \varepsilon_0 H(\tau)$ , Equation (28) becomes

$$\sigma(t) = \int_{-\infty}^t E_{\text{rel}}(t-\tau) \varepsilon_0 \delta(\tau) d\tau \quad (29)$$

or

$$\frac{\sigma(t)}{\varepsilon_0} = E_{\text{rel}}(t) \quad (30)$$

where  $H(\tau)$  is the Heaviside unit step function and  $\delta(\tau)$  is the Dirac delta function.

For a constant strain rate test, with strain rate  $R$  ( $\varepsilon = Rt$ ), Equation (28) yields

$$\sigma(t) = R \int_0^t E_{\text{rel}}(t-\tau) d\tau \quad (31)$$

Differentiating Equation (31) with respect to time,  $t$ , gives

$$\begin{aligned} \frac{d\sigma(t)}{dt} &= R E_{\text{rel}}(0) + R \int_0^t \frac{dE_{\text{rel}}(t-\tau)}{dt} d\tau \\ &= R E_{\text{rel}}(0) - R \int_0^t \frac{dE_{\text{rel}}(t-\tau)}{dt} d\tau \\ &= R E_{\text{rel}}(t) \end{aligned}$$

or

$$\left. \frac{d\sigma(t)}{d\varepsilon} \right|_{\varepsilon = Rt} = E_{\text{rel}}(t) \quad (32)$$

Thus, the relaxation modulus for a linear viscoelastic material can be deduced from differentiation of the stress-strain curve in a constant rate test.

An alternative method of measuring, and expressing, viscoelastic behavior is by considering steady-state response to forced vibrations. Creep and relaxation experiments are not capable of providing complete information concerning the mechanical behavior of viscoelastic solids. In certain cases the response of a structure is sought to a loading for times substantially shorter than the lower limit of time of usual creep or relaxation experiments.

For a linear system, both stress and strain will vary sinusoidally with the same frequency as the forcing frequency;

$$\epsilon(t) = \epsilon_0 e^{i\omega t} \rightarrow \sigma^*(\omega) e^{i\omega t}$$

$$\sigma(t) = \sigma_0 e^{i\omega t} \rightarrow \epsilon^*(\omega) e^{i\omega t}$$

If the input to a linearly viscoelastic material is an oscillatory stress,

$$\sigma(t) = \sigma_0 e^{i\omega t} \quad (33)$$

then the strain response will be an oscillation at the same frequency as the stress, but lagging behind by a phase angle  $\delta$ . Thus,

$$\epsilon(\omega) = \epsilon_0 e^{i(\omega t - \delta)} \quad (34)$$

where  $\varepsilon_0$  is the strain amplitude. The phase angle,  $\delta$ , is often called the loss angle and is a function of the internal friction. It is convenient to write Equation (34) in the form

$$\varepsilon(\omega) = (\varepsilon_0 e^{-i\delta}) e^{i\omega t} = \varepsilon^* e^{i\omega t} \quad (35)$$

where  $\varepsilon^*$  is the complex strain amplitude defined by

$$\begin{aligned} \varepsilon^* &= \varepsilon_0 e^{-i\gamma} = \varepsilon_0 (\cos\delta - i \sin\delta) \\ &= \frac{\varepsilon_0}{\cos\delta + i \sin\delta} \end{aligned} \quad (36)$$

If the input is an oscillatory strain,

$$\varepsilon(t) = \varepsilon_0 e^{i\omega t} \quad (37)$$


---

then the stress response will lead the strain by the phase angle  $\delta$ ,

$$\sigma(\omega) = \sigma_0 e^{i(\omega t + \delta)} = \sigma^* e^{i\omega t} \quad (38)$$

where

$$\sigma^* = \sigma_0 e^{i\delta} = \sigma_0 (\cos\delta + i \sin\delta) \quad (39)$$

The complex dynamic modulus is defined as the oscillatory stress response to an oscillatory strain input; that is,

$$\begin{aligned}
 E^*(\omega) - \frac{\sigma^*}{\epsilon_0} &= \frac{\sigma_0 e^{i\delta}}{\epsilon_0} \\
 &= \frac{\sigma_0}{\epsilon_0} (\cos\delta + i \sin\delta) \\
 &\equiv E'(\omega) + i E''(\omega)
 \end{aligned} \tag{40}$$

where  $E'(\omega)$  is in phase with the strain and is called the storage modulus,

$$E'(\omega) = \frac{\sigma_0}{\epsilon_0} \cos\delta \tag{41}$$

The second term of the last line of Equation (40),  $E''(\omega)$ , is often called the loss modulus and is defined by

$$E''(\omega) = \frac{\sigma_0}{\epsilon_0} \sin\delta \tag{42}$$

Equation (40) may also be written in the form

$$E^*(\omega) = |E^*| e^{i\delta} \tag{43}$$

where

$$|E^*| = \sqrt{(E')^2 + (E'')^2} = \sigma_0/\epsilon_0 \tag{44}$$

and

$$\delta = \tan^{-1} \left( \frac{E''}{E'} \right) \tag{45}$$

The ratio defining  $\tan\delta$  is called the loss tangent or mechanical loss. It gives a direct measure of the energy dissipation or damping characteristics of the material. For an elastic material  $\delta = 0$  and  $E'' = 0$  giving rise to an instantaneous response. For a viscous fluid  $\delta = \infty$  and  $E' = 0$  with the response 90 degrees out of phase. A viscoelastic solid has a loss tangent between these limits; i.e.,  $0 < \delta < \infty$ .

A representation for the complex dynamic modulus can be obtained in terms of the stress relaxation modulus by substituting Equation (37) into Equation (29). Then,

$$\sigma(t) = \epsilon_0 i\omega \int_{-\infty}^t E_{\text{rel}}(t-\tau) e^{i\omega\tau} d\tau \quad (46)$$

Performing a change of variables by letting  $u = t - \tau$ , Equation (46) becomes

$$\sigma(t) = \epsilon_0 i\omega e^{i\omega t} \int_0^\infty E_{\text{rel}}(u) e^{-i\omega u} du \quad (47)$$

or

$$E^*(\omega) = \frac{\sigma(t)}{\epsilon_0 e^{i\omega t}} = i\omega \int_0^\infty E_{\text{rel}}(u) e^{-i\omega u} du \quad (48)$$

Recalling the definition of the Laplace Transform, Equation (48) is seen to be

$$E^*(\omega) = i\omega \mathcal{L}[E_{\text{rel}}(u)] \Big|_{u=i\omega} \quad (49)$$

Thus, if the stress relaxation modulus is known, the dynamic modulus can be obtained by taking the Laplace transform, setting the transform

variable equal to  $(iw)$  and multiplying the result by  $(iw)$ . This observation is particularly useful if an exponential series (Prony Series or Dirichlet series) is used to represent the relaxation modulus. In this case,

$$E_{\text{rel}}(t) = E_e + \sum_{k=1}^n E_k \exp(-t/\tau_k) \quad (50)$$

where  $E_e$  is the equilibrium relaxation modulus, and  $E_k$  and  $\tau_k$  are constants chosen to fit the experimental data.  $E'$  and  $E''$  are readily determined from Equation (50) to be

$$E'(\omega) = E_e + \sum_{k=1}^n \frac{E_k (\omega \tau_k)^2}{1 + (\omega \tau_k)^2} \quad (51)$$

and

$$E''(\omega) = \sum_{k=1}^n \frac{E_k (\omega \tau_k)}{1 + (\omega \tau_k)^2} \quad (52)$$

For some viscoelastic materials,  $E_{\text{rel}}(t) = E'(\omega)$ .

#### 4.1.2 Time-Temperature Superposition

The analyses of the previous section apply to isothermal conditions, i.e., constant temperature conditions. In practice, it is impossible to obtain either relaxation data or dynamic data over the time scales and frequency ranges of practical interest in a solid rocket motor. In order to obtain data in these ranges the concept of time-temperature superposition is routinely employed. (See References 5, 6, 29, 30 and 31 for a general discussion.)

It has been widely found that temperature has the effect of expanding or contracting the time scale of response viscoelastic materials and

that an equivalence between time or frequency and temperature exists. Time and frequency are roughly the inverse of one another so that short time or high frequency response at one temperature corresponds to longer time or lower frequency response at a lower temperature. The converse holds true at higher temperatures. Thus, by obtaining the propellant response at several temperatures, a time-temperature shift function,  $a_T$ , relating the equivalence of time or frequency and temperature can be experimentally determined by horizontally "shifting" the test data so that it superimposes to form a single curve at some given reference temperature, usually 21 to 25°C. The resulting curve is known as the "master" response curve and is expressed in terms of temperature-reduced time,  $t/a_T$ , in the case of the master relaxation modulus curve, or in terms of temperature-reduced frequency,  $\omega a_T$ , in the case of the master dynamic moduli curves.

Thus, the previous analyses remain valid in terms of the master relaxation and dynamic moduli if time,  $t$ , and frequency,  $\omega$ , in the previous expressions are replaced by temperature-reduced time,  $t/a_T$ , and temperature-reduced frequency,  $\omega a_T$ , respectively.

The procedure for carrying out the analyses of this and the previous section are discussed further in Section V in connection with validation of the dynamic response model developed during this program.

#### 4.2 HUMIDITY EFFECTS

The presence of moisture may severely degrade the mechanical and chemical properties of solid propellants [4, 5, 29]. This degradation is typically manifest as swelling of the binder matrix, reduction in

modulus and retardation of propellant ignition. Often, leaching of surface oxidizer particles is observed. The mechanism of this degradation is primarily a reversion process in which chemical scission of polymer network cross-links and consequent reduction in modulus is caused by hydrolytic attack at cross-links.

Epoxide cured propellants are relatively insensitive to hydrolytic attack except for Mapo-epoxy cured CTPB propellants. Imine cured propellants have varying degrees of susceptibility. Double-base propellants are usually less influenced by moisture than composite propellants.

Inasmuch as the shuttle SRM propellant is an epoxy cured PBAN propellant, it may be anticipated that it will be relatively insensitive to, at least, short time exposure to moderate humidity levels. This belief has been borne out by relative humidity tests on the inert UTI-610 propellant used in the NASA/Langley dynamic model tests [3], in which some effect was observed on constant strain rate response but no noticeable effect was observed on dynamic response for exposure up to 14 days at 70% R.H.

Furthermore, moisture enters a solid propellant or liner-propellant interface through a diffusion process. The depth of penetration appears to be controlled by the relative humidity level, the ratio of volume to surface area exposed and the duration of exposure. The time constant associated with diffusion is much slower than that associated with temperature changes, where, in the case of the SRM, an equilibrium temperature will not be achieved for 60 - 90 days following a step temperature change. Accordingly, under normal circumstances moisture

will, at most, have only a local effect on the surface of the SRM propellant. Even this local effect can be avoided to a large extent by sealing the SRM motor segments and dessicating the interior.

The effects of relative humidity have also been observed to be reversible to a certain extent. The original properties of a propellant grain which has been inadvertently exposed to a high humidity level but which has not yet structurally failed, are substantially recovered by dessication of the motor interior. As a general rule, the drying recovery time is the same as the exposure time to moisture. Dessication of unaged propellants also tends to remove water introduced during mixing, casting and curing operations.

In view of the above comments it is concluded that it is not necessary to specifically account for moisture effects in the dynamic response model for the SRM propellant. It is recommended that the SRM segments be sealed and dessicated during all handling, transportation and storage operations prior to firing launch. If a segment should inadvertently be exposed to excessive humidity levels (say, greater than 50% R.H.) for an extended period of time (say, 14 days), then the segment should be sealed and dessicated for the appropriate period of time. If it is necessary to evaluate the dynamic response of the SRM under high moisture conditions, this can be accomplished conducting laboratory dynamic characterization tests under the appropriate moisture-exposure conditions and inputting this laboratory data into the dynamic response model developed herein.

Alternatively, moisture versus exposure-time tests can be conducted over a broad range of humidity levels, exposure times and temperatures

and a moisture-time-temperature shift function developed in a manner analogous to the time-temperature shift factor development. A master dynamic modulus versus moisture-temperature-reduced frequency curve can then be determined and directly input to the dynamic response model developed herein.

#### 4.3 STRAIN LEVEL EFFECTS

Strictly speaking, the response of a linear viscoelastic material cannot be a function of strain level; otherwise the material is no longer linear. However, many propellants have been shown to have strain dependent properties, particularly at strain levels where substantial dewetting takes place (see, for example [5,6,32,33]). Further impetus for concern over strain level effects comes from the IBM dynamic analysis of the shuttle SRM, reported earlier in Section 3.3 [4]. As noted in Section 3.3 they used dynamic properties which were, in fact, strain dependent. The modulus used for low strains, however, as noted previously, was obtained from unrealistically low strain level tests (on the order of microinches/inch) where it is well known that abnormally high values of moduli result which are not representative of conditions in an actual rocket motor under its expected use conditions.

Thus, one aspect of this program involved evaluating the extent of nonlinearity, if any, that could be expected of the relaxation and dynamic moduli of the SRM propellant and incorporating such effects, if necessary, into the propellant dynamic response model.

It may be noted that if the propellant properties do depend upon strain level it is still frequently possible to use the analysis of Section 4.1 by incorporating a "strain-level shift function" in a manner analogous to that by which a time-temperature or moisture-time temperature shift factor is introduced [4,5,32].

As it turns out, however, based upon the analyses and discussion in the following two sections, and the experimental test data presented in Section 4.3.3, it is concluded that neither static nor dynamic strain levels in the SRM are such as to have a statistically observable effect on dynamic moduli.

#### 4.3.1 General Discussion of Strain Level Effects on Propellant Response

As mentioned previously, it has often been observed that the response moduli of solid propellants appear to be influenced by strain level. This phenomenon is caused by several interacting effects:

- A. Dewetting
- 
- B. Finite Strain Levels
- C. Free Volume

Dewetting is the result, under strain, of the propellant's polymeric matrix adhesively failing at the surface of the ammonium perchlorate and/or aluminum particles. Quite often under strain, voids may form in the polymeric matrix itself. In any event, the result is the creation of a solid propellant with many distributed voids. The observed effects on propellant response are a drop in the various moduli, and a volumetric expansion.

Generally, strain-induced moduli weakening for propellants with an 86% solids-weight ratio do not show this effect until strain levels

are of the order of 10% at room temperature. For 88% solids loading, the onset of dewetting is generally below 10% strain and for very low temperatures, dewetting occurs at even lower strain levels.

Factors which apparently inhibit the dewetting phenomena below 10% strain in the 86% (by weight) solids loaded Thiokol SRM propellant, are:

- A. The balanced size distribution of perchlorate particles.
- B. The excellent elongation capabilities of the PBAN propellant at temperatures in the vicinity of room temperature.

A second factor affecting moduli under strain is the finite strain produced by normal stresses during shear testing. An ordinary lap shear testing apparatus does not, generally, provide the transverse restraint required for simple shear. Certain special test fixtures do. The Gottenberg disk test apparatus by its construction provides inherent capability to prevent motion normal to the shear direction, i.e., in the radial direction under shearing in the direction of the symmetry axis.

The free-volume effect under high overall compression can lead to increased observed moduli. However, as noted in the following section, very large transverse compression of the order of 14% is required for this increase to occur. With the properties of the SRM, this degree of transverse compression could only be reached at pressure levels of exceedingly high values. For example, assuming the bulk modulus of the SRM as a constant under very large degrees of compression

(which it is not but eventually increases with pressure) we can calculate a lower bound for the case pressure wherein the free-volume decrease would produce shear modulus changes. For a 10% volumetric change the mean pressure would be of the order of  $350,000 \text{ KN/m}^2$ , or over 50 times the SRM maximum expected operating pressure.

#### 4.3.2 Second Order Deformation Effects in Simple Shearing and Torsion Tests

Before discussing the experimental implications of the previous section, some second order elasticity effects are first introduced. These effects have been known for many years based upon observation and experiment.

The first phenomenon which is associated with simple shearing is called the "Kelvin" effect. It exhibits itself in the tendency of some materials requiring a finite transverse force to maintain a simple shear geometry. Highly filled polymers exhibit these second-order effects rather strongly. Thus, consideration must be given to second-order effects in the SRM propellant,

The second phenomenon, associated with torsion, is the "Poynting" effect. It exhibits itself in the tendency of some materials to elongate when subjected to torsion.

Let us consider in some detail the simple shear test as shown in Figure 1. In order to formulate the stress response, we assume that the propellant is (1) incompressible, and (ii) has a strain energy function,  $W$ . Without loss of generality for our purpose, we assume that the strain energy function has the form of a Mooney-Rivlin material.

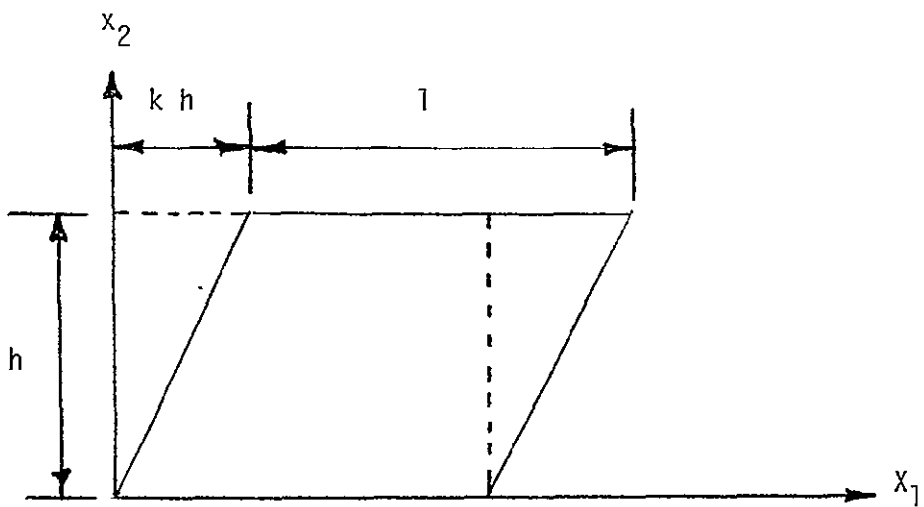


FIGURE 1. SIMPLE SHEAR GEOMETRY

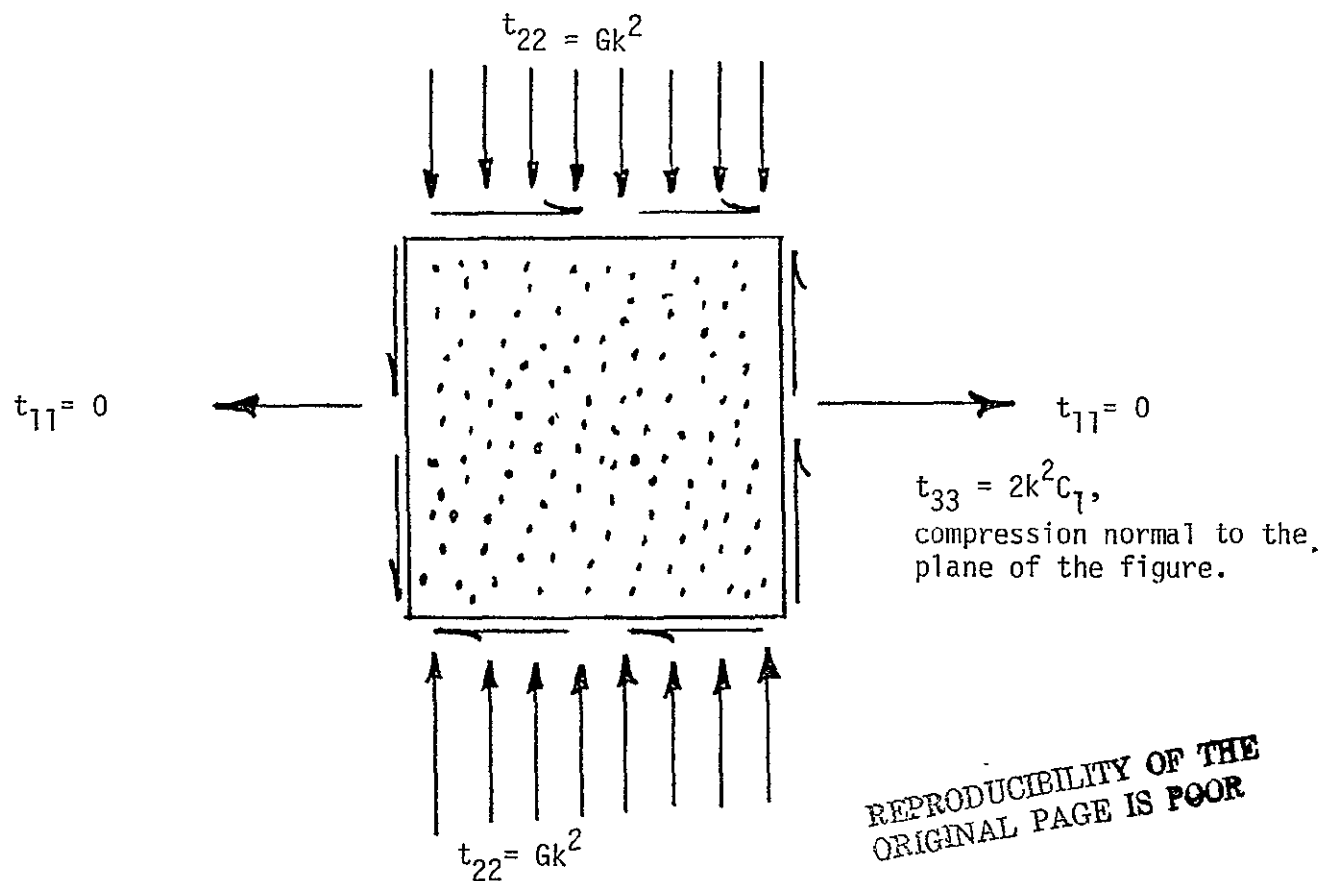


FIGURE 2. SIMPLE SHEAR STRESS STATE

This assumption is known to apply fairly well to polymeric materials. Without going through the details of the derivation, which are widely available [34], we simply state the results.

The Mooney-Rivlin form of the strain energy function is given by

$$W = C_1(I_1 - 3) + C_2(I_2 - 3) \quad (53)$$

where  $C_1$ ,  $C_2$  are constants and  $I_1$ ,  $I_2$  are the first and second invariants of the deformation tensor. For the geometry of the simple shear test shown in Figure 1, these invariants are equal and given by

$$I_1 = I_2 = 3 + k^2 \quad (54)$$

Assuming that the stress component parallel to the  $x_1$ -axis acting on a face perpendicular to the  $x_1$ -axis is zero, the stress components are given by

$$\begin{aligned} t_{11} &= 0 \\ t_{22} &= -k^2(C_1 + C_2) \\ t_{33} &= -2k^2C_1 \\ t_{23} &= t_{32} = 0 \\ t_{12} &= 2k(C_1 + C_2) \end{aligned} \quad (55)$$

The notation  $t_{12}$  means the stress component in the  $x_1$ -direction acting on a face normal to the  $x_2$ -direction, i.e., the simple shear. It is noted that  $t_{12}$  is linear in the displacement  $k$  with a constant of

proportionality,  $2(C_1 + C_2)$ . Defining this constant as the ordinary shear modulus,  $G$ , Equation (55) can be rewritten as

$$\begin{aligned} t_{11} &= 0 \\ t_{12} &= Gk \\ t_{33} &= -2k^2C_1 \\ t_{22} &= -Gk^2 \end{aligned} \quad (56)$$

Thus the stress system needed to maintain the simple shear geometry postulated as the defining test for the shear modulus,  $G$ , is as shown in Figure 2 (noting that  $t_{12} = t_{21}$  by the symmetry of the Cauchy stress tensor).

The mean stress is the average of the three principal stresses,

$$t_m = \frac{1}{3}(t_{11} + t_{22} + t_{33}) \quad (57)$$

which, from Equation (55) and (56) may be written in the form

$$t_m = -\frac{2}{3}(2C_1 + C_2)k^2 = -\frac{1}{3}(G + 2C_1)k^2 \quad (58)$$

For propellants, the ratio  $C_2/C_1$  is approximately 0.2 so that Equation (58) becomes

$$t_m = -1.45 C_1 k^2 = -0.6 k^2 G \quad (59)$$

Since the shear stress, given by Equation (56) is linear in  $k$  we can rewrite  $t_{22}$  and  $t_m$  as

$$t_{22} = -k t_{12} \quad (60a)$$

$$t_m = -0.6 k t_{12} \quad (60b)$$

with

$$t_{12} = Gk \quad (60c)$$

Thus, the prediction for simple shear is that the shear stress is linear in the shear strain,  $k$ , even for large deformations. This fact is borne out by experiments on propellants for shear strains up to 50%,  $k = 0.5$  [12,15].

Consider now the practical implications of the above results in a properly run simple shear test, such as the double-lap chevron specimen of Figure 3. For a typical propellant, let us set the value of  $G$  equal to 1000 psi ( $6.95 \times 10^6$  N/m $^2$ ). Let the static shear strain be typical of that found in a solid rocket motor under thermal cooling stresses, say 10% ( $k = 0.1$ ). Equation (60) then yields

$$\begin{aligned} t_{12} &= 100 \text{ psi } (6.95 \times 10^5 \text{ N/m}^2) \\ t_{22} &= -10 \text{ psi } (-6.95 \times 10^4 \text{ N/m}^2) \\ t_m &= -6 \text{ psi } (-4.17 \times 10^4 \text{ N/m}^2) \end{aligned} \quad (61)$$

For the more highly strained regions, a value of  $k = 0.2$  may be more typical, yielding

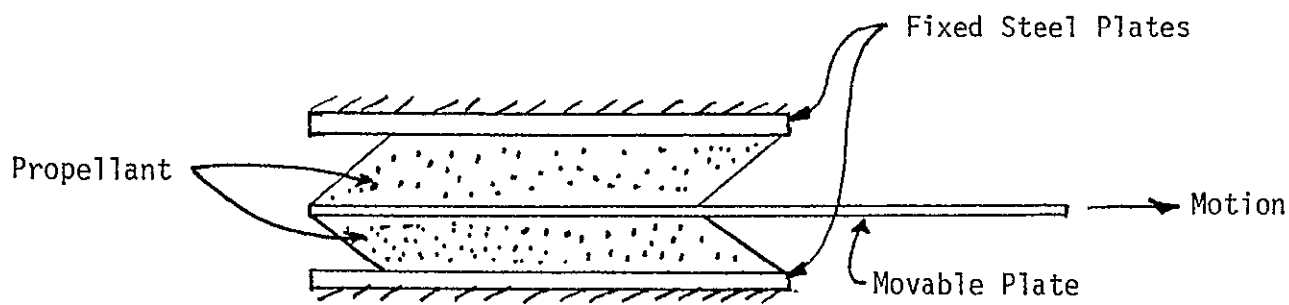


FIGURE 3. DOUBLE-LAP CHEVRON  
SHEAR TEST SPECIMEN (REF.12)

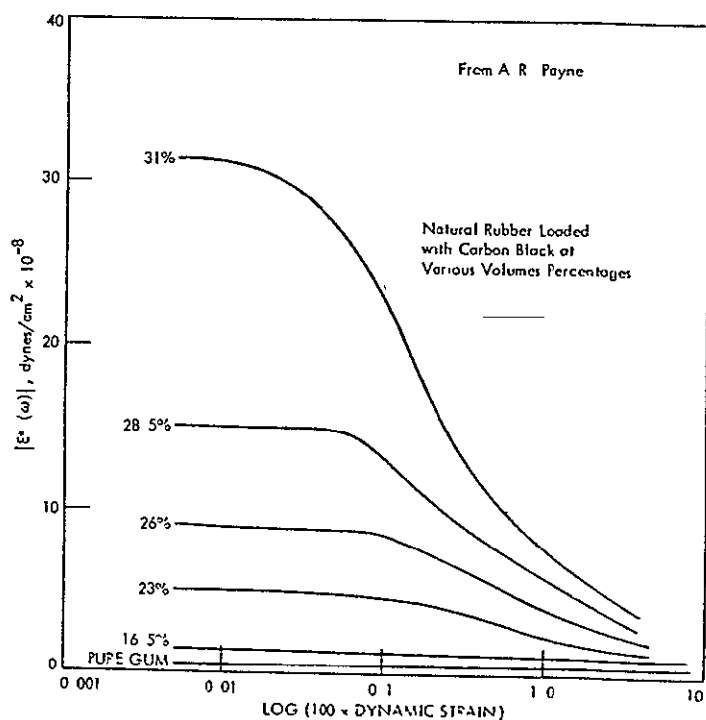


FIGURE 4. ABSOLUTE TENSILE MODULUS  
VS. AMPLITUDE FOR SINUSOIDAL STRAIN  
AT 0.5 HERTZ

$$\begin{aligned}
 t_{12} &= 200 \text{ psi } (13.9 \times 10^5 \text{ N/m}^2) \\
 t_{22} &= -40 \text{ psi } (-27.8 \times 10^4 \text{ N/m}^2) \\
 t_m &= -24 \text{ psi } (-16.7 \times 10^4 \text{ N/m}^2)
 \end{aligned} \tag{62}$$

Low strain areas, say  $k = 0.01$  yield stresses

$$\begin{aligned}
 t_{12} &= 10 \text{ psi } (6.95 \times 10^4 \text{ N/m}^2) \\
 t_{22} &= -1 \text{ psi } (-6.95 \times 10^3 \text{ N/m}^2) \\
 t_m &= 0.6 \text{ psi } (-4.17 \times 10^3 \text{ N/m}^2)
 \end{aligned} \tag{63}$$

It may thus be seen from Equations (62) and (63) that the transverse normal force required to run a correct simple shear test varies from a negligible value at low strains to a value of several atmospheres compression at higher strains. Unfortunately, many of the shear tests run on propellants (and other polymers) do not provide the necessary transverse, compressive restraining force,  $t_{22}$ . At very low shear strain measurements, this above fact is of no consequence. For the case, however, of large dynamic strains at high frequencies, the experimental observations can be very misleading. For example, Beyer [35], reporting on some published work by Payne (Figure 4) shows a drop in the dynamic shear modulus by a factor of 3 as the sinusoidal strain increases from 1% to 10% at 0.5 Hertz for a 31% carbon black filled natural rubber. The pure gum stock showed no change in modulus with strain level.

Beyer's results can be examined in light of second-order elastic effects. The shear modulus from the reference was  $G = 30 \times 10^7$  or

14,400 psi.\*

For low strain,  $k = 0.01$ ,  $G = 30 \times 10^7 \text{ N/m}^2$  (43,200 psi)

$$t_{12} = Gk = 30 \times 10^5 \text{ N/m}^2 \quad (432 \text{ psi})$$

$$t_{22} = -kt_{12} = -30 \times 10^3 \text{ N/m}^2 \quad (-4.3 \text{ psi})$$

$$t_m = -0.6 t_{22} = -18 \times 10^3 \text{ N/m}^2 \quad (-2.5 \text{ psi})$$

For medium strain,  $k = 0.1$ ,  $G = 30 \times 10^7 \text{ N/m}^2$

$$t_{12} = Gk = 30 \times 10^6 \text{ N/m}^2 \quad (4320 \text{ psi})$$

$$t_{22} = -kt_{12} = -30 \times 10^5 \text{ N/m}^2 \quad (-430 \text{ psi})$$

$$t_m = -0.6 t_{22} = -18 \times 10^5 \text{ N/m}^2 \quad (-250 \text{ psi})$$

Figure 4 shows an observed modulus at  $k = 0.1$  of  $G = 10 \times 10^7 \text{ N/m}^2$  (14,400 psi). However, the test method used did not provide the transverse constraining stress of  $30 \times 10^5 \text{ N/m}^2$  (430 psi) nor the accompanying average confining pressure of  $t_m = -18 \times 10^5 \text{ N/m}^2$  (250 psi hydrostatic compression).

The fact is, that dynamic (or static) shear tests run without the required transverse pressures (or equivalent hydrostatic confinement) yield results for the shear modulus  $G$  which are far too low. This is because in the absence of, in the above case, the  $t_{22}$  transverse pressure, we have the equivalent of a shear test run under tension. This

---

\*The ordinate listed as  $E$  in Beyer's paper was actually  $G$  in the original.

situation is shown in Figure 5. The properly run confined shear test field is shown as element A with the (in the previous case) confining compressive stress for a 10% shear strain of

$$t_{22} = -30 \times 10^5 \text{ N/m}^2 (-430 \text{ psi}).$$

A vertical motion is now allowed by superposing in B, a tensile stress of  $t_{22} = 30 \times 10^5 \text{ N/m}^2$  (430 psi).\* The resultant stress field is shown in, C, for simple shear stresses only.

The physical action of the tensile field, B, is to cause extensive dewetting of the matrix to oxidizer particles in the propellant, leading to a greatly lowered modulus as observed by Beyer and Payne. This reduction is not a reduction in G measured in true simple shear, but is a reduction of the apparent G when the sample is elongated vertically (dewetted) and then tested in simple shear.

The assumption of incompressibility holds when there is no dewetting. With dewetting, a volume expansion occurs and all elastic (viscoelastic) moduli decrease.

Again, for the test results shown above, if the simple shear tests were run under a superposed hydrostatic pressure but with no deliberate transverse constraint, one could conclude that if the hydrostatic pressure equaled a  $t_m$  of  $18 \times 10^5 \text{ N/m}^2$  (250 psi hydrostatic compression), then no decrease in dynamic shear modulus would be observed at a shear

---

\*While we can superpose the stress fields, we do not imply the strain fields superpose linearly.

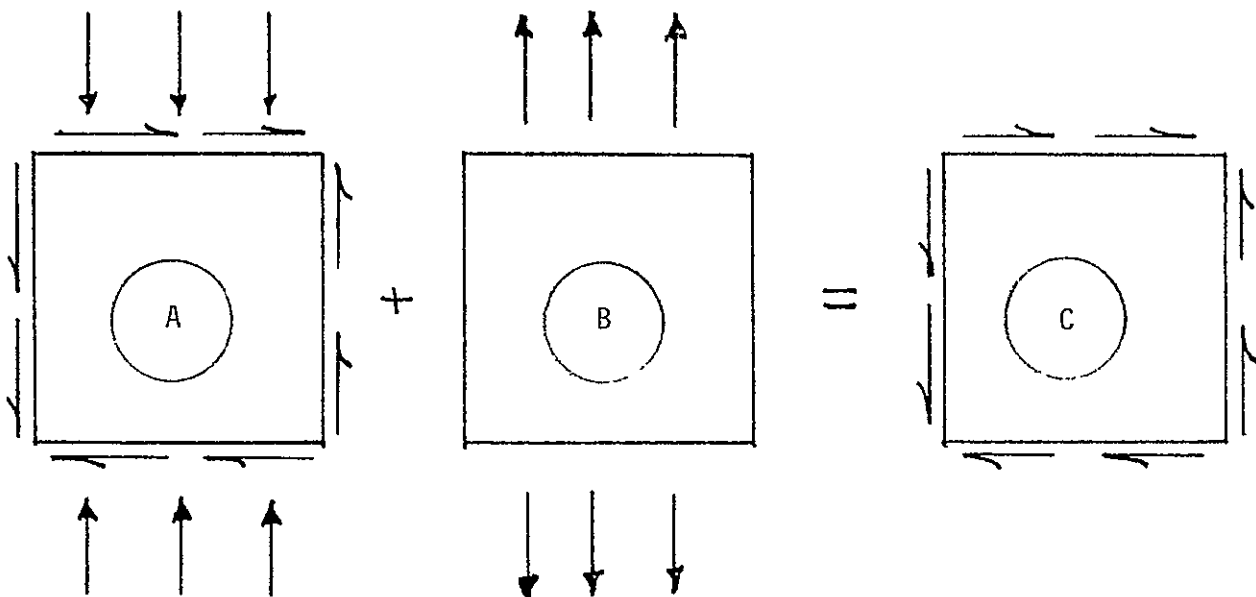


FIGURE 5. UNCONFINED SHEAR TEST  
STRESS FIELD

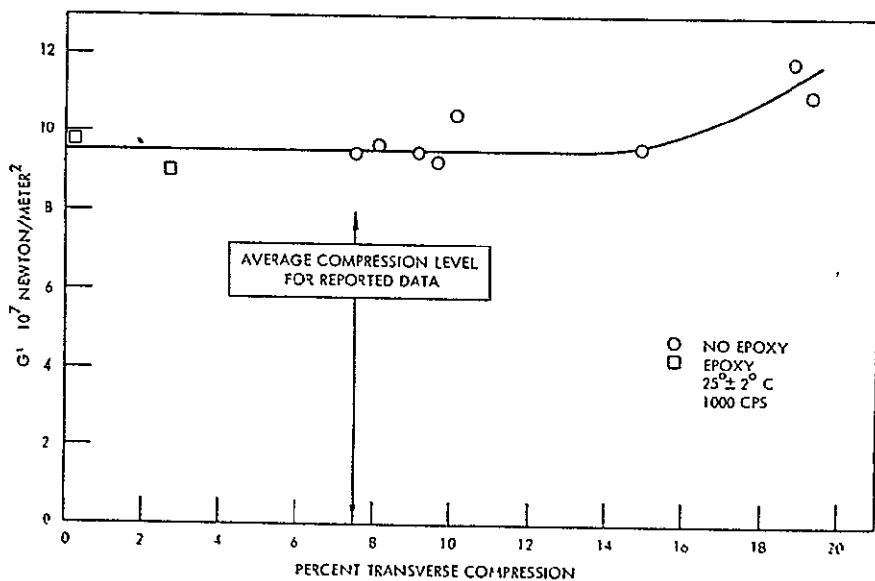


FIGURE 6. REAL PART OF SHEAR  
MODULUS FOR VARIOUS TRANSVERSE  
COMPRESSIONS

REPRODUCIBILITY OF THE  
ORIGINAL PAGE IS POOR

strain of 10%. Commensurate results can be produced for any other level of shear strain.

A second confirmation of the above argument can be seen in Figure 6, which is reproduced from Figure 17 in Beyer's paper [35]. This figure shows the independence of shear modulus  $G$  on transverse compression strain for strain values up to 15%. Again, the suppression here of the transverse extension serves to suppress dewetting, hence, leaving the shear modulus essentially unchanged.

Since the SRM will be operating at internal pressure levels well over the above figure, dynamic calculations should use the shear modulus determined from very small fixture strain, unpressurized tests with the Gottenberg disk test which provides the needed restraint. One should, however, run a large strain pressurized test to confirm the above analysis when simple tension tests are used to obtain the data.

#### 4.3.3 Experimental Data on the Effects of Strain on Propellant Dynamic Response Properties

Dynamic tests have been conducted at the University of Utah [3] on the inert UTI-610 PBAN propellant used in the NASA/Langley dynamic model tests and by Thiokol/Wasatch [2] on live and inert TP-H1123 PBAN propellant which closely resembles the actual SRM propellant.

Dynamic tension and shear tests were conducted at the University of Utah [3] using a Rheovibron dynamic tester. Thin slabs, 0.1 cm by 0.3 cm by 0.2 cm (0.04 in by 0.12 in by 0.8 in) were used for the dynamic tension tests and slabs 0.15 cm by 0.15 cm by 0.3 cm (0.06 in by 0.06 in by 0.12 in) were used for the dynamic shear tests.

Dynamic tension tests were carried out at 3.5, 11, 35 and 110 Hz and 0.1, 0.5, 1.0, 2.5 and 5.0 percent static strain levels at 18°C (0°F), 4°C (40°F), 25°C (77°F) and 49°C (120°F). Dynamic shear tests were carried out at the same frequencies and temperatures at strain levels of 0.5, 1.0, 2.5 and 5.0 percent pre-imposed static strain.

A fixed half-amplitude dynamic displacement of 50  $\mu\text{m}$  was used for all dynamic tests. The length of the specimens for the 0.1 percent strain level tests was 5 cm (2 in) rather than the 2 cm mentioned previously. For this test the dynamic strain level was equal to the imposed static strain of 0.1 percent. In all other dynamic tests, the dynamic strain level varied between 0.23 and 0.25 percent.

The average dynamic tension results of at least four specimens are tabulated in Tables II-a through II-d and the average dynamic shear results are tabulated in Tables III-a through III-d.

With the exception of the 0.1 percent static strain tension tests, no dependence on strain level is noted. This static strain is considerably below that which will occur in the SRM as a result of thermal cool down from the cure temperature to ambient temperature and axial or radial slump.

Thiokol [2] conducted dynamic shear tests using a modified Gottenberg disk test technique on live and inert TP-H1123 propellant; a propellant, which as noted previously is very similar to the actual SRM propellant.

In Thiokol's test, a cylindrical disk of propellant 3.31 inches outer diameter by 0.33 inch thickness with an inner diameter of

TABLE II-a  
DYNAMIC TENSION TEST RESULTS  
AT A FREQUENCY OF 3.5 Hz

STATIC STRAIN (%)	TEMPERATURE (°C)	$\tan \delta$	$ E $ (MN/m <sup>2</sup> )	$E'$ (MN/m <sup>2</sup> )	$E''$ (MN/m <sup>2</sup> )
0.1	-18	0.32	313	299	95.1
	4	0.47	65.3	59.0	27.8
	25	0.45	16.5	15.0	6.74
	49	0.38	3.92	3.68	1.36
0.5	-18	0.32	179	170	54.4
	4	0.45	45.6	41.5	18.8
	25	0.43	13.5	12.4	5.3
	49	0.32	5.91	5.58	1.82
1.0	-18	0.33	175	166	53.7
	4	0.45	43.8	40	17.9
	25	0.43	12.6	11.6	4.67
	49	0.30	5.42	5.17	1.58
2.5	-18	0.34	166	158	52.3
	4	0.45	39.9	36.6	16.3
	25	0.42	11.6	10.53	4.34
	49	0.30	4.68	4.48	1.35
5.0	-18	0.35	138	131	42.3
	4	0.43	34.8	32.1	13.4
	25	0.39	10.9	9.42	3.11
	49	0.26	4.0	3.85	1.09

TABLE II-b  
DYNAMIC TENSION TEST RESULTS  
AT A FREQUENCY OF 11 Hz

STATIC STRAIN (%)	TEMPERATURE (°C)	$\tan \delta$	$ E $ (MN/m <sup>2</sup> )	$E'$ (MN/m <sup>2</sup> )	$E''$ (MN/m <sup>2</sup> )
0.1	-18	0.34	333	315	107
	4	0.50	70.8	63.3	31.5
	25	0.47	19.7	17.8	8.35
	49	0.42	6.75	6.17	2.72
0.5	-18	0.33	207	197	63.3
	4	0.48	53.8	48.5	23.5
	25	0.48	15.0	13.6	6.49
	49	0.38	5.99	5.6	2.11
1.0	-18	0.33	214	204	66.4
	4	0.49	52.5	47.2	23.2
	25	0.47	14.0	12.6	6.0
	49	0.37	6.22	5.85	2.13
2.5	-18	0.32	213	204	62.6
	4	0.48	55.8	50.33	24.2
	25	0.47	14.7	13.2	6.32
	49	0.36	6.48	6.08	2.24
5.0	-18	0.33	185	177	52.5
	4	0.46	48.5	44.0	20.5
	25	0.44	13.8	12.6	5.64
	49	0.35	5.88	5.54	1.97

TABLE II-c  
DYNAMIC TENSION TEST RESULTS  
AT A FREQUENCY OF 35 Hz

STATIC STRAIN (%)	TEMPERATURE (°C)	$\tan \delta$	$ E $ (MN/m <sup>2</sup> )	$E'$ (MN/m <sup>2</sup> )	$E''$ (MN/m <sup>2</sup> )
0.1	-18	0.42	405	374	153
	-4	0.68	71.2	58.9	39.7
	25	1.08	25.0	17.2	18.0
	49	0.64	8.8	7.43	4.72
0.5	-18	0.26	269	260	67.3
	-4	0.55	75.2	65.9	36.2
	25	0.62	21.8	18.5	11.4
	49	0.47	8.37	7.56	3.57
1.0	-18	0.26	276	267	69.3
	-4	0.55	75.2	65.9	36.2
	25	0.62	21.8	18.5	11.4
	49	0.47	8.37	7.56	3.57
2.5	-18	0.26	263	254	66.1
	-4	0.52	76.3	68	34.7
	25	0.58	21.6	18.8	10.7
	49	0.46	8.66	7.85	3.64
5.0	-18	0.27	243	234	61.8
	-4	0.48	71	64	30.8
	25	0.50	18.6	16.7	8.24
	49	0.45	7.92	7.23	3.24

TABLE II-d  
DYNAMIC TENSION TEST RESULTS  
AT A FREQUENCY OF 110 Hz

STATIC STRAIN (%)	TEMPERATURE (°C)	$\tan \delta$	$ E $ (MN/m <sup>2</sup> )	$E'$ (MN/m <sup>2</sup> )	$E''$ (MN/m <sup>2</sup> )
0.1	-18	0.375	512	482	171
	4	1.1	120	87.2	78.1
	25	1.24	33.5	27.1	24.2
	49	1.25	12.3	8.06	8.94
0.5	-18	0.27	316	304	81.4
	4	0.53	102	90.4	48.0
	25	0.59	30.2	26.0	15.4
	49	0.54	12.2	10.8	5.81
1.0	-18	0.26	328	308	80.7
	4	0.53	105	92.6	49.2
	25	0.58	31.1	26.8	15.8
	49	0.53	12.2	10.7	5.72
2.5	-18	0.25	324	314	75.8
	4	0.50	108	96.9	47.8
	25	0.56	31.6	27.6	15.5
	49	0.51	12.3	11.3	5.59
5.0	-18	0.26	299	289	73.4
	4	0.48	103	92.0	44.4
	25	0.52	30.3	26.8	14.0
	49	0.48	11.7	10.6	5.12

TABLE III-a  
DYNAMIC SHEAR TEST RESULTS  
AT A FREQUENCY OF 3.5 Hz

STATIC STRAIN (%)	TEMPERATURE (°C)	$\tan \delta$	$ G $ (MN/m <sup>2</sup> )	$G'$ (MN/m <sup>2</sup> )	$G''$ (MN/m <sup>2</sup> )
0.5	-18	0.052	11.2	11.2	0.59
	4	0.174	8.06	7.94	1.33
	25	0.29	4.33	4.16	1.18
	49	0.31	1.89	1.81	0.55
1.0	-18	0.061	11.0	11.0	0.67
	4	0.21	7.35	7.16	1.49
	25	0.33	3.44	3.27	1.05
	49	0.31	1.71	1.64	0.51
2.5	-18	0.061	11.1	11.1	0.68
	4	0.21	7.29	7.13	1.48
	25	0.33	3.26	3.12	1.01
	49	0.32	1.59	1.52	0.48
5.0	-18	0.059	11.1	11.1	0.66
	4	0.205	7.35	7.2	1.45
	25	0.33	3.26	3.1	1.01
	49	0.32	1.54	1.47	0.47

TABLE III-b  
DYNAMIC SHEAR TEST RESULTS AT  
A FREQUENCY OF 11 Hz

STATIC STRAIN (%)	TEMPERATURE (°C)	$\tan \delta$	$ G $ (MN/m <sup>2</sup> )	$G'$ (MN/m <sup>2</sup> )	$G''$ (MN/m <sup>2</sup> )
0.5	-18	0.023	12.63	12.6	0.30
	4	0.10	10.5	10.4	1.08
	25	0.24	6.5	6.32	1.51
	49	0.31	3.42	3.28	0.99
1.0	-18	0.023	12.8	12.8	0.31
	4	0.1	10.4	10.3	1.14
	25	0.27	6.0	5.78	1.55
	49	0.33	2.99	2.67	0.95
2.5	-18	0.023	12.8	12.8	0.31
	4	0.11	10.5	10.4	1.11
	25	0.27	5.86	5.64	1.59
	49	0.34	2.82	2.67	0.91
5.0	-18	0.023	12.8	12.8	0.30
	4	0.093	10.5	10.4	1.02
	25	0.28	5.55	5.33	1.53
	49	0.34	2.58	2.43	0.85

TABLE III-c  
DYNAMIC SHEAR TEST RESULTS  
AT A FREQUENCY OF 35 Hz

STATIC STRAIN	TEMPERATURE (°C)	$\tan \delta$	$ G $ (MN/m <sup>2</sup> )	$G'$ (MN/m <sup>2</sup> )	$G''$ (MN/m <sup>2</sup> )
0.5	-18	0.036	14.67	14.67	0.58
	4	0.15	11.5	11.4	1.82
	25	0.31	6.26	5.97	1.85
	49	0.41	2.46	2.29	0.91
1.0	-18	0.045	14.3	14.3	0.68
	4	0.22	9.83	9.58	2.18
	25	0.41	3.8	3.52	1.43
	49	0.42	1.59	1.47	0.61
2.5	-18	0.05	14.0	13.9	0.75
	4	0.23	9.13	8.85	2.16
	25	0.44	3.28	3.01	1.28
	49	0.42	1.23	1.13	0.47
5.0	-18	0.072	13.2	13.2	1.03
	4	0.28	7.8	7.5	2.09
	25	0.45	2.97	2.72	1.23
	49	0.42	0.99	0.91	0.37

TABLE III-d  
DYNAMIC SHEAR TEST RESULTS AT A  
FREQUENCY OF 110 Hz

STATIC STRAIN (%)	TEMPERATURE (°C)	$\tan \delta$	$ G $ (MN/m <sup>2</sup> )	$G'$ (MN/m <sup>2</sup> )	$G''$ (MN/m <sup>2</sup> )
0.5	-18	0.036	22.0	22.0	0.84
	4	0.12	18.0	17.9	2.13
	25	0.29	10.9	10.4	2.98
	49	0.41	4.99	4.65	1.91
1.0	-18	0.046	22.2	22.2	1.08
	4	0.14	17.6	17.4	2.50
	25	0.34	9.77	9.25	3.08
	49	0.43	4.48	4.12	1.77
2.5	-18	0.046	22.4	22.4	1.12
	4	0.15	17.2	17.0	2.58
	25	0.35	9.33	8.8	3.09
	49	0.45	4.01	3.65	1.66
5.0	-18	0.049	22.0	22.0	1.14
	4	0.16	16.8	16.6	2.66
	25	0.37	8.49	7.96	2.94
	49	0.46	3.07	2.79	1.30

0.688 inch is used as a test specimen. The propellant disk is bonded to steel outer and center rings.

Tests were carried out at frequencies ranging from 10 to 50 Hz at 40°F, 70°F and 90°F. Analytical studies of the shuttle SRM center segment and the Göttingen disk test specimen were performed to arrive at appropriate static and dynamic displacements for the test. A Göttingen disk static center body deflection of 0.015 inch was required to simulate the propellant strains resulting from the worst case SRM thermal shrinkage, while a vibratory (dynamic) center body displacement of 0.0006 inch peak-to-peak is required to simulate maximum propellant strains resulting from a 0.5 g zero-to-peak, 2 to 50 Hz, longitudinal, sinusoidal vibration input to the case. Since the above dynamic displacement was below the minimum amplitude limit of the test apparatus, tests were conducted at dynamic displacement amplitudes ranging from 0.001 to 0.004 inch and imposed center body, static displacements ranging from 0.009 to 0.022 inches.

Experimental test results as a function of dynamic displacement are presented in Table IV for TP-H1123 live propellant and in Table V for TP-H1123 inert propellant (designated H-B). Similar results are presented in Tables VI and VII as a function of static displacement.

While the data presented in Tables IV through VII indicate significant influence of temperature and frequency, as expected, a Duncan Multiple Range Test indicated no statistical influence of static or dynamic displacement amplitude..

TABLE IV  
DYNAMIC SHEAR MODULUS OF LIVE TP-H 1123 PROPELLANT  
TEST DATA FOR VARIOUS DYNAMIC DISPLACEMENTS

Dynamic Displacement (Inches)	Frequency (Hz)	Temperature (°F)	$\tan\delta$	$ G $ (psi)	$G'$ (psi)	$G''$ (psi)
0.001	50	40	.44	3597	3064	1363
	40		.52	3014	2670	1398
	30		.47	2573	2328	1095
	20		.38	2168	2029	765
	15		.32	1949	1856	596
	10		.25	1757	1705	423
0.002	50	40	.53	3294	2909	1545
		70	.58	1472	1206	704
		90	.62	801	680	423
	40	40	.52	2856	2532	1322
		70	.58	1178	1019	590
		90	.61	660	562	345
	30	40	.47	2426	2196	1030
		70	.53	974	859	457
		90	.57	331	402	262
	20	40	.38	2017	1888	710
		70	.41	782	722	298
		90	.47	414	374	177
0.0027	15	40	.32	1824	1737	558
		70	.33	680	656	220
		90	.39	366	334	130
	10	40	.25	1632	1584	393
		70	.24	606	590	140
		90	.28	298	287	79.7
	50	40	.53	3292	2908	1544
	40		.52	2852	2592	1319
	30		.47	2438	2200	1032
	20		.38	2026	1896	714
	15		.32	1828	1740	558
	10		.24	1655	1608	392

TABLE IV (continued)  
 DYNAMIC SHEAR MODULUS OF LIVE TP-H1123 PROPELLANT  
 TEST DATA FOR VARIOUS DYNAMIC DISPLACEMENTS

Dynamic Displacement (Inches)	Frequency (Hz)	Temperature (°F)	$\tan\delta$	$ G $ (psi)	$G'$ (psi)	$G''$ (psi)
0.003	50	70	.58	1289	1116	645
		90	.62	793	674	417
	40	70	.58	1089	942	544
		90	.61	655	559	342
	30	70	.53	904	797	425
		90	.57	526	458	259
	20	70	.42	733	676	283
		90	.48	397	357	173
	15	70	.34	699	618	209
		90	.43	322	295	128
0.004	50	70	.24	547	532	127
		90	.30	277	265	80.3
	40	70	.57	1315	1140	656
		90	.52	777	663	406
	30	70	.56	1106	960	542
		90	.61	645	552	335
	20	70	.52	908	807	416
		90	.47	398	360	169
	15	70	.42	726	669	282
		90	.47	398	360	169
	10	70	.35	636	601	208
		90	.39	343	320	125
						148
				288	278	79.0

TABLE V  
DYNAMIC SHEAR MODULI OF H-13 INERT PROPELLANT  
TEST DATA FOR VARIOUS DYNAMIC DISPLACEMENTS

Dynamic Displacement (Inches)	Frequency (Hz)	Temperature (°F)	$\tan\delta$	$ G $ (psi)	$G'$ (psi)	$G''$ (psi)
0.0011	50	40	.52	2504	2220	1153
		70	.64	998	841	538
		90	.77	710	561	430
	40	40	.51	2197	1953	998
		70	.63	836	708	445
		90	.77	599	473	364
	30	40	.50	1909	1707	849
		70	.58	678	588	340
		90	.73	494	397	290
	20	40	.46	1642	1486	689
		70	.47	533	482	227
		90	.63	398	335	211
	15	40	.44	1510	1331	604
		70	.41	462	428	175
		90	.55	349	304	148
	10	40	.41	1382	1277	519
		70	.31	400	382	118
		90	.43	305	280	119
0.002	50	40	.52	2292	2030	1060
		70	.64	995	838	536
		90	.58	616	532	310
	40	40	.51	1981	1764	897
		70	.63	837	708	445
		90	.56	507	443	247
	30	40	.47	1676	1514	714
		70	.57	680	592	336
		90	.5	407	364	182

TABLE V (continued)

DYNAMIC SHEAR MODULI OF H-13 INERT PROPELLANT  
TEST DATA FOR VARIOUS DYNAMIC DISPLACEMENTS

Dynamic Displacement (Inches)	Frequency (Hz)	Temperature (°F)	tan	G (psi)	G' (psi)	G'' (psi)
0.002	20	40	.43	1391	1277	545
		70	.47	536	484	228
		90	.44	315	288	126
	15	40	.36	1252	1177	422
		70	.31	396	378	116
		90	.33	232	220	72.5
	50	70	.77	946	751	575
		40	.75	796	636	478
		30	.73	648	524	382
		20	.61	506	433	262
		15	.50	439	392	197
		10	.37	371	349	130

TABLE VI  
DYNAMIC SHEAR MODULI OF TP-H1123 LIVE PROPELLANT  
AS Affected BY VARIOUS STATIC DISPLACEMENTS

Static Displacement (inches)	0.0098	0.0177	0.0217	0.0197
<u>Frequency (Hz)</u>	<u>G' (psi)</u>			
50	1153	1178	1163	1153
40	982	1003	992	982
30	828	850	839	828
20	694	723	718	694
15	627	650	650	627
10	558	588	582	558
	<u>G" (psi)</u>			
50	656	674	663	656
40	551	565	558	551
30	421	433	427	421
15	197	204	204	197
10	122	128	127	122
	<u> G  (psi)</u>			
50	1327	1357	1339	1327
40	1126	1151	1138	1126
30	929	954	941	923
20	745	777	771	745
15	657	681	681	657
10	571	602	596	871

Note: Tested at 70°F, ambient pressure and a dynamic displacement of 0.002 inch peak to peak.

TABLE VII  
DYNAMIC SHEAR MODULI OF H-13 INERT PROPELLANT  
AS AFFECTED BY VARIOUS STATIC DISPLACEMENTS.

Static Displacement (inches)	0.0217	0.0098	0.0086	0.0017
<u>Frequency</u> <u>(Hz)</u>	<u>G' (psi)</u>			
50	1046	986	1076	1001
40	899	837	925	853
30	765	706	798	722
20	652	589	675	594
15	588	523	617	535
10	532	477	554	471
	<u>G" (psi)</u>			
50	602	557	624	568
40	506	464	524	475
30	393	359	412	368
20	261	234	271	243
15	195	173	205	177
10	121	108	128	107
	<u>G*(psi)</u>			
50	1207	1132	1244	1151
40	1032	957	1063	976
30	860	792	898	810
20	702	634	727	642
15	619	551	650	564
10	546	489	569	483

Note: Tested at 70°F and ambient pressure.

Thiokol also performed additional tests to investigate the influence of pressure on dynamic response. These test results are reported in the following section.

The dynamic test results presented in Tables II through VII are used subsequently in Section V in the validation of the dynamic response model.

#### 4.4 PRESSURE EFFECTS

As pointed out in Section 4.3.1 the decrease in moduli of strained solid propellants is caused primarily by dewetting and subsequent void formation. When this voiding problem occurs, the effect of hydrostatic pressure is to collapse or close the voids and, hence, nullify the reduction in moduli. When tests are conducted under imposed hydrostatic pressure, the pressure serves to suppress the formation of voids. Thus, no decrease in moduli is observed until, if at all, strain levels very near the ultimate strain are reached, i.e., 25% to 40% under high pressure.

Furthermore, as discussed in Section 4.3.2, the transverse constraint provided by the Göttenberg disk specimen produces dynamic shear modulus results as though some degree of hydrostatic pressure were present.

In addition to the dynamic shear tests discussed in Section 4.3.3, Thiokol [2] conducted Göttenberg disk tests on TP-H1123 live propellant in a pressure vessel at ambient, 500 and 1000 psi by confining pressures. Their test results are presented in Table VIII. As may be noted, these

TABLE VIII  
DYNAMIC SHEAR MODULI OF TP-H1123 LIVE  
PROPELLANT AS Affected BY PRESSURE

Pressure (psi)	Ambient			500		1000		
				<u>G' (psi)</u>				
Frequency (Hz)	50	40	30	20	50	40	30	20
50	1196	1209	1176	1207	1194	1187	1182	1189
40	986	995	989	982	989	1000	975	989
30	826	841	829	826	826	848	816	826
20	678	691	676	671	686	688	680	691
<u>G'' (psi)</u>								
50	700	709	685	708	698	693	741	695
40	565	571	566	562	566	574	600	566
30	429	437	430	429	429	441	457	429
20	300	305	298	295	303	304	327	305
<u> G  (psi)</u>								
50	1386	1402	1361	1399	1383	1374	1395	1377
40	1136	1147	1140	1131	1140	1153	1145	1140
30	931	948	934	931	931	956	935	931
20	741	755	739	733	750	752	755	755

Note: Tested at 70°F and at a dynamic displacement of 0.0045 inch peak to peak.

data are well within the statistical limits established by the ambient pressure tests previously presented in Section 4.3.3.

Therefore, it is concluded that pressure will have an insignificant effect on the SRM propellant dynamic response at the static and dynamic strain levels existing in the shuttle SRM.

#### 4.5 AGING EFFECTS

Solid propellants, in general, experience changes due to normal aging during long term storage (see Equations 5,6,23,29,36-38). However, in the case of the space shuttle SRM, the planned casting and firing schedule of the shuttle is such that aging effects will be inconsequential, and, hence, need not be included in the propellant dynamic response model.

If motors are stored longer than six months between casting and firing, then dynamic tests should be conducted on propellant the appropriate age of the SRM at the time-of firing and these data input to the dynamic response model to compute appropriate dynamic moduli. As a rule of thumb, if the time between casting and firing exceeds one year, provided the dynamic moduli curves versus frequency are only shifted with aging and not rotated, (i.e., provided the slope  $n$  remains constant) an effective baseline modulus,  $E_0^*$ , can be calculated according to

$$E_0^* = E_0 (1 + 0.2 t) \quad (64)$$

where  $E_0$  is the original unaged value and the time,  $t$ , is expressed in years. This relation is based on the observation that propellants

typically degrade approximately 10 to 20 percent during the first year of aging [5,6]. As such, Equation (64) should be approximately valid for two to three years aging. For longer aging times actual aging test data should be employed. Past experience indicates that the aging degradation relation will be a straight line on a log-log plot.

During the first six months following casting of the SRM, the softening effect due to hydrolytic chain scission in the curing process apparently compensates for the hardening effect of oxidative and post-cure cross-linking since, the modulus is observed to be essentially unchanged during this period.

#### 4.5.1 General Discussion of Aging of Solid Propellants

Solid propellants experience changes due to normal aging during long term storage. These changes are reflected in changes in the chemical and physical properties of the propellant and liner-propellant bond. Unlike the effects of moisture, however, the effects of aging are irreversible. Most propellants typically exhibit between 25 and 50 percent degradation during aging. The discussion here is restricted to chemorheological aging. Mechanical aging degradation results from sustained or cyclic application of loads and is normally handled through cumulative damage considerations.

Several factors are known to influence the aging characteristics of propellants which in turn affect the shelf-life of a solid rocket motor. The dominant aging mechanisms affecting propellant behavior, which normally occur simultaneously, are continued post-curing, oxidative cross-linking and polymer chain scission. Additional

consideration must also be given to surface versus bulk aging characteristics and migration effects. The influence of these factors is dependent to a greater or lesser extent upon the propellant polymer and cure system, cure cycle, cure catalysts, ballistic modifiers and aging temperature.

Post-cure curative reactions result from the slow continuation of reactions not driven to completion during the normal cure cycle. These reactions result in an increase in the propellant modulus due to the formation of additional network cross-links.

Oxidative cross-linking is primarily a surface phenomenon which results from free-radical attack at double bonds in the polymer chain backbone. This mechanism also results in an increase in stress and decrease in the strain properties of solid propellants.

Chain scission is largely determined by the cure system and results in softening of the propellant. This phenomenon, as mentioned before, is accentuated by the presence of moisture; however, Hydroxy-terminated (HTPB) and Carboxy-terminated polybutadiene (CTPB) propellants frequently display this reversion process during high temperature aging. Polyurethane propellants also undergo chain scission during aging due to splitting of functional linkage.

Distinct differences between the surface and bulk aging characteristics of propellants have been noted primarily due to surface oxidation of the propellant. This surface oxidative cross-linking results in a considerably stiffer propellant surface. Surface skin effects, notably hardening of the grain inner bore, has been observed

to a depth of one-half inch in some cases. Significant variations in the aging behavior of propellant aging in sample cartons and propellant aged in rocket motors has also been observed. These variations have been attributed in part to the fact that motors are characteristically cured at a higher temperature than the oven temperature because of internal exothermic reactions. Cartons, on the other hand, are cured at a temperature more nearly equal to the oven temperature.

Migration of soluble species is of major concern at the propellant-liner-insulation bond interfaces. Soluble species such as low molecular weight polymer, burning rate catalysts, plasticizers, moisture and degradation products may migrate across bond interfaces causing both chemical and physical changes. An exact relation between ingredient migration and the physical and chemical changes is not presently known. Such a relation is influenced in a complicated manner by time, temperature, concentration and relative solubility of the migrating species. The predominant physical effect of all migratory species is degradation of the adhesive bond between the liner, and propellant or liner and insulation or case. In addition, the propellant and the liner or insulation may harden or soften either separately or jointly. Typically, migrating species from the propellant into the liner or insulation act as plasticizers causing the liner or insulation to soften and swell and the propellant to harden and shrink resulting in high localized stresses and strains at the bond interface as well as a weakened adhesive bond. Plasticizer migration from certain elastomeric insulations into the propellant, on the other hand, normally softens the propellant. In other

situations, such as a curative imbalance between the liner and the propellant, a hardening of either or both the propellant and the liner may result. Cross migration of other ingredients may have similar results depending on the particular ingredients and concentrations involved. It suffices to observe that migration invariably degrades the adhesive bond system.

Migration in composite propellants has been observed to be particularly critical in CTPB propellants, and for propellants employing liquid alkylferrocene ballistic modifiers. Migratory behavior has also been observed of dioctyl azelate (DOZ) and circo light oil.

The storage or aging temperature influences the rate at which the above processes occur, the relative severity of degradation, and, to a certain extent, if a given aging mechanism will occur. In general, increasing the aging temperature accelerates the rate at which degradation takes place. It is also noted that the degradation in propellant and liner-propellant properties observed during high temperature (accelerated) aging is significantly greater than the degradation observed during ambient temperature aging, even for prolonged periods of time. Post-cure curative reaction rates are accelerated by increasing the storage temperature. In this situation, high temperature aging completes the normal cure process. Migration rates and the relative degradation of the liner-propellant adhesive bond due to migration are significantly increased at high temperatures.

Surface hardening due to oxidative cross-linking also appears to be accentuated at elevated temperatures. On the other hand, propellant softening due to excess chain scission over continued post-cure

cross-linking, noticeably absent under ambient temperature storage conditions, has been observed in CTPB, HTPB and polyurethane propellants during high temperature aging.

For the most part, the processes discussed in the previous paragraph are de-emphasized under low temperature storage conditions. However, an alternate problem may be introduced for composite propellants containing liquid alkylferrocenes which may crystallize during low temperature storage.

In addition to the primarily physical effects discussed previously, aging also affects the ballistic properties of solid propellant grains. The normal ballistic changes are changes in burn rate, pressure and temperature sensitivity of burn rate and ignitability caused primarily by hardening of the propellant and evaporation and migration of volatile catalysis.

The problem of controlling and minimizing aging effects has only been partially solved by the propellant chemist. The problem facing the propellant chemist is that of formulating completely stable solid propellants which undergo insignificant changes in all aging environments. This goal has effectively been attained only for polybutadiene-acrylnitrile acrylic acid terpolymer (PBAN) propellants, which typically undergo about a 25% decrease in strain properties during the first year of aging and then remain relatively stable thereafter.

Continued post-cure cross-linking is exhibited by all composite propellants to a greater or lesser extent. One effective means of controlling post-cure reactions has been to extend the cure cycle to assure completion of all normal cure reactions. This technique, although

effective in minimizing continued cross-linking during storage, may frequently result in undesirable, and unacceptable unaged propellant physical properties. The most desirable method of controlling the effects of post-cure reactions is to maintain a balance between post-cure cross-linking and chemical scission of polymer chains. For this situation the aging behavior obtained from conventional aging of bulk samples is indistinguishable from the unaged properties inasmuch as polymer chains are broken and new cross-links are formed in an unstressed state. In a composite solid propellant grain under ambient storage conditions, the polymer chains that are broken are in a strained state; however, the new cross-links formed are still in an unstrained state. Forming new cross-links in an unstrained state in propellant which was previously strained de-emphasizes the importance of the effects of previous loadings. In essence, the propellant has no memory for prior loadings.

Oxidative cross-linking is primarily a surface phenomenon which is suppressed to a certain extent, but not eliminated by the presence of antioxidants in the propellant prepolymer. This effect is further minimized by sealing the rocket motor interior in an inert gas environment.

Migration effects may be reduced to tolerable levels through consideration of the equilibrium concentrations of migrating species and the use of migration barriers. Primarily, effort has been directed toward the elimination or reduction of the degradation of adhesive bonds attributed to plasticizer migration.

## 4.6 EPOXY/CURATIVE RATIO EFFECTS

Chemical effects represent an additional variable, in particular the epoxy/curative ratio investigated during the program, since the Thiokol SRM propellant is an epoxy cured PBAN propellant. It is a common practice to vary the epoxy/curative ratio to maintain quality control in large production propellant castings. Usually the stress relaxation modulus at some fixed time or the strain at maximum stress in a constant strain rate test [29] is selected as the appropriate mechanical property governing quality control limits. It is also known that epoxy/curative ratio variations affect the dynamic response [13,15]. Therefore, an investigation was carried out to determine the extent and significance of chemical changes on the SRM propellant dynamic response.

For the shuttle SRM program, the variable epoxy/curative ratio is inherent in the manufacturing process for maintaining quality control over physical properties; hence, the epoxy/curative ratio has no effect on the dynamic response model.

### 4.6.1 General Discussion of Epoxy/Curative Ratio Effects

The epoxy/curative ratio in a solid propellant is very influential in determining the value of the dynamic moduli. Ideally, this ratio is equal to 1.0 in order to provide just enough curative to guarantee cross-linking of all available chain ends with none left over for post-cure reactions nor none deficient possibly leading to initial undercure and subsequent oxidative hardening.

The practice at Thiokol/Wasatch however, is to:

1. Determine the functionality of the various polymer batches making up the PBAN (Polybutadiene acrylic-acid acrilo-nitrite terpolymer).
2. Calculate the epoxide-curable ratio so that the proper amount of curative is added to achieve the designated tensile modulus.
3. Use quality control constant rate tension tests to confirm that the specified value of tensile modulus is met within acceptable tolerance limits.

#### 4.7 INTERNAL HEAT GENERATION

As noted previously in Section 3.1, a problem associated with vibration is that of generating local temperature increases sufficient to cause either that of generating local temperature increases sufficient to cause either spontaneous ignition of the propellant or severe mechanical degradation. The rate of energy dissipation into heat for a linear viscoelastic material is proportional to the frequency of vibration, material stiffness, (i.e., the real part of the complex modulus) and the square of the magnitude of the deformation. Thus, the vibration problem is typically most severe for conventional motors under the low frequency, first resonant mode, at high temperatures. In this situation the propellant stiffness is a minimum for vibration conditions, and the motion of free surfaces (e.g., a starpoint) is greatest, resulting in maximum energy dissipation into heat. The problem is further complicated by the characteristically strong temperature

dependence of propellant mechanical properties. This temperature dependence makes the energy dissipation very sensitive to temperature variations so that a continuing periodic forced motion can give rise to substantial temperature increases.

Typical thermomechanical response and heat generation for dynamic double-lap shear tests of a PBAA propellant showing the potential magnitude of the problem are presented in Figures 7 through 11, taken from Reference 31.

It is not likely that autoignition or chemomechanical degradation of the shuttle SRM propellant will be encountered; however, temperature increases sufficient to change the viscoelastic dynamic response properties during vibration could develop for certain vibration modes. An analysis based on longitudinal, through-the-thickness shear vibration [6] yielded an estimated temperature increase of less than 1°K. This increase is not sufficient to alter the propellant properties significantly.

The shuttle SRM would need a burn and flight time in excess of 10 - 20 minutes before sufficient viscous dissipation could occur to produce temperature changes sufficient to meaningfully affect the propellant dynamic modulus. Hence, it is concluded that internal heat generation can be neglected in the SRM propellant dynamic response model.

#### 4.8 DAMAGE EFFECTS

Based upon our extensive studies of the nonlinear permanent memory behavior of solid propellants over the past few years we were initially concerned that the response of the SRM propellant could be

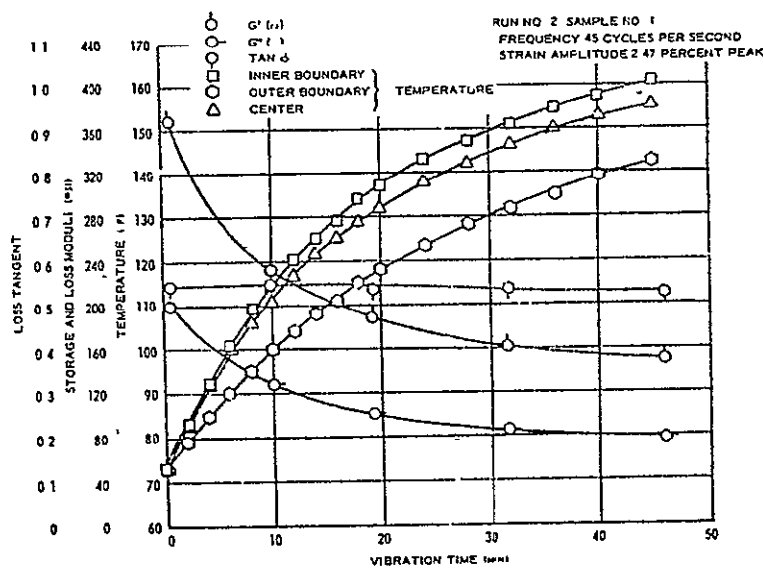


Fig. 7. Thermomechanical response, constant strain amplitude excitation, adiabatic boundary conditions, PBAA propellant

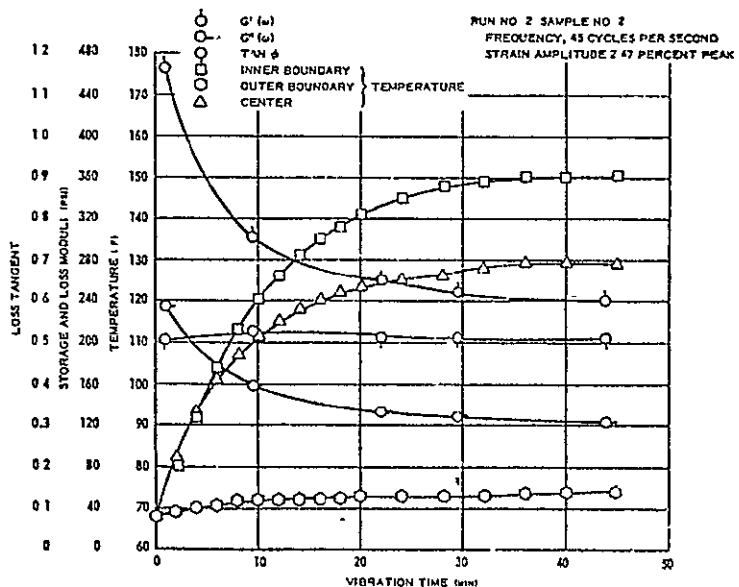
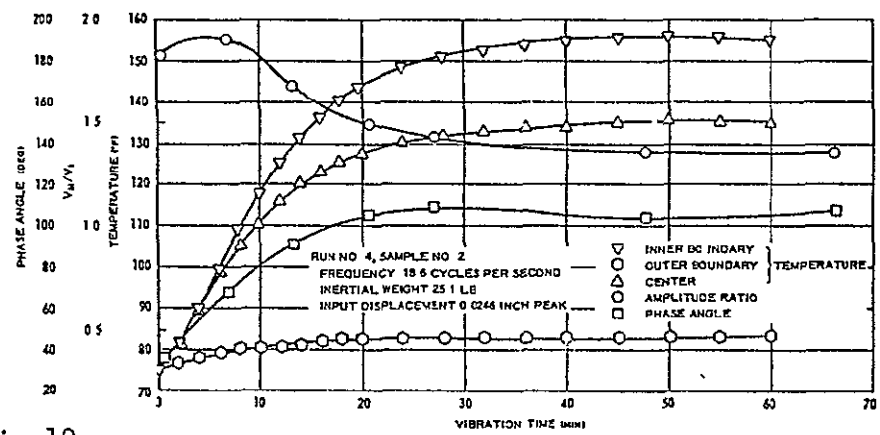
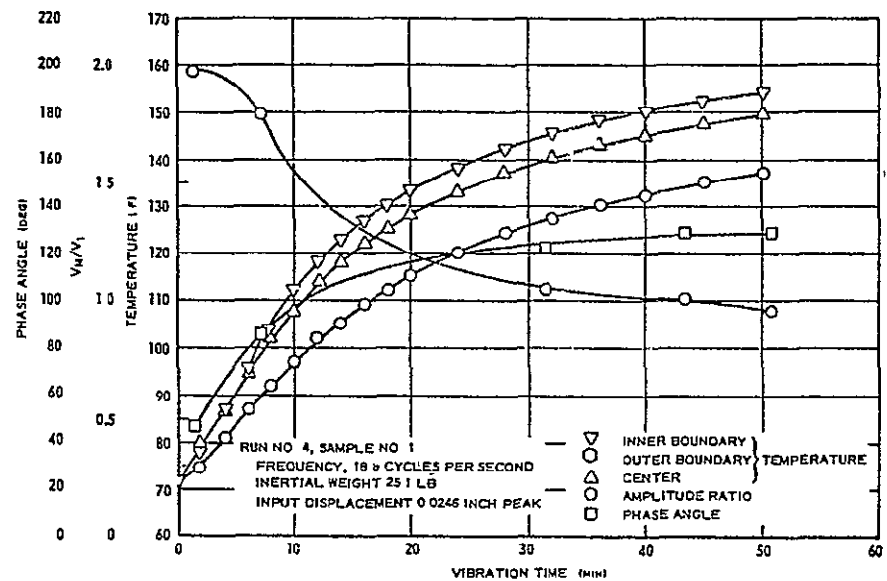


Fig. 8. Thermomechanical response, constant strain amplitude excitation, isothermal boundary conditions, PBAA propellant



REPRODUCIBILITY OF THE  
FLUCTION IS POOR

ANALYSIS AND DESIGN OF SOLID PROPELLANT GRAINS

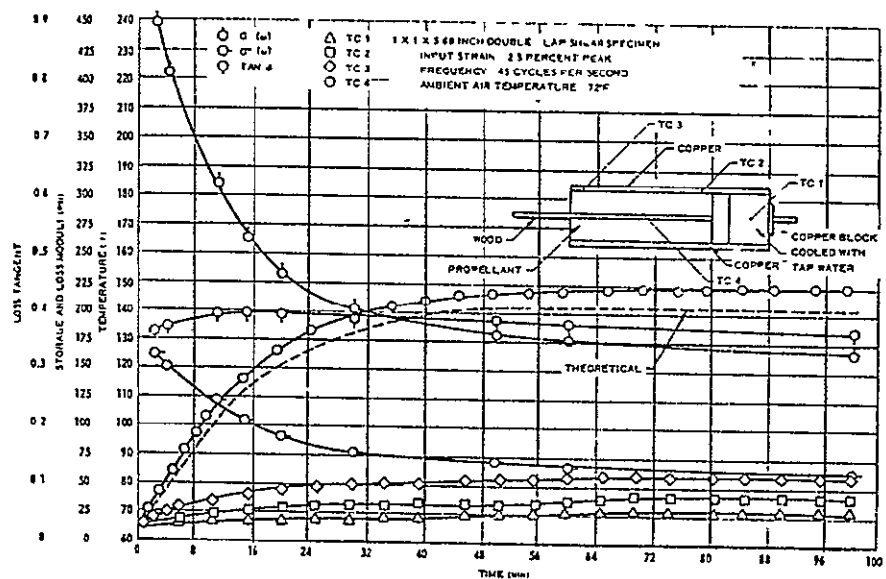


Fig. 11. Dynamic heating, isothermal boundary conditions, PBAA propellant.

REPRODUCIBILITY OF THE  
ORIGINAL PAGE IS POOR

considerably different during vibration if the SRM has previously seen vibration at a higher frequency analogous to the static behavior of many propellants at modest strain levels (see Equation (33)). In this situation, the propellant stiffness at the lower frequency following previous vibration at a higher frequency could be lower. Amplitude changes could also give this effect.

Based on subsequent investigation's we have concluded, however, that damage or permanent memory effects are negligible over the domain of operation of the shuttle SRM.

Strictly speaking, the statement that there are no damage effects present is not true. The fact that propellant dynamic data typically do not translate into comparable stress relaxation data according to linear viscoelasticity theory, is one indication of damage effects. However we are not herein using relaxation data to obtain the dynamic moduli, but are directly utilizing dynamic tests. Thus, if the propellant is "damaged" under a few cycles of dynamic testing, this fact is not observable since all data is obtained under steady state dynamic conditions. Thus, any intrinsic damage is implicit in the moduli obtained at the various frequencies, strains and temperatures.

Again, as noted in Section 4.3, the strain levels are apparently sufficiently low to have no effect; thus, the "cycling" damage is not observable.

## V. DEVELOPMENT OF THE SRM PROPELLANT DYNAMIC RESPONSE MODEL

Based on the arguments of the previous sections it has been concluded that the SRM propellant dynamic response model need only account for temperature and frequency. The particular model selected, as noted previously in Section 2.2, is a power law (i.e., straight-line curve on a log-log plot of the form

$$E = E_0 (\omega a_T)^n \quad (1)$$

where  $E$  here can represent the real or imaginary part of either the dynamic tensile or shear modulus,  $E_0$  is the modulus at  $\omega a_T = 1$  and  $n$  is the slope on a log  $E$  versus log  $\omega a_T$  plot. The time-temperature shift factor was selected to have the form

$$a_T = \left( \frac{T_R - T_a}{T - T_a} \right)^m \quad (65)$$

where  $T_R$  is the reference temperature to which data at other temperatures is shifted and  $T_a$  and  $m$  are empirically determined parameters.

Equations (1) and (65) have been incorporated into a computer program which performs a least-squares curve-fit of laboratory data to determine the coefficient  $E_0$  and the exponent  $n$  and/or predict the dynamic moduli at any frequency and temperature.

The following sections describe the rationale for selecting the model given by Equations (1) and (65), and validation of the model using UTI-610, TP-H1123 and H-13 propellant data, and a general discussion of the computer program. A listing, documentation and a user's manual for the computer program is presented in Appendix B.

### 5.1 RATIONALE FOR SELECTION OF THE RESPONSE MODEL

The analysis of Section 4.1 resulted in some very useful expressions interrelating the behavior of linear viscoelastic materials under different test nodes. The expressions of interest to the discussions here are

$$\left. \frac{\partial \sigma(t)}{\partial \varepsilon} \right|_{\varepsilon=Rt} = E_{rel}(t) \quad (32)$$

$$E^*(\omega) = i\omega \mathcal{L}[E_{rel}(u)] \Big|_{u=i\omega} \quad (49)$$

$$E_{rel}(t) = E_e + \sum_{k=1}^n E_k \exp(-t/\tau_k) \quad (50)$$

$$E'(\omega) = E_e + \sum_{k=1}^n \frac{E_k (\omega \tau_k)^2}{1 + (\omega \tau_k)^2} \quad (51)$$

and

$$E''(\omega) = \sum_{k=1}^n \frac{E_k (\omega \tau_k)}{1 + (\omega \tau_k)^2} \quad (52)$$

As pointed out in Section 4.1, Equation (32) expresses the fact that for a linear viscoelastic material the instantaneous slope of the

stress-strain curve, in a constant strain rate test with strain rate  $R$ , evaluated at  $\epsilon = Rt$ , gives the stress relaxation modulus at time,  $t$ .

Equation (49) expresses the fact that for a linear viscoelastic material, the complex cynamic modulus is given by the Laplace transform of the relaxation modulus evaluated at  $i\omega$  and multiplied by  $i\omega$ . Using Equation (49) and the Dirichlet exponential series in Equation (50) to represent the relaxation modulus, then the storage and loss components of the complex dynamic modulus are readily determined, as given by Equations (51) and (52), in terms of the parameters describing the relaxation behavior of the material.

The significance of the above comments is that for a linear viscoelastic material any single test is sufficient to uniquely determine the material response to any other test. Unfortunately, in the case of solid propellants, whereas the propellant may appear to be linear under any one given test condition, such as constant strain rate, constant stress, oscillatory stress or strain, attempts at converting the data to another test condition are seldom successful.

Part of the test program carried out at the University of Utah on UTI-610 propellant for the NASA/Langley facility involved investigating the validity of the relations given by Equation (32) and (49) to (52). Figure 12 presents the master stress relaxation modulus versus temperature-reduced time as determined from direct experimental observations and calculated from Equation (32). Without belaboring the point, the agreement is quite poor. The errors become even worse when one carries out the next step of converting the constant strain rate and relaxation data to dynamic data as shown in Figure 13 for the storage modulus in tension and shear.

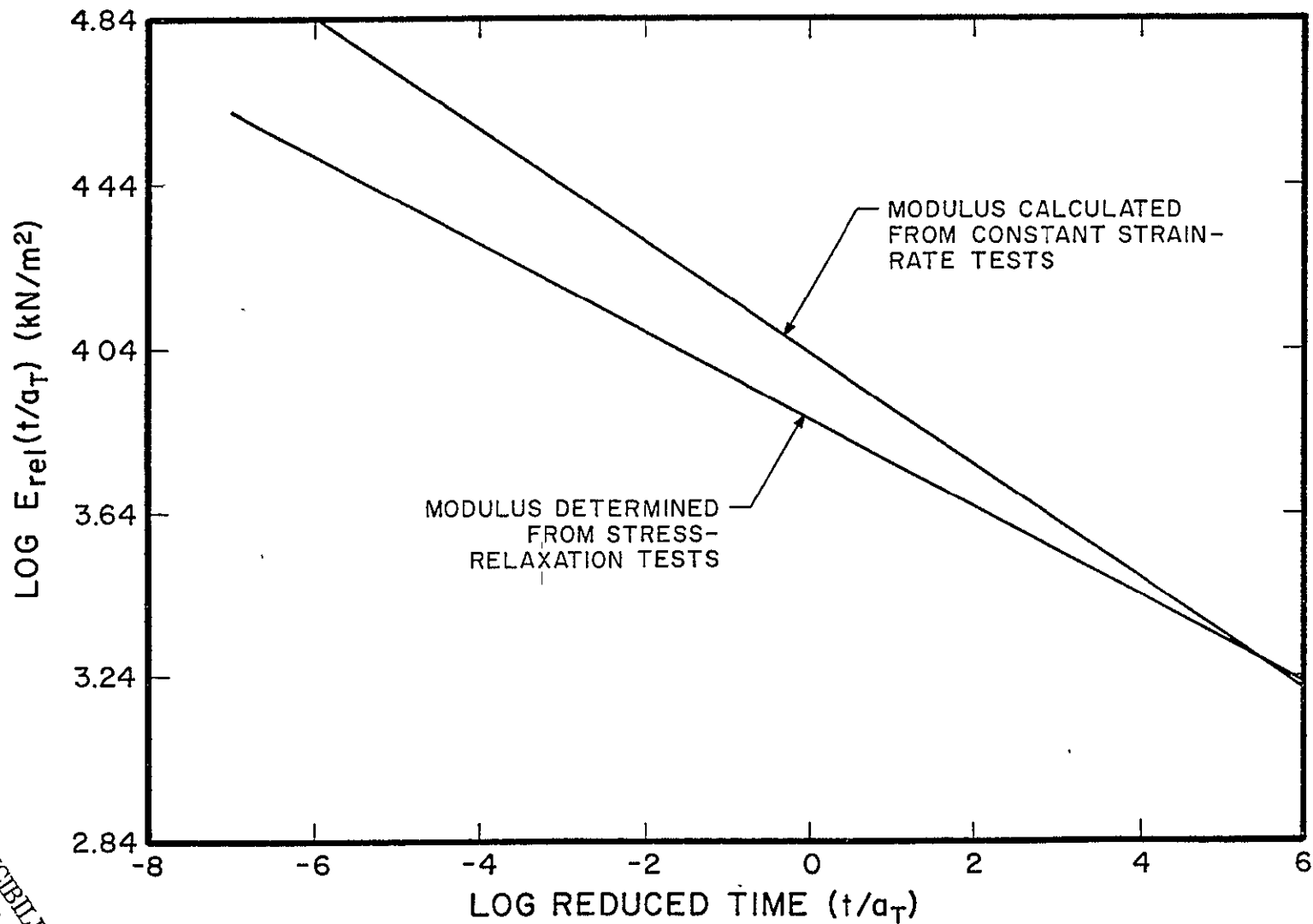


FIGURE 12. Master Stress Relaxation  
Modulus Versus Temperature Reduced Time

REPRODUCIBILITY OF THE  
ORIGINAL PAGE IS POOR

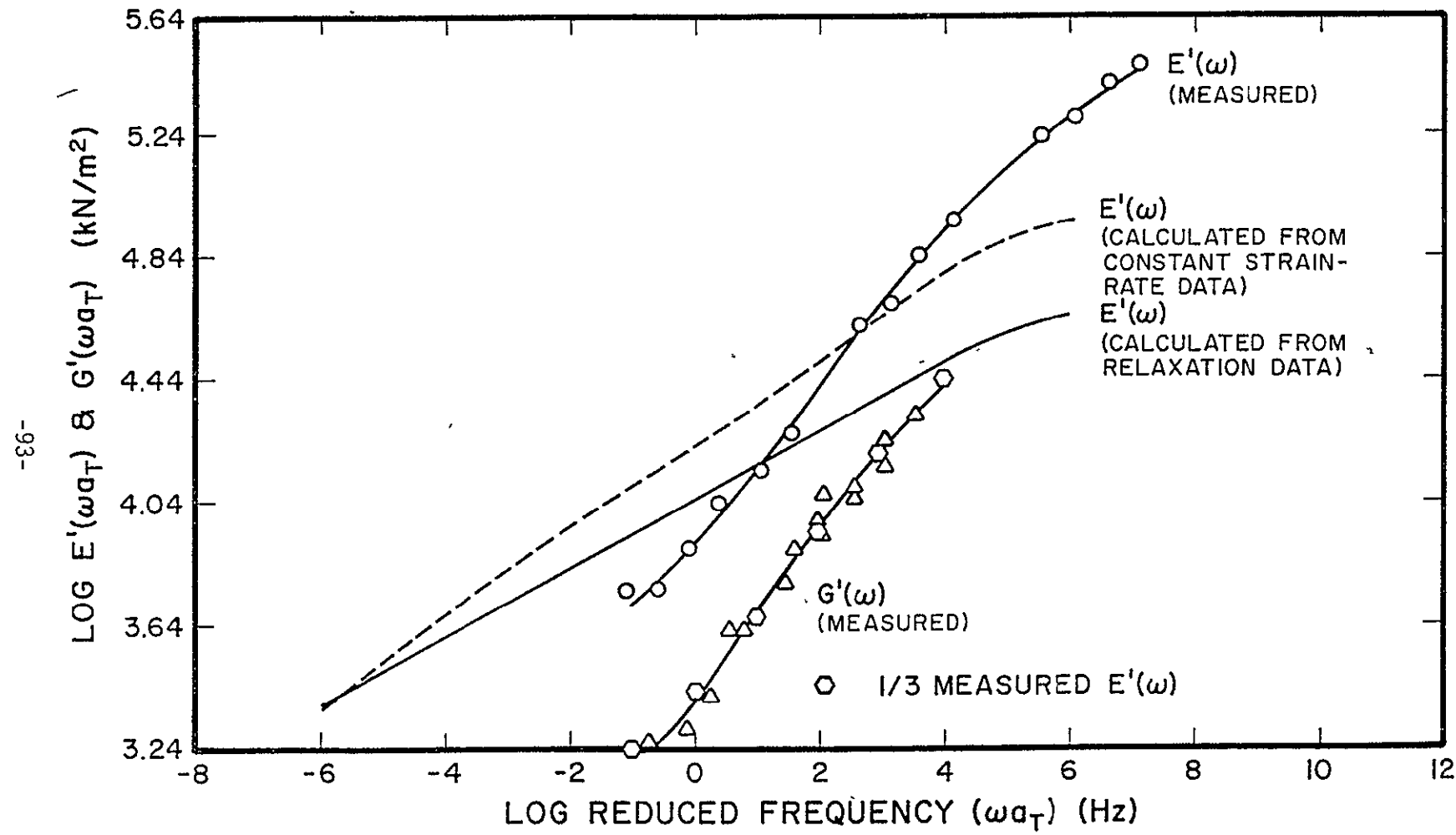


FIGURE 13 - MASTER DYNAMIC MODULUS VERSUS  
TEMPERATURE REDUCED FREQUENCY

One additional interesting observation from Figure 13 is that the measured dynamic tensile modulus is very nearly one-third the measured dynamic tensile modulus, thus supporting the normal assumption that propellants behave as incompressible materials (i.e.,  $\nu = \frac{1}{2}$ ).

Based on the above observations another representation of the dynamic moduli was sought. Other expressions used to represent the relaxation modulus include [5,6] a modified power law

$$E_{\text{rel}}(t) = E_e + \frac{E_g - E_e}{[1+t/\tau_0]^n} \quad (66)$$

where  $E_e$  is the long-time equilibrium modulus,  $E_g$  is the short-time glassy modulus,  $\tau_0$  is a characteristic time taken to be the midpoint of the transition region from glassy to rubbery response and  $n$  is the slope of the modulus curve through the transition region. Equation (66), however, while capable of representing other polymeric material behavior does not work well with solid propellants since it is extremely difficult to conduct tests over a short enough or long enough period of time to define the glassy and rubbery moduli, respectively. Most propellants exhibit the behavior shown in Figure 12 of a straight-line behavior over many decades of time. Also, Equation (66) is not well suited for taking the Laplace transform to determine the dynamic moduli; and one would still not expect much better agreement than that shown in Figure 12.

The relaxation behavior in Figure 12 is easily represented by the simple power law

$$E_{rel}(t) = E_1(t/a_T)^n \quad (67)$$

However, this equation is also difficult to Laplace transform for  $n$  not equal to an integer ( $n$  typically ranges from 0.1 to 0.3).

A more direct approach based on the observed behavior of  $E'$  and  $G'$  in Figure 13 and Thiokol data to be presented subsequently over the anticipated temperature-reduced frequency of interest to the shuttle SRM (1 to 1000 Hz) is to utilize the simple power law given by Equation (1) directly; which is what we have chosen to do.

The efficient utilization of the model given by Equation (1) in a computer program requires analytical specification of the time-temperature shift function. Several representations are commonly used to represent  $a_T$ . The most famous is the WLF equation

$$\log a_T = \frac{-8.86 (T-T_g)}{101.6 + (T-T_g)} \quad (68)$$

where the temperature,  $T$  is measured in degrees Kelvin. The temperature,  $T_g$  is approximately equal to the glass transition temperature  $T_g + 50^\circ$ . Equation (68) works well for amorphous polymers for which it was developed, but does not always fit propellant data very well.

Another representation frequently used in numerical computational schemes involves approximating the shift-factor curve by piece-wise log-linear curves of the form

$$a_T = 10^{n(T-T_R)} \quad (69)$$

Equation (69) is complicated to use with the dynamic response model selected since more computational time would be spent in locating the transition temperatures for the straight line segments than in evaluating the model.

A better representation than either Equation (68) or (69) for representing the shift-factor for a solid propellant is obtained using the modified power law representation given by Equation (65).

Figure 14 shows the experimentally determined shift factors used in generating the curves presented in Figures 12 and 13 compared with the analytical fit using Equations (68) and (65). The temperature  $T_s$  was chosen to be 323°K in Equation (68) and the parameters in Equation (65) were determined to be

$$T_R = 298^\circ\text{K}$$

$$T_a = 233^\circ\text{K}$$

$$m = 15.0$$

Even though the WLF equation, Equation (68) gives results within the  $\pm 3 \sigma$  limits of the experimentally determined shift factor, Equation (65) more closely approximates the mean values of the experimental shift factor curve.

## 5.2 VERIFICATION OF THE DYNAMIC RESPONSE MODEL

As mentioned previously, the SRM propellant dynamic model was validated using test data obtained at Thiokol [2] and at the University of Utah [3]. Figure 15 presents the real and imaginary parts of the dynamic shear modulus for TP-H1123 live propellant and H-13 inert propellant versus temperature-reduced frequency.

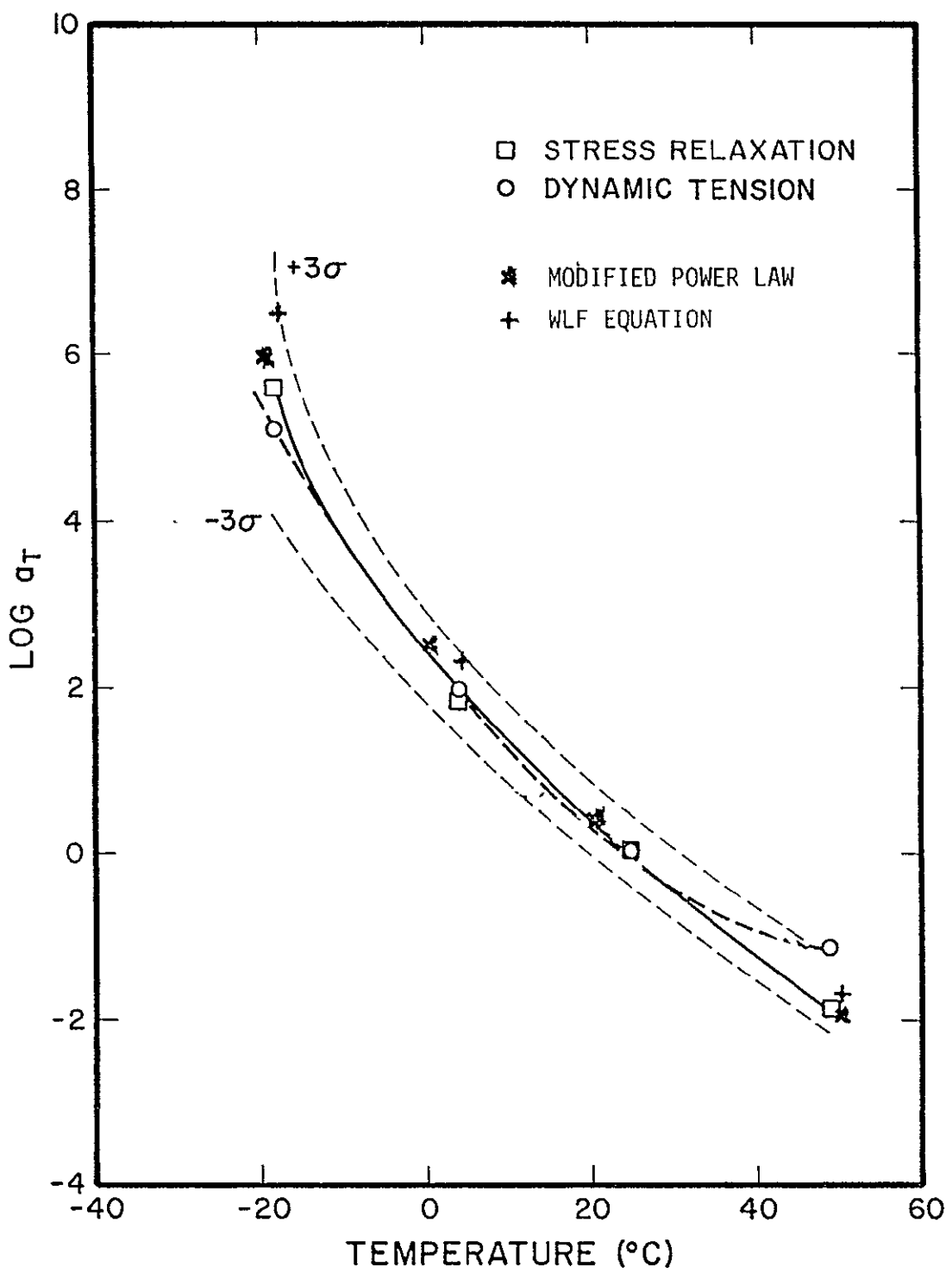


FIGURE 14- Time-Temperature Shift Factor Versus Temperature

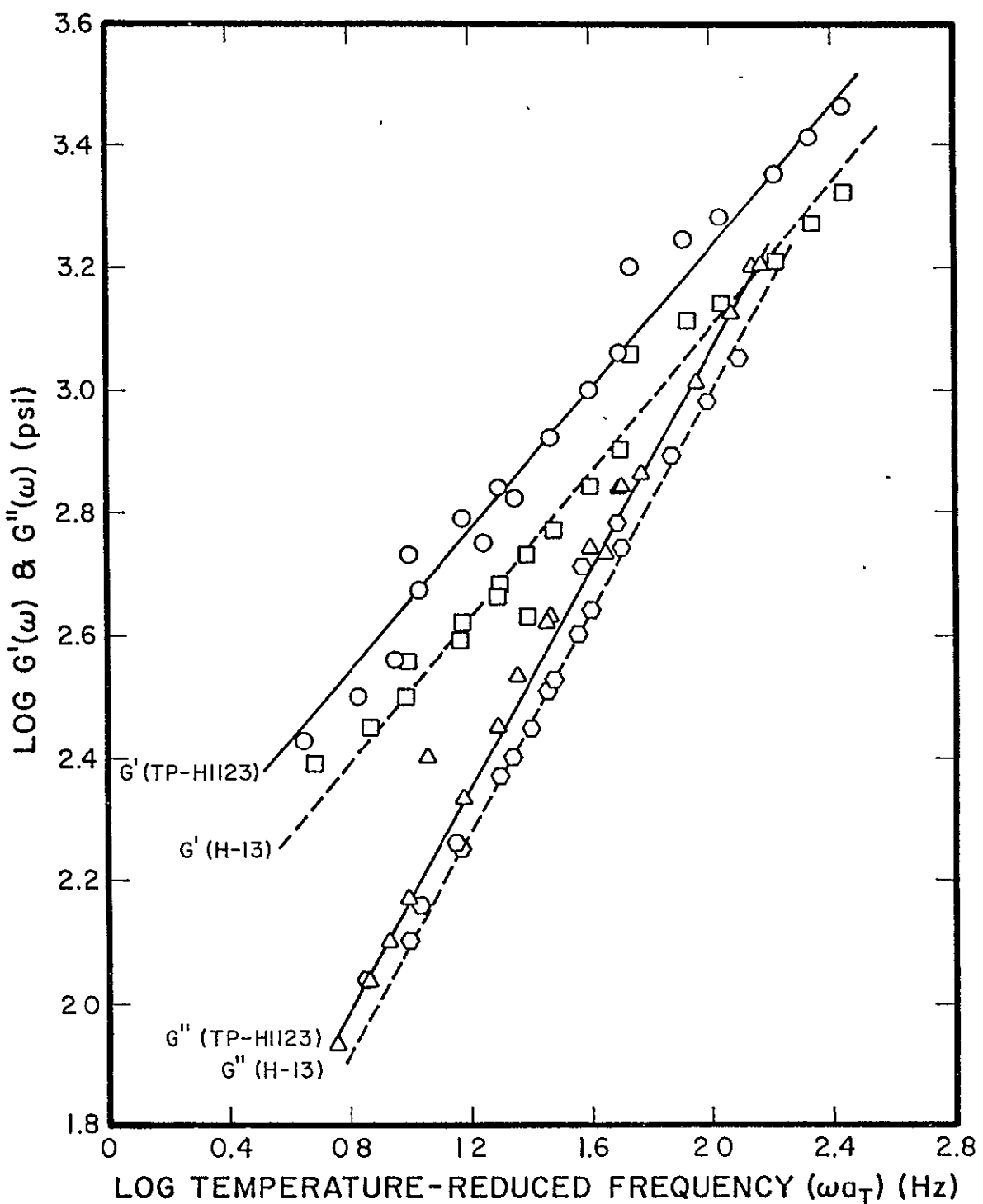


Figure 15. Dynamic Shear Modulus Versus Temperature Reduced Frequency for TP-H1123 and H-13 Propellant

Fitting the model given by Equation (1) to the data presented in Figures 13 and 15 gave the results presented in Table IX for the coefficient  $E_0$  and the exponent  $n$ .

A comparison of measured dynamic response with calculated moduli using the model parameters in Table IX is shown in Table X. It is seen that even though there is considerable experimental data scatter, the selected model for the SRM propellant dynamic response describes the behavior very well.

TABLE IX  
MODEL PARAMETERS

	<u>UTI-610</u>	<u>TP-H1123</u>		<u>H - 13</u>	
	<u><math>E'</math> (kN/m<sup>2</sup>)</u>	<u><math>G'</math> (psi)</u>	<u><math>G''</math> (psi)</u>	<u><math>G'</math> (psi)</u>	<u><math>G''</math> (psi)</u>
$E_0$	7867	-120	19	83	15.8
$n$	0.26	0.58	0.89	0.59	0.9

### 5.3 COMPUTER PROGRAM FOR THE DYNAMIC RESPONSE MODEL

The SRM propellant dynamic response model given by Equation (1) was programmed using Standard ANSI FORTRAN IV. Detailed input instructions for the code are provided in Appendix B. A brief general discussion of the program capabilities is described herein.

The use of the code begins by constructing a master dynamic modulus curve versus temperature-reduced frequency from tests conducted

TABLE X  
COMPARISON OF PREDICTED AND MEASURED DYNAMIC MODULUS

Temperature- Reduced Frequency	UTI-610		TP-H1123				H - 13			
	E' (kN/m <sup>2</sup> )		G' (psi)	G'' (psi)		G' (psi)	G'' (psi)			
	meas.	calc.	meas.	calc.	meas.	calc.	meas.	calc.	meas.	calc.
6	11,900	12,500	346	339	93.3	93.6	243	238	79	79.2
10	12,900	14,300	452	456	148	148	320	323	126	126
15	14,500	15,900	575	577	216	212	407	410	174	181
20	15,500	17,140	716	682	272	273	484	486	232	234
50	20,000	21,700	1150	1160	617	618	832	835	525	534
100	25,000	26,050	1720	1730	1150	1140	1260	1260	989	997

at several temperatures. Data points from this curve are input and a least-squares curve-fit is carried out to determine the coefficient  $E_0$  and the exponent  $n$  in the constitutive relation, Equation (1).

The code has the capability of simultaneously curve-fitting the real and imaginary parts of either the dynamic tensile or dynamic shear modulus at different frequencies and at a different number of points. If both the real and imaginary part of a modulus are curve-fit then the loss tangent is also calculated.

Simultaneous with the curve-fitting procedure, predictions of dynamic response for the real and/or imaginary parts of the modulus can be made at different frequencies and different temperatures. In this case the parameters describing the temperature shift function given by Equation (65) must be input. The curve-fitting procedure is carried out in terms of the temperature-reduced frequency with respect to a given reference temperature. In making predictions, however, the actual frequency at a given temperature where the response is desired is input and the temperature shift function calculated according to Equation (65).

Finally, as a third alternative if the parameters  $E_0$  and  $n$  have been previously determined, the curve fitting routine is by-passed and predictions directly made.

The code has the output formatted in SI units; however, it may be seen from Equations (1) and (65) that the calculations within the code are independent of the system of limits selected.

## VI. DYNAMIC SCALING AND COUPLING BETWEEN MOTOR CASE AND SRM PROPELLANT

### 6.1 DYNAMIC SCALING LAWS FOR SPACE SHUTTLE SRM

Dynamic tests of 1/8-scale models of the Shuttle External Tank, Solid Rocket Boosters and the Mated model have been conducted at the NASA/Langley Research Center [27]. These tests have been concerned with determination of resonant frequencies and mode shapes and evaluation of the NASTRAN dynamic model. Additional dynamic tests of SRM segments are planned. As a tool for the evaluation of the NASTRAN dynamic model, it is not necessary that relations between the SRM model response and the full-scale shuttle SRM's be determined. However, if information from dynamic model tests is to be used to deduce information about the vibration response of the full-scale or prototype SRM then appropriate scaling laws must be developed. For elastic materials in which the material properties (i.e., Young's modulus, E, and shear modulus, G) are independent of time or frequency simple geometric scaling of frequencies or amplitudes is sufficient. However, for viscoelastic materials with E and G strongly frequency dependent, simple geometric scaling is usually not valid.

For the viscous damping associated with solid rocket motor vibration, normalized mode shapes are unaffected by scaling. Therefore, the discussion that follows is concerned with developing scaling laws relating the resonant frequency response of the model and the prototype. The analysis considers:

- A. Longitudinal shear vibration of an infinitely long thick-walled hollow cylinder bonded to a rigid casing material;
- B. Axial vibration of a finite-length composite cylindrical rod,
- C. Bending of a composite cylindrical beam,
- D. Torsion of a composite cylindrical rod,
- E. Lateral vibration of a star point

Two approaches are commonly used for determining the relationships between a model and its prototype. The conditions of similarity may be expressed in mathematical form, using established laws of structural mechanics, and the principles of similitude rigorously deduced from them, or the principles of similitude may be deduced using dimensional analysis and the well known "Buckingham Pi-Theorem." The latter approach is not dependent upon specific knowledge of the equations governing the system response, but does require that all variables affecting the system behavior be included.

The first method is generally employed when the equations describing the system response are known. This approach is followed subsequently. The dynamic scaling laws are deduced from appropriate elastic formulae by replacing the elastic modulus with the storage modulus or real component of the viscoelastic modulus written in complex form.

In this situation an iterative procedure is followed until the calculated frequency agrees with the initial assumed frequency (or by finding the intersection of curves of modulus versus frequency and

resonant frequency versus modulus). Stresses and strains, if desired, may then be calculated using viscoelastic properties at the frequency of interest.

It is possible to carry out more refined analysis using NASTRAN or some other structural code; however, in view of the agreement shown in Section 3.3 between a simple model analysis and a NASTRAN analysis, such refinements are not required and add nothing new beyond the effects discussed herein.

### 6.1.1 Longitudinal Shear Vibration

We consider the longitudinal shear vibrations of a thick-walled hollow cylinder bonded to a rigid case as shown in Figure 16.

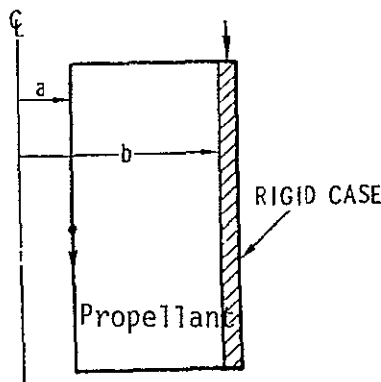


Fig. 16 Longitudinal Shear Vibration

The resonant frequency,  $\omega_n$ , is given by

$$\omega_n = \frac{\Omega_n}{2} \sqrt{\frac{G'(\omega_n)}{\rho b^2} g} \quad (70)$$

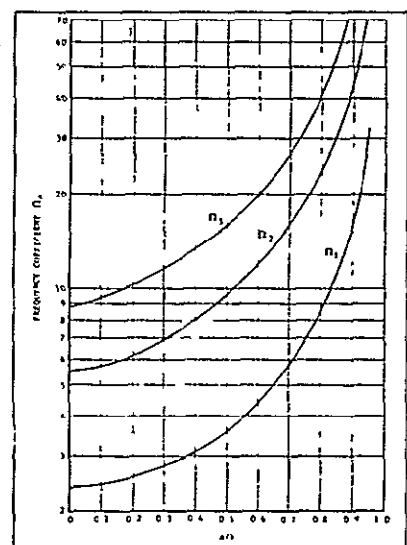


Fig. 17 Circular Frequency Coefficient

REPRODUCIBILITY OF THE  
ORIGINAL PAGE IS POOR

where

$\Omega_n$  = circular frequency coefficient shown in Figure 17 as  
a function of  $a/b$

$\rho$  = density

$g$  = acceleration due to gravity = 386 ips<sup>2</sup>

$G'(\omega_n)$  = real part of complex shear modulus evaluated at  
frequency  $\omega_n$ .

Letting the superscript, or subscript,  $m$  denote model parameters and assuming linear scaling according to

$$a^m = ka$$

$$b^m = kb$$

$$\rho^m = \rho$$

where  $k$  is the scale factor, it follows that

$$\frac{\omega_n^m}{\omega_n} = \frac{1}{K} \sqrt{\frac{G'(\omega_n^m)}{G'(\omega_n)}} \quad (71)$$

Thus, it may be seen that resonant frequencies do not scale directly, but depend also upon the square-root of the ratio of moduli evaluated at the appropriate model and prototype resonant frequencies. It may also be noted that had we attempted to match resonant frequencies in the model and the prototype, it would have been necessary to use a full-scale model, as concluded in the initial IBM study [4].

### 6.1.2 Axial Vibration of A Composite Rod

The previous analysis did not consider end-effects. Finite-length effects are brought in for the geometry shown in Figure 18, which for free-ends has the resonant frequency equation

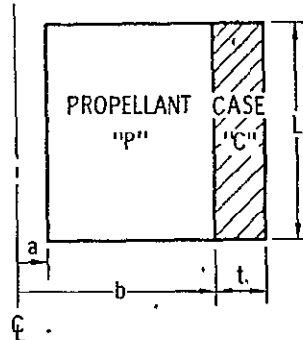
$$\omega_n = \frac{n}{2L} \sqrt{\frac{g A_c E_c + A_p E'_p}{A_c \rho_c + A_p \rho_p}} \quad (72)$$

where,

$$A_c = 2\pi b t$$

$$A_p = \pi(b^2 - a^2)$$

$L$  = grain length.



Again assuming linear scaling

such that

Fig. 18 Axial Vibration Model .

$$a^m = ka$$

$$b^m = kb$$

$$L^m = kL$$

$$t^m = k_1 t$$

$$\rho_p^m = \rho_p$$

$$A_p^m = k^2 A_p$$

$$A_c^m = kk_1 A_c$$

then

$$\frac{\omega_n^m}{\omega_n} = \frac{1}{k} \sqrt{\frac{k_1 A_c E_c^m + k A_p E_p^m}{k_1 A_c \rho_c^m + k A_p \rho_p}} \cdot \frac{A_c \rho_c + A_p \rho_p}{A_c E_c + A_p E_p} \quad (73)$$

Equation (73) can be used to evaluate the scaled frequency response for axial vibration. However, certain simplifications result if one considers constructing the model with an aluminum case compared to the prototype with a steel case. In this case

$$E_c^m \approx \frac{E_c}{3}$$

and

$$\rho_c^m \approx \frac{\rho_c}{3}$$

which gives that  $k_1 = 3k$ , and Equation (73) reduces to

$$\frac{\omega_n^m}{\omega_n} = \frac{1}{k} \sqrt{\frac{A_c E_c + A_p E_p(\omega_n^m)}{A_c E_c + A_p E_p(\omega_n)}} \quad (74)$$

Since  $E_c \gg E_p$ , the sensitivity of the frequency response with  $E_p$  can be investigated by writing Equation (74) in the form

$$\frac{\omega_n^m}{\omega_n} = \frac{1}{k} \sqrt{\frac{1 + \frac{A_p E_p(\omega_n^m)}{A_c E_c}}{1 + \frac{A_p E_p(\omega_n)}{A_c E_c}}} \quad (75)$$

At one extreme, for  $E_p(\omega_n^m) = E_p(\omega_n)$ ,

$$\frac{\omega_n^m}{\omega_n} = \frac{1}{k} \quad (76)$$

which implies simple direct scaling. At the other extreme, suppose  $E_p(\omega_n^m) = 10 E_p(\omega_n)$  which is considerably more stiffening than propellants actually exhibit. Then choosing

$$a = 22.5"$$

$$b = 76.5"$$

$$t = .75"$$

$$E_c = 30 \times 10^6 \text{ psi}$$

as representative of the SRB case properties, and  $E'(\omega_n) = 3000$  as a maximum expected storage modulus at the frequencies of interest, Equation (75) yields

$$\frac{\omega_n^m}{\omega} = \frac{1}{k} (1.021) \quad (77)$$

or approximately a two percent increase over direct linear scaling. It should be noted that the same results are obtained if one uses the same casing material in the model and prototype and the same scaling factor as for other length parameters. However, reducing the case thickness by a factor of 8, for example for the 1/8<sup>th</sup> scale model could lead to buckling instability problems.

As a more direct example, consider the model test results obtained at NASA/Langley [27] and discussed in Section 3.3. For the situation being discussed herein, they found the first resonant axial mode at 149.7 Hz. Using this value for  $\omega_n^m$  in Equation (75) and assuming that the tests were conducted at a temperature near 25°C (70°F) with  $E'(\omega_n^m)$  determined to be 28.8 kN/m<sup>2</sup> (4170 psi) from Figure 13, the corresponding resonant frequency for the SRM is determined to be  $\omega_n = 18.7$  Hz where the following parameters, appropriate to the one-eighth scale lift-off configuration have been used in the calculation:

$$\begin{aligned}
 t_c &= 0.1875 \text{ in} \\
 a &= 6.1875 \text{ in} \\
 b &= 9.5625 \text{ in} \\
 A_c &= 11.376 \text{ in}^2 \\
 A_p &= 167 \text{ in}^2 \\
 E_c &= 10 \times 10^6 \text{ psi} \\
 k &= 0.125
 \end{aligned}$$

Direct scaling also gives  $\omega_n = 18.7$  Hz indicating that the stiffness of the propellant is negligible compared to that of the case.

### 6.1.3 Beam Bending Vibration

Consider the bending of a composite cylindrical beam as shown in Figure 18.

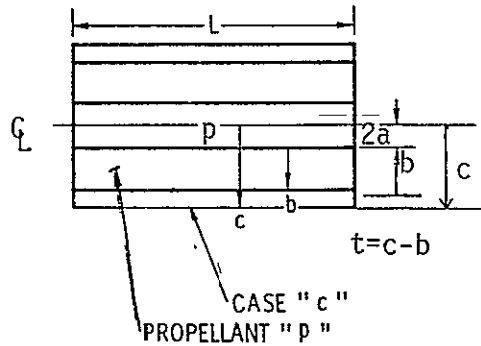


Fig. 18 Beam Bending Model

The resonant frequency,  $\omega_n$ , is given by

$$\omega_n = \frac{A_n}{L^2} \sqrt{\frac{EI}{\rho}} g \quad (78)$$

where  $A_n$  is a parameter which depends on end conditions as shown in Table XI and

$$EI = (EI)_p + (EI)_c$$

$$\rho = \frac{A_c \rho_c + A_p \rho_p}{A_c + A_p}$$

End Cond	n	A <sub>n</sub>		
		1	2	3
CANTILEVER		0.561	3.57	9.82
PINNED-PINNED		1.57	6.29	14.15
FIXED-FIXED		3.57	9.82	19.26
FREE-FREE		3.57	9.82	19.26

Table XI. End Condition Parameter

where

$$I_p = \frac{\pi}{4} (b^4 - a^4)$$

$$I_c = \frac{\pi}{4} (c^4 - b^4) \cong \pi b^3 t$$

$$A_c = \pi(c^2 - b^2) \cong 2\pi b t$$

$$A_p = \pi(b^2 - a^2)$$

Assuming linear scaling again such that

$$a^m = ka$$

$$b^m = kb$$

$$L^m = kL$$

$$t^m = k_1 t$$

$$\rho_p^m = \rho_p$$

It follows that

$$I_p^m = k^4 I_p$$

$$I_c^m = k^3 k_1 I_c$$

$$A_p^m = k^2 A_p$$

$$A_c^m = k k_1 A_c$$

$$\begin{aligned}
 (EI)^m &= E_p'(\omega_n^m) k^4 I_p + k^3 k_1 E_c^m I_c \\
 &= k^3 [k E_p'(\omega_n^m) I_p + k_1 E_c^m I_c] \quad (79)
 \end{aligned}$$

$$\rho^m = \frac{k_1 A_c \rho_c^m + k A_p \rho_p}{k_1 A_c + k A_p} \quad (80)$$

If we again consider the prototype case material to be steel and the model to be aluminum, it again follows that  $k_1 = 3k$ ,  $\rho_c^m = \rho_c/3$ ,  $E_c^m = E_c/3$  and Equations (79) and (80) reduce to

$$(EI)^m = k^4 [E_p'(\omega_n^m) I_p + E_c I_c] \quad (81)$$

and

$$\rho^m = \rho$$

Then,

$$\frac{\omega_n^m}{\omega_n} = \sqrt{\frac{E_p'(\omega_n^m) + E_c I_c}{E_p'(\omega_n) + E_c I_c}} \quad (82)$$

From Equation (82) it is seen that geometric scale factors have no influence on the frequency response under bending, and therefore,  $E_p'(\omega_n^m) = E_p'(\omega_n)$  so that Equation (82) gives  $\omega_n^m = \omega_n$ .

#### 6.1.4 Torsional Vibrations

We consider the torsional oscillations of a thick-walled, finite-length, hollow cylinder bonded to a thin elastic casing. The resonant frequency response is given by

$$\omega_n = \frac{n\pi}{L} \sqrt{\frac{G_c G_p'(\omega_n)}{\rho_p}} \cdot \sqrt{\frac{I_c}{\rho_p I_p + \rho_c I_c}} \quad (83)$$

where  $I_c$  and  $I_p$  are as given before.

Again assuming

$$a^m = ka$$

$$b^m = kb$$

$$L^m = kL$$

$$t^m = k_1 t$$

$$\rho_p^m = \rho_p$$

it follows that

$$\frac{\omega_n^m}{\omega_n} = \frac{1}{k} \sqrt{\frac{G_c^m G_p'(\omega_n^m)}{G_c G_p(\omega_n)}} \sqrt{k^3 k_1} \sqrt{\frac{\rho_p I_p + \rho_c I_c}{k^4 \rho_p I_p + k^3 k_1 \rho_c I_c}} \quad (84)$$

Again, selecting aluminum as the model case material, with  $G_c^m = G_c/3$  and  $k_1 = 3k$ , Equation (84) reduces to

$$\frac{\omega_n^m}{\omega_n} = \frac{1}{k} \sqrt{\frac{G_p'(\omega_n^m)}{G_p(\omega_n)}} \quad (85)$$

### 6.1.5 Lateral Vibration of A Star Point

The geometry for the lateral vibration of a star point is shown in Figure 19. The analysis treats the star-point as a cantilevered beam. The first resonant frequency is given by

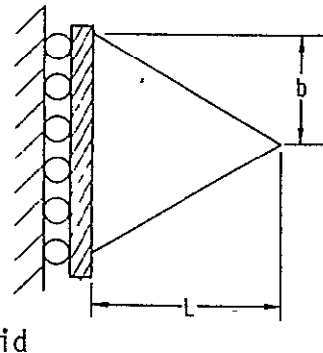
$$\omega_1 = 0.488 \frac{b}{L^2} \sqrt{\frac{E'(\omega_1)g}{\rho}} \quad (86)$$

For linear scaling,

$$b^m = kb$$

$$L^m = kL$$

$$\rho^m = \rho$$



Therefore

Fig. 19. Star Point Model

$$\frac{\omega_1^m}{\omega_1} = \frac{1}{k} \sqrt{\frac{E'(\omega_1^m)}{E'(\omega_1)}} \quad (87)$$

The lateral vibration of a star point gives rise to the only reasonable situation where a temperature rise due to sustained vibration may be of concern. The adiabatic temperature rise rate at the first resonance is given by

$$\frac{d\theta}{dt} = \frac{3}{8} \frac{(2\pi\omega_1)\beta_p}{E'(\omega_1)c} |\sigma_{max}|^2$$

with

$$\sigma_{max} = \rho \frac{L^2}{b} \frac{1}{\delta} n$$

where a stress concentration factor of 2.0 is assumed at the base corner and

$\delta$  = propellant loss tangent

$c$  = propellant specific heat

$n$  = acceleration in g's.

From Equations (88) and (89)

$$\frac{(d\theta/dt)_m}{(d\theta/dt)} = k \sqrt{\frac{E'(\omega_1)}{E'(\omega_m)}} \frac{\beta}{\beta_m} \frac{n_m^2}{n^2} \quad (90)$$

where use has been made of the relation

$$\frac{\sigma_{max}^m}{\sigma_{max}} = k \frac{n^m}{n} \frac{\beta}{\beta^m} \quad (91)$$

#### 6.1.6 Summary of Scaling Laws

Scaling laws have been presented for the primary modes of vibration of the shuttle solid rocket boosters. These equations are obtained from the equivalent elastic formulae by substituting the tensile or shear storage modulus at an assumed frequency of interest for the elastic moduli. In practice it is usually necessary to iterate until the calculated frequencies agree with the assumed frequency. Only two or three iterations are usually required.

It can be seen, that in contrast to elastic structures with frequency independent properties, relations between resonant frequencies of the model

and prototype may in principle, depend also on the respective propellant storage moduli; particularly under shearing type loading conditions. However, as a practical matter as illustrated in the previous section, this stiffness of the propellant is negligible compared to the case stiffness.

As a practical matter, it may also be seen that certain simplifications in the scaling laws result when aluminum is selected for the casing material of the model in place of the steel in the prototype due to nearly constant relations between  $E$ ,  $G$  and  $\rho$  for steel and aluminum. The use of aluminum as the model case material allows a thicker case than would be allowed from direct scaling of steel. For example, for 1/8-scale models such as those tested at NASA, Langley Research Center, the aluminum case thickness could be .375t or approximately 0.28" compared with 0.094" for direct linear scaling. Furthermore, it would seem that a 1/10 or 1/12 scale model would be the practical limit to prevent buckling instability and keep resonant frequencies of the model in an easily measurable range. For example, for a 1/10<sup>th</sup>-scale model with a variation of, say 2, in the storage modulus in the frequency range of interest, the resonant frequency of the model would be about 14 times the resonant frequency of the prototype. This would seem to be a practical limit of readily available dynamic recording equipment.

## 6.2 COUPLING BETWEEN THE SRM PROPELLANT AND MOTOR CASE

It has been mentioned several times previously that in the vibration of solid rocket motors the propellant provides all of the mass and the motor case provides all of the stiffness. This fact was illustrated for the one-eighth scale model tests in the previous sections. With regard to the full-scale SRM, the equations of Section 6.1 can be used to reach the same conclusion by specializing the propellant modulus to zero and comparing the results

obtained to the situation where they are taken to be non-zero. For example, in the case of longitudinal composite-rod vibration, Equation (72) becomes

$$\omega_n = \frac{n}{2L} \sqrt{g \frac{A_c E_c}{A_p \rho_p + A_c \rho_c}} \quad (92)$$

Using the following properties [4]

$$g = 386 \text{ ips}^2$$

$$L = 1200 \text{ in}$$

$$A_c = 222 \text{ in}^2$$

$$E_c = 28 \times 10^6 \text{ psi}$$

$$A_p = 14,358 \text{ in}^2$$

$$\rho_c = 0.28 \text{ lb/in}^3$$

$$\rho_p = 0.064 \text{ lb/in}^3$$

Equation (92) then yields  $\omega_1 = 20.604 \text{ Hz}$ . Using Equation (72) with  $E_b'(\omega) = 2510$  from Figure 13, gives  $\omega_1 = 20.664 \text{ Hz}$ , a negligible difference.

Similar results are obtained for the simple beam bending model in Equation (78).

Thus, coupling between the case and propellant is nonconsequential. The case will provide stiffness and the propellant will provide the mass and damping characteristics.

## VII. CONCLUSIONS AND RECOMMENDATIONS

### 7.1 CONCLUSIONS

Based on an extensive literature survey it has been determined that the only significant variables that need to be included in a dynamic constitutive relation for the shuttle are frequency and temperature. The possible effects of humidity level, static and dynamic, strain level, hydrostatic pressure, aging, epoxy/curative ratio, internal heat generation and damage or permanent memory effects were investigated and found to be inconsequential for the shuttle SRM.

Accordingly, experimental test data on PBAN propellants [2,3] related to the SRM propellant were used to generate the dynamic response model in the form of a simple power law,

$$E'(\omega) = E_0' (w a_T)^n$$

$$E''(\omega) = E_0'' (w a_T)^n$$

$$G'(\omega) = G_0' (w a_T)^n$$

$$G''(\omega) = G_0'' (w a_T)^n$$

\* Temperature is accounted for through the time-temperature shift factor which was taken in the modified power law form

$$a_T = \left( \frac{T_R - T_a}{T - T_a} \right)^m$$

A computer program was written for curve-fitting laboratory dynamic test data to determine the parameters of the constitutive model and for predicting dynamic moduli at any desired frequency and temperature.

Additional studies were conducted to investigate scaling laws and coupling between the SRM propellant and the motor case. Certain advantages are obtained if scale models of the SRM use aluminum for the case material. Even so, it seems that a one-tenth scale model is about the practical limit for scaling.

Due to the fact that the SRM motor case is so much stiffer than the propellant and the propellant mass so much greater than the case, the case provides overall stiffness to the system and the propellant the mass and damping characteristics. This fact results in the resonant frequencies between a scaled SRM and the prototype SRM being approximately equal.

Near propellant burn-out, the vibration characteristics are dominated by the case.

## 7.2 RECOMMENDATIONS

While the results of this study have produced a workable dynamic model which includes all of the pertinent variables affecting the dynamic response of the shuttle SRM propellant, there are still several aspects relating to the dynamic response and structural integrity of the SRM which remain to be investigated.

With regard to the propellant, these include:

- A. Development of correlation between static test and dynamic test properties for the SRM propellant since routine static testing will be conducted to maintain

quality control of production propellant castings  
and not dynamic tests.

- B. Extend SRM propellant dynamic model to a probabilistic model in order to assess the inherent stochastic variations of propellant properties.

With regard to the overall SRM vehicle dynamics, additional work necessary includes:

- A. Development of a simple lumped-mass model of the SRM for input to the external tank dynamic studies.
- B. Evaluation of material property gradients throughout propellant web, due to temperature gradients, on the dynamic response of the SRM.

In addition, there should be continuous and independent assessment of material property test results and structural integrity investigations to insure that the most appropriate material properties are used in structural analyses, to assess any potential degradation of material properties, and to provide assistance should unforeseen structural problems arise related to the SRM propellant grain.

## VIII. REFERENCES

1. Hufferd, W. L., "Solid Propellant Viscoelastic Dynamic Model - Literature Survey," Special Report No. 1, J. E. Fitzgerald & Associates, August 1975,
2. Stoker, J. H. and Mason, D. R., "Space Shuttle SRM Propellant Dynamic Properties," TWR-10543, Thiokol/Wasatch Division, June 1975.
3. Hufferd, W. L., "Measured Properties of Propellant For Solid Rocket Booster of One-Eighth Scale Dynamic Shuttle Model," UTEC CE 75-178, University of Utah, November 1975.
4. Anon, "Dynamic Characterization of Solid Rockets," Report No. 13W-00241, IBM, Federal Systems Division, Electronics System Center, Huntsville, Alabama, September 1973.
5. Hufferd, W. L. and Fitzgerald, J. E., "JANNAF Solid Propellant Structural Integrity Handbook," CPIA Publ. No. 230, The Johns Hopkins University, University of Utah UTEC CE 72-160, September 1972.
6. Fitzgerald, J. E. and Hufferd, W. L., "Handbook for the Engineering Structural Analysis of Solid Propellants," CPIA Publ. No. 214, The Johns Hopkins University, University of Utah UTEC CE 71-089, May 1971.
7. Achenbach, J. D., "Dynamic Response Problems of Solid Propellant Rockets," Feature Article, Solid Rocket Structural Integrity Abstracts, The University of Utah, Vol. 5, No. 1, pp. 1-34, January 1968.
8. Baltrukonis, J. H., "The Dynamics of Solid Propellant Rocket Motors," in Mechanics and Chemistry of Solid Propellants, edited by A. C. Eringen, H. Liebowitz, S. L. Koh, and J. M. Crowley, Pergamon Press, pp. 297-332, 1967 (also published as NASA CR-658, December 1966).
9. Huang, N. C. and Lee, E. H., "Thermomechanical Coupling Behavior of Viscoelastic Rods Subjected to Cyclic Loading," Paper No. 66 WA/APM-29, Winter Meeting of BMB, 1966.
10. Huang, N. C. and Lee, E. H., "Analysis of Coupled Thermoviscoelastic Response of Rods and Slabs Subjected to Cyclic Loading," Bulletin of the 5th ICRPG Mechanical Behavior Working Group Meeting, CPIA Publication No. 119, Vol. I, The Johns Hopkins University, p. 339, October 1966.

11. Schapery, R. A., "Effect of Cyclic Loading on Temperature in Viscoelastic Media with Variable Properties," AIAA Journal, Vol. 2, p. 827, May 1964.
12. Cantey, D. E., "Solid Propellant Structural Integrity Investigations, Dynamic Response and Failure Mechanisms," Final Report No. RPL-TDR 64-32, Vol. I, (LPC Report No. 618-F), Lockheed Propulsion Company, May 1964.
13. Jones, J. W. and Cantey, D. E., "Investigations of Propellant Dynamic Response, Viscoelastic Linearity and Thermorheological Behavior," Bulletin of the Third ICRPG Working Group on Mechanical Behavior Meeting, CPIA publication No. 610, Vol. I, The Johns Hopkins University, pp. 203-244, October 1964.
14. Cantey, D. E., "An Apparatus for Measurement of Dynamic Effects in Rheological Materials," Bulletin of the Fourth ICRPG Working Group on Mechanical Behavior Meeting, CPIA Publication No. 940, Vol. I, The Johns Hopkins University, pp. 255-268, October 1965.
15. Cantey, D. E., "Solid Propellant Structural Integrity Investigations, Dynamic Response and Failure Mechanisms," AFRPL-TR-65-171, (LPC Report No. 667-F), Lockheed Propulsion Company, November 1965.
16. Schapery, R. A. and Cantey, D. E., "Thermomechanical Response Studies of Solid Propellants Subjected to Cyclic and Random Loading," AIAA Journal, Vol. 4, pp. 244-255, 1966.
17. Tormey, J. F. and Britton, S. C., "Effect of Cyclic Loading on Solid Propellant Grain Structures," AIAA Journal, Vol. 1, No. 8, August 1963.
18. Volterra, E. and Zachmanoglou, E. C., Dynamics of Vibrations, C. E. Merrill Books, Inc., Columbus, Ohio, 1965.
19. Göttenberg, W. G., "Experimental Study of the Vibrations of a Circular Cylindrical Shell," J. Acoust. Soc. Am., Vol. 32, p. 1002, 1960.
20. Leadbetter, S. A., Alley, V. A., Herr, R. W., and Gerringer, A. H., "An Experimental and Analytical Investigation of the Natural Frequencies and Mode Shapes of a Four-stage Solid Propellant Rocket Vehicle," NASA TN-0-1354, August 1962.
21. Anderson, J. M., "Adaptation of the Finite-element Stiffness Method to Viscoelastic Steady-State Vibration Solutions," Proceedings of the 5th ICRPG Mechanical Behavior Working Group Meeting, CPIA Publication No. 119, Vol. 1, The Johns Hopkins University, pp. 297-318, October 1966:

22. Baker, W. E. and Daly, J. M., "Dynamic Analysis of Solid Propellant Grains Using the Finite Element Method (Direct Stiffness Method)," Proceedings of the 5th ICRPG Mechanical Behavior Working Group Meeting, CPIA Publication No. 119, Vol. 1, The Johns Hopkins University, pp. 319-338, October 1966.
23. Leeming, H., et al., "Solid Propellant Structural Test Vehicle, Systems Analysis and Cumulative Damage Program," Appendix A, AFRPL-TR-68-130, Lockheed Propulsion Company, October 1968.
24. Ghosh, S. and Wilson, E., "Dynamic Stress Analysis of Axisymmetric Structures Under Arbitrary Loading," Report No. EERG 69-10, University of California, Berkeley, September 1969.
25. Goudreau, G. L., "Evaluation of Discrete Methods for the Linear Dynamic Response of Elastic and Viscoelastic Solids," Report No. 69-15, University of California, Berkeley, June 1970.
26. Anon., "Dynamic Analysis of the Solid Rocket Motor for the Space Shuttle," IBM Report No. 75W-00144, IBM Federal Systems Division, Huntsville, Alabama, July 1975.
27. Anon., "January/February 1975 Progress Report on Langley Space Shuttle Dynamics Model Programs," NASA Langley Research Center, Hampton, Virginia, March 1975.
28. Levy, A., Zalesak, J., Bernstein, M. and Mason, P. W., "Development of Technology for Modeling of 1/8-Scale Dynamic Model of the Shuttle Solid Rocket Booster (SRB)," NASA-CR-132492, Grumman Aerospace Corporation, July 1974.
29. CPIA Publication No. 21, "JANNAF Solid Propellant Mechanical Behavior Manual," The Johns Hopkins University, original publication, November 1963, subject to continuous revision.
30. Williams, M. L., Blatz, P. J. and Schapery, R. A., "Fundamental Studies Relating to Systems Analysis of Solid Propellants," GALCIT SM 61-5, Guggenheim Aeronautical Laboratory, California Institute of Technology, February 1961.
31. Fitzgerald, J. E., "Analysis and Design of Solid Propellant Grains," in Mechanics and Chemistry of Solid Propellants, edited by A. C. Eringen, H. Liebowitz, S. L. Koh, and J. M. Crowley, Pergamon Press, pp. 19-46, 1967.
32. Schapery, R. A., "Recent Developments in the Nonlinear Viscoelastic Characterization of Solid Propellants," Solid Rocket Structural Integrity Abstracts, The University of Utah, Vol. 8, No. 2, pp. 1-66, April 1967.

33. Hufford, W. L. and Fitzgerald, J. E., "Permanent Memory Effects in Solid Propellants," Proceedings of the 1974 Combined JANNAF OSWG and S&MBWG, CPIA Publication No. 253, The Johns Hopkins University, pp. 345-370, July 1974.
34. Rivlin, R. S., "Large Elastic Deformations of Isotropic Materials. I. Fundamental Concepts," Phil. Trans. A., Vol. 240, p. 459, 1948.
35. Beyer, R. B., "Nonlinear Mechanical Behavior of Solid Propellants," AIAA Paper No. 65-159, AIAA 6th Solid Propellant Rocket Conference, Washington, D. C., February 1-3, 1965.
36. Kelley, F. N., "Solid Propellant Mechanical Properties Testing, Failure Criteria and Aging," Advances in Chemistry Series, Number 88, "Propellants, Manufacture, Hazards and Testing," American Chemical Society, pp. 188-243, 1969.
37. Layton, L. H., Bennett, S. J. and Stoker, J. H., "Chemical Structural Aging Effects," Proceedings of the JANNAF Combined OSWG and S&MBWG Annual Meeting, CPIA Publication No. 253, The Johns Hopkins University, pp. 99-116, July 1974.
38. Layton, L. H. and Bennett, S. J., "Applications of Aging Models to Predictions of Propellant Long Term Aging Characteristics," Proceedings of the Combined Annual OSWG and S&MBWG Meeting, CPIA Publication No. 264, The Johns Hopkins University, pp. 1-18, May 1975.

APPENDIX A

LITERATURE SURVEY

This literature search has been conducted with the objectives of identifying (1) the pertinent variables which influence the dynamic viscoelastic response of solid propellants, (2) appropriate representations for dynamic response of solid propellants, and (3) appropriate analysis tools and techniques for analysis of the dynamic response of Solid Propellant Rocket Motors.

For convenience the literature has been divided into four categories:

1. Dynamic Viscoelastic Characterization
2. Dynamic Analysis
3. Representation of Dynamic Properties and Theoretical Developments
4. Thermomechanical Coupling

Abstracts are numbered sequentially within each section and an author index is provided for easy cross-referencing.

No attempt has been made to provide a comprehensive literature search of all aspects of the dynamics or vibration of structures. Rather, attention has been deliberately specialized to the dynamics of solid propellant rocket motors and dynamic viscoelasticity as applied to solid propellants only. Thus, references to literature of a more general nature are kept to a minimum.

The specific format for presentation of the literature survey was chosen to allow easy updating of the reference material from time to time in the future.

## I. DYNAMIC VISCOELASTIC CHARACTERIZATION

- I-001 "Dynamic Mechanical Properties of Solid Propellants," Quarterly Technical Summary Report, for period 1 April 1962 - 30 June 1962, Atlantic Research Corporation, Alexandria, Virginia, (ARPA Order No 22-61, Project Code No 009-06-001, Contract No N0w 61-1054-C), July 30, 1962.
- Measurements of the two components of dynamic shear compliance of the following propellants are reported PBAN propellant, TP-H-1001, at 64.6°C and at room temperature, PBAA propellant, "Propellant D", at 35 1°C, and polyurethane propellant, AEBA-10, at room temperature
- Preliminary measurements indicate that the amount of compression applied to the sample to keep it from slipping in the sample holder may have a significant effect on the compliance
- A second thirty-five pound trial batch of IP-H-1001 was mixed. Delivery of the high-pressure enclosure has been delayed because the first casting of the shell did not meet specifications regarding magnetic properties
- I-002 "Dynamic Mechanical Properties of Solid Propellants," Quarterly Technical Summary Report, for period 1 July 1962 - 30 September 1962, Atlantic Research Corporation, Alexandria, Virginia, (ARPA Order No 22-61, Project Code No 009-06-001, Contract No N0w 61-1054-C), October 30, 1962
- Measurements of the dynamic shear compliance of a polyurethane propellant, AEBA-10, are reported for approximate intervals of ten degrees centigrade from -15°C to +65°C. The data appear inconsistent, particularly above room temperature, and additional investigation is required.
- I-003 "Dynamic Mechanical Properties of Solid Propellants. Quarterly Technical Summary Report, 1 October 1962 - 31 December 1962." Atlantic Research Corporation, Alexandria, Virginia, ARPA Order No 22-61, Contract N0w 61-1054-C, December 31, 1962
- Measurements of the dynamic shear compliance of a polyurethane propellant, AEBA-10, are reported for temperature intervals of approximately ten degrees centigrade from +25°C to +65°C. The humidity environment was more closely controlled and monitored during these measurements to determine if the moisture content of the samples was a contributing factor in some of the inconsistencies previously reported
- I-004 "Dynamic Mechanical Properties of Solid Propellants," Quarterly Technical Summary Report, for period 1 January 1963 - 31 March 1963, Atlantic Research Corporation, Alexandria, Virginia, (ARPA Order No. 22-61, Project Code No 009-06-001, Contract No N0w 61-1054-C), May 10, 1963.
- Measurements of the two components of the complex dynamic shear compliance of a polyurethane propellant, AEBA-10, are reported for approximate temperature intervals of ten degrees centigrade from -15 to +65. These measurements represent a duplication of some of the previous work using new samples of the same material previously measured. The objective here was to resolve some of the inconsistencies previously reported
- I-005 "Dynamic Mechanical Properties of Solid Propellants - Final Summary Report 32 June 1961 - 31 July 1963" Atlantic Research Corporation, Alexandria, Virginia, January 15, 1964. This report summarizes the work performed under Contract No N0w 61-1054-C concerned with the measurement of certain dynamic mechanical properties of solid propellants
- The objective of this program was to define the dynamic shear properties of selected propellants at frequencies between 25 cps and 2, 000 cps at temperature of -50°C to 75°C and at pressures up to 1, 000 psig
- Measurements are conducted with a Fitzgerald Apparatus which applies a sinusoidal shear stress and shear strain to a coin-size sample of propellant. Continuous smooth curves depicting compliance of propellants having a hydrocarbon binder and a polyurethane binder as a function of frequency and temperature have been constructed
- Cure time of the hydrocarbon-type propellant was found to influence compliance measurements. Propellant cured under representative conditions of actual grains continued to change with time, particularly as the temperature was raised through a sequence of measurements. Propellant cured for longer lengths of time was stabilized, as evidenced by the approximate duplication of properties at ambient temperature at the beginning and end of a test series. Small changes in moisture content were shown to effect the compliance. Increasing static compressive strain normal to the shear plane appeared to decrease compliance markedly. Attempts to apply the method of reduced variables to these data have not been successful
- I-006 "Dynamic Mechanical Properties of Solid Propellants - Quarterly Technical Summary Report No. 2, 1 March 1964 to 31 May 1964", Atlantic Research Corporation, Alexandria, Virginia, July 1964
- The calibration of the Fitzgerald Apparatus at ambient and elevated temperatures was completed. Dynamic shear modulus measurements were made on a new batch of the polyurethane propellant in order to determine the degree of similarity between this batch and the previous batch on which the basic data were obtained. Data have been obtained showing the effects of hydrostatic pressure and accelerated aging on dynamic shear modulus of a polyurethane propellant. Samples of two propellants have been placed in constant humidity atmospheres for conditioning prior to studying the effect of absorbed moisture on the dynamic shear modulus.

THE  
ORIGINAL PAGE IS POOR

I-007 Robinson, C. N. "Dynamic Mechanical Properties of Solid Propellants - Quarterly Technical Summary Report No. 3, 1 June 1964 - 31 August 1964." Atlantic Research Corporation, Alexandria, Virginia, October 1964.

Problems in the Fitzgerald Apparatus temperature monitoring system have been eliminated and the earlier data corrected to reflect the effect of these changes. Dynamic shear modulus measurements were made on a new batch of the TPH-1001 PBAN propellant. Comparisons of these data with results from an earlier batch indicate a significant difference between the mixes. Dynamic shear modulus data have also been obtained showing the effects of accelerated aging on the TPH-1001 propellant and the effect of moisture on the AEBA-10 propellant.

I-008 Robinson, C. N. "Dynamic Mechanical Properties of Solid Propellants", TR-PL-6313-01, Annual Technical Summary Report for period of 27 November 1963 to 26 November 1964, Atlantic Research Corporation, Alexandria, Virginia, April 1965.

The objective of this program is the continued measurement of the complex dynamic shear properties of a PBAN and a polyurethane propellant system as a function of frequency. The Fitzgerald Apparatus is the primary experimental tool for this study. Measurements have been made indicating the effects of temperature, pressure, aging and humidity on the dynamic properties of these propellants.

Data have been obtained showing the effect of temperature on the dynamic properties of new batches of both the PBAN and PU propellants. These results appear to be consistent with the prediction of the WLF Time-Temperature superposition principle. However, while the data for the polyurethane propellant were in excellent agreement with earlier results, the data for the PBAN propellant were significantly different from previously obtained results. The reason for this discrepancy is not apparent.

Data obtained on the polyurethane propellant at pressures up to 1000 psig have indicated no effect of hydrostatic pressure on dynamic shear properties. This result is consistent with theoretical considerations.

The results of short-term accelerated aging at 65°C indicate only minor changes in dynamic shear properties of both propellants. These results are in general agreement with data published by others concerning the aging characteristics of these propellants.

Experimental data have also been obtained showing the effect of moisture content on the dynamic properties of both propellant systems. According to these results, the polyurethane propellant showed the more pronounced effects of moisture. The effects of moisture on the PBAN propellant were not as pronounced and less sharply defined. These results are also in good agreement with data reported elsewhere for the propellant system.

I-009

Robinson, C. N., Graham, P. H. "Dynamic Mechanical Properties of Solid Propellants," Quarterly Technical Summary Report, 1 June to 31 August, 1965, Atlantic Research Corporation, Alexandria, Virginia, 1965.

The dynamic mechanical properties of TPH-1001 PBAN binder have been determined over a range of frequency and temperature in the Fitzgerald apparatus. A comparison between interconverted tensile data reported previously and current measurements reduced to a common reference temperature shows substantial agreement between prediction and experiment.

A CTPB propellant and binder system has been selected for continuation studies and the embedded gage investigation. This propellant has been characterized in the uniaxial tension test over a broad range of temperatures and straining rates and the binder has been tested in the Fitzgerald apparatus. The results are presented in tabular form and profile plots.

The marked similarity in behavior for both the CTPB and PBAN formulations is discussed and difficulties inherent in the definition of a reference temperature are described.

A composite double-base formulation, Arcocel 322, has been characterized in the Fitzgerald apparatus. The experimental data superposes smoothly with WLF  $\alpha_T$  values computed for a  $T_s$  of 299°K.

I-010

Robinson, C.N., Graham, P.H. "Dynamic Mechanical Properties of Solid Propellants," TR-PL-9294, Final Technical Summary Report 27 November 1963 to 26 November 1965, Atlantic Research Corp., Alexandria, Virginia, 1967.

The objective of this program has been the measurement of the complex dynamics shear properties of several propellants and propellant binders. Several attempts have been made to predict dynamic shear properties based on the interconversion of uniaxial tensile data using Atlantic Research Corporation developed computer programs. The uniaxial tensile data were obtained over a broad range of strain rates and temperatures. Dynamic data and uniaxial tensile data are presented to show the effect of moisture and accelerated aging on these properties.

I-011

Tschoegl, N. W., Smith, J. R.; Smith, T. L. "Viscoelastic Properties of Solid Propellants and Propellant Binders" Quarterly Technical Summary Report No. 2, Stanford Research Institute, Menlo Park, California, February 15, 1964.

Improvements have been made in the design and operation of the low frequency dynamic shear tester. Special techniques have been evaluated for determining precisely the phase angle between the applied displacement and the resultant force. In addition, theoretical work was directed toward determining the manner in which the specimen shape-factor depends on the laterally applied compressive force.

A complete description is given of a dynamic bulk compressibility apparatus and of the calibration and evaluating work done to date.

A-5

INTRODUCIBILITY OF THE  
ORIGINAL PAGE IS POOR

I-012

Tschoegl, N. W., Smith, J. R., Smith, T. L. "Viscoelastic Properties of Solid Propellants and Propellant Binders", Quarterly Technical Summary Report (Report No. 2 for Contract Period)(Report No. 14 of Series), Stanford Research Institute, Menlo Park, California, for period December 16, 1964 to March 15, 1965

Studies supplementary to the determination of the dynamic shear modulus are reported. The effect of specimen geometry and the magnitude of shear strain on the dynamic modulus of polyurethane propellant AEBA-10 was studied. A method was worked out to correct measurements to the same level of shear strain to allow a direct comparison under all experimental conditions. An evaluation of the differential Lissajous method for determining small phase angles has shown that, at frequencies as low as 0.05 cps, a phase angle of the order of a few thousandths of a radian can be measured with good precision. An evaluation was made of the static compressibility apparatus by determining the compressibility of dioctylsebacate at 25 and 50°C and at pressures up to 2000 psi. The results are in excellent agreement with reported data. Factors that influence the reproducibility of data obtained with the dynamic compressibility apparatus have been investigated.

I-013

Tschoegl, N. W., Smith, J. R.: "Viscoelastic Properties of Solid Propellants and Propellant Binders," SRI Project FRU-5174, Quarterly Technical Summary Report (Report No. 3 for Contract Period, Report No. 15 for Series) for period March 16 to June 15, 1965, Stanford Research Institute, Menlo Park, California, (Contract No. N0W 65-0061-d), 1965.

Data were obtained on the dependence of the shear moduli of a polyurethane propellant on shear strain at different frequencies and temperatures, and on the time of storage at low temperatures. The propellant was then tested in the dynamic shear tester over extended ranges of temperature and frequency. The data are presented in graphical form

I-014

Smith, Thor L., Smith, James R., Tschoegl, Nicholas W. "Viscoelastic Properties of Solid Propellants and Propellant Binders," Final Technical Summary Report, 1 July 1961 to 15 April 1966, Stanford Research Institute, Menlo Park, California, April 15, 1966.

This final report presents the results of a four-year research program on the mechanical properties of solid propellants and unfilled elastomers. Studies were made of (1) dynamic shear properties; (2) dependence of specific volume on pressure, temperature, and time; and (3) tensile properties at constant strain rates

The storage and loss moduli of a polyurethane propellant were determined at frequencies between 0.06 and 25 cps and at temperatures between -40 and 60°C, data at different

temperatures could be precisely superposed to yield composite curves. In addition, the influence of specimen geometry, lateral compression, and shear strain on the dynamic moduli of the propellant and of an unfilled styrene-butadiene rubber was investigated.

The static bulk compressibility of polyurethane propellants containing 70% and 80% solids was determined at temperatures between about -43 to 45°C and at pressures up to about 1500 psi, and the dynamic compressibility of the 80% solids propellant was studied between -30 and 45°C at static pressures from 300 to 2000 psi. The storage compressibility at frequencies between 0.5 and 100 cps was sensibly independent of both frequency and pressure, its temperature dependence was essentially the same as that for the static compressibility. The loss compressibility was estimated to be quite small. The influence of moisture on the glass temperature,  $T_g$ , of a polyurethane propellant was briefly investigated as well as the effect of time and pressure on the  $T_g$  of an unfilled polyurethane polymer.

Stress-strain data obtained on a polyurethane propellant in uniaxial tension at various extension rates and temperatures were analyzed to obtain the constant strain rate modulus. From these data, the storage and loss dynamic moduli were computed.

I-015

Cantey, D. "Solid Propellant Structural Integrity Investigations. Dynamic Response and Failure Mechanisms." RTD-TDR-63-113, Lockheed Propulsion Company, Redlands, California, December 6, 1963.

The program effort is divided into two phases. Phase I covers dynamic response in solid propellants. Effort during the reporting period was directed toward theoretical resolution of experimental data obtained during the first three quarters of the program and on systematic collection of additional propellant physical property data. Transient and dynamic viscoelastic behavior of additional propellant formulations was determined, equivalence of transient and periodic propellant characterization was investigated, and dielectric investigation of binder polymers and curing effect was carried out.

I-016

Fitzgerald, J. E. "Solid Propellant Structural Integrity Investigations. Dynamic Response and Failure Mechanisms" Research Status Report No. 12 for 21 October-20 November 1963, Lockheed Propulsion Company, Redlands, California, December 12, 1963.

Measurement of sinusoidal viscoelastic moduli has been completed for Polycarburene-R propellant at temperatures from -45°F to +138°F. Good agreement has been obtained between dynamic moduli calculated from shear stress relaxation and directly measured shear dynamic moduli for the same sample. Stress relaxation characterization has been completed for the Polycarburene-R cross-link density and recast oxidizer particle size formulation variations. Significant variations in relaxation response are observed for the cross-link density variations.

- I-017 Fitzgerald, J. E. "Solid Propellant Structural Integrity Investigations. Dynamic Response and Failure Mechanisms" Research Contract Status Report No 11 for 21 November-20 December 1963, Lockheed Propulsion Company, Redlands, California, January 8, 1964.  
Progress is reported in the investigation of dynamic response behavior of composite propellants, and in the study of the mechanism of propellant rupture. Also reported is progress in the general areas of finite deformation study, vibration mode analysis for case-bonded viscoelastic grains under isothermal and nonisothermal steady state thermal field conditions, and dynamic heat generation in viscoelastic materials
- I-018 Canley, D. "Solid Propellant Structural Integrity Investigations Dynamic Response and Failure Mechanisms." Final Technical Documentary Report No RPL-TDR 64-32, Vol 1, Lockheed Propulsion Company, Redlands, California, April 17, 1964, LPC Report 618F  
This document presents the results and conclusions of a theoretical and experimental research program to correlate mechanical response and failure in solid propellants with basic material structural characteristics. The program was concentrated on the study of propellant dynamic physical properties and structural failure phenomena. Major emphasis in the program, directed at the complementary problems of propellant viscoelastic properties and failure mechanisms together with examination of the effects of propellant binder and filler physical characteristics on these general aspects of its behavior, is reported upon. Measurements of viscoelastic properties of various propellants using transient techniques are demonstrated and results are presented. Investigation of propellant viscoelastic properties in dynamic shear is also discussed.
- I-019 Canley, D. E. "Solid Propellant Structural Integrity Investigations Dynamic Response and Failure Mechanisms" LPC Report No 667-Q-1, Technical Documentary Report No AFRPL-TR-64-148, Volume 1, Lockheed Propulsion Company, Redlands, California,  
The results of an investigation of viscoelastic and failure properties of highly filled PBAA and PBAN propellants as a function of solids loading are reported. The temperature rise in shear specimens under constant large amplitude dynamic strains was investigated and compared with analytical predictions. The theory of thermomechanical effects is extended to include inertia loading and stationary random loading conditions. Initial results obtained from piezoelectrical test devices for measuring dynamic bulk and shear properties of propellants are reported.
- I-020 Canley, D. E. "Solid Propellant Structural Integrity Investigations Dynamic Response and Failure Mechanisms." LPC Report No 667-Q-2, Technical Documentary Report No AFRPL-TR-65-20, Lockheed Propulsion Company, Redlands, California, 15 January 1965.  
The results of an investigation of viscoelastic and failure properties of highly filled PBAA and PBAN propellants as a function of solids loading are reported. Failure surface study results are reported, and the results of a limited study of the relationship between crack propagation velocity and propellant physical characteristics are discussed. Propellant dynamic shear and bulk properties were investigated with small deformation piezoelectric devices. An experimental investigation of propellant thermomechanical response to sustained cyclic inertial loading was completed, and the results in agreement with theory are presented. Also discussed are experimental investigations of transient thermoviscoelastic response of propellant under constant cyclic strain amplitude and inertial loading
- I-021 Ferry, J. D., Fitzgerald, E. R., Grandine, L. D., Williams, M. L. "Temperature Dependence of Dynamic Properties of Elastomers, Relaxation Distributions." Industrial and Engineering Chemistry, Vol 44, No 4, April 1952, pp. 703-706.  
By the use of reduced variables, the temperature dependence and frequency dependence of dynamic mechanical properties of rubberlike materials can be interrelated without any arbitrary assumptions about the functional form of either. The definitions of the reduced variables are based on some simple assumptions regarding the nature of relaxation processes. The real part of the reduced dynamic rigidity, plotted against the reduced frequency, gives a single composite curve for data over wide ranges of frequency and temperature, this is true also for the imaginary part of the rigidity or the dynamic viscosity. The real and imaginary parts of the rigidity, although independent measurements, are interrelated through the distribution function of relaxation times, and this relation provides a check on experimental results. First and second approximation methods of calculating the distribution function from dynamic data are given. The use of the distribution function to predict various types of time-dependent mechanical behavior is illustrated.
- I-022 Lee, E. H., Bland, D. R. "The Analysis of Dynamic Tests of Visco-Elastic Materials" Technical Report No 7, Brown University, PA-TR/7, June 1954, Contract Nord 11496  
In this report methods of analysis of dynamic tests of viscoelastic materials are examined. It is shown that it is important to develop the analysis on the basis of a general stress-strain relation, since the particular form of the relation for the material under test is not known in advance,

and any arbitrary assumption about it may lead to contradictions. Such a general method of analysis is discussed for a simple longitudinal stress test, and for the vibrating reed test. References to the published literature indicate that such contradictions appear in currently accepted analyses, and their influence is detailed. In seeking a visco-elastic model of springs and dashpots to represent the behaviour of the material, the method presented separates the analysis of the test results from the determination of the appropriate model.

- I-023 Bland, D. R.; Lee, E. H. "Calculation of the Complex Modulus of Linear Viscoelastic Materials from Vibrating Reed Measurements." *Journal of Applied Physics*, Vol 26, No. 12, December 1955, pp 1497-1503.

Two methods of determining the variation of real and complex modulus with frequency from vibrating reed test results are detailed. One is based on measurements of the relative amplitude and phase lag of the motion of the free and driven ends of the reed, the other on amplitude resonance measurements only. The analysis is based on a general linear viscoelastic law, and takes into account the influence of the frequency dependent moduli of the material on the frequency and amplitude of the resonance peaks. This influence has not been correctly accounted for in previous analyses which have included the assumption that the material behaves according to a particular, simple viscoelastic law, which will in general not be borne out by the final results.

The method is applied to a series of tests. For the material and frequency range used the imaginary part of the complex modulus was small compared with the real part, and the influence mentioned in the foregoing was small. A simpler method of analysis might thus be justified, but in other cases it will be necessary to carry out the complete analysis in order to obtain a satisfactory interpretation of test results.

- I-024 Benbow, J. J. "The Determination of Dynamic Moduli and Internal Friction of High Polymers from Creep Measurements." *Proc Phys. Soc B*, Vol 69, 1956, pp. 885-892

An account is given of the use of Fourier analysis to transform creep measurements to dynamic quantities with specific reference to some measurements made on polythene. The method is based on a technique described by Roesler, but additional theory is given which eliminates the necessity of determining the retardation spectrum explicitly. Using the derived dynamic quantities as a standard it is shown that more approximate methods provide sufficiently accurate transformations for many practical purposes if the retardation spectrum of the material is very flat.

- I-025 Jones, J W "Viscoelastic Characterization of Solid Propellants by Transient Test Techniques." *Journal of Applied Polymer Science*, Vol 6, 1962, p 331.

The experimental determination of solid propellant viscoelastic physical characteristics using specialized test procedures is described. Experimental and analytical difficulties connected with propellant physical characterization in the millisecond time domain are discussed. Viscoelastic property specification by linear differential operator techniques is described.

- I-026 Layton, L. H., Sheppard, G. A., Bennett, S. J "Determination of the Dynamic Shear Modulus of a Composite Solid Propellant." *Review of Scientific Instruments*, Vol. 34, December 1963, pp. 1333-1340.

Theoretical analysis of the principles of high- and low-frequency measurement of the dynamic behavior of viscoelastic materials, and application of these principles to determine the shear modulus of a composite solid propellant, in the frequency range from 0.10 to 1,000 cps. The test specimen consists of two concentric metal rings carried by a flat plate of propellant. The high frequency data (70-1000 cps) are obtained by applying a known sinusoidal motion to the outer ring and measuring the response at the center. The transducer and center mounting are used as an inertial mass and are included in the analysis of the viscoelastic plate. The low frequency data (0.10-45 cps) are obtained by applying a known sinusoidal motion to the center of the specimen with the outer edge in a clamped position. The applied force and displacement are both measured at the center of the specimen. Typical results for the complex dynamic shear modulus with its real and imaginary parts, as well as the loss tangent, are given for a composite solid propellant. These data indicate a precision of approximately  $\pm 10\%$ .

- I-027 Knauss, W G "On the Mechanical Properties of an H-C Rubber." GALCIT SM 63-1, California Institute of Technology, Pasadena, California, September 1963 Presented at ICRPG Meeting, Hill AFB, Utah, November 1963

The material properties of H-C binder including dynamic shear compliance, relaxation modulus, creep compliance, ultimate stress and ultimate strain are reported. Further useful information in the form of Modified Power Law and Prony Series curve fits are included as well as a master curve of reduced stress versus strain.

All tests are performed using standard procedures, however some inconsistency in material properties has been found. It was further determined that the time-temperature shift principle is not directly applicable in its simplest form, however, upon postulating two molecular mechanisms responsible for gross deformations it is found that each one can be associated with a different characteristic glass transition temperature such that, e.g. the dynamic compliance  $J(w)$  is the sum of two compliances  $J_\alpha$  and  $J_\gamma$

$$J(w, t) = J_\alpha (w, T_{glass}^\alpha) + J_\gamma (w, T_{glass}^\gamma)$$

which individually follow the time temperature superposition principle.

- I-028 Smith, T. L. "Mechanical Response of a Polyurethane Propellant to Constant Extension Rates and to Sinusoidally Varying Strains" Bulletin of the 2nd Meeting ICRPG Working Group on Mechanical Behavior, November 1963, pp. 375-394.

Tensile stress-strain curves were determined on a polyurethane propellant at a large number of strain rates at nine temperatures between -50 and  $70^{\circ}\text{C}$ . At each temperature, the data at strains below some critical value could be represented quite precisely by the constant strain rate modulus defined as  $F(t) = \lambda \sigma / (\lambda - 1)$ , where  $\sigma$  is the nominal stress and  $\lambda$  is the extension ratio. Data obtained at different temperatures were superposed to give a master plot of  $\log F(t) 298/T$  vs.  $\log t/a_T$ . Values of  $\log a_T$  obtained by superposing the curves were in agreement with the WLF equation based on the so-called universal constants, except for  $\log a_T$  values resulting from shifting -20 and  $-30^{\circ}\text{C}$  data. At -20 and  $-30^{\circ}\text{C}$ , values of  $F(t)$  were unexpectedly large, apparently because propellant embrittlement occurred during the test periods. The master curve could be represented precisely by the equation  $\log [F(t) - 350] = -0.26 \log t + 2.83$  over the range  $-8 < \log t < 3$ , where  $F(t)$  is in psi and  $t$  is in minutes. By the use of interconversion equations which are essentially exact, calculations were made of the storage and loss shear moduli,  $G'(\omega)$  and  $G''(\omega)$  and of the storage and loss compliances,  $J'(\omega)$  and  $J''(\omega)$ . A comparison of the calculated dynamic data with limited data obtained by direct experimental methods showed that the computed values are at least as reliable as the experimental ones.

- I-029 Layton, L. H. "Dynamic Testing of Solid Propellants," Bulletin of the 2nd Meeting ICRPG Working Group on Mechanical Behavior, November 1963, pp. 95-96

In the study of viscoelastic materials, interest is centered mainly on effects which depend upon time rather than upon stress. The great majority of such studies are made with

testing procedures which assume an approximate viscoelastic behavior. This type of behavior is in evidence when the stress-strain ratio, which is a function of time, is independent of stress. This restricts studies on most materials to low stress measurements. The basic aim of mechanical properties investigations pertaining to viscoelastic materials is the measurement of stress-strain ratios resulting from some kind of time-dependent loading pattern. Equations are available for translating results of one type of experiment into those of another.

The dynamic behavior of viscoelastic materials can be characterized by a complex modulus  $E^*(\omega) = E'(\omega) + iE''(\omega)$  which is defined as the stress developed under a sinusoidally varying strain. The stress then becomes a function of the strain and the complex modulus so that  $\sigma = E^*(\omega)\epsilon$  and the strain become  $\epsilon = \epsilon_0 e^{i\omega t}$ .

In order to obtain quantitative information pertaining to the mechanical properties of viscoelastic materials, it is necessary to devise suitable test apparatus to perform laboratory tests. If the test material in question is linearly viscoelastic, one test procedure will suffice. Technical simplicity and convenience may decide the performance of one or the other test method. Real materials are not always linearly viscoelastic, resulting in discrepancies when the mathematical transformation is attempted. For this reason many mechanical test methods have been used and, in the past few years, several dynamic test methods have been devised for use with solid propellant.

One of the first dynamic testers which was adapted to solid propellant was described by Fitzgerald and Ferry in 1953. This apparatus was described for measurements of complex shear modulus or compliance on samples ranging from soft gels to stiff solids at -50 to  $+150^{\circ}\text{C}$  over the frequency range 25 to 5000 cps. This apparatus was used in several laboratories in the past few years to measure the dynamic shear compliance of solid propellants. A second apparatus was described by Baltrukonis, Gottenberg and Schreiner in 1962. This covers approximately the same frequency range as the Fitzgerald apparatus, but is experimentally simpler to operate. The analysis and data reduction are complex and most conveniently performed with an electronic digital computer. The temperature range is somewhat limited due to the necessity for bonding the specimen to a metal ring which restrains its geometry and introduces thermal stresses.

It was found by Layton, Sheppard, and Bennett that the data became very difficult to reduce at low frequencies, although with judicious and persistent treatment, it was sometimes possible to get a value. A low frequency tester was devised using the same disk specimen which extended the frequency range down to 0.1 cps. In addition, the data reduction becomes much simpler, making hand computations possible because certain inertial terms may be neglected.

All of these methods suffer from the necessary assumption of a value for Poisson's ratio. In order to avoid this a dynamic torsion tester was developed by Gottenberg and Christensen. The complete frequency range from  $2 \times 10^{-4}$  to  $10^3$  cps is covered by two testers. One is mechanically driven, the other is electrodynamically driven. The same specimen is used in each of the testers.

- I-030 Glauz, R. D. "Transient Analysis of a Vibrating Reed." *Journal of Polymer Science, Part A*, Vol. 1, 1963, pp. 1693-1700.
- A new simplified test for obtaining the physical properties of a viscoelastic material is described and analyzed. A reed, clamped at one end, is displaced at the free end and the damped oscillations measured. From measurements of the damping factor and frequency the complex modulus is computed. Tables of eigenvalues have been calculated for various masses and moments of inertia attached to the free end of the reed. Many experimental tests have shown the simplicity and usefulness of the method.
- I-031 Markovitz, H. "Free Vibration Experiment in the Theory of Linear Viscoelasticity." *Journal of Applied Physics*, Vol. 34, No. 1, January 1963, p. 21.
- An idealized free-vibration experiment is analyzed on the basis of the theory of infinitesimal linear viscoelasticity. The resulting motion can be expressed as a sum of terms, of which some are damped sinusoidal waves while others are negative exponentials in time. For some three parameter models of viscoelastic behavior, the results of this theory are compared with those of the usual treatment which leads to a simple damped sinusoidal wave.
- I-032 Lee, Tung-Ming "Method of Determining Dynamic Properties of Viscoelastic Solids Employing Forced Vibration." *Journal of Applied Physics*, Vol. 34, No. 5, May 1963, p. 1524.
- Both the longitudinal vibration method and the torsional vibration method are used for evaluating dynamic properties of viscoelastic solids. The criterion of using  $R_{max}$  (the maximum amplitude ratio of the free end of a sample to the end attached to a driver) and  $f_{ro}$  (the corresponding vibration frequency) is introduced. The complex modulus is used to describe the stress-strain relationship for a viscoelastic solid. Simple expressions relating dynamic properties to  $R_{max}$  and  $f_{ro}$  are obtained. When  $R_{max}$  and  $f_{ro}$  are measured from experiment, one may readily determine the dynamic properties of the sample.
- I-033 Baltruonis, J. H., Blomquist, D. S., Magrab, E. B.: "Measurement of the Complex Shear Modulus of a Linearly Viscoelastic Material". Technical Report No. 5, The Catholic University of America, Washington, D.C. 20017, May 1964.
- A detailed description is presented of an experimental system intended to measure the complex shear modulus of homogeneous, isotropic and linearly viscoelastic materials. The test is based on the torsional oscillations of a circular cylindrical sample of finite length. The test and data reduction procedures are described. A Fortran listing of the data reduction computer program is included in the Appendix. Actual measurements are presented on a sample of filled polyvinyl-chloride. Master curves of the shear storage modulus and shear loss tangent are plotted by making use of the time-temperature shifting principle.
- I-034 Blatz, P. J., George, N., Ko, W. L., Murthy, A., Yoh, J. "Physicomechanical Behavior of Rubberlike Materials", MA1SCI-PS-61-8, California Institute of Technology, Pasadena, California, (AD 608 229), September 1964.
- For the controlled evaluation of several gum-rubber vulcanizates in simple tension as a function of time, temperature, and strain rate, the geometry of the ring specimens are discussed, and the stress and strain variables to be obtained from the Instron record are defined. Other studies of the mechanical behavior of gum-rubber vulcanizates include estimation of the network entropy of polymer chains using nongaussian statistics, the derivation of a new distribution function for relaxation times to provide for rapid interconversion of creep, relaxation, strain rate, and dynamic loading data, and the comparison of experimental and predicted uniaxial constant strain-rate tensions.
- I-035 Robinson, Courtland N.; Graham, Phillip H. "Dynamic Mechanical Properties of Solid Propellants and Propellant Binders," Bulletin of the 4th Meeting ICRPG Working Group on Mechanical Behavior, Vol. 1, October 1965, pp. 183-216.
- This paper presents the results of an experimental program to study the dynamic shear properties of selected solid propellants and propellant binders. The main objective of this work has been to obtain data of a fundamental nature which would contribute to the understanding of the dynamic mechanical properties of composite viscoelastic media.
- A modified Fitzgerald Apparatus has been used to obtain dynamic shear modulus data over a range of frequencies and temperatures. Data obtained on both propellants and binders at pressures up to 1000 psig have indicated no effect of hydrostatic pressure on dynamic shear modulus. However, lateral clamping pressure has been shown to significantly effect the dynamic shear modulus of the propellants but not the unfilled binders.

REPRODUCIBILITY OF THE  
ORIGINAL PAGE IS POOR

A-10

The results of accelerated aging tests have shown significant changes in the small deformation dynamic shear properties of two propellant systems. In addition, experimental results for propellants stored under constant relative humidities have revealed some very interesting effects. Dynamic shear modulus was observed to increase with moisture constant in a polyurethane propellant while just the opposite effect was observed for a PBAN propellant.

I-036                   Sharma, M. G. "Dynamic Compressibility Measurements of an Inert Composite Propellant at Low Frequencies," Bulletin of the 4th Meeting ICRG Working Group on Mechanical Behavior, Vol 1, October 1965, pp. 153-168

The paper deals with dynamic compressibility measurements on an inert composite propellant in a frequency range of  $10^{-4}$  to  $10^{-1}$  cycles per second and at room temperature conditions. An apparatus for the dynamic compressibility measurements has been developed, which subjects a specimen confined with a fluid in a chamber to known periodic pressure changes and measures the associated volume changes. From the hysteresis curves obtained for specified pressure changes, dynamic compressibility (Dynamic Bulk Compliance), and phase angle between pressure and volume changes are evaluated. Results indicate that a decrease of a little over twenty per cent of dynamic compressibility was noticed with the increase of frequency from  $2.47 \times 10^{-4}$  to  $1.23 \times 10^{-1}$  cycles per sec (almost three decades of frequency). In addition, the bulk loss compliance distribution is found to show a peak in the above frequency region. Finally, the dynamic compressibility at various frequencies for the test material is predicted from static volumetric creep measurements, and verified with experimentally determined values.

I-037 Cantey, D. "An Apparatus for Measurement of Dynamic Effects in Rheological Materials," Bulletin of the 4th Meeting ICRPG Working Group on Mechanical Behavior, Vol 1, October 1965, pp 255-268

An apparatus is described which can be used for rapid and economical dynamic viscoelastic characterization of solid propellants or similar materials. Sinusoidal deformations of the order of 10 micro-inches are produced by a piezoelectric driver at frequencies which can be continuously varied from 20 to 1000 cycles per second. Force transmitted through the specimen is detected, measured and compared with the deformation sinusoid to yield the temporal phase angle between dynamic stress and strain.

This phase angle, together with measured specimen dimensions and the magnitude of the output force obtained by calibration, permit direct calculation of the components of the dynamic modulus. Multiple temperature measurements provide data useful in time-temperature superposition analysis.

I-038

Robinson, Courtland N., Graham, Phillip H. "Dynamic Mechanical Properties of Solid Propellants and Propellant Binders (II)," CPIA Publication No. 119, Vol. 1, Proceedings of the 5th ICPRG Meeting Mechanical Behavior Working Group, October 1966, p. 249.

The main objective of this work has been to obtain data of a fundamental nature which would contribute to the understanding of the dynamic mechanical properties of composite viscoelastic media. During the past year, additional experimental data have been obtained and analyzed. Analysis of the experimental data suggests that (a) Time-temperature equivalent behavior in the conventional sense is not exhibited by the PBAN and CTPB formulations and the respective binders examined, (b) The broad spectrum mechanical behavior of the PBAN and CTPB formulations examined is markedly similar, (c) Data reduction assuming that the observed behavior is comprised of a linear viscoelastic contribution combined with an Arrhenius-like temperature-dependent contribution results in qualitative and empirically quantitative agreement between prediction and experiment.

I-039 Tschocgl, N W, Smith, Thor L "Dynamic Shear Modulus of a Polyurethane Propellant," CPIA Publication No 119, Vol 1, Proceedings of the 5th ICRPC Meeting Mechanical Behavior Working Group, October 1966, p 267

The dynamic moduli of a polyurethane propellant were determined at 11 temperatures between -40 and 60°C and at as many as 14 frequencies between 0.064 and 24.5 cps at each temperature. Tests were made on conventionally bonded specimens 1.25 inches in diameter and 0.50 inch thick. The data were corrected to a shear strain amplitude of 0.01. Both the G' and G'' data at the different temperatures could be precisely superposed to give composite curves which show the dynamic moduli at frequencies in the range  $-2 < \log \omega_a < 9.6$ , where  $\omega_a$  is the circular frequency, in radians per second. Values of the shift factor  $a_T$  obtained by superposing the G' and G'' data were sensibly identical and corresponded to those predicted by the WLF equation. Over the frequency and temperature ranges covered, the storage modulus increased from about  $1.4 \times 10^7$  dynes/cm<sup>2</sup> (205 psi) to  $1.4 \times 10^9$  dynes/cm<sup>2</sup> (20,500 psi), the latter value being less than the expected glassy modulus by a factor of 8 to 10. The mechanical loss tangent had a shallow maximum at  $\log \omega_{aT} = 1.2$ , above  $\log \omega_{aT} = 6.0$ , it decreased rapidly with increasing frequency. In the range  $-2 < \log \omega_{aT} < 6$ , the loss tangent varied only +12% above the mean value in this frequency range.

T-040

Veyssiére, Béatrice, Long, V "On the  
Transmission from Harmonic to Transient  
State in Viscoelasticity," Séanc. Acad.  
Sci., Paris, No. 266 A, 1968, pp 366-369,  
(in French)

The problem considered is the derivation of the time functions (creep and relaxation functions) from the steady-state harmonic response (complex moduli and compliances) of a linearly viscoelastic material. An expression of the Laplace transforms of the required functions is sought in the form of a product

$$\prod_{i=0}^n p^{-1} \{ i + (T_1 p)^{\beta_1} \}^{-1},$$

which is said to be adequate for strongly damped materials. The method for determining those factors (with the help of a chart) is only hinted at here and is to be published in "Mémoires de l'Artillerie Française". This paper is essentially devoted to the inversion of the Laplace transformation, which involves confluent hypergeometric functions and multiple convolutions. As an example, the relaxation curve of a bituminous concrete is produced (without computational details, also to be published) as computed from the complex modulus by the authors' method, by Shapery's method and by Sayegh's. As far as this example is concerned, the present method yields results in agreement with those obtained by Shapery's procedure, these results are somewhat different from Sayegh's in the steepest part of the (log-log) relaxation curve, and in good agreement for very short times.

I-041

Sharma, M G , Lawrence, W F St "Investigation on the Dynamic Mechanical Behavior of a Filled Rubberlike Material," Fifth International Congress on Rheology, Kyoto, Japan, 1968

This paper is concerned with a study on the dynamic mechanical behavior of a rubberlike material (Solvilane 113) filled with finely divided aluminum spherical particles of prescribed volume concentrations at frequencies in the lower audiofrequency range, and at several temperatures above and below room temperature. The dynamic behavior of the material is studied by subjecting a specimen in the form of a rod to longitudinal vibrations and determining the resonant frequencies and the bandwidths of the mechanical resonance curve, corresponding to various modes of vibration.

From the dynamic mechanical data obtained at several temperatures and frequencies, reduced curves for the storage and loss moduli corresponding to a standard temperature are constructed for an extended frequency range by utilizing the time-temperature shift hypothesis. An examination of the dynamic data for various filler concentrations indicates that the viscoelastic transition region is shifted to lower frequencies with the increase in the volume fraction of the filler in the bulk material.

I-042

Nielsen, Lawrence E. "Dynamic Mechanical Properties of Filled Polymers," Applied Polymer Symposia, No. 12, 1969, pp. 249-265.

Review and interpretation of published experimental data on the dynamic mechanical properties of filled polymers. The effects of filler concentration, particle agglomeration, and ratio of particle modulus to polymer modulus on dynamic mechanical properties are reviewed. The reasons why moduli are lower than predicted are explained. In polyblends and polymers containing soft fillers, the modulus is lowered by the filler, and phase inversion can occur. A theory of phase inversion is described.

I-043

Kelley, Frank N. "Solid Propellant Mechanical Properties--Testing, Failure Criteria, and Aging," American Chemical Society (Advances in Chemistry Series, No. 88), 1969, pp. 188-243

Survey of current approaches and techniques for the characterization of the mechanical properties of solid propellants. Solid propellants are an integral part of the structure of solid rockets, although their chemical composition and overall configuration are dictated by ballistic requirements. If the propellant is viewed as a construction material, it must be characterized with respect to mechanical response, failure, and physical deterioration. The test techniques devised for such characterizations have undergone an evolutionary development in the direction of increased sophistication. The Joint Army-Navy-Air Force (JANAF) uniaxial test specimen is still the most widely used for routine quality control testing, but a variety of improved uniaxial and multiaxial measurements are becoming commonplace. It is pointed out that no completely general failure criterion has become available which may be used to evaluate either the propellant or the final grain design.

I-044

Gottenberg, W. G. "Semiannual Report on Vibrational Characteristics of Solid Propellant Rocket Engines", AFMMD-TR-60-113, STL/TR-60-0000-09197, Space Technology Laboratories, Inc., Los Angeles, California, for period of 1 January - 30 June 1960, (AD 242 737).

Four experimental methods for determining the dynamic mechanical properties of propellant-like materials are discussed in this report of progress under "Project Plan 165-29" for the period 1 January through 30 June 1960. In each case, the necessary experimental techniques have been developed. One of the tests, that for measuring the complex shear modulus, is investigated quite thoroughly and is actually used to obtain some properties for a representative material.

I-045 Volterra, E. "Vibrations of Elastic Systems

Having Hereditary Characteristics," Journal of Applied Mechanics, Vol 72, 1950, p. 363.

Results of experiments carried out on plastics and rubber-like materials at high rate of straining are given. It is shown that the dynamic stress-strain ( $\sigma$ ,  $\epsilon$ ) relationship for those materials can be expressed by the formula

$$\sigma = f(\epsilon) + \int_0^t \phi(t-T) \frac{d\epsilon(T)}{dT} dT$$

The first term represents the static stress-strain relationship, while the second depends on the rate of straining  $\frac{d\epsilon}{dt}$ . As a first approximation it is supposed that the materials follow Hooke's law when statically stressed. Equation [1] then becomes

$$\sigma = E\epsilon + \int_0^t \phi(t-T) \frac{d\epsilon(T)}{dt} dT$$

Materials which follow the second equation are called materials with "hereditary characteristics." Vibrations of single-degree-of-freedom systems having hereditary characteristics are considered. Methods of finding the hereditary function  $\phi(t)$  from forced vibrations are given. Free and forced vibrations of simply supported beams having hereditary characteristics are studied.

I-046

Jones, J. W., Cantey, D. E. "Investigations of Propellant Dynamic Response, Viscoelastic Linearity and Thermorheological Behavior," CPIA Publication No. 61U, Bulletin of the Third ICRPG Working Group on Mechanical Behavior, Vol. 1, October 1964, pp. 203-244.

Propellant dynamic response and viscoelastic behavior investigations at Lockheed Propulsion Company (LPC) have been directed toward the measurement of propellant response to transient and dynamic strains and stresses in tension and shear. Measurement of dynamic properties was performed at sinusoidal strain amplitudes from 0.5 to 10% peak on a machine designed at LPC. This paper discusses the correlation of dynamic moduli measured for uniaxial

A-12

REPRODUCIBILITY OF THE  
ORIGINAL PAGE IS POOR

tension-compression and simple shear stress geometries, with moduli calculated from reduced variable tensile and shear stress relaxation data. Viscoelastic heating effects under constant strain amplitude conditions are examined. Results of dynamic shear modulus measurements at  $10^{-2}$  % peak strain obtained on a piezoelectrically driven test device are discussed, along with dynamic bulk modulus measurements on the same propellant under conditions of superposed hydrostatic pressure

Transient viscoelastic response and thermorheological behavior of a variety of polybutadiene acrylic acid (PBAA) and carboxy-terminated polybutadiene propellants are presented as measured by stress relaxation and creep techniques. Propellant formulations investigated included variations in oxidizer specific surface area as well as cross-linker functionality and concentration for the two polymer types.

Nonlinear responses observed in both transient and dynamic tests are described, and their effects on analysis techniques are discussed.

I-047 Briar, H P , Wiegand, J H "Statistical Aspects of Propellant Behavior." Paper No 65-148, AIAA 6th Solid Propellant Rocket Conference, Washington, D. C., February 1-3, 1965

The variability of solid propellant mechanical properties complicates prediction of motor structural behavior. Such variability was accepted at one time, but the great advances in stress analysis now require that specific properties meet limits imposed by the design and the conditions of use. Typical variabilities of properties pertinent to static and dynamic analysis are examined to show the within-batch variability, associated apparently with the manufacturing operation, and the between-batch variability characteristics of binder cross-link density and other raw material variations.

I-048 Kolsky, H "Experimental Studies of the Mechanical Behavior of Linear Viscoelastic Solids," in Mechanics and Chemistry of Solid Propellants, edited by A. C. Eringen, H Liebowitz, S L Koh, J M. Crowley, p. 357 Pergamon Press, 1967

In order to characterize the linear viscoelastic behavior of a material, measurements must be made over a wide range of time scales. In considering the response to stresses varying sinusoidally with time, frequencies from one cycle per hour to tens of megacycles per second should be covered, and in creep and stress relaxation measurements, the time scale is further extended to months or even years. Thus an extremely large number of different experimental techniques have to be used, these are reviewed and discussed in this paper. In addition the representation of these experimental results by various mathematical and mechanical

models is considered, and the relation between chemical composition and viscoelastic properties is briefly discussed. Finally, recent experimental work on the propagation of stress waves in viscoelastic solids is described particularly from the point of view of the results obtained on the dilatational viscosity of some high polymers

I-049

Van der Wal, C W and Drent, R H J W A "Instrumentation of Thermomechanical Measurements, VI A Torsional-Creep Apparatus," Report nr. CL 67/10, Centraal Laboratorium TNO, October 1967,

This report describes a torsional creep apparatus for the determination of the creep compliance in shear as a function of time and the corresponding dynamic modulus and damping. The instrument is suitable for the measurement of compliances below  $5 \cdot 10^{-8}$  N<sup>2</sup>/N, in the time range between 1 and  $10^5$  seconds. The lowest corresponding damping that can be determined is several times  $10^{-3}$ . Within five minutes the temperature of the specimen can be adjusted to any value between -175°C and +200°C with an accuracy of 1°C.

I-050

Fitzgerald, E. R "Dynamic Mechanical Measurements on Viscoelastic Solids," Final Report, The Johns Hopkins University, September 1967

Work carried out under this contract had a twofold purpose 1) to develop apparatus for dynamic mechanical measurements, and 2) to carry out such measurements on various materials in order to gain new knowledge of their mechanical and/or acoustic properties. Accordingly much time and effort was devoted to modifying existing dynamic mechanical measurement equipment (e.g., The Fitzgerald Apparatus) in order to extend its frequency range of 50 to 5,000 cps and, in addition, several completely new systems of measurement were devised and prototype instruments constructed

I-051

Lepie, A., and Adicoff, A. "Characterization of Propellant Mechanical Behavior," Bulletin of the 8th JANNAF Structures and Mechanical Behavior Meeting, CPIA Publication No. 193, The Johns Hopkins University, p. 1970

This paper describes the results of simultaneous dynamic measurements in tension and torsion made on propellant samples. The complex dynamic moduli E', E", G', G" at low frequencies were determined within a temperature range from room temperature to -90°C. Time temperature-shift factors and reduced master curves for both tension and shear properties are discussed. The effect of dewetting on the dynamic properties in tension and shear was also investigated. A preliminary attempt is made to compute the degree of dewetting in a propellant by applying Beer-Lambert's law

I-052

Lawrence, W. St., and Sharma, M. G  
- "Dynamic Mechanical Behavior of A Composite Viscoelastic Material" Annual Report  
Pennsylvania State University, July 1967

An investigation was made into the dynamic mechanical behavior of a composite viscoelastic material. The material studied consisted of a soft binder material (Solithane 113), which had dispersed in it a number of small aluminum particles. By varying the volume fraction concentration of the filler material, the effect of the filler concentration on the dynamic characteristics was determined. Due to the nature of the composite material the dynamic investigation was limited to the lower part of the audio-frequency spectrum. To extend the frequency range over which the investigation would be applicable the material was studied at several temperatures, above and below room temperature. The time-temperature superposition principle was then applied to construct response functions that extended over several decades of frequency.

A theory was developed which considered the dynamic behavior of the composite material as a function of the moduli, and volume fraction of each constituent material. This theory was then used to predict the materials dynamic properties for filler concentrations, and frequencies studied in the experimental investigation.

The theoretically predicted moduli values were compared with the experimental results which showed that for low filler concentrations and at low frequencies the correlation between theory and experiment was good. At high frequencies and filler concentrations the correlation was found to be poor.

I-053

Beyer, R. B., "Nonlinear Mechanical Behavior of Solid Propellants," AIAA Paper No. 65-159, AIAA 6th Solid Propellant Rocket Conference, Washington, D. C., February 1-3, 1965.

The mechanical response of standard solid propellants was studied by extensive analysis of data measured under conditions of constant strain rate, constant strain, and dynamic shear strain. Nonlinear viscoelasticity has been found to occur when propellant samples are strained beyond a few tenths of one percent by tensile test methods currently used by most investigators.

Studies conducted over a wide range of strain rates ( $10^{-7}$  to  $10 \text{ min}^{-1}$ ) indicate that nonlinearity can occur (1) by loss of reinforcement due to dewetting and (2) by the "Mullins Effect" in a matrix with chemical adhesive bonding between binder and filler. In case (1) dewetting was observed to depend only on the applied stress and the temperature. The linear viscoelastic response obtained from small constant strain rate and dynamic data differed from the constant strain (2 to 5 percent) stress-relaxation modulus by as much as an order of magnitude. At very low strain rates equilibrium behavior was obtained up to strains as high as 7 percent. The time and temperature dependence of both the reinforced and nonreinforced modulus is discussed and related to long term ambient tests and actual motor behavior.

I-054

Francis, E. C., Structural Integrity of Propellant Grains," Vol. I, Final Report LPC-556-F, Lockheed Propulsion Co., January 1963.

Research effort in the investigations reported herein was directed with equal emphasis at methods for engineering evaluations of the viscoelastic properties of solid propellants, treating them as generalized linear materials, and at determinations of propellant failure characteristics. Viscoelastic propellant physical description is a fundamental necessity both to the determination of grain stresses and to the proper interpretation of grain failure criteria. Significant progress is reported in both the areas of effort. With considerable attention to analytical detail, engineering methods for propellant viscoelastic characterization requiring only standard laboratory test equipment were refined to routine practice.

I-055

Anon. "Solid Propellant Structural Integrity Investigations, Dynamic Response and Failure Mechanisms," TR No. RTD-TDR-63-1, Lockheed Propulsion Co., May 1963.

Experimental investigations of propellant dynamic behavior has been initiated using stress relaxation, small deflection mechanical oscillation, and dielectric response test techniques. Initial test results for Polycarburethane-R propellant are presented, along with fabrication progress on the large deflection mechanical test apparatus.

I-056

Cantey, D.; "Solid Propellant Structural Integrity Investigations, Dynamic Response and Failure Mechanisms," Final Report, AFRL-TR-65-71, Lockheed Propulsion Co., November 1965.

The results and conclusions of an experimental and theoretical research study of solid propellant dynamic response and failure behavior are presented. Experimentally verified analytic methods for treatment of propellant thermorheological response to vibration are described.

I-057

Tschoegl, H. W., Smith, J. R., and Smith, T. L., "Viscoelastic Properties of Solid Propellants and Propellant Binders," Quarterly Technical Report, Stanford Research Institute, for period September 16 to December 15, 1964,

Studies of the dynamic shear modulus and bulk compressibility are discussed. The storage shear modulus for a polyurethane propellant was found to increase linearly with lateral compression up to a compressive strain of 10-15%. In contrast, the storage modulus of an unfilled styrenebutadiene rubber decreased linearly with the lateral compression. The modulus also depended on specimen geometry, increasing linearly with the shape factor, i.e., the ratio of the (uncompressed) specimen thickness to the cross-sectional area. Within experimental error, the loss modulus did not depend on

specimen geometry. Some information was obtained on the heat build-up in propellant specimens during oscillatory testing. A qualitative discussion is given of work done to calibrate the dynamic and static bulk compressibility apparatus.

I-058

Fishman, N. and Rinde, J. M.: "Solid Propellant Mechanical Properties Investigations," Report No. 6, Stanford Research Institute, for period January 1 to April 1, 1964.

The overall objective of this research is to relate mechanical behavior and propellant failure mechanisms to processes of propellant microstructure. We are investigating the binder-particle interfacial processes and how they affect the mechanical response and ultimate properties of composite solid propellants. The research consists primarily of determining volume changes under selected test conditions to measure the separation between binder and filler particles and, by appropriate analysis of the test results, to quantitatively describe the interfacial processes and how they are influenced by time, temperature, and humidity.

I-059

Tschoegl, N. W. and Landel, R. F.: "A Research Program on Solid Propellant Physical Behavior," AFRPL-TR-68-106, California Institute of Technology, June 1968.

Part VI describes a continuation of earlier investigations of approximations to the spectral distribution functions of linear viscoelastic theory. It is shown that if the order of the highest derivative is  $k$ , then there exist  $k$  approximations from the step and the storage functions, and  $k + 1$  approximations from the loss functions. Thus a number of new, hitherto unknown, approximations are found, which include approximations of even order from the storage functions, and approximations of odd order from the loss functions. Of particular practical interest are the two approximations of first order from the loss functions. The interrelation between the  $k$  approximations of a given order, and the choice of the most suitable approximation is discussed. The relation of the more general method to the transform inversion method is examined, and it is shown that certain approximations in the current literature are in error because of lack of normalization of the associated intensity function, and, where applicable, because of failure to take into account that the time scale of the spectrum must be shifted by the appropriate amount if the maximum of the intensity function does not lie at the origin. Finally, the derivation of approximations from creep recovery, stress relaxation after cessation of steady flow, and deformation at constant rates of strain is discussed.

In Part VII the z-transform method for the numerical inversion of the Laplace transform is examined for possible application to viscoelastic problems. The method is found to be unsuited for viscoelastic functions which are given as logarithmic functions of time or frequency, because the logarithmic spacing of the variables leads to unstable solutions.

Part VIII predicts a general method for expressing the response of viscoelastic materials to the piecewise continuous excitation functions to which they are subjected in cumulative damage testing, as functions of the standard response functions such as

relaxation modulus and creep compliance, or, in case of periodic excitations, the dynamic moduli and compliances. It is expected that departures from the predicted behavior can be ascribed to cumulative damage. This could lead to the development of a non-destructive fatigue test.

I-060

Knauss, W. G., Clauser, J. F., and Landel, R. F.: "Second Report on the Selection of a Cross-Linked Polymer Standard," AFPL-TR-66-21, California Institute of Technology, January 1966.

The properties of the polyurethane, Solithane 113, were investigated in some detail both to explore its suitability as an interim standard polymer and to develop the tools and methods necessary for such standardization. The stress relaxation behavior from the rubbery to the glassy region was evaluated for five catalyst/prepolymer ratios.

Twelve computer programs written in IBMAP and FORTRAN IV, have been set up to convert  $E(t)$ ,  $E'(\omega)$ ,  $E''(\omega)$  and the constant strain rate modulus to  $H(\tau)$  and vice versa,  $D(t)$ ,  $D'(\omega)$ , and  $D''(\omega)$  to  $L(\tau)$  and vice versa,  $H(\tau)$  to  $D'$  and  $D''$ . Hence any characterizations may be calculated from any other. In addition,  $H(\tau)$  or  $L(\tau)$  can be converted to a Prony series. The programs are based on the numerical solution of a Fredholm equation of the first kind. Results are illustrated by calculating  $H(\tau)$ ,  $G'(\omega)$  and  $G''(\omega)$  from the stress relaxation data.

I-061

Anon: "ICRPG Solid Propellant Mechanical Behavior Manual," CPIA Publication No. 21, The Johns Hopkins University, September, 1963.

The Mechanical Behavior Manual covers experimental procedures used to test solid propellants, characterize their mechanical behavior, guide propellant development and for research on mechanical behavior. The manual is presented in looseleaf format and corrections, revisions, deletions and additions are continually made as progress is made.

I-062

Kruse, R. B.: "Laboratory Characterization of Solid Propellant Mechanical Properties," AIAA Paper No. 65-147, AIAA 6th Solid Propellant Rocket Conference, Washington, D. C., February 1-3, 1965.

The characterization of mechanical properties of solid propellants is complicated by the profound effects of temperature and rate upon these properties. Since it is not practical to test a sufficiently wide range of rates in the laboratory, the technique of time-temperature superposition has been generally employed in the solid propellant industry to characterize the viscoelastic response of solid propellants from glassy response to equilibrium behavior. In addition, it has been observed that most solid propellants exhibit ultimate properties which may be superposed on a temperature-reduced rate basis. An extension of the empirical superposition of ultimate properties is a curve of ultimate stress vs. ultimate strain, which provides a failure boundary for the propellant. The path dependence, or lack thereof, of the failure boundary is presently the subject of considerable experimental investigation, but it is generally agreed that failure boundaries provide the best currently available basis for comparison of

various propellants. The general problem of relating uniaxial failure measurements to behavior in combined stress or combined strain states by means of suitable failure criteria has proven extremely difficult of solution. Test techniques have been devised to measure failure of propellant in combined stress states, but one complicating factor appears to be qualitative differences in behavior among different types of propellants. At least for some propellants, the results can be rationalized with a deviatoric stress failure behavior in compression and dilatational failure in tension.

I-063

Nicholson, D E , Blomquist, D S and Lemon, R. H. "An Experimental Technique for Determining the Dynamic Tensile Modulus of Viscoelastic Materials," Bulletin 20th JANAFAN Panel on Physical Properties of Propellants, SPIA/PP14 V, Vol. I, p. 271, The Johns Hopkins University, October 1961.

This paper describes a vibrating reed test for the determination of the dynamic tensile moduli of a solid propellant. The analysis used in reducing the experimental data to plot storage moduli and loss tangent vs frequency is that of Bland and Lee for linear viscoelastic materials.

An experimental technique is presented that is simple to conduct, yet provides valuable, analyzable information. The results presented were gathered at ambient temperature. Tests were conducted on various sample configurations to obtain the optimum length to width ratio.

I-064

Kostyrko, G. J. "Development and Use of A Free Vibration Reed Test for Evaluation of Solid Propellants," Aerojet TN 229, Aerojet General Corp., August 1963.

I-065

Smith, T. L : "Mechanical Response of A Polyurethane Propellant to Constant Extension Rates and to Sinusoidally Varying Strains," Bulletin of the 2nd ICRPG Working Group on Mechanical Behavior Meeting, CPIA Publication No. 27, The Johns Hopkins University, p. 375, 1963.

I-066

Wagner, F. R. "Dynamic Testing of Solid Propellants at URIDC," Bulletin of the 1st ICRPG Working Group on Mechanical Behavior Meeting, CPIA Publication No. 2, The Johns Hopkins University, p 299, 1962,

I-067

Hoebel, J. F. "The Use of The Fil Dynamic Tester to Measure Propellant Dynamic Shear Properties," Bulletin of the 20th JANAFAN Panel on Physical Properties of Solid Propellants, SPIA/PP 14 v. Vol. II. The Johns Hopkins University, p. 13, October 1961.

I-068

Stoker, J. H. and Mason, O R . "Space Shuttle SRM Propellant Dynamic Properties," TWR-10543, Thiokol/Wasatch Division, June 1975.

This report summarizes dynamic characterization tests of live and inert propellants representative of the space shuttle SRM propellant

I-069

Hufferd, W L. "Measured Properties of Propellant for Solid Rocket Booster of One-Eighth Scale Dynamic Shuttle Model," UTEC CE 75-178, University of Utah, November 1975.

Static and dynamic material property tests were conducted on inert UTI-610 propellant to obtain basic mechanical response data for use in Analysis of the one-eighth scale model tests of the space shuttle SRB being dynamically tested at the NASA/Langley Research Center.

#### SEE ALSO ABSTRACTS NOS.:

II -057, -070, -071, -072, -073, -074, -078, -079, -080, -081, -086, -087, -088, -093

III -003, -003, -005, -007, -009, -010, -011, -014, -015, -016, -023, -029, -030, -035

REPRODUCIBILITY OF THE  
ORIGINAL PAGE IS POOR

## II. DYNAMIC ANALYSIS

- II-001 Baltrukonis, J. H.; Gottenberg, W. G.: "Thickness-Shear Vibrations of Circular Bars" *The Journal of the Acoustical Society of America*, Vol 31, No. 6, June 1959, pp. 734-739.  
Exact general solutions of the three-dimensional elasticity equations of motion in polar, cylindrical coordinates are obtained for axisymmetric and antisymmetric thickness-shear vibrations. These solutions are applied in solving five solid and hollow circular bar problems. Natural frequencies are tabulated.
- II-002 Baltrukonis, J. H. "Free Transverse Vibrations of an Incompressible Elastic Mass Contained by an Infinitely Long, Rigid, Circular-Cylindrical Tank" EM 9-21, Space Technology Laboratories, Inc., P O Box 95001, Los Angeles, 45, California, October 29, 1959  
Natural circular frequencies of free transverse vibrations of an incompressible elastic mass contained by an infinitely long, rigid, circular-cylindrical tank are obtained as exact solutions of the equations of elasticity. Frequency coefficients are tabulated for solid and hollow cores and for, at least, four frequencies in each of the first four modes of vibration.
- II-003 Baltrukonis, J. H. "Free, Transverse Vibrations of a Solid Elastic Mass in an Infinitely Long Rigid, Circular-Cylindrical Tank." *Journal of Applied Mechanics*, Vol 27, December 1960, pp. 663-668.  
Making use of the field equations of elasticity, the frequency equation is derived for the free, transverse vibrations of a solid elastic mass contained by an infinitely long, rigid, circular-cylindrical tank. This frequency equation relates the natural circular frequencies and Poisson's ratio. This relationship is plotted revealing a very interesting step-like variation of the natural frequency with Poisson's ratio. Displacement fields are plotted for two natural frequencies in each of the first three modes.
- II-004 Baltrukonis, J. H., Gottenberg, W. G., Schreiner, R. N. "Dynamics of a Hollow, Elastic Cylinder Contained by an Infinitely Long Rigid Circular-Cylindrical Tank." *The Journal of the Acoustical Society of America*, Vol 32, No. 12, December 1960, pp. 1539-1546.  
Dispersion equations are derived for the propagation of transverse waves within an infinitely long thick-walled hollow elastic cylinder which is perfectly bonded along its outer cylindrical surface to an infinitely long rigid circular-cylindrical tank. In the case of infinite wavelength the dispersion equations reduce to two uncoupled frequency equations, one defining the natural frequencies of free vibrations of the hollow elastic core in the antisymmetric axial shear mode and the other defining the natural frequencies of plane strain vibrations. Some numerical results are presented for the dispersion equations and the two frequency equations and references are given to more detailed results.
- II-005 Baltrukonis, J. H.; Gottenberg, W. G., Schreiner, R. N. "Axial-Shear Vibrations of an Infinitely Long Composite Circular Cylinder." *The Journal of the Acoustical Society of America*, Vol 33, No. 11, November 1961.  
Exact general solutions of the three-dimensional elasticity equations of motion in polar cylindrical coordinates are written for axisymmetric and antisymmetric axial-shear vibrations. The frequency equation follows immediately from the boundary conditions for the problem of the infinitely long, composite cylinder with two concentric circular-cylindrical layers which are perfectly bonded at their interface. The branches of the frequency equation are plotted and analyzed. The conditions are pointed out under which it is possible to obtain reasonably accurate estimates of the natural frequencies by assuming that the motions of the casing and core are uncoupled.
- II-006 Baltrukonis, J. H., Chi, M.; Gottenberg, W. G. "Free Transverse Vibrations in an Infinitely-Long, Layered Elastic Cylinder." *The Catholic University of America, Washington 17, D. C., Technical Report No. 3, NASA Research Grant NsG-125-61 (Suppl. 1-62)* August 1962.  
Baltrukonis, J. H., Chi, M., Laura, P. A. "Axial-Shear Vibrations of Star Shaped Bars - An Application of Conformal Transformation" *The Catholic University of America, Washington 17, D. C., Technical Report No. 4, NASA Research Grant NsG-126-61 (Suppl. 1-62)*, October 1962  
The conformal transformation method is applied to the problem of calculating the natural frequencies of free, axial-shear vibrations of infinitely-long, prismatic bars with epitrochoidal cross-sections. In the real plane the boundary conditions are relatively complicated but on conformal transformation of the cross-section onto a unit circle, the boundary conditions become quite simple and can be identically satisfied. However, the governing differential equation becomes relatively complicated on transformation and an exact solution is not possible. Two different collocation techniques are used to calculate approximate natural circular frequency coefficients for bars with free and clamped boundaries.
- II-007 Baltrukonis, J. H., Casey, K. B., Chi, M., Laura, P. A. "Axial-Shear Vibrations of Star Shaped Bars - An Application of Conformal Transformation" *The Catholic University of America, Washington 17, D. C., Technical Report No. 4, NASA Research Grant NsG-126-61 (Suppl. 1-62)*, October 1962  
The conformal transformation method is applied to the problem of calculating the natural frequencies of free, axial-shear vibrations of infinitely-long, prismatic bars with epitrochoidal cross-sections. In the real plane the boundary conditions are relatively complicated but on conformal transformation of the cross-section onto a unit circle, the boundary conditions become quite simple and can be identically satisfied. However, the governing differential equation becomes relatively complicated on transformation and an exact solution is not possible. Two different collocation techniques are used to calculate approximate natural circular frequency coefficients for bars with free and clamped boundaries.
- II-008 Baltrukonis, J. H., Gottenberg, W. G., Schreiner, R. N. "Solution and Experimental Results for a Problem in Linear Viscoelasticity" *Transactions of the Society of Rheology*, Vol 6, 1962, pp. 41-60.  
A solution is obtained for the problem of the axial vibrations of a rigid circular rod embedded in a linear, viscoelastic material which is, in turn, contained within a rigid circular casing. It is assumed that the entire assembly is infinitely long. The response of the embedded rod to steady-state,

harmonic oscillation of the casing is calculated within the framework of the small deformation theory of linear viscoelasticity. This result is applied in devising an experimental method to measure the complex shear modulus of the embedding, linear viscoelastic material as a continuous function of frequency. Experimental data are presented to illustrate the method and to demonstrate some of the associated difficulties.

- II-009 Baltrukonis, J. H. "Forced Transverse Vibrations of a Solid, Elastic Core Case-Bonded to an Infinitely-Long, Rigid Cylinder" Technical Report No. 1, The Catholic University of America, Washington 17, D. C., NASA Research Grant No NsG-125-61, August 1961

The problem is solved of the forced, transverse vibrations of a solid, compressible, elastic core case-bonded to an infinitely-long, rigid cylinder. It is shown that the ratio of the amplitude response of the core axis to the amplitude of the casing depends on both the frequency of the forced vibration and Poisson's ratio for the core material. By plotting amplitude ratio versus frequency curves for different values of Poisson's ratio it is demonstrated that the amplitude ratio versus frequency plot for an incompressible, elastic core is a simple line spectrum.

- II-010 Baltrukonis, J. H. "Final Report". The Catholic University of America, Washington 17, D. C., September 1963.

This is a final report summarizing progress at The Catholic University of America in viscoelastic stress analyses of solid propellant rocket motors under the two-year term of Research and Development Subcontract No. 72, Navor 16640 with the Allegany Ballistics Laboratory of Rocket Center, West Virginia. Completed work and work remaining is detailed in five technical areas. The highlight of our research is a very careful study of the tensile stress relaxation experiment including inertia effects, elasticity of the testing machine and internal heat generation. Methods for the treatment of quasi-static and dynamic problems involving infinitesimal displacements in real, linearly-viscoelastic materials are now well-developed.

- II-011 Baltrukonis, J. H., Magrab, E. B.: "Dynamic Internal Pressurization of an Infinitely-Long, Thick-Walled, Linearly-Viscoelastic Cylinder Case-Bonded to a Thin Elastic Tank" Technical Report No. 2, The Catholic University of America, Washington, D. C., February 1964. Transient and quasi-static stress and strain responses are calculated due to rapid pressurization in an infinitely-long, two-layered cylinder considered as an idealization of a solid propellant rocket motor. The casing is taken as an incompressible, elastic material while the core is considered an incompressible, linearly-viscoelastic material. Actual measured data are used for the mechanical properties of both casing and core. The pressurization program

is expressed analytically as a difference of sine integrals resulting in a program that has much the same shape as actual, measured pressurization programs and it embodies certain important analytical advantages which are discussed. Numerical data are obtained in several specific cases and the results are discussed and explained.

- II-012 Baltrukonis, J. H. "The Dynamics of Solid Propellant Rocket Motors," Technical Report No. 9, The Catholic University of America, Washington, D. C., June 1965,

From the point of view of dynamics, a solid propellant rocket motor is an unique structure in that it is composed of a substantial mass of propellant material case-bonded to a relatively massless, thin-walled cylinder. The mechanical properties of the propellant are such that it contributes little to the stiffness of the composite structure but it does contribute to the dynamic characteristic of the structure because of its mass. Furthermore, due to the viscoelastic character of the propellant, it can be expected to provide considerable damping to the system. At this point in the development of the art of design a solid propellant rocket motors there are no clear-cut or well-founded methods to quantitatively evaluate the contributions of the propellant to the dynamic responses of the composite structure. It is clear that unless such methods are devised, it will be difficult to arrive at accurate missile designs.

In the paper, a survey of the dynamic problems of solid propellant rocket motors is presented starting from the simplest model thereof and proceeding, step-by-step, to the consideration of more sophisticated and realistic models. The consideration is restricted to infinitesimal deformations of propellant grains with linear mechanical properties.

- II-013 Baltrukonis, J. H. "A Survey of Structural Dynamics of Solid Propellant Rocket Motors," NASA CR-658, National Aeronautics and Space Administration, Washington, D. C., December 1966

In the paper a survey of the dynamic problems of solid propellant rocket motors is presented starting from the simplest model thereof and proceeding, step-by-step, to the consideration of more sophisticated and realistic models. The consideration is restricted to infinitesimal deformations of propellant grains with linear mechanical properties.

- II-014 Achenbach, J. D. "Dynamic Response of a Long Case-Bonded Viscoelastic Cylinder." AIAA Journal, Vol. 3, No. 4, April 1965, pp 673-677

Time-dependent pressures are applied in an encased viscoelastic cylinder and on the surface of the case. The resulting dynamic response of the cylinder-case system is the subject of a theoretical analysis. The viscoelastic material of the cylinder is assumed to be incompressible and a forced vibration is therefore excited without initial wave effects. The cylinder is viscoelastic in shear, showing short-time elastic behavior and delayed elasticity. The displacement, the circumferential stress, and the radial stress are investigated. If a time-dependent pressure is

applied to the case, the radial bond stress at the cylinder-case interface is periodic and shows tensile peaks for high values ( $\sim 10^4$ ) of the ratio of Young's modulus of the shell to the rubbery shear modulus of the cylinder. The stresses are damped exponentially to the compressive quasi-static solution. Analytical solutions are presented for step loading and standard linear viscoelastic shear behavior.

- II-015 Achenbach, J. D. "Dynamic Response of an Encased Elastic Cylinder with Ablating Inner Surface", AIAA Journal, Vol. 3, No. 6, June 1965, p 1142

- II-016 Achenbach, J. D. "Forced Vibrations of a Burning Rocket," AIAA Journal, Vol. 3, No. 7, 1965, pp 1333-1336

The loss of mass and stiffness of a burning cylindrical grain affects the dynamic response of a solid-propellant rocket. The viscoelastic behavior of the solid-propellant material is another factor that influences the forced vibrations of a burning rocket. In the present note the effects of ablation and viscoelastic damping are considered in a study of the dynamic response of an encased viscoelastic cylinder with an ablating inner surface.

A time-dependent pressure is applied at the ablating inner surface of the cylinder. The cylinder material is viscoelastic in shear, and it is assumed incompressible in bulk. As a consequence of the incompressibility assumption the dilatational wave velocity is infinite, and a forced vibration is immediately started without initial wave effects

- II-017 Achenbach, J. D. "Thickness Shear Vibrations of an Ablating Rocket," Technical Report No. 65-3, Northwestern University, The Technological Institute, Department of Civil Engineering, Structural Mechanics Laboratory, Evanston, Illinois, (Contract Nonr-1228(34)), July 1965

The loss of momentum and stiffness due to ablation may significantly influence the vibrations of a solid propellant grain. This paper presents an analytical study of the axial shear vibrations of a long hollow cylinder that is subjected to time dependent body forces in the axial direction. The outer surface of the cylinder is bonded to a rigid case, and the inner radius increases monotonically with time. An expression is determined for the shear stress at the bond-interface. It is shown that the frequency of the shear-bond stress increases, and that its amplitude decreases towards burnout time. The shear stress is studied for various ablation rates. Conventional methods of analysis, such as separation of variables and Fourier-Bessel analysis, are not directly applicable in this problem, since the boundary conditions are prescribed on a time dependent surface. A modified Fourier-Bessel mode is defined that satisfies the boundary conditions. By substituting this mode into the equation of motion, a solution is obtained by asymptotic methods in the vicinity of the bond-interface. The analysis

is extended to include the axial shear vibrations of an ablating viscoelastic cylinder. Viscoelasticity is introduced by means of the relaxation function in shear

- II-018

- Achenbach, J. D., Herrmann, G. "Forced Vibrations of an Encased Cylinder with Eroding Inner Surface," Bulletin of the 4th Meeting ICRPG Working Group on Mechanical Behavior, Vol. 1, October 1965, p. 517

Grain ablation affects the vibratory response of a solid propellant rocket. This paper presents an analytical study of the axially symmetric vibrations of a long hollow cylinder that is subjected to time-dependent internal pressure. The inner radius of the cylinder increases monotonically with time and the outer surface is bonded to a thin elastic shell. The material of the cylinder is assumed to be incompressible in bulk and elastic or viscoelastic in shear. For an internal pressure harmonic in time, the radial response consists of the superposition of a maintained vibration and a transient vibration. The maintained vibration takes into account the loss of mass and stiffness in a quasi-static manner. The internal pressure is a step function the radial response consists of the superposition of a quasi-static response and a transient vibration. In both examples the transient vibrations are subjected to viscoelastic damping

- II-019

- Achenbach, J. D. "Dynamic Response of a Viscoelastic Cylinder with Ablating Inner Surface," Technical Report 65-6, Northwestern University, Evanston, Illinois, December 1965

The effects of ablation and viscoelasticity on the vibratory response of a hollow cylinder are investigated. The cylinder is subjected to a time-dependent internal pressure. Solutions are presented for the circumferential stress at the eroding inner surface and for the displacement in the axial direction. It is found that due to ablation, frequency decrease and amplitudes increase. The increases in amplitudes due to ablation are counteracted by viscoelastic damping. In this analysis it is assumed that the material is incompressible in bulk and viscoelastic in shear

- II-020

- Achenbach, J. D. "Torsional Oscillations of an Encased Hollow Cylinder of Finite Length," Paper presented at the AIAA/ASME Seventh Structures and Materials Conference, Cocoa Beach, Florida, April 18-20, 1966. (See also Technical Report No. 66-3, Northwestern University, Evanston, Illinois, February 1966.)

A hollow elastic or viscoelastic cylinder of finite length is encased in a thin elastic shell. The analysis of

free torsional vibrations of the elastic system yields a transcendental frequency equation that is solved numerically. The modes of free torsional motion are discussed and the proper relation establishing orthogonality of the principal modes is determined. The elementary mode of a free circular cylinder, wherein each transverse section rotates as a whole, does not occur for an encased cylinder. The exact frequencies are compared with estimates based on the assumption that the material of the core is very compliant as compared to the material of the shell. The regions are discussed in which these estimates are acceptable. Fourier-Bessel analysis is used for the problem of forced torsional motion of the encased elastic core, for arbitrary dependence on radial coordinate and time of the prescribed displacements or stresses at the end sections. For time-harmonic forcing functions the analysis is extended to forced torsional motion of an encased viscoelastic cylinder. The viscoelastic solutions are derived in terms of the complex shear modulus.

- II-021** "Dynamic Response Problems of Solid Propellant Rockets," J. D. Achenbach Feature Article, Solid Rocket Structural Integrity Abstracts, Vol. 5, No. 1, pp. 1-34, January 1968

A survey of dynamic effects on the response of solid rocket motors is presented. The service loads that impart dynamic loads to solid rocket structures are discussed and the various techniques for solving dynamic response problems of solid rocket motors are reviewed.

- II-022** "The Structural Dynamics of Solid Propellant Rockets," J. D. Achenbach, Applied Mechanics Reviews, Vol. 21, pp. 549-555, June 1968.

Methods of investigating the dynamic response of solid rocket motors are reviewed.

- II-023** "Circumferential Modes of Vibration of A Model For A Solid Propellant Rocket," J. D. Achenbach and F. H. Chou, J. Spacedraft & Rockets, Vol. 5, pp. 964-968, August 1968.

A thick-walled solid cylinder with a gas filling the circular cylindrical cavity is encased in a thin elastic shell. The material of the solid cylinder is incompressible and the behavior in

shear is dependent on frequency. The transcendental frequency equation for free nonaxially symmetrical motion in the plane strain of the gas-solid-case system is derived and is solved numerically. For various values of the relative thickness of the shell and for a large number of modes, the frequencies are shown versus the ratio of inner and outer radius of the cylinder. The dynamic interaction between gas and solid is discussed.

- II-024**

"Axial Shear Vibrations of A Cylinder of Decreasing Thickness," J. D. Achenbach, AIAA Journal, Vol. 4, pp. 1233-1240, July 1966.

This paper presents an analytical study of the axial shear vibrations of a long hollow cylinder that is subjected to time-dependent body forces in the axial direction. An expression is determined for the shear stress at the bond interface. It is shown that the instantaneous frequency of the shear bond stress increases, and that its amplitude decreases toward burnout time. Various ablation rates are considered. A modified Fourier-Bessel mode is defined that satisfies the boundary conditions. Substituting this mode into the equation of motion, a solution is obtained by asymptotic methods in the vicinity of the bond interface. The axial shear vibrations of an ablating viscoelastic cylinder are discussed briefly.

- II-025**

"Effect of Elastic Case on Stability of Radial Modes in Solid Propellant Rockets," by J. E. Achenbach and C. T. Sun, J. Spacecraft & Rockets, Vol. 4, pp. 214-219, February 1967.

The coupling of the combustion process and the mechanical vibrations of a solid propellant rocket may result in acoustic instability if a mechanical disturbance is amplified by energy release in the combustion zone. Acoustic stability depends on the balance of energy sources and energy sinks. Energy dissipations in the gas and the viscoelastic solid propellant binder are taken into account. The instantaneous frequencies of the structural system are determined from the undamped system. In this paper the influence of relative thickness of the elastic case on acoustic stability of the lowest radial mode is discussed. It is found that in the early part of the burning process a thicker case makes a more stable motor. Near burnout, however, the motor becomes more stable for a thinner case.

NOT LEGIBLE  
ORIGINAL PAGE IS POOR

- II-026 Achenbach, J D. "Vibrations of a Viscoelastic Body," AIAA Journal, Vol. 5, No. 6, 1967, pp 1213-1214, AD-657 495
- It was concluded that for a body of viscoelastic material of constant Poisson's ratio subjected to surface tractions, the dynamic displacement can be obtained, provided that (1) the static boundary-value problem for the corresponding elastic body subjected to the surface tractions can be solved, (2) the normal modes of free vibration of the corresponding elastic body are known.
- II-026a Williams, M L. "The Axial Vibration of a Viscoelastic Rod" GALCIT SM 63-9, California Institute of Technology, Pasadena, California, April 1963.
- II-027 Ghosh, Sukumar and Wilson, Edward. "Dynamic Stress Analysis of Axisymmetric Structures under Arbitrary Loading". University of California at Berkeley, Earthquake Engineering Research Center, California, Report No EERC-69-10, September 1969, 207 p., (PB-189 026)
- A finite element method is presented for the dynamic analysis of complex axisymmetric structures subjected to any arbitrary static or dynamic loading or base acceleration. The three-dimensional axisymmetric continuum is represented either as an axisymmetric thin shell, a solid of revolution, or as a combination of both. Hamilton's variational principle is used to derive the equations of motion for this discrete structure. This leads to a mass matrix, stiffness matrix, and load vectors which are all consistent with the assumed displacement field. To minimize computer storage and execution time, a diagonal mass matrix has been assumed in writing the computer program. For an earthquake analysis, the response spectrum technique may be used to obtain approximate values of the maximum response quantities if detailed time history of the response is not desired. This method of analysis is applied to various practical cases.
- II-028 Fitzgerald, E A. "The Dynamic Response of Linearly Viscoelastic Cylindrical Shells to Periodic or Transient Loading." Shock and Vibration Bulletin, Naval Research Laboratory No. 58, Part 3, Nov. 1968, pp. 121-137.
- Author discusses the correspondence principle of Biot governing the use of elastic equations to solve the analogous viscoelastic problem and shows that correspondence will exist for cylindrical shells only for sinusoidal mode shapes. Considering multilayer cylindrical shells, he uses a Donnell-type analysis, somewhat more general than that of Bieniek and Freudenthal and adapts Cowper's method to allow for transverse shear. The solution, in terms of normal mode theory, is used to determine the response of various multilayer shells to impulsive, harmonic and random loads.
- II-029 Magrib, Edward B. "Transient Response of a Case-Bonded Nonlinear Viscoelastic Cylinder," AIAA Journal, Vol. 7, No. 4, April 1969
- The problem of a rapidly pressurized, infinitely long, thick-walled viscoelastic cylinder bonded to a thin elastic shell is considered. The plane strain solution is obtained in the strain  $\epsilon$  and deformation rate  $d$  in the viscoelastic cylinder are such that terms of order three and higher in  $\epsilon$  and  $d$  can be neglected in comparison with  $\epsilon$  and  $d$ . The strains in the shell, however, are restricted to magnitudes for which infinitesimal elasticity theory applies. The effect of inertia of the viscoelastic cylinder is included in the analysis. The cylinder is internally pressurized by two types of pressure programs: a step pressure and a ramp pressure with four different rise-times. For these loadings the Eulerian strain and circumferential stress response at the inner and outer radii of the viscoelastic cylinder are obtained using a second-order constitutive relation in which the stress depends only on the displacement and velocity gradients.
- II-030 Marinescu, Al. "Concerning the Oscillations of the Rocket," Revue Roumaine des Sciences Techniques, Serie de Mecanique Appliquee, Vol. 12, No. 3, 1967, pp 1145-1164, (In German)
- Examination of a model rocket which has the shape of a rod with one free end and is characterized by variable mass and rigidity. The free oscillations of the rod are investigated by means of the bending theory, as well as from the standpoint of rotational inertia, shear forces, inner damping, hydrodynamic damping, and axial forces. Finally, forced oscillations resulting from the combined action of harmonic, accidental, and unsteady perturbations are studied. Numerical examples of these three types of perturbing force are presented.
- II-031 Laura, Patricio A., Shihady, Paul A. "Longitudinal Vibrations of a Solid Propellant Rocket Motor," Developments in Theoretical and Applied Mechanics, Vol. 3, Southeastern Conference on Theoretical and Applied Mechanics, 3rd, University of South Carolina, Columbia, S C, March 31-April 1, 1966, Proceedings, ed P A Shaw, 1967, pp 623-633
- Study of the problem of calculating the lower natural frequency of a long clamped circular cylinder with a star-shaped stress-free internal perforation vibrating in axial-shear mode. This problem is interpreted as a first approximation for a typical long, solid-propellant rocket motor. It is pointed out that the method described is directly applicable in determining the cutoff frequencies of wave-guides of very general cross section.
- II-032 Liu, C K., Chang, C H. "Wave Propagation in Hollow Elastic Cylinders with End Constraints," Developments in Mechanics, Vol. 3, 9th Midwestern Mechanics Conf., University of Wisconsin, Madison, Ws, Aug. 16-18, 1965, Proceedings, Part II, Dynamics and Fluid Mechanics, ed T C Huang, M W Johnson, Jr., 1967, pp 203-214
- Solution for the dynamic displacements (and stresses) in a thick-walled finite elastic cylinder, which is subjected to an internal blast-loading. The ends of the cylinder are well lubricated, but they are prevented from axial movement. The analysis has applications to some rocket-motor thrust chamber components, which are to withstand the transient loading of thrust buildup without interference with gimbaling.
- II-033 Anderson, C. "Plane-Strain Vibrations of a Hollow Cylinder Bonded to a Thin Shell," Acoustical Society of America, Journal, Vol. 43, May 1968, pp 1180-8'
- Frequency equations for elastic plane-strain vibrations of an infinitely long hollow elastic cylinder bonded on the outer curved surface to a thin elastic casing are discussed and compared with similar equations appropriate for hollow cylinders with (1) traction-free surfaces and (2) one traction-free and one clamped surface. The axisymmetric mode uncouples into a shear mode and a radial-extensional mode. The effects of shell thickness, mass density, and elastic properties on the natural circular frequency coefficients associated with the shear and extensional modes are discussed, and graphs of the natural circular frequency coefficients and of a displacement ratio are included.

REPRODUCIBILITY OF THE  
ORIGINAL PAGE IS POOR

II-034

Anderson, G. "Elastic Axial Shear Vibrations of a Hollow Cylinder Bonded to a Thin Shell," Acoustical Society of America, Journal, Vol. 43, May 1968, pp. 1182-84

Frequency equations and displacement ratios for elastic axial shear vibrations of an infinitely long hollow elastic cylinder bonded on its outer curved surface to a thin elastic casing are derived and compared with similar equations appropriate for hollow cylinders with (1) traction-free surfaces and (2) one traction-free and one clamped surface. Various plots of the natural circular frequency coefficients and displacement ratios have been made in order to display their dependence on shell thickness, core thickness, mass density, and elastic properties.

II-035

Knobloch, G. W.; Shulman, Yechiel. "Dynamic Response of a Composite Shell," American Institute of Aeronautics and Astronautics, and American Society of Mechanical Engineers, Structures, Structural Dynamics and Materials Conference, 9th, Palm Springs, Calif., 1-3 April 1968, AIAA Paper 68-351

An approximate analytic solution is obtained to the transient response of an infinitely long cylindrical shell surrounded by a viscoelastic medium. A uniform, axisymmetric pressure pulse is applied to the interior of the shell. Cases are treated where the shell is considered to be (1) elastic and (2) the shell is considered to be a composite shell consisting of an inner elastic layer and an outer viscoelastic layer. The viscoelastic media are described by the complex modulus representation of the constitutive relations. The elastic shell is described by thin-shell theory. The results indicate the nature of the response over a wide range of viscoelastic properties. The approximate solution corresponds favorably with results obtained by numerical techniques. A composite shell with a viscoelastic layer having high shear and bulk moduli which is surrounded by a viscoelastic medium having relatively low moduli is found to respond in a manner similar to that of an elastic shell surrounded by a viscoelastic medium with high moduli.

II-036

Shaffer, Bernard W., Sann, Robert I. "Optimum Relaxation Time for a Maxwell Core During Forced Vibration of a Rocket Assembly," New York University, School of Engineering Science, Department of Mechanical Engineering, University Heights, New York, December 1967

When the core of a case-bonded viscoelastic assembly is made of a Maxwell solid, an optimum relaxation time is found which minimizes the displacement amplitude and the bond stress response at resonance. For a Voigt solid the displacement amplitude and the bond stress response at resonance decreases with retardation time, but no optimum time exists in the same sense.

II-037

Sciammarella, C. A.; Chiang, Fu-pen. "Dynamical Stresses and Strains in Propellant Grains," Intergency Chemical Rocket Propulsion Group, Mechanical Behavior Working Group, 6th Meeting, December 5-6, 1967, Jet Propulsion Laboratory, Pasadena, Calif., CPRA Publication No 158, Vol. 1, October 1967

The main purpose of the research program presented in this paper is to study experimentally the transient phenomena that take place in propellant grains at the initiation of ignition. As the first problem in the analysis of transient phenomena, the effect of energy dissipation in the propellant in the reduction of maximum chamber pressure at the beginning of ignition is undertaken. A hollow cylinder case-bonded propellant grain is used as a model. A ring section of the cylinder is utilized as representing the propellant behavior. A discussion of the similitude condition is given. It is shown that the plane stress condition prevailing in the ring gives results that differ substantially from the plane strain condition existing in a long cylinder. A loading device able to simulate the pressure generated by the ignition is designed. The moiré method is utilized as the experimental stress technique. The dynamic moiré patterns produced by the applied

load are recorded by high speed photography. Two other quantities are measured, pressure history applied to the propellant and the strains of the fiberglass casing.

II-038

Kelkar, Vasant S. "Vibrations of a Hollow Plastic Cylinder Bonded to a Thin Casing of a Different Material," National Aeronautics and Space Administration, Ames Research Center, Moffett Field, California, November 1967

Exact solutions are obtained to determine the natural frequencies and mode shapes of a thin cylindrical shell supported by a hollow core of a different material. Materials for both shell and core are assumed to be homogeneous, isotropic, and linearly elastic. A perfect bond is assumed at the junction of the shell and the core. The composite cylinder is free from stresses at its curved boundaries and is supported by a diaphragm at its flat ends. The solutions for the core are based on three-dimensional elasticity theory and for the shell on bending theory. Curves are plotted to show the variation of the frequency with the variation in circumferential and axial wave numbers and in the ratio of inner to outer radii of the core.

II-039

Sciammarella, C. A.; Chiang, Fu-pen. "Structural Integrity Studies a Study of the Transient Behavior of Propellant Grains Under Dynamic Loads By Means of the Notch Technique," Report No. TR-1, Florida University, Gainesville, Dept. of Engineering Science and Mechanics, Dec 1966.

The main purpose of this research program was to study experimentally the transient phenomena that take place in propellant grains at the initiation of ignition. As a first step in the analysis of the transient phenomena, the effect of energy dissipation in the propellant, in the reduction of the maximum chamber pressure at the beginning of ignition was undertaken.

II-040

Sann, Robert I., Shaffer, Bernard W. "Free Transverse Elastic Vibrations of a Solid Cylinder Bonded to a Thin Casing," Siam Journal on Applied Mathematics, Vol. 14, No. 2, March 1966, pp. 266-285.

Frequency equations and mode displacement functions have been derived for the plane strain, free transverse vibration of a cylindrical assembly consisting of a solid elastic core bonded to a thin elastic shell. Deformation of the elastic core obeys Navier's equation of elastodynamics while deformation of the casing in extension and in bending occurs in accordance with the equations of thin shell theory. Two different solutions are presented, one is applicable to a compressible and the other to an incompressible core material. It is found that with a compressible core, the rotationally symmetric mode has two uncoupled motions, one is a rigid body rotation of the casing with a twisting of the cylinder and the other is a radial "breathing" of the casing and the cylinder. The breathing mode is not present with an incompressible core. Some simplified frequency equations are also presented for limiting extremes of rigidity and density.

II-041

Magrab, Edward B. "Transient Vibrations of a Rapidly Pressurized Nonlinear Viscoelastic Cylinder Bonded to a Thin Elastic Shell," Paper presented at the Fifth U S National Congress of Applied Mechanics, June 1966, (abstract only in Proceedings)

The problem of a rapidly pressurized, infinitely long, thick-walled viscoelastic cylinder bonded to a thin elastic shell is considered. The plane strain solution is obtained when the strain,  $\epsilon$ , and deformation rates,  $d$ , in the viscoelastic cylinder are such that terms of order three and higher in  $\epsilon$  and  $d$  can be neglected in comparison with  $\epsilon$  and  $d$ . The strains in the shell, however, are restricted to magnitudes for which infinitesimal elasticity theory adequately applies. The effect of inertia of the viscoelastic cylinder is included in the analysis. The cylinder is internally pressurized by two types of pressure programs - a step pressure and a ramp pressure with four different rise-times. A second order constitutive relation is developed for an isotropic, incompressible viscoelastic material in which the stress depends only on the displacement and velocity gradients. The constitutive relation contains seven material constants which can be determined from four experimental tests. These tests are described in an appendix. The constitutive relation is used to obtain the Eulerian strain and normal stress responses at the inner and outer radii of the viscoelastic cylinder to both the step and ramp pressure loadings.

complex modulus and a stress fringe value as functions of frequency are determined by means of sinusoidal oscillation tests. These are converted into a relaxation modulus and a stress fringe value as functions of time. Two approaches are discussed. In the first one, measured strains in the model and the material relaxation modulus are used for the computation of stresses by numerical integration of the integral constitutive relations of viscoelasticity. In the other approach, birefringent measurements in the model and the stress fringe value of the material are used for the computation of the principal stress difference by numerical integration of the integral stress-optic relation. The application of these methods is demonstrated in the cases of a strut and a plate subjected to the impact of a falling weight. Results obtained independently by the two methods are in satisfactory agreement.

II-044

Elder, A. S. "Derivation of Formulas for Calculating the Transient Response of a Viscoelastic Torsional Pendulum," Bulletin of the 2nd Meeting ICRPG Working Group on Mechanical Behavior, November 1963, pp. 141-160.

The pendulum consists of a circular viscoelastic rod fixed at one end and attached to a disc at the other end. The disc, initially at rest, is subjected to a step function of torque. The subsequent motion is analyzed in terms of normal modes and normal coordinates. The normal modes are found by separation of variables. The characteristic numbers associated with these modes depend only on the moments of inertia of the rod and disc, and not on the mechanical properties of the rod. The normal coordinates are solutions of integro-differential equations of the Volterra type. These equations may be solved by means of the Laplace transform if the mechanical properties of the rod are represented in differential operator form.

After the response to a step function of torque has been obtained, the response to an arbitrary torque may be obtained by means of Duhamel's integral.

This method of analysis may be applied to other dynamic problems in linear viscoelasticity provided the characteristic equation can be reduced to a form that does not involve the mechanical properties of the material.

II-042

Marinescu, Al. "Approximate Analysis of Forced Vibration of Rockets," Revue Roumaine des Sciences Techniques, Série de Mécanique Appliquée, Vol 9, No 5, 1964, pp 1115-34.

A discussion of the forced vibrations of rockets, when the latter are considered as beams of variable mass with free cross sections at the ends. Forced vibrations under the action of external harmonic forces are first considered. Subsequently, such vibrations are examined under the action of external random forces followed by a discussion of discontinuous external forces. In all cases the equations for forced vibrations examined include the effect of internal and aerodynamic dampings as well as the effect of axial and restoring forces.

II-043

Daniel, I. M. "Experimental Methods for Dynamic Stress Analysis in Viscoelastic Materials," Journal of Applied Mechanics, Series E, Vol 32, No. 3, September 1965, pp. 598-606

This paper deals with experimental methods of dynamic stress analysis in viscoelastic materials. Plasticized polyvinyl chloride is used as the model material. Dynamic properties, both mechanical and optical, in the form of a

II-045

Henry, L. A., Freudenthal, A. M. "Forced Vibrations of a Visco-Elastic Cylinder Case-Bonded to a Thin Elastic Shell," Technical Report No. 22, Columbia University, New York City, January 1964

This paper is concerned with the forced vibrations of case-bonded solid propellant grains. Special attention is paid to the interaction between the thin elastic shell (case) and the thick-walled propellant cylinder. The effects of material damping in the propellant are explored.

Frequency-response functions are computed, which can be used for analysis in situations where the loading is arbitrary deterministic or random (stationary).

II-046

Henry, L. A.; Freudenthal, A. M. "Forced Vibrations of a Finite Viscoelastic Cylinder Case-Bonded to a Thin Shell." Paper No. 65-173, AIAA 6th Solid Propellant Rocket Conference, Washington, D. C., February 1-3, 1965.

Frequency-response functions are determined for the stresses and displacements in a viscoelastic thick-walled cylinder case-bonded to a thin cylindrical shell. A radially symmetric solution is obtained in three steps. 1) the solution is obtained for a thick-walled cylinder with oscillating pressures on the inner and outer surfaces and a tangential stress on the outer surface in the axial direction, 2) the solution is obtained for a thin cylindrical shell with internal pressure and tangential stress in the axial direction on the inner surface and with the outer surface traction free, and 3) combinations of solutions 1 and 2, requiring continuous displacements at the interface, give the solution to the problem. The equations of linear elasticity are used for the thick-walled cylinder. Membrane theory is used for the shell. Damping is introduced by means of complex moduli. The boundary conditions require that the radial displacement and the normal stress in the axial direction both be zero at each end. Numerical results are presented for the first barreling mode of the structure. These computations illustrate the effect of the coupling of the cylinder and shell on the natural frequencies of the system in the range considered. The effect of various degrees of damping in the thick-walled cylinder is also clearly illustrated.

II-047

Kingsbury, H. B.; Vinson, J. R., Soler, A. I. "Lobar and Longitudinal Vibrations of Solid Propellant Rocket Motors." Paper No. 65-172, AIAA 6th Solid Propellant Rocket Conference, Washington, D. C., February 1-3, 1965.

Approximate analytical methods are developed to determine the lobar (breathing) mode shapes and natural frequencies of a solid propellant motor, the axially symmetric propellant mode shapes and natural frequencies during longitudinal vibration, and the propellant stresses during forced longitudinal vibration. Such methods are essential to the study of motor structural integrity during transportation and handling. For lobar vibrations, the Reissner Functional is formulated utilizing a plane strain solution of the motor undergoing arbitrary inextensional deformations of the case. Employing a variational technique, analytical expressions for the lobar natural frequencies and mode shapes are determined. For longitudinal vibrations, the propellant is considered as a thick, hollow, elastic, finite cylinder. Functional forms for stresses and displacements are assumed with arbitrary radial and axial dependence. The repeated use of Reissner's Principle yields equations applicable to various boundary conditions. From these, natural frequencies and mode shapes are determined. Numerical results using the expressions developed predicted fundamental lobar and longitudinal frequencies within 2% of those obtained from full-scale rocket motor tests. Finally,

an approximate method is developed to determine stresses and displacements in closed form for motors under forced longitudinal vibration. Its range of applicability includes the frequencies associated with transportation and handling

## REPRODUCIBILITY OF THE ORIGINAL PAGE IS POOR

II-048

Barrett, R. E. "Techniques for Predicting Localized Vibratory Environments of Rocket Vehicles" Technical Note D-1836, National Aeronautics and Space Administration, Marshall Space Flight Center, Huntsville, Alabama, October 1963.

It is imperative that the vibration environment of future vehicles be predicted prior to design and development so that satisfactory design and test procedures can be established. These criteria are essential to the establishment of high reliability standards necessary for man-rated vehicles. The methods and techniques presented herein allow adequate predictions of future vehicle environments.

These techniques rely upon typical structural configurations which have been sufficiently defined by measured data. Subsequent statistical analyses describe the dynamic characteristics of the structure with statistical certainty. Thus, with only a knowledge of the structural geometry and mass characteristics, the anticipated dynamic environment may be established. These techniques are applicable to all rocket vehicle structure including corrugated and sandwich skin construction.

The predicted environments represent a statistical estimation since the reference spectra are established by statistical techniques. Consequently, the probability of the actual environment not exceeding the predicted environment of a future vehicle is established with a 97.5 percent confidence. This does not infer that the predicted environment will accurately correspond to a single measured environment. Certainly, some of the measured responses of a new vehicle will be significantly lower than the predicted. This is to be expected since the criterion is such that the prediction will envelope 97.5 percent of the situations. However, this problem is alleviated somewhat by the techniques utilized of separating rocket vehicle structure into eight (8) basic categories -- each possessing essentially similar dynamic characteristics. This reduces the variance about the mean so that the mode value (most likely to occur) is not greatly less than the higher confidence limits. Therefore, the 97.5 percent criterion may be used without the concern of over conservatism in regard to a specific problem.

II-049

Arveson, W. B. "Dynamics of a Rocket with an Axis of Symmetry." NAVWES Report 7958, NOIS TP 3000, U S Naval Ordnance Test Station, China Lake, California, July 1963

A fundamental analysis of the dynamics of a short-range rocket-propelled vehicle with an axis of symmetry is presented. The treatment is rigorous and comprehensive,

stressing the interpretation and application of physical principles to this problem.

The number of initial assumptions has been kept small. The final equations are quite general, and are carried through a series of approximations and restrictions.

II-050

Sarkar, S. K. "Torsional Vibration of a Semi-Infinite Viscoelastic Circular Cylinder Due to Transient Torsional Couple." AIAA Journal, Vol. 1, No. 6, June 1963, p. 1427.

This paper is concerned with the determination of displacement in a semi-infinite viscoelastic cylinder when a torque, exponentially decreasing with time, is applied on a prescribed region of the plane end.

II-051

Cook, K. S., Chappell, R. N. "An Analog Solution to Viscoelastic Structural Problems." CPIA Publication No. 61U, Bulletin of the Third ICRPG Working Group on Mechanical Behavior, Vol. 1, October 1964, pp 141-152.

An analog computer solution to transient, viscoelastic structural problems is presented. The general form of a computer diagram for quasi-static problems is developed, and it is shown that dynamic problems may also be analyzed by the same methods. The quasi-static and dynamic responses to internal pressurization of a viscoelastic propellant grain in an elastic case are given as examples. Computed results are compared with test results. The method utilizes the relaxation modulus rather than the complex dynamic modulus.

II-052

Burton, J. D.; Jones, W. B., Frazee, J. D. "Viscoelastic Vibrations." CPIA Publication No. 61U, Bulletin of the Third ICRPG Working Group on Mechanical Behavior, Vol. 1, October 1964, pp 191-202.

Fatigue testing of solid propellants has been conducted at Rocketdyne since it was discovered that prolonged, large amplitude, relatively high-frequency vibration of solid propellants caused structural failure of that viscoelastic material. Small models have been used for this testing to minimize the expense and complexity of the study program. One model used is a longitudinally-vibrating weighted column. Expressions developed by Williams from basic equations of motion were solved to give the response of the column. The solutions, while complex, consider body forces and describe the motion of a plane within the model as a function of time. Uniaxial tensile test data in the form of relaxation modulus curves have been transformed to determine parameters for a mathematical model used to describe the propellant properties in vibration. The relations were then evaluated to predict the model response. It is shown that predicted and experimental response are in good agreement.

II-053

Garrison, U. E. "Final Report - Resonance Search and Response Test Stage I Minuteman Motor with Embedded Instrumentation (TU-122-1834.1062, TTM 009)." Thiokol Chemical Corporation, Brigham City, Utah, May 1964.

A total of thirteen vibration tests were performed using a live Stage I Minuteman motor with both external and embedded instrumentation. Ten of the tests utilized the electrodynamic exciter system and three of the tests utilized the electrohydraulic exciter system. Five tests were performed with the excitation applied parallel with the longitudinal axis of the motor. Six tests were performed with the excitation applied perpendicular to the longitudinal axis (transverse). Two tests were performed with asynchronous excitation applied at each side of the motor center, i.e. the driving forces directly opposed, were 180 deg out of phase with each other.

Driving point mechanical impedance measurements were found to be an excellent means of detecting resonance. In some cases, antiresonances by impedance may indicate erroneous results but can be verified by mode shape analysis.

II-054

Bynum, Douglas, Jr. "Vibration-test Evaluation of an ULLAGE Solid-propellant Rocket Motor," Experimental Mechanics, Vol. 10, No. 2, February 1970, pp 57-63

The mission of the ULLAGE motor is to maintain a positive acceleration of the Saturn rocket during the period between burnout of the first stage and ignition of the second stage. The eight ULLAGE motors attached to the Saturn second stage are fired during separation from the first stage. They must withstand intense sound levels and vibrations transferred through the first stage and the interstage structures.

Vibration tests were performed on an inert ULLAGE motor to safely educe the approximate response of the design configuration. The results served as a basis for improved definitions of the control parameters in subsequent vibration tests performed during the development program. The motor was tested while subjected to harmonic (sinusoidal) displacing excitation, as well as to random distribution of random vibration. The transmissibilities and power spectral densities were obtained for forcing functions in the longitudinal, radial, and tangential directions. Summaries of all the vibration tests were prepared and the critical frequencies were enumerated and discussed.

II-055

Shaffer, Bernard W., Sann, Robert I. "Forced Transverse Vibration of a Solid Viscoelastic Cylinder Bonded to a Thin Casing," Journal of Applied Mechanics, Vol. 36, No. 4, December 1969, pp 827-834

The amplitude versus frequency-response spectra of stress and displacement components within a solid viscoelastic cylinder bonded to a thin plastic casing are obtained when arbitrary normal and tangential stresses are applied to the outer surface of the casing. Special consideration is given to assemblies whose cores are made either of a Voigt material or a Maxwell material. A quantitative comparison of the bond stress amplitude spectrum at the lowest circumferential wave number reveals for both Voigt and Maxwell cores, and for small values of retardation time and relaxation time, respectively, that the amplitude ratio between the radial bond stress and the lateral pressure decreases with increasing values of the time constant. As the time constants get larger, the resonant amplitude increases for the Maxwell material, and decreases for the Voigt material. The Voigt core essentially behaves like an elastic solid at small values of its retardation time, and like a viscous fluid at large values of its retardation time. The Maxwell core essentially behaves like a nonviscous fluid at small values of its relaxation time and like an elastic solid at large values of its relaxation time.

II-056

Pan, H. H. "Axisymmetrical Vibrations of a Circular Sandwich Shell with a Viscoelastic Core Layer," Journal of Sound and Vibration, Vol 9, No 2, March 1969, pp 338-348.

The author presents a thorough derivation of the governing equation of motion for a three-layered cylindrical sandwich shell of finite length. The derivation is general in that each layer is allowed to have independent thicknesses and elastic properties. The derivation is restricted to axisymmetric vibration. In solving the governing equation, the frequency equation and corresponding composite loss-factor equation are developed. It is found that the composite loss-factor is independent of the boundary conditions, but that the natural frequencies and damping effect of the viscoelastic core will be different under different boundary conditions. The analytical results are compared with limiting cases of transverse vibration of sandwich plates and beams.

II-057

Hoekel, T. F.: "The Structural Design of Solid Propellant Grains," Emerson Electric Report No. 2123, 3 January 1967.

The report was prepared to serve as reference material for a lecture course. The material is presented in elementary fashion to serve the needs of personnel other than those directly concerned with structural analysis. The report initiates with strength of materials and elementary elasticity. Viscoelastic behavior, environmental influences and failure data are covered in brief. The majority of the contents are devoted to design problems and preliminary design analysis which are employed to study the problems.

II-058

Anderson, J. McKay "Adaptation of the Finite-Element Stiffness Method to Viscoelastic Steady-State Sinusoidal Vibration Solutions," CPIA Publication No 119, Vol I, Proceedings of the 5th ICRPC Meeting Mechanical Behavior Working Group, October 1966, p 297.

A procedure is outlined for adapting the finite-element stiffness method to the solution of steady-state sinusoidal vibration problems considering general linear viscoelastic material property representations. The kinetic energy for the finite-element model is written in terms of the nodal displacement coordinates. Lagrange's equation is then applied to the kinetic energy expression to determine the inertia terms in the equations of motion. Static equilibrium equations, obtained from the elastic finite-element formulation, are used in combination with the inertia terms to complete the equations of motion. The steady-state frequency response solution to the equations of motion is obtained and the elastic-viscoelastic correspondence principle is then used to transform the elastic solution into a steady-state viscoelastic solution.

Finite-element computer programs at Hercules Inc., modified to obtain frequency response solutions, provide viscoelastic solutions which are generally in excellent agreement with known solutions. A detailed frequency response analysis of a two-layered, finite-length cylinder is presented which exhibits typical core deformation and stress patterns at several of the resonant frequencies. Fundamental modes for conditions in which the core is not restrained by the case at the ends are primarily axial-shear modes of the core. When the core is restrained at the ends by rigid plates attached to the case, fundamental modes exhibit strong coupling between the core and the case.

II-059

Baker, W. F., Daly, J. M. "Dynamic Analysis of Solid Propellant Grains Using the Finite Element Method (Direct Stiffness Method)," CPIA Publication No 119, Vol I, Proceedings of the 5th ICRPC Meeting Mechanical Behavior Working Group, October 1966, p 319.

Presented is a method of dynamic analysis of complex continuum bodies by the extension of the finite element method. Both the axisymmetric and plane stress/strain formulations together with the associated computer programs have been developed. The analysis was developed using viscous damping and the assumption that classical modes exist. The undamped frequencies and mode shapes are first calculated and are used through a mode superposition method to calculate the response to an arbitrary dynamic loading. The method is proposed for application on solid propellant grains as a first approximation of the natural frequencies and dynamic response. Discussed are the theoretical development, correlation studies, applications, and some of the limitations of the analysis.

II-060

Hill, James L., Becker, Eric B. "Dynamic Stress in a Case-Bonded Cylinder Due to Transient Angular Acceleration," ASME Journal, Vol 7, No 3, March 1969

In one applications, case-bonded elastic cylinders are given high rates of spin quite rapidly. To gain some insight about the dynamic stresses in the cylinder during such loading, the transient response of an elastic circular cylinder that is bonded to a more rigid case is investigated. The case is given a specified angular acceleration as a function of time. Specifically, the case is given an impulsive angular acceleration and a step function angular acceleration. Numerical results of these rotations are presented. The numerical results for the step function angular acceleration are for an incompressible elastic cylinder. In all instances, the cylinder is considered to be in a state of plane strain.

II-061

Malone, David W., Connor, Jerome F. "Transient Dynamic Response of Linearly Viscoelastic Structures and Conclusions," American Society of Mechanical Engineers and American Institute of Aeronautics and Astronautics, Structures, Structural Dynamics, and Materials Conference, 10th, Proceedings, New Orleans, La., 14-16 April 1969, pp 349-356.

Description of a finite-element displacement formulation for the direct determination of the dynamic response of structural systems composed of arbitrary materials. In order to investigate the practicability of such an approach, the procedure is implemented for a linear viscoelastic material. The concept of internal coordinates, based upon an exponential expansion of the relaxation modulus, is used directly in the solution procedure to avoid carrying along the strain histories. From numerical considerations of the discretized form of the constitutive relation, it is shown that only a few terms in the exponential expansion may be necessary for satisfactory accuracy in a structural analysis problem. The method has been implemented for plane-stress/plane-strain boundary-value problems using first-order triangular and rectangular elements and a viscoelastic material with constant Poisson's ratio. Results are presented for two simple situations which were used to check out the computer program.

II-062

Goudreau, G. L. "Evaluation of Discrete Methods for the Linear Dynamic Response of Elastic and Viscoelastic Solids," University of California at Berkeley, Structural Engineering Laboratory, California, Report No SESM-69-15, June 1970, 131 p., (PB-194 286).

Governing field equations are given for the linear mechanical theory of solids, including the extension of Hamilton's principle to viscoelastic solids. Through the use of convolutions, a principle is constructed whose Euler equations are the integral equations of motion, containing the initial conditions. Closed form solutions are presented for the lumped and consistent mass finite element models of the simple bar, membrane, and beam operators. Further, the spectral approximation to the two radial mode Mindlin-Hermann bar theory is studied. Step-by-step schemes for the time integration of discrete systems are discussed. A property of the explicit time integration scheme which gives it the power to capture discontinuities in the propagation of stress waves is also discussed. The method embodies the 'direct' or 'discontinuous step' method of Nefta and Divids and Koenig in conjunction with a finite element spatial discretization.

II-063

Dunham, Robert S. "Dynamic Stress Analysis of One-Dimensional Thermorheologically Simple Viscoelastic Solids with Nonlinear Heat Conduction Analysis," U.S. Army Missile Command, Redstone Arsenal, Alabama, Report No RK-TK-70-13, July 1970.

This report presents a computer code for the dynamic stress analysis of one-dimensional plane, axisymmetric and spherical thermorheologically simple viscoelastic solids in a transient thermal environment. The uncoupled heat conduction equation is also solved for these geometries, with the option of temperature-dependent conductivities and specific heats. A user's manual, program listing, and typical input-output data are included.

II-064

Hunter, S. C., 'The Solution of Boundary Value Problems in Linear Viscoelasticity,' in Mechanics and Chemistry of Solid Propellants, edited by A. C. Eringen, H. Liebowitz, S. L. Koh and J. M. Crowley, p. 257, Pergamon Press, 1967.

Methods for the solution of boundary value problems in linear viscoelasticity are surveyed and applied to a number of physical problems, including dynamic problems

II-065

"The Dynamics of Solid Propellant Rocket Motors," J. H. Baltrukonis in Mechanics and Chemistry of Solid Propellants, edited by A. C. Eringen, H. Liebowitz, S. L. Koh, J. M. Crowley, p. 297, Pergamon Press, 1967.

At this point in the development of the art of design of solid propellant rocket motors there are no clear cut or well founded methods to evaluate quantitatively the contributions of the propellant to the dynamic responses of the composite structure. In this paper a survey of the dynamic problems of solid propellant rocket motors is presented starting from the simplest model thereof and proceeding, step-by-step, to the consideration of more sophisticated and realistic models. The consideration is restricted to infinitesimal deformations of propellant grains with linear mechanical properties. Substantial progress has been achieved towards the solution of many important dynamical problems.

II-066

Durelli, A. J., "Experimental Strain and Stress Analysis of Solid Propellant Rocket Motors," in Mechanics and Chemistry of Solid Propellants, edited by A. C. Eringen, H. Liebowitz, S. L. Koh, J. M. Crowley, p. 381, Pergamon Press, 1967.

A review is made of the methods used to strain-analyze solid propellant rocket motor shells and grains when subjected to different loading conditions. The review includes methods directed at the determination of strains in actual rockets and also at the determination of strains in rocket models. The surveyed methods include two- and three-dimensional photo-elasticity, brittle coatings, electrical strain gages, moiré, grids, etc.

II-067

Jones, J. P. and Shittier, J. S., "A Simplified Method for Dynamic Stress Analysis of Axially Symmetric Solid Propellant Grains," Report No. TDR-469 (240-10) - 9, (SSD-TR-65-176), Ballistic Systems and Space Division, November 1965

Response to transient axially symmetric end pressure of a finite length hollow circular cylinder with a fixed outer surface is considered. Axially symmetric thickness shear motion is assumed predominant and a correspondingly simplified equation of motion is derived. It is found that, for forced motion problems, considerable simplification is obtained if, instead of solving the equation of motion exactly, one uses Galerkin's method. One and two term Galerkin expansions are compared with exact solutions

for free vibrations and for transient response to suddenly applied pressure. Agreement is good for the one-term expansion and excellent for the two term expansion. Although the equations are derived for a standard linear solid as well as an elastic grain, calculations are performed for the elastic grain only

II-068

Bill, E. H., Bolland, R. J. H., Pister, K. S., Sackman, J. L. and Taylor, R. L., "Structural Integrity Studies," MSNW Report No. 69-50-1, Mathematical Sciences Northwest, Inc., December 1969.

This report examines the role of structural integrity analysis in engineering systems design wherein structural performance is an important factor, illustrates the actual role of the analyst by application to a solid propellant rocket motor system; and reviews in depth (a) numerical methods for structural integrity analysis, (b) response of motors to dynamic loadings, and (c) material characterization

II-069

Valanis, K. C. and Lianis, G., "Studies in Dynamic Stresses in Thermorheologically Simple Viscoelastic Materials," A & ES 62-16, Purdue University, November 1962.

Dynamic stresses in linear viscoelastic elastic solids under non-isothermal conditions are still an unexplored field. In the present report progress has been made by limiting attention to incompressible viscoelastic materials, in the sense that volumetric changes either due to mechanical forces or temperature fields are zero. Consequently the dynamic stresses examined here, arise because of the time wise variation of the mechanical forces (stresses) applied at the boundary.

Consideration is limited to the configurations of the sphere and the infinite hollow cylinder, both with polar symmetry, so that the dependent variables are functions of radius and time only. On the other hand, within this restriction, temperature fields are both non-homogeneous and transient in nature. The solutions of both problems reduce to Volterra integral equations of the second kind, which can be systematically solved numerically without undue difficulty.

II-070

Williams, M. L. and Arenz, R. J., "Dynamic Analysis in Viscoelastic Media," GALCIT SM 62-38, California Institute of Technology, August 1962

Distinguishing characteristics of viscoelastic media are reviewed with special reference to dynamic stress analysis. To circumvent the inherent computational difficulties in the usual transform type of solutions, an extension of the Schapery method is proposed for approximating the viscoelastic strain distribution due to wave effects. From an experimental standpoint, the use of photoelastic materials to model the responses due to dynamic loading is discussed. It is emphasized that quantitative analysis depends upon knowing the birefringence as a function of a strain rate and temperature. The association of the stress and strain optic coefficients to mechanical properties is derived and suggestions are made as to the determination of material characterization as a function of reduced strain rate.

II-071

Bornstein, G. A., Schapery, R. A. and Robinson, E. W. "Simulation Tests and Analytical Methods for Predicting the Vibrational Response of Air-Launched Rocket Motors," Report No ES2-24-3-71, Naval Ordnance Station, April 1971

The objective of this work is to generate needed vibrational analysis techniques for Navy air-launched solid propellant rocket motors. The work includes (1) developing simulation tests to obtain data for use in vibrational analysis, and (2) establishing analytical procedures necessary for the successful application of these data.

The present report develops the underlying theory for the vibrational experimental designs (polyurethane cylinders),

II-072

Bornstein, G. A., Schapery, R. A., and Lipton, L.: "Simulation Tests and Analytical Methods for Predicting the Vibrational Response of Air-Launched Rocket Motors," Naval Ordnance Station, July 1971.

The objective of this work is to generate needed vibrational analysis techniques for Navy air-launched solid propellant rocket motors. The work includes (1) developing simulation tests to obtain data for use in vibrational analysis, and (2) establishing analytical procedures necessary for the successful application of these data.

Vibration testing of analogue motors has begun. A computer program has been written, which calculates the results of the theoretical analysis for a massless hollow viscoelastic cylinder with an inertial rod.

The theoretical groundwork has been worked out for prediction of the vibrational response of the cylinder model.

II-073

Bornstein, G. A.: "Simulation Tests and Analytical Methods for Predicting the Vibrational Response of Air-Launched Rocket Motors," Naval Ordnance Station, November 1971.

The objective of this work is to generate needed vibrational analysis techniques for Navy air-launched solid propellant rocket motors. The work includes (1) developing simulation tests to obtain data for use in vibrational analysis, and (2) establishing analytical procedures necessary for the successful application of these data

The observed vibrational response of the analogue motor has been compared with computer predictions with good results. The complex shear modulus of a small sample of polyurethane was measured and the values used as input for the computer programs. The agreement between the analytical prediction (using small-sample data) and "full scale" tests demonstrates the feasibility of the approach for larger motors.

II-074

Bornstein, G. A., "Simulation Tests and Analytical Methods for Predicting the Vibrational Response of Air-Launched Rocket Motors," Naval Ordnance Station, January 1972.

The objective of this work is to generate needed vibrational analysis techniques for Navy air-launched solid propellant rocket motors. The work includes (1) developing simulation tests to obtain data for use in vibrational analysis, and (2) establishing

analytical procedures necessary for the successful application of these data.

The complex shear modulus has been measured at 77°F for SPU-1C (Sidewinder) propellant, a composite AP-Al-binder type material. An improved computer program was used to predict the vibrational response of an analogue motor using this propellant.

II-075

Anon. "Structural Vibration Prediction," NASA SP-8050, June 1970.

This monograph is concerned with the determination of the space-vehicle structural vibration resulting from induced or natural environments, and with determining internal structural loads and stresses caused by such vibrations. The vibration sources are assumed to be described adequately; the content of the monograph is therefore an assessment of analytical and experimental methods of determining the resulting vibrations, and internal loads and stresses, and an enumeration of means of demonstrating the validity of these data

II-076

Wagner, F. R.: "Solid Load Definition Study: The Vibration Environment," AFRL-TR-68-140, University of Utah, January 1969.

This study was initiated to investigate the rationale behind present load determinations and specifications for solid propellant rocket motors. As a point of departure, special emphasis has been focussed upon interactions between the viscoelastic solid propellant grain and its housing when the motor assembly is subjected to a vibration environment. The vibration environment was selected for this study since it is the load which has the greatest uncertainty associated with it, and it is a load for which significant amounts of development funds and time have been expended in order to achieve a satisfactory design.

II-077

Bushnell, D.: "Axisymmetric Dynamic Response of A Ring Supported Cylinder to Time-Dependent Loads," AIAA Paper No. 66-83, AIAA 3rd Aerospace Sciences Meeting, New York, January 24-26, 1966.

Hamilton's principle is used to derive differential equations of motion and boundary conditions for the axisymmetric free vibrations of a pre-stressed, core-supported cylindrical shell, ring-stiffened at one end and simply supported at the other. The core carries no shear stress and produces a normal pressure on the shell proportional to the radial displacement. A digital computer program computes the free vibration characteristics and modal stresses for any desired range of the eigenvalue, which is the square of the normalized angular frequency, and the dynamic response to any axisymmetric time-dependent load is calculated in a subroutine of this program. Numerical examples are given in which the dynamic response to a uniform unit dimensionless radial impulse is determined. In the early time response under such loading most of the shell moves inward uniformly, and an edge effect propagates into the shell from the boundaries. High moment resultants at the juncture between the shell and ring immediately after the loading is applied are generated by the rotatory inertia of the ring. The convergence of all of the response quantities is found to be adequate.

II-078

Leeming, H., Williams, M. L., Fitzgerald, J. E., Bolland, R. J. H., Pister, K. S., Knauss, W. G., and Schapery, R. A. "Solid Propellant Structural Test Vehicle, Systems Analysis and Cumulative Damage Program," AFRPL-TR-68-130, Lockheed Propulsion Co., October 1968.

This report covers a one year program of work concerned with the development of instrumented Structural Test Vehicles (STV's), studies related to damage accumulation with propellants and studies of systems analysis as applied to solid propellant motor design. Section 2 of this report details the experimental propellant characterization tests carried out at LPC. Stress relaxation and failure data are given as well as the effects of storage on the propellant properties. Section 3 considers STV design and the instrumentation problem areas. Various stress-strain sensors and gage calibration procedures are reviewed. Experimental bore strain and case-grain stress data are given. Section 4 details the analytical work performed for the STV configurations and the gage-grain problem area. Two new computer programs are given and the problems of material nonlinearities are reviewed. Also, experimental STV stress-strain data are compared with the analytical predictions. Section 5 is concerned with two areas related to cumulative damage (1) the use of propellant volumetric dilatation-as a damage index and (2) the calculation of transient thermal stresses. The experimental volumetric dilatation data suggest dewetting is a stress determined phenomenon. Transient thermal investigations are discussed and it is shown that experimental data do not agree with the predictions. Further work is indicated. Section 6 illustrates the technique for using a systems analysis approach to rocket motor structural design problems by means of a specific example. Further uses of the systems approach for motor design optimization are discussed.

II-079

Leeming, H. "Solid Propellant Structural Test Vehicle and Systems Analysis," Special Report 966-S-1, Lockheed Propulsion Co., June 1969.

This special report summarizes the progress made in the Structural Test Vehicle and Systems Analysis program by the end of March of 1969. The intention is to present the experimental and analytical STV data currently available and to point out gaps in the information that will have to be filled during the current year's work.

Similarly, the progress in gage design and evaluation techniques is reviewed.

Finally, a brief outline is provided of the proposed work plan for the remainder of the program.

II-080

Leeming, H., Williams, M. L., Fitzgerald, J. E., Bolland, R. J. H., Pister, K., Schapery, R. A., Knauss, W. G., and Noel, J. "Solid Propellant Structural Test Vehicle and Systems Analysis," AFRPL-TR-70-10, Lockheed Propulsion Co., March 1970.

This report covers the second year of a program for the development of instrumented Structural Test Vehicles (STV's) and systems

analysis for solid propellant motor design. The work follows that described in AFRPL-TR-68-130. This report supplements and uses data given in that earlier report. Additional data for 0064-61E propellant, Solithane 113 elastomer, and a new inert propellant are detailed. The problems of STV grain analysis, gage-grain interaction, and gage output interpretation, i.e., calibration techniques, also are covered. Nonisothermal grain analysis remains the largest problem area. Failure prediction for STV's and inert analog motors is discussed. Predictions are based on conventional techniques, fracture mechanics, and cumulative damage approaches.

STV test data are presented for isothermal pressurization, slow cooling and heating and transient or temperature cycling conditions. Data include failure tests on STV's and inert analog motors. Details of a new STV also are presented. The data are compared with analytical predictions to show that despite improved analyses and extensive propellant characterization, predictions of grain stresses and failure leave much to be desired. Further work is described on methods of applying systems analysis to motor design.

II-081

Anon. "Dynamic Characterization of Solid Rockets," Report No. 73W-00271, IBM, Federal Systems Division, September 1971.

This report describes a study task dealing with the structural dynamics of solid rockets. The method used in gaining background material and the use of this material in evaluating the structural dynamics of the SRB are described. Propellant modes which are self-excited are analyzed in detail. The necessity of testing propellant modes is established and the requirements for this test are described.

II-082

Parr, C. H.: "The Application of Numerical Methods to The Solution of Structural Integrity Problems of Solid Propellant Rockets," Feature Article, Solid Rocket Structural Integrity Abstracts, California Institute of Technology, Vol. 1, No. 2, pp. 1-56, October 1964.

This article reviews and documents the application of numerical methods by high speed digital computation to the problems of stress analysis of solid propellant grains. One feature of the review article is a collection and description of a large number of computer programs pertaining to solid rocket structural analysis.

II-083

Hilton, H. H. "A Summary of Linear Viscoelastic Stress Analysis," Feature Article, Solid Rocket Structural Integrity Abstracts, California Institute of Technology, Vol. 2, No. 2, pp. 1-56, April 1965.

This article briefly summarizes present developments in linear viscoelastic stress analysis as they affect solid propellant grain analysis.

- II-084 Hilton, H. H. "An Introduction to Visco-Elastic Analysis," in Engineering Design for Plastics, pp. 199-276, Reinhold Publishing Corp., New York, 1964
- The handbook is a comprehensive textbook type presentation of methods for structural analysis of solid propellant grains. Discussions of the accuracy and range of applicability conventional methods of analysis are provided. A critical re-examination of current methods is made and much emphasis is given to experimental verification of analysis methods.
- II-084A Parr, C. H. "The Application of Numerical Methods to The Solution of Structural Integrity Problems of Solid Propellant Rockets -II," UTEC SI 67-001, University of Utah, January 1967
- This survey supplements the previous survey written two years earlier and documents the progress and computer programs developed during the intervening period.
- II-085 Anderson, J. M.: "A Review of The Finite Element Stiffness Method as Applied to Propellant Grain Stress Analysis," Feature Article, Solid Rocket Structural Integrity Abstracts, University of Utah, Vol. 6, No. 4, pp. 1-54, October 1969
- The underlying theory for the finite element stiffness method is reviewed in this article. The emphasis is on linear, elastic solutions. Specific element formulations are described in some detail with emphasis on behavior for Poisson's ratio near 0.5.
- II-086 Hufferd, W. L. and Fitzgerald, J. E., editors. "Solid Propellant Structural Integrity Handbook," CPIA Publication No. 230, The Johns Hopkins University, September 1972.
- The JANNAF Solid Propellant Grain Structural Integrity Handbook provides, in revisable and expandable form, the most currently acceptable methods for predicting the structural integrity of solid propellant rocket motor grains.
- II-087 Anon.: "Solid Propellant Structural Integrity Analysis," NASA SP-8073, 1970.
- This monograph reviews and assesses current practices and provides guidance in the stress analysis of solid propellant grains. Sections of the monograph are concerned with state-of-the-art, design criteria, and recommended practices. Main sections are grain geometries, propellant property characterizations, specific loadings, stress-strain and displacement analysis techniques, and failure analysis.
- II-088 Fitzgerald, J. E. and Hufferd, W. L. "Handbook For The Engineering Structural Analysis of Solid Propellants," CPIA Publication No. 214, The Johns Hopkins University, May 1971.
- II-089 Malone, D. W. and Connor, J. J. "Finite Elements and Dynamic Viscoelasticity," J. of Engineering Mechanics Division, ASCE, EM4, pp. 1145-1158, August 1971
- A direct numerical approach, based on the finite element method, is proposed for determining the transient dynamic response of structures or bodies containing linearly viscoelastic materials.
- II-090 Robertson, S. R.: "Using Measured Material Parameters in Solving Forced Motion Problems in Viscoelasticity," J. Sound and Vibration, Vol. 19, pp. 95-109, 1971.
- A method is given for handling forced motion problems in viscoelasticity when experimental data is used to represent the material data instead of a model. A cubic spline series is used to interpolate between data points and thus to represent the data in a logical fashion that can be handled analytically. The solution to the time part of the problem is found in terms of the Laplace transform which is inverted numerically.
- II-091 Freudenthal, A. M. and Henry, L. A.; "One Dimensional Response of Linear Viscoelastic Media," Tech. Report No. 2, Columbia University, June 1961.
- In the present investigation the response of compressible linear viscoelastic media under a stationary state of small-amplitude oscillation is analyzed with the help of complex moduli and compliances as well as of the complex Poisson ratio functions. It is easily shown that the relatively sharp differentiation between the simple types of viscoelastic response in shear vanishes as soon as the assumption of incompressibility is abandoned.
- II-092 Lee, E. H. "Viscoelastic Stress Analysis," in Structural Mechanics, edited by J. N. Goodier and N. J. Hoff, p. 456, Pergamon Press, 1960.
- The need for the application of viscoelastic stress analysis in order to include the influence of time effects in material behavior is pointed out, and features of the resulting variation of stress distributions which are in marked contrast to results of elastic analysis are detailed. It is shown that while many aspects of linear theory have been developed to enable technologically important stress analysis problems to be solved further developments are needed for the complete solution of design problems on

this basis. In particular, methods of accurate measurement of viscoelastic material properties for combined stresses are lacking. The relations between forms of representation of viscoelastic behavior are discussed, and also their influence on the methods of attack on stress analysis problems. Simple practical tests for viscoelasticity and linearity are suggested. The influence of temperature variation and the development of nonlinear theory are mentioned briefly.

II-093 Moskvitin, V. V. "The Strength of Viscoelastic Materials As Applied to Changes of Solid Propellant Rocket Engines," FID-MT-24-714-73, Foreign Technology Division, Air Force Systems Command, October 1973.

General theoretical principles and methods of staging and solving problems dealing with determination of the stresses and strains and analysis of the strength of load-bearing structures made of polymeric materials, particularly solid-propellant rocket engines, are given. Certain specific solutions which can be used in practical calculations, are also presented.

The first four chapters of this monograph present information from the mechanics of continuous deformable media. The use of relationships from the linear theory of elasticity is stipulated by the fact that the corresponding solutions are studied in a great many cases for constructing solutions in the viscoelastic case.

In the chapter on the deformation of viscoelastic media various equations of state are presented as well as methods for determining the material functions and constants, and methods for solving the appropriate problems. Specific questions discussed here include: the deformation of media whose equations of state take into consideration the influence of the form of the stressed state, hereditary deformation of media with consideration of the influence of the degree of accumulated damage, simple loadings for linear and nonlinear viscoelastic media, statement of problems on determining the stresses that arise during polymerization of the material of a viscoelastic structure, generalization of the Bailey principle, etc.

All subsequent chapters are devoted primarily to solving specific problems. Problems on the effect of pressure, determination of thermal stresses, and deformation of structures during overloads and under prolonged storage conditions are examined. Also, certain problems on dynamic loadings and specific problems on heat formation with a cyclic change in external loads and determination of the limiting states with a cyclic change in temperature are discussed.

II-094

Levy, A., Zalesak, J., Bernstein, M., and Mason, P. W.: "Development of Technology for Modeling of a 1/8-scale Dynamic Model of the Shuttle Solid Rocket Booster," NASA CR-132492, Grumman Aerospace Corp., July 1974.

This report describes a NASTRAN analysis of the solid rocket booster (SRB) substructure of the space shuttle 1/8-scale structural dynamic model.

II-095

Anon. "Dynamic Analysis of the Solid Rocket Motor For the Space Shuttle," IBM Federal Systems Division, Huntsville, Alabama, July 1975

Analyses were conducted on three different analytical models of the Space Shuttle Solid Rocket Motor (SRM) to show the effects of various degrees of modeling complexity on the results. Analysis was also conducted on a short test segment of the SRM, with and without a test fixture, to evaluate the longitudinal dynamic characteristics of the test segment and to demonstrate the feasibility of determining these modes by testing with a 100,000 force-pound vibration exciter.

—SEE ALSO ABSTRACTS NOS :

I -017, -048

III -007, -011, -027

IV -003, -004, -006, -008, -009, -010, -015, -022, -023, -024

REPRODUCIBILITY OF THE  
ORIGINAL PAGE IS POOR

III. REPRESENTATION OF DYNAMIC PROPERTIES  
AND THEORETICAL DEVELOPMENTS

- III-001 Hilton, H. H. "Analytical Determination of Generalized, Linear Viscoelastic Stress-Strain Relations from Uniaxial, Biaxial, and Triaxial Experimental Creep and Relaxation Data." Technical Memorandum No. 180 SRP, Aerojet-General Corporation, Solid Rocket Plant, Sacramento, California, December 1961
- Analytical relations and procedures are formulated for the determination of linear viscoelastic stress-strain relations from actual creep and relaxation data. Uniaxial, biaxial, and triaxial experimental conditions are interpreted in terms of the fundamental deviatoric and volumetric stress-strain laws in either the general differential or integral forms. The analytical results are applied to some uniaxial and biaxial relaxation data for solid propellants and material property constants are computed for four, five, and six-parameter generalized Kelvin models
- III-002 Smith, T. L. "Approximate Equations for Interconverting the Various Mechanical Properties of Linear Viscoelastic Materials" Translation of Society of Rheology II, 1958, pp 131-51.
- Approximate equations are given for interconverting the storage modulus  $G'$ , the loss modulus  $G''$ , and the stress relaxation modulus  $G(t)$  by using the relaxation spectrum  $H$ , and similarly for interconverting the storage compliance  $J'$ , the loss compliance  $J''$ , and the creep compliance  $J(t)$  by using the retardation spectrum  $L$ . Approximations to the exact equations of Gross are also given for interconverting  $H$  and  $L$ . All approximate equations are based on the assumption that  $H \propto t^{-m}$  and  $L \propto t^n$  over a relatively narrow region of the time-scale. To indicate the accuracy of the approximate equations, calculations were made using published data on the NBS polyisobutylene
- III-003 Schapery, R. A. "A Simple Collocation Method for Fitting Viscoelastic Models to Experimental Data" GALCIT SM 61-23A, California Institute of Technology, Pasadena, California, February 1962.
- An easily applied collocation method is discussed for fitting the response of finite-element viscoelastic models to experimental stress-strain curves. It can be used with creep, relaxation, and steady-state oscillation data. The method is illustrated by means of two examples. As the first one, a model is obtained utilizing the dynamic shear compliance of polyisobutylene. In the second example we calculate a model from the tensile relaxation modulus of polymethyl methacrylate. With each case the model's response agreed with the experimental data within graphical accuracy over the entire frequency (or time) scale
- III-004 Biot, M. A. "Dynamics of Viscoelastic Anisotropic Media." Proceedings of the 2nd Mid-western Conference on Solid Mechanics, 1955.
- New principles are introduced for the formulation of dynamic problems in viscoelasticity for the most general case of anisotropy. One is a variational principle derived from irreversible thermodynamics the other a correspondence principle between viscoelasticity and elasticity. Applications to the dynamics of viscoelastic plates and rods are developed as examples. The variational principles are applied in conjunction with a very general method of approximation by expanding the deformation in a power series across the thickness. The method is applicable to viscoelastic shells. The concept of partial mode as a generalization of that of vibration mode for the elastic case is also introduced.
- III-005 Williams, M. L. "The Structural Analysis of Viscoelastic Materials." AIAA Journal, Vol 2, No. 5, May 1964, pp. 785-809
- In a paper several years ago, the author discussed certain background materials relating to the strain analysis of viscoelastic solid propellant grains. At that time it was indicated that the engineering stress analysis of viscoelastic materials was relatively new. Hence after reviewing certain basic principles of mathematical representation of the material behavior, the differences between elastic and viscoelastic stress analysis, and failure behavior as a function of the applied strain history, it was recommended that increasing effort be directed toward developing techniques which could be incorporated into future designs in order to more closely evaluate the structural integrity with a consequent decrease in cost and increasing reliability. Since that time there has indeed been considerable effort devoted to this subject and it is felt appropriate to review this progress particularly as the engineering analysis of viscoelastic materials is not necessarily restricted solely to solid propellant rocket motors.
- This paper therefore first presents a summary of methods of material characterization especially in terms of the broadband responses of the relaxation moduli and creep compliances as a function of reduced strain rate; second, as most stress analyses of linear viscoelastic materials have been based upon the "correspondence rule" relating to an associated elastic problem obtained by Laplace transformation, the alternative of exact and approximate inversion techniques are explored.
- III-006 Lockett, F. J.; Gurtin, M. E.: "Frequency Response of Non-Linear Viscoelastic Solids." Technical Report No. 7, CII-90, Brown University, March 1964, Contract Nonr 562(30)/7.

- III-007** Hunter, S C "Possible Equations to Describe Transient Stress, Strain and Temperature Fields in Viscoelastic Solids." Brown University, Technical Report No 2, 1960, Contract Nord-18594/2  
The purpose of the present investigation is to derive a complete set of equations governing the propagation of stress, strain and temperature transients in viscoelastic solids. While the analysis is undertaken within the framework of the usual assumptions of linear viscoelasticity, the inclusion of temperature variation entails non-linear equations. The propagation of shear and dilatational waves is investigated in a linear approximation whose range of validity is ascertained, thermomechanical effects appear to be more severe than in the corresponding elastic problem
- III-008** Glauz, R D. "The Viscoelastic Vibrating Reed." Technical Report No 4, Brown University, PA-TR-4/22, May 1953, Contract Nord 11496.  
The amplitude of vibration of a viscoelastic vibrating reed with a mass attached to the free end is found for a general linearly time dependent stress-strain law. The particular case of zero mass and a Voight stress-strain law is considered in greater detail with tables and formulas developed for obtaining the complex modulus and physical constants. The use of the complex modulus in fitting experimental data with a stress-strain law is discussed.
- III-009** Bland, D R , Lee, E H "The Calculation of the Complex Modulus of Linear Visco-Elastic Materials from Vibrating Reed Measurements." Technical Report No 9, Brown University, PA-TR/9, January 1955, Contract Nord 11496  
Two methods of determining the variation of real and complex-modulus with frequency from vibrating reed test results are detailed. One is based on measurements of the relative amplitude and phase lag of the motion of the free and driven ends of the reed, the other on amplitude resonance-measurements only. The analysis is based on a general linear viscoelastic law, and takes into account the influence of the frequency dependent moduli of the material on the frequency and amplitude of the resonance peaks. This influence has not been correctly accounted for in previous analyses which have included the assumption that the material behaves according to a particular simple visco-elastic law, which will in general not be borne out by the final results  
The method is applied to a series of tests. For the material and frequency range used the imaginary part of the complex modulus was small compared with the real part, and the influence mentioned above was small. A simpler method of analysis might thus be justified, but in other cases it will be necessary to carry out the complete analysis in order to obtain a satisfactory interpretation of tests results
- III-010** Achenbach, J D , Chao, C C.: "A Three-Parameter Viscoelastic Model Particularly Suited for Dynamic Problems" J Mech Phys. Solids, Vol 10, 1962, pp. 245-252.  
In this paper a stress-strain relation is proposed for a linearly viscoelastic solid of the three-parameter type. The mechanical model representation includes a mass. An analysis of the creep function and the elastic modulus shows the similarity of these functions with those of the standard linear solid. As opposed to the stress-strain relation of the standard linear solid the present relation leads to simple solutions of dynamic problems. A wave propagation example is treated
- III-011** Hunter, S C. "Tentative Equations for the Propagation of Stress, Strain and Temperature Fields in Viscoelastic Solids " J. Mech. Phys Solids, Vol. 9, 1961, pp 39-51.  
A thermodynamic analysis of the "thermo-rheologically" simple solid proposed by Schwarzl and Staverman (1952) leads to a set of thermomechanically coupled equations for the propagation of stress, strain and temperature fields in viscoelastic solids. The propagation of harmonic dilatational waves is investigated in a linear approximation whose range of validity is ascertained, thermomechanical coupling effects appear to be more severe than for elastic solids.
- III-012** Snowdon, J.C. "Representation of the Mechanical Damping Possessed by Rubberlike Materials and Structures." J. Acoust Soc. Am., Vol 35, June 1963, pp. 821-829.  
Discussed in detail is the manner in which the damping possessed by rubberlike materials and structures experiencing sinusoidal vibration may be represented by the ratio of the imaginary to the real part of a complex elastic modulus. Examples are given of the way in which the damping possessed by low- and high-damping rubbers depends on frequency. Equations that predict the response to vibration of distributed systems, such as damped rods and beams and a simple structure comprised of two damped beams and a lumped element of mass are derived. Representative computations of input impedance and transmissibility are presented.
- III-013** Cost, T. L. "Approximate Laplace Transform Inversions in Viscoelastic Stress Analysis " AIAA Journal, Vol. 2, No. 12, December 1964, p 2157.  
An investigation was made of approximate methods for inverting Laplace transforms that occur in viscoelastic stress analysis when use is made of the elastic-viscoelastic analogy. Alfrey's and ter Haar's methods and Schapery's direct method were examined and shown to be special cases of a general inversion formula due to Widder.

Schapery's least squares method and several techniques based on orthogonal function theory were also examined. Viscoelastic solutions to two problems involving deformations and stresses in solid propellant rocket motors under axial and transverse acceleration loads were obtained by use of several of the methods discussed. The problems were typical of the type where the associated elastic solution is known only numerically. The use of the orthogonal polynomial methods is explained in detail, and the limitations discussed. From the investigation described, it was concluded that Schapery's direct method and ter Haar's method generally give good results when applicable. Wiener's general inversion formula, which includes Alfrey's method as a special case, is not useable for the type problems of interest here. Although the orthogonal polynomial methods possess characteristics that make them especially suited to the type problems considered, their use appears limited by severe computational difficulties. Schapery's least squares method gives good results to most problems of interest.

III-014 Arenz, R. J. "Theoretical and Experimental Studies of Wave Propagation in Viscoelastic Materials." Dissertation, GALCIT SM 63-41, California Institute of Technology, Pasadena, California, 1964.

The phenomenon of wave propagation in viscoelastic materials is investigated both theoretically and experimentally, with attention directed to two areas. First, analytical methods of solution are developed for certain wave propagation problems in one and two dimensions utilizing realistic material properties. This is accomplished by use of time-dependent material property characterization through a Dirichlet series representation to overcome the limitations of the widely-used simple spring and dashpot models involving two or three elements. The Laplace transformed solutions are then inverted by an extension of the Schapery collocation method to dynamic situations.

III-015 Arenz, R. J. "Two-Dimensional Wave Propagation in Realistic Viscoelastic Materials." GALCIT SM 64-1, California Institute of Technology, Pasadena, California, January 1964 Paper No. 64-WA/APM-13, presented at Annual Meeting of ASME, November 29-December 4, 1964, New York, to be published in Journal of Applied Mechanics.

A solution method using realistic (broad-band) viscoelastic response characteristics covering approximately ten decades of logarithmic time is presented for wave propagation in two-dimensional geometries. A Prony series representation of the viscoelastic mechanical properties, and a numerical collocation inversion procedure, overcome many of the computational difficulties associated with the Laplace transform approach to dynamic linear viscoelasticity and also afford a complete time solution. Stress distributions are given for two complementary

cases, the viscoelastic half-space and semi-infinite thin plate subjected on the upper surface to the steady motion of a step pressure load moving supersonically relative to any wave speed in the material.

III-016

Percival, C. M. "Interconversion of Viscoelastic Material Properties for Minuteman Stage III Propellants," Task 9 Minuteman Support Program, Hercules Powder Co., Magna, Utah, September, 1963

This document describes an analytical procedure which can be used to extend the known ranges of the stress relaxation modulus and the complex dynamic modulus of linear viscoelastic materials. The technique makes use of the digital computer to evaluate numerical approximations of the expressions relating the various material properties. This report includes a discussion of the interconversion procedure and gives a presentation of stress relaxation and dynamic material properties for CYH and EJC propellants.

III-017

Cost, Thomas L., Becker, Eric B. "The Multidata Method of Approximate Laplace Transform Inversion," Special Report No S-51, Rohm & Haas Company, Redstone Arsenal Research Division, Huntsville, Alabama, September 7, 1965 (Contract No DA-01-021 AMC-11536(7))

A newly developed approximate Laplace transform inversion method is described. A derivation of the method, termed the "multi-data method," is presented along with a derivation of Schapery's collocation method. Similarities and differences between the two methods are described and discussed. Results of parameter studies of both methods are presented which demonstrate the sensitivity to error displayed by the collocation method and the improved accuracy obtainable with the multidata method as compared with the collocation method when errors exist in the function to be inverted. Computer program listings and operating instructions for both methods are presented.

III-018

Chae, Yong Suk. "Viscoelastic Properties of Solids as Specified by Their Dependence on Frequency," Paper presented at the F. U. S. National Congress of Applied Mechanics, June 1966, (abstract only in Proceedings)

The frequency dependence of dynamic properties of the viscoelastic solids is studied theoretically based on the principles of linear viscoelasticity. The variation of complex dynamic moduli, viscosity, and the loss factor with frequency is evaluated under an assumption of linearity in the distribution function of creep curves, and the effects of time limits are studied in detail. It is quite evident that

the relaxation characteristics could have been used just as well, but the use of creep function as basic data was preferred because the determination of the relaxation characteristics is usually more difficult. It is also shown that as far as small deformations are concerned the dynamic moduli or compliance vs. frequency curve provides a description of all the mechanical properties of a viscoelastic material. Cases of non-linearity, when deformations are large, are discussed briefly.

Employing a newly developed technique of determining the dynamic response of materials, which enables one to obtain the test results at any desired frequency including resonance, experimental results are obtained from steady-state vibration over a large range of frequency. It is shown that the theory developed is approximately obeyed by the test results on snow, but the deviation from the theory is noted for the soil (Ottawa sand) used. In general, the dynamic moduli of both snow and soil increase slightly with frequency, the dynamic viscosity shows a decrease, and the loss factor remains more or less constant with frequency. This study shows that the relation of dynamic properties to frequency can be used to specify the viscoelastic properties of a material, and that the results from creep and vibration tests can be correlated.

III-019 Gatignol, Philippe "Propagation of Sinusoidal Vibrations in Certain Viscoelastic Media," Académie des Sciences (Paris), Comptes Rendus, Vol. 261, No. 1, July 5, 1965, pp. 45-48, (in French)

Description of a method for evaluating and defining the four velocities observed when a forced sinusoidal vibration propagates through a linear, viscoelastic medium. These velocities are the wavefront velocity, the precursor's maximum velocity, the phase velocity with which the vibration is propagated, and the speed at which the amplitude of the vibration becomes preponderant. The waveform can be derived from the values for these velocity terms.

III-020 Fisher, George M C ; Leitman, Marshall J "A Correspondence Principle for Free Vibrations of a Viscoelastic Solid," Paper presented at the Fifth U S National Congress of Applied Mechanics, June 1966, (abstract only in Proceedings)

In this note we establish a correspondence principle for free vibrations in the classical linearized theory of viscoelasticity. We show that for motions which are either irrotational or solenoidal there is always an associated elastic problem with the following properties: (i) every mode shape for the viscoelastic problem is also a mode shape for the elastic problem, and (ii) the viscoelastic frequencies can, in principle, be calculated from a knowledge of the elastic spectrum and the relevant relaxation function. We further

## UCIBILITY OF THE ORIGINAL PAGE IS POOR

show that, in general, for motions which are neither irrotational nor solenoidal, this correspondence exists only for the restricted class of viscoelastic materials for which the behavior depends essentially upon one relaxation function. We conclude with the observation that the correspondence also exists for those approximate theories in which there appears only one relaxation function.

III-021 Struik, L C E. "Free Damped Vibrations of Linear Viscoelastic Materials," Rheol Acta, Vol. 6, 1967, pp. 119-129.

For linear viscoelastic materials possessing a positive discrete relaxation spectrum, a careful discussion is given of the theory underlying methods of determining the complex dynamic modulus (as defined for undamped sinusoidal oscillations) from the observed frequency and logarithmic decrement for free damped oscillations when the material is combined with a specified inertia.

III-022 Davis, Julian L. "Dynamical Aspects of Viscoelasticity," Society of Rheology, Transactions, Vol. 10, part 2, 1966, pp. 449-65

This paper is concerned with some aspects of the dynamic response of a three-dimensional linear viscoelastic medium to prescribed boundary conditions. The constitutive equations, expressed in operator form, are applied to a three-dimensional continuum and are combined with the equations of motion to yield a system of linear partial differential equations. This system may be expressed in terms of a scalar and vector potential and parameters called 'generalized velocities  $c_1^*$  and  $c_2^*$ ' (operators describing the properties of the medium). The free radial vibrations of a viscoelastic sphere and spherical shell are worked out for the prescribed boundary conditions. In particular the phase velocity is obtained as a function of the wave number and a complex frequency. The wave number is obtained from the roots of a transcendental equation. The free longitudinal vibrations of a viscoelastic cylinder are determined by solving the equations for the scalar and vector potentials with the appropriate boundary conditions. The phase velocity is obtained for the Voigt and Maxwell models. In addition, asymptotic results are obtained which reduce to either the thin rod or the Pochhammer approximation.

III-023 Schwarzl, F R : "On the Interconversions of the Viscoelastic Functions," Rheol Acta, Vol. 7, 1968, pp. 13-18

The practical problem of calculating the dynamics storage and loss compliance from the creep compliance is analyzed.

III-024 Barenblatt, G I et al. "Vibrations of Creep of Polymer Materials," Journal of Applied Mechanics and Technical Physics, No. 5, September-October 1965, pp. 44-48

In the mechanics of deformed solids it is usually assumed that superposing small amplitude vibrations on a static load has no effect on the over-all characteristics of a material under strain. This hypothesis is reflected in the fact that the existing equations of state for the case of static loads with superposed small vibrations give deformation characteristics which differ little from the corresponding parameters of deformation processes taking place in the absence of excitations. At the same time, substantial changes in the deformation characteristics of a number of materials are observed under certain conditions after the application of alternating stresses of small amplitude. Reports on studies of creep of metals, elastomers, and concrete have been published, in which the fatigue curves obtained with small vibrations superposed on static loads lie above curves obtained for static loads corresponding to the maximum pulsating load level. Attempts have been made to explain this effect from the standpoint of the molecular-kinetic and phenomenological theories. Certain theoretical considerations and experimental data, discussed

in this article, show that superposing a small dynamic component on a static load leads to an increase in the rate of creep of several polymer materials. This effect, which is due mainly to an increase in the polymer temperature, is a result of dissipation of vibrational energy. This differs from the 'vibration effect' observed on elastomers by Slonimskii and Alickseev, in which the temperature rise due to the heat generated by vibrations plays no substantial part.

### III-025

Nowacki, W K , Raniecki, B "Remarks on the Solutions for Some Dynamic Problems of Thermo-Viscoelasticity," Archivum Mechaniki Stosowanej, Vol 20, No 3, 1968 pp 337-346

Description of a method for obtaining the particular solution of the basic equation of thermoviscoelasticity for a fairly broad class of dynamic problems. The absence of body forces and heat sources is assumed, and homogeneous initial conditions for the temperature field and for the quantities characterizing the strain state are introduced. Particular solutions are obtained using the elastic-viscoelastic analogy, and the discussion is based on the results of Nowacki and Raniecki (1967) concerning an elastic medium. The particular solution in the space of transforms for a medium described with polynomial differential operators is presented. The inverse transforms are determined for both Voigt and Maxwell models. The general solution of the one-dimensional problem for a half-space with an arbitrary boundary condition for the temperature field is presented.

### III-026

Roscoe, R "Bounds for the Real and Imaginary Parts of the Dynamic Moduli of Composite Viscoelastic Systems," Journal of the Mechanics and Physics of Solids, Vol 17, No 1, February 1969, pp 17-22

If a system, consisting of firmly bonded isotropic linearly viscoelastic phases, behaves macroscopically as a homogeneous isotropic material under oscillatory deformation, upper and lower bounds can be set to both the real and imaginary parts of the complex rigidity and bulk moduli of the system. These reduce to the Voigt and Reuss bounds on the elastic moduli when the phases are purely elastic, and to the corresponding bounds on the shear viscosity when the phases are purely viscous.

### III-027

Mirrab, Edward B , Ochsner, Donald J "Transient Response of a Viscoelastic Bar Subjected to a Time Dependent End-Displacement," SIAM Journal of Applied Mathematics, Vol 16, No. 6, November 1968.

A numerical Fourier inversion technique is used to determine the transient response of a viscoelastic bar rigidly mounted at one end and subjected to a time dependent displacement at its free end. The displacement and stress of the midpoint of the bar are given for an end displacement which approximates a step loading in the short time region. An experimentally determined complex tensile modulus is used to describe the viscoelastic material. The results indicate that this numerical technique is accurate and can readily be extended to problems with a more complicated geometry. In addition, it is shown that a distinct advantage of the technique is that actual measured viscoelastic material properties can be used without resorting to parametric models, i.e., Maxwell, Voigt.

### III-028

Graffi, Dario, "Uniqueness Theorem in the Dynamics of Viscoelastic Bodies," Revue Roumaine de Mathématiques Pures et Appliquées, Vol 13, No 9, 1968, pp 1335-1342, (in Italian).

Demonstration of the uniqueness theorem for the equations of the dynamics of viscoelastic bodies on the basis of energy considerations. The demonstration is stated to be interesting from the teaching standpoint. It uses considerations of hereditary elasticity developed by Volterra and requires hypotheses that, although seeming to be restrictive from the mathematical standpoint, are hardly so from the physical standpoint.

### III-029

Straik, I C F , Schwarzl, F R "Conversion of Dynamic into Transient Properties, and Vice Versa," Rheologica Acta, Vol 8, No. 2, July 1969, pp. 134-141

A short review is given of a recent theory for converting into each other dynamic and transient properties of linear viscoelastic materials. The applicability is illustrated for a polymer in the glass-rubber transition range.

### III-030.

Goldberg, W and Dean, N. W. "Determination of Viscoelastic Model Constants from Dynamic Mechanical Properties of Linear Viscoelastic Materials," Report no 1180, Ballistic Research Laboratories, November 1962

A semi-analytical method of determining the generalized Voigt model which represents the dynamic mechanical properties of a linear viscoelastic material over a range of frequencies of three decades is presented. This model representation is shown to be equivalent to the differential operator formulation of the linear viscoelastic stress-strain law. The method is applied to complex creep compliance data for NBS polyisobutylene at 22 different temperatures. In general, the compliances calculated from the models differ from the experimental data by less than 5%.

A summary of spring-dashpot model theory is presented in Appendix A. The equivalence of the differential operator stress-strain relation and the generalized Voigt model is demonstrated in Appendix B.

### III-031

Hopkins, I. L . "Iterative Calculation of Relaxation Spectrum from Free Vibration Data," J. Appl. Pol. Sci., Vol. 7, pp. 771-992, 1963.

The complex elastic modulus  $G^*(\omega) = G'(\omega) + iG''(\omega)$  is shown to be a function not only of the frequency ( $\omega$ ) but also of the damping factor  $a$  if the strain is of the form  $x = x_0 \exp[-at] \sin \omega t$ . The general equations for  $G^*(\omega, a) = G'(\omega, a) + iG''(\omega, a) =$  are derived in terms of the relaxation spectrum. The use of a spring to aid the specimen and reduce the ratio  $a/\omega$  is discussed, and its desirability demonstrated. If data are thus available in terms of either  $G''(\omega)$  or  $G''(\omega, a)$  the iterated second approximation of Hinomura and Ferry provides a rapid and powerful method of finding the relaxation spectrum. To the accuracy to which the time-temperature reduction factor  $a_T$  is known or can be predicted by means such, for example, as the WLF equation, the function  $G''(\omega, a)$  over a temperature range at nearly constant frequency can be translated into terms of  $G''(\omega, a)$  at constant temperature and varying frequency. In such cases, the relatively simple torsional pendulum, or some analogue of it, can economically provide a characterization of the viscoelastic behavior of the material over an extended time or frequency range.

**III-032** Huang, H. C. and Lee, E. H.: "Nonlinear Viscoelasticity for Short Time Ranges," J. Appl. Mech., p. 313, June 1966,

Approximate constitutive equations for nonlinear viscoelastic incompressible materials under small finite deformation and for short time ranges are derived. The error bound of such a constitutive equation is investigated. Nonlinear creep is analyzed on the basis of the proposed equation, and also the problem of a pressurized viscoelastic hollow cylinder bonded to an elastic casing. Numerical solutions, evaluated by assuming particular forms of kernel functions in the constitutive equation, are obtained by means of an inverse interpolation technique, and the effects of nonlinearity of material properties are discussed. An experimental procedure is also proposed for measuring kernel functions from uniaxial tension tests for real materials.

**III-033** Fitzgerald, J. E.: "Analysis and Design of Solid Propellant Grains," in Mechanics and Chemistry of Solid Propellants, edited by A. C. Eringen, H. Liebowitz, S. L. Koh, J. M. Crowley, p. 19, Pergamon Press, 1967

The present paper covers in some detail several pertinent aspects of engineering grain stress analysis:

(1) A brief review of linear viscoelastic theory with emphasis on time-temperature relations, (2) More details on thermal relations including a redefinition of Lee's reduced time parameter, (3) Presentation of a master relaxation curve for typical 84 percent solids loaded systems, (4) Discussion of relative thermal equilibrium and relaxation times for several motor sizes and design implications therefrom, (5) A generalization of the "freezing point" concept for uniformly cooled grains resulting in a new "material characteristic," (6) Thermo-mechanically coupled experimental data, (7) Comments on cree-relaxation reciprocal relations and, finally, (8) Recommendations relative to methods of analysis for physically nonlinear materials which appear promising for future engineering utilization

**III-034** Duffin, R. J.: "The Influence of Poisson's Ratio on The Vibrational Spectrum," SIAM J. Appl. Math., Vol. 17, p. 179, 1969

This note concerns the normal modes of vibration of an elastic body subject to standard boundary conditions. The Poisson coefficient enters into the boundary value problem in a rather complex way. To simplify this situation the Rayleigh-Ritz variational principle is introduced in order to define the normal mode frequencies as stationary values. This leads to a perturbation formula for the frequencies as a function of the Poisson coefficient. In some cases it is found that this formula can be evaluated exactly. In any case the formula furnishes upper and lower bounds for the variation

**III-035** Smith, T. L.: "Empirical Equations for Representing Viscoelastic Functions and For Deriving Spectra," J. Polymer Sci., Part C, pp. 39-50, 1971

Several equations containing two empirical constants are considered for representing  $G(t)$ ,  $T'(\omega)$ , and  $J(t)$  in the glass-to-rubber dispersion zone. With these equations, data on the NBS polyisobutylene can be closely represented. The relaxation spectrum  $H(\tau)$  and the retardation spectrum  $L(\tau)$  were derived exactly from the equations for  $G'(\tau)$  and  $J'(\tau)$  respectively. The derived equations have the same functional form, and thus  $H(\tau)$  and  $L(\tau)$  can be interconverted, under certain conditions, by employing an auxiliary equation that interrelates the relaxation and retardation times at which the spectra maximize. An exact transformation of an equation for  $G(t)$  gave a second equation for  $H(\tau)$ , from the constants in this equation,  $L(\tau)$  was calculated. The methods for obtaining and interconverting  $H(\tau)$  for  $L(\tau)$  for polyisobutylene gave results that agree satisfactorily with literature data obtained by the usual approximation methods.

#### SEE ALSO ABSTRACTS NOS.:

I -005, -006, -008, -011, -012, -015, -016, -017, -018, -021, -022, -023, -024, -025, -027, -028, -029, -020, -031, -032, -034, -038, -040, -045, -046, -048, -052, -053, -054, -056, -059, -060, -061, -062

II -044, -052, -057, -064, -070, -072, -073, -074, -081, -082, -083, -084, -085, -086, -088, -090, -091, -092, -093

IV -008, -009, -010, -015, -016

REPRODUCIBILITY OF THE  
ORIGINAL PAGE IS POOR

IV. THERMOMECHANICAL COUPLING

IV-001

Schapery, R. A. "Heating of Thermo-Rheologically Simple Viscoelastic Media Due to Cyclic Loading." A and ES 63-4, Purdue University, School of Aeronautical and Engineering Sciences, Lafayette, Indiana, May 1963.

Steady-state and transient temperature distributions resulting from dissipation are calculated for a viscoelastic slab and hollow cylinder subjected to cyclic shear loading. Temperature dependence of the dissipation function is introduced through the usual assumption of thermo-rheologically simple behavior, wherein frequency-dependent mechanical properties measured at different temperatures are superposed by shifting the logarithmic frequency scale. This assumption leads to a nonlinear heat conduction equation, and an exact closed-form solution is obtained for just the steady-state temperature distribution. In order to solve the transient problem, some approximate methods of analysis are proposed. Numerical results for a solid propellant are given, and it is found that a large temperature rise will occur as the result of a thermal instability when the shear stress is above a certain critical value. In this present paper inertia is neglected, however, many of the considerations, including the approximate methods, are potentially applicable to dynamic problems.

IV-002

Tasi, J. "Thermoelastic Dissipation in Vibrating Plates" Journal of Applied Mechanics, Vol 30, No 4, December 1963, p. 562

The thermal dissipation associated with the natural modes of free vibration of a thermoelastic medium is obtained as an integral formula involving the mode of vibration and the temperature produced in the mode. The integral formula for dissipation is applied to an infinite isotropic plate, and numerical results are given for the three lowest, real, symmetric branches of the spectrum. Finally, it is shown that low-frequency extensional vibrations of plates can be adiabatic or isothermal, depending on whether adiabatic or isothermal boundary conditions are specified on the faces of the plate

--

IV-003

Suhubi, E. S. "Longitudinal Vibrations of a Circular Cylinder Coupled with a Thermal Field" Journal of Mech Phys Solids, Vol 12, 1964, pp 69-75

In this paper the longitudinal vibration of a circular infinite cylinder in presence of a temperature field has been studied. The frequency equation has been obtained for two particular cases, namely constant temperature and zero heat flux on the surface of the cylinder. The resulting equations have been solved for small radii and weak coupling between fields. For the former case no first order thermal effect has been observed. In the latter, expressions have been found for the velocity of propagation and damping factor, which indicate the effect of thermal field on the elastic waves and which coincide, if the lateral contraction is neglected, with those found earlier by Sneddon for the very short and very long wave lengths

IV-004

Schapery, R. A. "Effect of Cyclic Loading on the Temperature in Viscoelastic Media with Variable Properties" AIAA Journal, Vol. 2, May 1964, pp 827-835

Determination of steady-state and transient temperature distributions resulting from dissipation calculated for a linear viscoelastic slab and hollow cylinder subjected to cyclic shear loading. Temperature dependence of the dissipation function is introduced through the familiar assumption of thermorheologically simple behavior, wherein frequency-dependent mechanical properties measured at different temperatures are superposed by shifting with respect to the logarithmic frequency scale. This assumption leads to a nonlinear heat-conduction equation, and an exact closed-form solution is obtained for just the steady-state temperature distribution. In order to solve the transient problem two approximate methods of analysis are proposed. Numerical results for a solid propellant are given, and it is found that a large temperature rise will occur as the result of a thermal instability when the shear stress is above a certain critical value that depends on thermal and mechanical properties and geometry. In this paper, inertia is neglected, however, many of the considerations, including the approximate methods, are potentially applicable to dynamic problems as well as to other configurations and loading conditions

IV-005

Humphreys, J.S.; Martin, G.J.: "Determination of Transient Thermal Stresses in a Slab with Temperature-Dependent Viscoelastic Properties." Transactions of the Society of Rheology, Vol. 7, 1963.

The general problem considered is predicting thermal stresses in a thin layer of material whose mechanical properties vary with both time and temperature, due to temperature changes on the exterior. The analytical development followed falls within the framework of linear viscoelasticity and is based on recent work by Muki and Sternberg and by Lee and Rogers. The effect of temperature variation is accounted for using the log-time-temperature superposition hypothesis. A specific case is worked through for a rigid aluminum slab covered by a layer of an AVCO-developed epoxy resin material. Stress relaxation curves as a function of temperature, which are determined by averaging the results of a series of relaxation experiments on the material, are presented. Then, by using a prescribed exterior temperature drop and the heat conduction equation to determine a temperature distribution, in-plane thermal stresses are found numerically on a high-speed computer. The results of direct elastic calculations and of simplified calculations using constant-temperature properties are presented along with more complete calculations including the variation of properties with temperature.

IV-006

Petroi, R. C.; Gratch, S. "Wave Propagation in a Viscoelastic Material with Temperature-Dependent Properties and Thermomechanical Coupling." Paper No. 64-APM-8, presented at Summer Conference of the Applied Mechanics Division of The American Society of Mechanical Engineers, Boulder, Colorado, June 9-11, 1964.

A numerical method is developed for the analysis of one-dimensional wave propagation in viscoelastic media with temperature-dependent properties when thermomechanical coupling is significant. The method is applied to a specific case of longitudinal wave propagation in a finite rod with essentially sinusoidal stress variation at the two ends. The results show that, contrary to the usual assumption, such a system does not have the same response as a single-degree-of-freedom elastic system with viscous damping, as long as a realistic stress-strain relation is used.

IV-007

Schapery, R. A.: "Application of Thermodynamics to Thermomechanical, Fracture, and Birefringent Phenomena in Viscoelastic Media". *Journal of Applied Physics*, Vol. 35, No. 5, May 1964, pp. 1451-1465.

A unified theory of the thermomechanical behavior of viscoelastic media is developed from studying the thermodynamics of irreversible processes, and includes discussions of the general equations of motion, crack propagation, and birefringence. The equations of motion in terms of generalized coordinates and forces are derived for systems in the neighborhood of a stable equilibrium state. They represent a modification of Biot's theory in that they contain explicit temperature dependence and a thermodynamically consistent inclusion of the time-temperature superposition principle for treating media with temperature-dependent viscosity coefficients. The stress-strain-temperature and energy equations for small deformation behavior follow immediately from the general equations and, along with equilibrium and strain-displacement relations, they form a complete set for the description of the thermomechanical behavior of media with temperature-dependent viscosity.

IV-008

Schapery, R. A., "Thermomechanical Behavior of Viscoelastic Media with Variable Properties Subjected to Cyclic Loading." CPIA Publication No. 61U, Bulletin of the Third ICRPG Working Group on Mechanical Behavior, Vol. 1, October 1964, pp. 245-66.

The interaction between heating and dynamic response of viscoelastic bodies with temperature-dependent properties is studied. Firstly, equations governing the small deformation thermomechanical response to sinusoidal loading are shown to be equivalent to a set of two variational principles. Viscoelastic properties of a solid propellant

are characterized and then used in numerical examples dealing with sinusoidal shear loading of slabs and cylinders. As the first problem, an approximate variational method is used to calculate one-dimensional transient and steady-state temperature distributions in a massless slab. An exact steady-state solution is obtained for the thermomechanical behavior of a slab with concentrated mass, and is then used to deduce the solution for a similarly loaded cylinder. Finally, the influence of distributed mass in a cylinder is studied using a variational principle. It is found that without inertia a large temperature rise may occur when the applied stress amplitude is above a certain critical value which depends on thermal and mechanical properties, geometry, and frequency. On the other hand, the combination of temperature-dependent properties and inertia leads to temperature and displacement jump instabilities that are similar to those existing in a nonlinear spring-mass system with a spring that softens with increasing displacement.

IV-009

Schapery, R. A. "On the Thermomechanical Analysis and Behavior of Viscoelastic Media Subjected to Cyclic Loading" A and ES 64-3, Purdue University, Lafayette, Indiana, January 1964

The interaction between heating and dynamic response of viscoelastic bodies with temperature-dependent properties is studied. Equations governing the thermo-mechanical response to sinusoidal loading are developed and shown to be equivalent to a set of two variational principles. Viscoelastic properties of a solid propellant are characterized and then used in numerical examples dealing with sinusoidal shear loading of slabs and cylinders. As the first problem, an approximate variational method is used to calculate one-dimensional transient and steady-state temperature distributions in a massless slab. An exact steady-state solution is obtained for the thermomechanical behavior of a slab with concentrated mass, and is then used to deduce the solution for a similarly loaded cylinder. Finally, the influence of distributed mass in a slab and cylinder is studied using variational principles. It is found that with or without inertia a large temperature rise may occur when the stress is above a certain critical value which depends on thermal and mechanical properties and geometry. Furthermore, the combination of temperature-dependent properties and inertia leads to dynamic jump instabilities that are similar to those existing in a nonlinear spring-mass system.

IV-010

Tormey, J. F.; Britton, S. C. "Effect of Cyclic Loading on Solid Propellant Grain Structures." AIAA Journal, Vol. 1, No. 3, August 1963, p. 1763.

IV-011 Schapery, R. A., Cantey, D. E. "Thermo-mechanical Response Studies of Solid Propellants Subjected to Cyclic and Random Loading," Paper No. 65-160, AIAA 6th Solid Propellant Rocket Conference, Washington, D. C., February 1-3, 1965

An analytical and experimental study of the interaction between heating and dynamic response of solid propellant is presented. Emphasis is placed on the nature of thermal instabilities which exist under certain loading conditions, and on evaluation of linear viscoelastic theory in predicting thermal mechanical behavior of solid propellants. For analytical and experimental simplicity, the investigation considers a specimen which is loaded in simple shear and insulated such that heat flow is restricted to occur normal to the direction of shear. Two types of loadings are considered constant displacement amplitude and inertial driving. Steady-state response to both cyclic and stationary random-loading processes is determined analytically, and it is shown that large temperature increases may occur in the specimen with attached mass due to thermal instabilities. Although good agreement between experiment and theory was obtained over most of the range of strain and frequency, some strain-induced anisotropy and gradual propellant degradation were observed.

IV-012 Tauchert, T. R.. "Coupled Thermoviscoelasticity of the Standard Linear Solid," Department of Aerospace and Mechanical Sciences, Princeton University, Princeton, New Jersey

This paper reports an investigation of temperature distributions in a viscoelastic solid which result solely from mechanical deformations (i.e., no external heat is supplied to the body through its boundary). The solid is assumed to be isotropic and linear, and one which can be represented by the "Standard Linear Solid." A coupled energy equation for such a material is presented, and is used to calculate the transient and steady-state temperature distributions in a thin-walled tube subjected to torsional oscillations.

IV-013 Wolosewick, R. M., Gratch, S. "Transient Response in a Viscoelastic Material with Temperature-Dependent Properties and Thermo-mechanical Coupling," Journal of Applied Mechanics, Series E, Vol. 32, No. 3, September 1965, pp. 620-622

The transient response of a semi-infinite, viscoelastic rod after application of a sinusoidal stress variation at one end has been investigated by a numerical method. Account has been taken of temperature dependence of properties and of thermomechanical coupling. It is found that, with values of physical properties typical for polymeric materials, temperature approaches steady state several orders of magnitude more slowly than would be the case for stress and strain in the absence of thermomechanical coupling.

REPRODUCIBILITY OF THE  
ORIGINAL PAGE IS POOR

IV-014 Herrmann, George, Achenbach, Jan D "Some Dynamic Problems of Coupled Thermoelasticity," Paper presented at IUTAM Symposium on "Irreversible Aspects in Continuum Mechanics" held in Vienna, Austria, June 22-25, 1966 (Proceedings to be published by Springer-Verlag, Vienna and New York, 1967.)

Recent work at Northwestern University on dynamics of thermoelastic and viscoelastic continuous media is briefly reviewed. Some current studies on the propagation of dilatational discontinuities with plane, cylindrical and spherical fronts in a medium which includes coupling between thermal and linearly viscoelastic mechanical effects are described. The constitutive relations are assumed to contain a temperature dependence of the functions which characterize the mechanical response. The results exhibit an exponential decay of the magnitude of the discontinuity due to both viscoelastic and thermomechanical coupling effects.

IV-015 Clemmer, L. E. "Thermomechanical Response of a Viscoelastic Cantilever Plate," Bulletin of the 4th Meeting ICRPC Working Group on Mechanical Behavior, October 1965, pp. 371-382

An analytical study of the thermomechanical response of a viscoelastic cantilever plate under the action of steady-state cyclic loading is presented. This model may be considered as providing a first approximation for estimating dissipative heating due to propellant grain star-point vibration. The energy equation is derived considering dissipation and temperature-dependent material properties. The material is assumed to obey linear viscoelastic theory and to be thermorheologically simple. Two cases are treated 1) constant amplitude harmonic force input and 2) inertial loading in which the mass of the plate is approximated by a concentrated mass at the free edge of the cantilever. Analytical solutions for adiabatic heating have been obtained and numerical results are given using thermal and mechanical properties of a solid propellant. The amount of heating, as measured by the maximum temperature in the plate, is compared with the temperature rise in a viscoelastic slab subjected to simple cyclic shear loading.

IV-016 Hung, N. C. "Dissipation Function in Thermomechanical Phenomena of Viscoelastic Solids," Technical Report No. 1, Department of the Aerospace and Mechanical Engineering Sciences, University of California, San Diego, La Jolla, Calif., October 1966

In this paper, an explicit form of the dissipation function associated with thermomechanical phenomena of viscoelastic solids is derived. This function is expressed in terms of the observable quantities such as stress rates, strain rates, and their second time derivatives, etc. The formulation is based on the theory of irreversible thermodynamics of deformable bodies developed by Biot and generalized by Ziegler and Schapery. The proposed dissipation function can be used conveniently for both experimental and theoretical purposes.

IV-017

Huang, N C , Lee, E H "Analysis of Coupled Thermo-Viscoelastic Response of Rods and Slabs Subjected to Cyclic Loading," CPIA Publication No 119, Vol 1, Proceedings of the 5th ICPG Meeting Mechanical Behavior Working Group, October 1966, p 339

This report deals with the problem of longitudinal waves in a viscoelastic rod caused by a sinusoidal stress applied at one end. It is assumed that a quasi-steady state of wave motion follows after a few cycles of oscillation, with the stress and strain effectively periodic, but with a slow change in amplitude associated with the slow rise in temperature due to the continuous transformation of mechanical energy into heat. The mechanical properties of the rod are temperature dependent so that the wave speed and its shape change with time. Since the temperature at one end of the rod is fixed and a radiation condition is prescribed at the other end, heat flux flows out from both ends. Finally, a steady state of temperature distribution is reached. The object of this report is to find the temperature distribution as well as the stress distribution at various times

IV-018

Huang, N C., Lee, E H.: "Thermomechanical Coupling Behavior of Viscoelastic Rods Subjected to Cyclic Loading," University of California, San Diego, LaJolla, Dept of the Aerospace and Mechanical Engineering Sciences, Journal of Applied Mechanics, March 1967, pp 127-132

The problem of longitudinal oscillation of a viscoelastic rod of finite length including the effect of thermomechanical coupling was studied. The material is assumed to be thermorheologically simple. The almost steady oscillation superposed on a slowly varying temperature distribution permits representation as a boundary-value problem which is solved numerically by iterative procedures. Calculations are made for different stress levels and frequencies. It is found that the temperature increases considerably after a length of time of vibration although the stress level is low. A steady state of temperature can be reached if the temperature at one end of the rod is fixed and a radiation boundary condition is prescribed at the other end.

IV-019

Tauchert, T R "Heat Generation in a Viscoelastic Solid," Acta Mechanica, Vol 3, No 4, 1967

The temperature distributions in a viscoelastic solid which result from mechanical deformations are investigated. The solid is assumed to be isotropic and linear. A coupled energy equation is used to calculate the transient and steady-state temperature distributions in a thin-walled tube subjected to torsional oscillations. The heating is determined solely by the materials mechanical behavior and by consistency with thermodynamics

IV-020

Torvik, Peter J. "Temperature Rise and Stresses due to Internal Heating," Air Force Inst of Tech, Wright-Patterson AFB, Ohio, School of Engineering, Technical Report, January 1968, AD-664 052

A finite amount of heat is generated in each cycle when a material is subjected to a cycled load. This internal heat generation causes changes in the temperature of the body which, under certain conditions, may be appreciable. Expressions are developed for the temperature distribution and resulting thermal stress, and from them, the parameters which determine the magnitude of temperature rise and stress are obtained. Quantitative agreement with previous experiments exists in the area of temperature rises. Thermal stresses are appreciable only in very unusual circumstances

IV-021

Tauchert, T R "Transient Temperature Distributions in Viscoelastic Solids to Cyclic Deformations," Acta Mechanica, Vol 6, No 2-3, 1968, pp 239-252

Study of the effect of heat dissipation resulting from deformation of a viscoelastic solid on the temperature field in the solid. The coupled heat equation is used to calculate the transient and steady-state temperature distributions in two situations: (1) simple shear of an infinite slab, and (2) torsional oscillation of a circular rod

IV-022

Cost, Thomas L. "Thermomechanical Coupling Phenomena in Non-Isothermal Viscoelastic Solids," Rohm and Haas Company, Pedstone Research Laboratories, Huntsville, Alabama, Technical Report S-226, August 1969, 122p

The increasing use of viscoelastic materials in cyclic loading applications has created a need for an understanding of the thermomechanical coupling phenomenon by which mechanical energy exerted in deforming a material is converted into thermal energy. Three basic approaches to a mathematical analysis of this phenomenon, presented by Biot, Lekhnitskii, and Stavermann and Schwarzl, are reviewed and discussed in a similar mathematical notation is possible. The basic constitutive behavior, including dissipative effects, of "thermorheologically simple" materials is developed by use of each of these theories. The relation of the three approaches to one another is demonstrated in this development. The theories are shown to produce similar forms for the constitutive relations although the basic approaches are considerably different. The significance of the derived dissipation function is investigated by solving the energy equation, with the dissipation function included, for the case of a solid circular cylinder undergoing torsional vibrations. It is shown that thermorheologically simple materials produce less heat than isothermal viscoelastic materials under similar conditions. An experiment was performed on a solid circular cylinder of a polyurethane rubber by applying a periodic torsional displacement to one end of the cylinder while holding the other end fixed. The temperature was recorded at several stations in the cylinder as a function of time. The experimental results indicate that the heat generated in viscoelastic materials by cyclic loading at frequencies of about 10 Hz and strain magnitudes of about 5% can produce temperature changes of at least 30°F

IV-023

Kovlenko, A D , Tiuplia, V. I. "Propagation of Longitudinal Waves in a Viscoelastic Cylinder with Allowance for Thermomechanical Coupling," Prikladnaya Mekhanika, Vol 6, January 1970, pp 3-9, (in Russian).

Analysis of the influence of the interaction between the strain and temperature fields on the propagation of harmonic viscoelastic longitudinal waves in an infinite solid cylinder insulated at the surface. The problem is solved in linear formulation without allowance for the temperature dependence of the thermophysical and mechanical characteristics of the medium. Approximate expressions for the phase velocities and attenuation coefficients are obtained for a predominantly viscoelastic wave and a wave similar in nature to a pure thermal wave. Numerical values for these wave characteristics are obtained for a modified viscoelastic longitudinal wave propagating in a polyethylene cylinder

IV-024

Achenbach, J D., Herrmann, G "Propagation of Second-order Thermomechanical Disturbances in Viscoelastic Solids," IUTAM Symposium East Kilbride, Proceedings June 25-28, 1968, Springer-Verlag, New York.

The change of magnitude of a strain discontinuity is studied as it propagates in a heat conducting viscoelastic medium. The paper includes an investigation of the effects of thermomechanical coupling, viscous flow, second-order strains, and temperature-dependent material properties.

REPRODUCIBILITY OF THE  
ORIGINAL PAGE IS POOR

IV-025

Cost, Thomas L. "Dissipation of Mechanical Energy in Viscoelastic Materials," JANNF Mechanical Behavior Working Group 8th Meeting, Chemical Propulsion Information Agency, Johns Hopkins University, Applied Physics Lab., Silver Spring, Md., CPIA Publication No. 193, Vol. 1, March 1970.

When solid propellant rocket motors experience sustained cyclic loads, dissipation of part of the mechanical energy imparted to the propellant grain results in significant amounts of heat being generated. This heat strongly influences the strength and rigidity of solid propellant. No additional characterization of the solid propellant is required to describe the dissipative behavior in an analysis beyond that necessary to describe the stress constitutive equations. Results from a cyclic loading experiment on an unfilled polyurethane rubber indicate that sufficient heat is generated in viscoelastic materials tested at frequencies of about 1000 cpm and at strain levels of about 5% to produce temperature increases of about 30°F. A prediction of the amount of heat generated depends upon whether or not the viscoelastic mechanical properties are assumed to be temperature dependent. Predictions based upon assumed isothermal behavior appear to overestimate the amount of heat generated whereas the assumption of "thermorheologically simple" behavior results in an underestimate.

IV-026

Tauchert, T. R. "Thermomechanical Coupling in Viscoelastic Solids," Thermoviscoelasticity (IUTAM Symposium 1968 East Kilbride), edited by B. A. Boley, Springer-Verlag, New York, 1970, pp. 316-326.

Experimental data on the heat generated in polymeric specimens undergoing oscillatory deformations are presented. Various factors which affect the hysteresis, including strain amplitude, frequency and mode of loading, and ambient temperature are investigated. It is observed that not all of the energy added to a specimen during a cycle of deformation is dissipated as heat. A comparison of theory and experiment demonstrates that the remaining (or "stored") energy must be accounted for in predicting the thermomechanical behavior of such materials.

IV-027

Mukherjee, S.: "Variational Principles in Dynamic Thermoviscoelasticity," SUDAM Report No. 72-3, Stanford University, April 1972

Dual variational principles for steady state wave propagation in three dimensional thermoviscoelastic media are presented. The first one, for the equations of motion, involves only the complex displacement function. The second principle is for the energy equation. The specialized versions of these principles in two dimensional polar coordinates and then in one dimension are obtained. A one dimensional example, that of wave propagation in a thermoviscoelastic rod insulated on its lateral surface and driven by a sinusoidal stress at one end, is solved using the Rayleigh-Ritz method. The displacement and temperature functions are expressed as series of polynomials. Successive approximations for the solution are compared with a solution obtained by a method of finite differences, and an estimate of the degree of accuracy as a function of the number of terms taken in the series is obtained. It is found that as long as the spatial distribution of stress and temperature are sufficiently smooth, rapid convergence to the correct solution is obtained. If the stress is a rapidly oscillating function of the distance along the rod, polynomials are no longer efficient and other test functions must be chosen.

IV-028

Mukherjee, S. "Thermal Instabilities in A Viscoelastic Rod Under Cyclic Loading," SUDAM Report No. 72-9, Stanford University, June 1972

Thermal instabilities in a viscoelastic rod under cyclic loading are discussed by determining the stresses and temperature in a viscoelastic rod insulated on its lateral surface and driven by a sinusoidal stress at one end. Temperature dependence of the complex Young's modulus of the rod and the effect of thermo-mechanical coupling are included in the analysis. A method of finite differences is used to directly determine the steady state stresses and temperature without obtaining the complete time history of the process. The iterative algorithm used is very useful and converges rapidly for a wide range of driving stress amplitudes and frequencies. It is found that rapid rise of temperature to dangerous levels occurs for relatively low values of driving stress amplitudes especially if the driving frequency is close to one of the critical frequencies of the rod. Drastic softening of the rod leads to large strains. Thus, failure of the rod could occur at low values of the driving stress.

#### SEE ALSO ABSTRACTS NOS.:

I -017, -019, -020, -046, -056, -062

II -086, -088, -093

III -025, -033

REPRODUCIBILITY OF THE  
ORIGINAL PAGE IS POOR

V. AUTHOR INDEX

Achenbach, J. D. ....II-014, -015, -016, -017, -018, -019,  
-020, -021, -022, -023, -024, -025, -026,  
III-010, IV-014, -024

Adicoff, A. ....I-051

Anderson, G. ....II-033, -034

Anderson, J. M. ....II-058, -085  
Anon .....II-095  
Arveson, W. B. ....II-049

Atlanta Research Corporation...I-001, -002, -003, -004, -005, -006

Baker, W. E. ....II-059 >

Baltrukonis, J. H. ....I-033, II-001, -002, -003, -004, -009,  
-010, -011, -012, -013, -065

Barenblatt, G. I. ....III-024

Barrett, R. E. ....II-048

Becker, E. B. ....II-060, III-017

Benbow, J. J. ....I-024

Bennett, S. J. ....I-026 —

Beyer, R. B. ....I-053

Biot, M. A. ....III-004

Bland, D. R. ....I-022, -023, III-009

Blatz, P. J. ....I-034

Blomquist, D. S. ....I-033, -063

Bollard, R. J. H. ....II-067, -078, -080

Bornstein, G. A. ....II-071, -072, -073, -074

Briar, H. P. ....I-047

Britton, S. C. ....IV-010

Burton, J. D. ....II-052

Bushness, D. ....II-077

Bynum, D., Jr. ....II-054

Cantey, D. .... I-015, -018, -019, -020, -037, -046,  
-056, IV-011

Chae, Y. S. .... III-018

Chao, C. C. .... III-010

Chang, C. H. .... II-032, -039

Chiang, F. .... II-037

Chappell, R. N. .... II-051

Chou, F. H. .... II-023

Clauser, J. F. .... I-060

Clemmer, L. E. .... IV-015

Connor, J. J. .... II-061, -089

Cook, K. S. .... II-051

Cost, T. L. .... III-013, -017, IV-022, -025

CPIA .... I-061

Daly, J. M. .... II-059

Daniel, I. M. .... II-043

Davis, J. L. .... III-022

Dean, N. W. .... III-030

Dill, E. H. .... II-068

Drent, R. H. J. W. A. .... I-049

Duffin, R. J. .... III-034

Dunham, R. S. .... II-063

Durelli, A. J. .... II-066

Elder, A. S. .... II-044

Ferry, J. D. ....I-021  
Fisher, G. M. C. ....III-020  
Fishman, N. ....I-058  
Fitzgerald, J. E. ....I-016, -017, -021, -050, II-028, -078,  
-080, -086, -088, -033  
Francis, E. C. ...., I-054  
Frazee, J. D. ....II-052  
Freudenthal, A. M. ....II-045, -046, -091

Garrison, U. E. ...., II-053  
Gatignol, P. ...., III-019  
George, N. ...., I-034  
Glaus, R. D. ...., I-030, III-008  
Goldberg, W. ...., III-030  
Gottenberg, W. G. ...., I-044, II-001, -004  
Goudreau, G. L. ...., II-062  
Graffi, D. ...., III-028  
Graham, P. H. ...., I-009, -010, -035, -038  
Grandine, L. D. ...., I-021  
Gratch, S. ...., IV-006, -013  
Gurtin, M. E. ...., III-006

Henry, L. A. ...., II-045, -046, -091  
Herrmann, G. ...., II-018, IV-014, -024  
Hill, J. L. ...., II-060  
Hilton, H. H. ...., II-083, -084, III-001  
Hoebel, J. F. ...., I-067

Hoekel, T. F. ....II-057  
Hopkins, I. L. ....III-031  
Huang, N. C. ....III-032, IV-016, -017, -018  
Hufferd, W. L. ....I-069; II-086, -088  
Humphries, J. S. ....IV-005  
Hunter, S. C. ....II-064, III-007, -0111

IBM Federal Systems Division ...II-081

Jones, J. P. ....II-067  
Jones, J. W. ....I-025, -046  
Jones, W. B. ....II-052

Kelkar, V. S. ....II-038  
Kelley, F. N. ....I-043  
Kingsbury, H. B. ....II-047  
Knauss, W. G. ....I-027, -060, -078, -080  
Knobelock, G. W. ....II-035  
Ko, W. L. ....I-034  
Kolsky, H. ....I-048  
Kostryko, G. J. ....I-064  
Kovalenko, A. D. ....IV-023  
Kruse, R. B. ....I-062

Landel, R. F. ....I-059, -060  
Laura, P. A. ....II-031  
Lawrence, W. F. St. ....I-041, -052

Layton, L. H. ....I-026, -029  
Lee, E. H. ....I-022, I-023, II-091, III-009, -032,  
IV-017, -018  
Lee, T. M. ....I-032  
Leeming, H. ....II-018, -079, -080  
Leitman, M. J. ....III-020  
Lemon, R. H. ....I-063  
Levy, A. et al. ....II-094  
Lepie, A. ....I-051  
Lianis, G. ....II-069  
Lipton, L. ....II-072  
Liu, C. K. ....II-032  
Lockheed Propulsion Co. ....I-055  
Lockett, F. J. ....III-006

Magrab, E. B. ....I-033, II-011, -029, -041, III-027  
Malone, D. W. ....II-061  
Marinescu, Al. ....II-030, -042  
Markovitz, H. ....I-031  
Marshall, J. ....III-020  
Martin, C. J. ....IV-005  
Moskvitin, V. V. ....II-093  
Mukherjee, S. ....IV-027, -028  
Murphy, A. ....I-034

NASA .....II-075, -077  
Nicholson, D. E. ....I-063  
Nielsen, L. E. ....I-042

Noel, J. .... II-080  
Nowacki, W. K. .... III-025

Ochsner, D. J. .... III-027

Pan, H. H. .... II-056  
Parr, C. H. .... II-082, 84A  
Percival, C. M. .... III-016  
Petrof, R. C. .... IV-006  
Pister, K. S. .... II-068, -078, -080

Raniecki, B. .... III-025  
Rinde, J. M. .... II-058  
Robertson, S. R. .... II-090  
Robinson, C. N. .... I-007, -008, -009, -010, -035, -038  
Robinson, E. W. .... II-071  
Roscoe, R. .... III-026

Sackman, J. L. .... II-068  
Sann, R. J. .... II-036, -040, -055  
Sarkar, S. K. .... II-050  
Schapery, R. A. .... II-071, -072, -078, -080, III-003, IV-001,  
-004, -007, -008, -009, -011  
Schwarzl, F. R. .... III-023, -029  
Sciammarella, C. A. .... II-037, -039  
Schreiner, R. N. .... II-004  
Shaffer, B. W. .... II-036, -040, -055

- Shahady, P. A. ....II-031  
Sharma, M. G. ....I-036, -041, -052  
Sheppard, G. A. ....I-026  
Shittier, J. S. ....II-067  
Shulman, Y. ....II-035  
Smith, J. R. ....I-011, -012, -013, -014, -039, -057  
Smith, T. L. ....I-011, -012, -014, -028, -039, -057, -065,  
                  III-002, -035  
Snowdon, J. C. ....III-012  
Soler, A. L. ....II-047  
Stoker, J. H. ....I-068  
Struik, L. C. E. ....III-021, -029  
Suhubi, E. S. ....IV-003  
Sun, T. ....II-025
- Tasi, J. ....IV-002  
Tauchert, T. R. ....IV-012, -019, -021, -026  
Taylor, R. L. ....II-068  
Tiuptia, V. I. ....IV-023  
Tormey, J. F. ....IV-010  
Torvic, P. J. ....IV-020
- Valanis, K. C. ....II-069  
Van der Wal, C. W. ....I-049  
Vleysseyre, R. ....I-040  
Vinson, J. R. ....II-047  
Volterra, E. ....I-045

Wagner, F. R. ....I-066, II-076  
Wiegand, J. H. ....I-047  
Williams, M. L. ....I-021, II-026A, -070, -078, -080, III-005  
Wilson, E. ....II-027  
Wolosewick, R. M. ....IV-013  
  
Yoh, J. ....I-034

APPENDIX B

DYNVIS  
COMPUTER PROGRAM  
FOR SRM PROPELLANT  
DYNAMIC RESPONSE

B - 1

DYNVIS  
PROGRAM DOCUMENTATION

### B-1.1 GENERAL DISCUSSION

The SRM propellant dynamic response model is given by the power-law

$$E(\omega a_T) = E_0 (\omega a_T)^n \quad (B-1)$$

where the temperature shift-factor is given by the modified power-law

$$a_T = \left( \frac{T_R - T_a}{T - T_a} \right)^m \quad (B-2)$$

where

$E_0$  = dynamic modulus at a temperature-reduced frequency  $\omega a_T = 1$

$\omega$  = frequency

$n$  = log-log slope of master dynamic modulus curve versus temperature-reduced frequency,  $\omega a_T$

$T_R$  = reference temperature at which master dynamic modulus curve versus temperature-reduced frequency was generated,

$T_a, m$  = experimentally determined constants chosen to represent the temperature shift-factor by Eq. (B-2).

Equation (B-1) is used to represent the real or imaginary part of the tensile or shear modulus.

A computer code was written for Eqs. (B-1) and (B-2) using standard ANSI FORTRAN IV. The code has three options:

- (1) A least-squares curve-fit of Eq. (B-1) may be accomplished to determine the parameters  $E_0$  and  $n$ .
- (2) Simultaneous with the curve-fitting, calculations of the dynamic modulus may be made at any combination of frequencies and temperatures up to a maximum of 20 each.
- (3) Calculations of the dynamic modulus may be made without the curve-fitting at any combination of frequencies and temperatures up to a maximum of 20 each.

In all three options, calculations may be made with the real or imaginary part of the dynamic modulus or both.

Explicit definition of the input-output variables is given with the user's manual in Appendix B-2.

The least-squares curve-fitting option can be used in two ways. On the one hand, a master dynamic modulus curve versus temperature-reduced frequency may be constructed from dynamic tests conducted at several temperatures. Data points (up to a maximum of 20) from this curve are then input as a function of temperature-reduced frequency and the least-squares curve fit carried out to determine the coefficient  $E_0$  and the exponent  $n$  in the constitutive relation, Eq. (B-1). In this procedure Eq. (B-2) must be fit to the temperature shift-factor curve generated

during construction of the master dynamic modulus curve and the parameters  $T_a$  and  $m$  in Eq. (B-2), determined for input to the code.

Alternatively, if the curve-fit is desired at a single temperature, then this temperature may be defined as the reference temperature with  $T = T_R$  in Eq. (B-2) and, thus,  $a_T = 1$  in Eq. (B-1). Any values may then be input for  $T_a$  and  $m$ , including zero;

The curve-fitting procedure is carried out in terms of the temperature-reduced frequency,  $\omega a_T$ , with respect to a given reference temperature,  $T_R$ . In calculating dynamic response, however, the actual frequency,  $\omega$ , at the temperature,  $T$ , where the response is desired is input and the temperature shift-function calculated according to Eq. (B-2). In this case it is necessary to input the reference temperature,  $T_R$ , and the parameters  $T_a$  and  $m$ . If calculations are desired at a single temperature where  $E_0$  and  $n$  are known, or are to be determined from the program, then, the temperature  $T$  can be set equal to the reference temperature  $T_R$  and arbitrary values input for  $T_a$  and  $m$ .

The code has the output formatted in SI units; however, it may be seen that Eq. (B-2) only involves temperature differences and the units of the dynamic modulus are carried in the coefficient  $E_0$  in Eq. (B-1). Therefore, the calculations within the computer code are actually independent of the system of units used.

## B-1.2 LEAST-SQUARES CURVE-FIT

The least-squares curve-fit of Eq. (B-1) is accomplished in the following fashion. Defining  $t \equiv wa_T$ , then Eq. (B-1) may be written in the form

$$\log_e E(t) = \log_e E_0 + n \log_e(t) \quad (B-3)$$

where  $\log_e$  denotes the natural logarithm. Next, defining  $S$  by

$$S = \sum_{i=1}^N [\log_e E(t_i) - \log_e E_0 - n \log_e(t_i)]^2 \quad (B-4)$$

and setting  $dS/dE_0 = 0$ , it follows that

$$\begin{aligned} N \log_e E_0 + \sum_{i=1}^N n \log_e(t_i) &= \sum_{i=1}^N n (\log_e(t_i))^2 \\ &= \sum_{i=1}^N [(\log_e E(t_i)) (\log_e(t_i))] \end{aligned} \quad (B-5)$$

The solution for  $\log_e E_0$  and  $n$  from Eqs. (B-5) and (B-6) is then given by

$$\log_e E_0 = \frac{\begin{vmatrix} \sum_{i=1}^N \log_e E(t_i) & \sum_{i=1}^N \log_e(t_i) \\ \sum_{i=1}^N [\log_e E(t_i) \log_e(t_i)] & \sum_{i=1}^N (\log_e(t_i))^2 \end{vmatrix}}{\Delta} \quad (B-7)$$

and

$$n = \frac{\begin{vmatrix} N & \sum_{i=1}^N \log_e E(t_i) \\ \sum_{i=1}^N \log_e (t_i) & \sum_{i=1}^N [\log_e E(t_i) \log_e (t_i)] \end{vmatrix}}{\Delta}$$

where

$$\Delta = \begin{vmatrix} N & \sum_{i=1}^N \log_e (t_i) \\ \sum_{i=1}^N \log_e (t_i) & \sum_{i=1}^N (\log_e (t_i))^2 \end{vmatrix}$$

B - 2

DYNVIS  
USER'S MANUAL

B\_9  
 QELT,L \*DYNVIS.USER  
 ELTUT7 RLIB70 05/08-15:13:10-(0,)  
 000001 000 C\*\*\* \*\*\*USE00100  
 000002 000 C\*\*\* \*\*\*USE00200  
 000003 000 C\*\*\*  
 000004 000 C\*\*\*  
 000005 000 C\*\*\* SOLID PROPELLANT VISCOELASTIC DYNAMIC RESPONSE MODEL \*\*\*USE00500  
 000006 000 C\*\*\* \*\*\*USE00600  
 000007 000 C\*\*\* \*\*\*USE00700  
 000008 000 C\*\*\* \*\*\*USE00800  
 000009 000 C\*\*\* \*\*\*USE00900  
 000010 000 C\*\*\* DEVELOPED BY \*\*\*USE01000  
 000011 000 C\*\*\* \*\*\*USE01100  
 000012 000 C\*\*\* W L HUFFED \*\*\*USE01200  
 000013 000 C\*\*\* \*\*\*USE01300  
 000014 000 C\*\*\* \*\*\*USE01400  
 000015 000 C\*\*\* \*\*\*USE01500  
 000016 000 C\*\*\* J. E. FITZGERALD & ASSOCIATES \*\*\*USE01600  
 000017 000 C\*\*\* ATLANTA, GEORGIA \*\*\*USE01700  
 000018 000 C\*\*\* \*\*\*USE01800  
 000019 000 C\*\*\* \*\*\*USE01900  
 000020 000 C\*\*\* \*\*\*USE02000  
 000021 000 C\*\*\* USER'S MANUAL \*\*\*USE02100  
 000022 000 C\*\*\* \*\*\*USE02200  
 000023 000 C\*\*\* \*\*\*USE02300  
 000024 000 C\*\*\* THIS PROGRAM PERFORMS A LEAST-SQUARES CURVE-FIT TO DYNAMIC \*\*\*USE02400  
 000025 000 C\*\*\* LABORATORY TEST DATA TO DETERMINE THE COEFFICIENTS IN A \*\*\*USE02500  
 000026 000 C\*\*\* POWER LAW REPRESENTATION OF THE FORM: \*\*\*USE02600  
 000027 000 C\*\*\*  
 000028 000 C\*\*\*  $E = E_{ZERO} * (\Omega * \alpha_{SUBT})^{** N}$  . (1) \*\*\*USE02800  
 000029 000 C\*\*\* \*\*\*USE02900  
 000030 000 C\*\*\* AND/OR MAKES PREDICTIONS OF THE REAL AND/OR IMAGINARY \*\*\*USE03000  
 000031 000 C\*\*\* COMPONENTS OF THE DYNAMIC MODULUS. THE PROGRAM IS VALID \*\*\*USE03100  
 000032 000 C\*\*\* FOR THE REAL AND/OR IMAGINARY COMPONENTS OF THE DYNAMIC \*\*\*USE03200  
 000033 000 C\*\*\* TENSILE OR SHEAR MODULI. \*\*\*USE03300  
 000034 000 C\*\*\* \*\*\*USE03400  
 000035 000 C\*\*\* TEMPERATURE IS ACCOUNTED FOR THROUGH THE USE OF A TIME - \*\*\*USE03500  
 000036 000 C\*\*\* TEMPERATURE SHIFT FUNCTION REPRESENTED IN THE FORM OF A \*\*\*USE03600  
 000037 000 C\*\*\* MODIFIED POWER LAW: \*\*\*USE03700

REPRODUCIBILITY OF THE  
 ORIGINAL PAGE IS POOR

B  
10

000038	000	C***				***USE03800
000039	000	C***				***USE03900
000040	000	C***				***USE04000
000041	000	C***	WHERE			***USE04100
000042	000	C***		TREF = REFERENCE TEMPERATURE (DEGREES KELVIN).	(2)	***USE04200
000043	000	C***				***USE04300
000044	000	C***		TA,TM = EXPERIMENTALLY DETERMINED PARAMETERS TO		***USE04400
000045	000	C***		FIT EQ. (2) TO THE ASUBT SHIFT CURVE		***USE04500
000046	000	C***		VERSUS TEMPERATURE.		***USE04600
000047	000	C***				***USE04700
000048	000	C***		THE CURVE-FITTING IS CARRIED OUT IN TERMS OF THE		***USE04800
000049	000	C***		TEMPERATURE - REDUCED FREQUENCY, OMEGA * ASUBT; BUT		***USE04900
000050	000	C***		PREDICTIONS ARE MADE IN TERMS OF ACTUAL FREQUENCY AT ANY		***USE05000
000051	000	C***		DESIRED TEMPERATURE. INPUT VALUES OF DYNAMIC MODULI FOR		***USE05100
000052	000	C***		THE CURVE-FITTING SHOULD BE IN KILONEWTONS PER SQUARE		***USE05200
000053	000	C***		METER AND TEMPERATURE IN DEGREES KELVIN. (ALTHOUGH, THE		***USE05300
000054	000	C***		INTERNAL LOGIC IS VALID AND WILL SATISFACTORILY EXECUTE		***USE05400
000055	000	C***		FOR ANY CONSISTENT SET OF UNITS)		***USE05500
000056	000	C***				***USE05600
000057	000	C***				***USE05700
000058	000	C***				***USE05800
000059	000	C***				***USE05900
000060	000	CAKD	COLUMNS	FORMAT	IN F O R M A T I O N	USE06000
000061	000	---	-----	-----		USE06100
000062	000					USE06200
000063	000		1	1 - 80	20A4 TITLE INFORMATION. PRINTED WITH OUTPUT.	USE06300
000064	000					USE06400
000065	000		2	1 - 5	I5 NRFIN = NUMBER OF TEMPERATURE - REDUCED	USE06500
000066	000				FREQUENCIES AT WHICH THE REAL	USE06600
000067	000				PART OF THE DYNAMIC MODULUS IS	USE06700
000068	000				TO BE CURVE-FIT.	USE06800
000069	000					USE06900
000070	000		2	6 - 10	I5 NRFOUT = NUMBER OF ACTUAL FREQUENCIES	USE07000
000071	000				(NOT TEMPERATURE - REDUCED	USE07100
000072	000				FREQUENCIES) AT WHICH	USE07200
000073	000				CALCULATIONS OF THE REAL PART	USE07300
000074	000				OF THE DYNAMIC MODULUS ARE	USE07400
000075	000				DESIRED.	USE07500
000076	000					USE07600

PRODUCIBILITY OF THE  
ORIGINAL PAGE IS POOR

000077 000 2 11 - 15 . I5 NRTEMP = NUMBER OF TEMPERATURES FOR USE07700  
 000078 000 WHICH CALCULATIONS OF THE REAL USE07800  
 000079 000 PART OF THE DYNAMIC MODULUS USE07900  
 000080 000 ARE DESIRED. USE08000  
 000081 000  
 000082 000 2 16 - 20 I5 NIFIN = NUMBER OF TEMPERATURE - REDUCED USE08200  
 000083 000 FREQUENCIES AT WHICH THE USE08300  
 000084 000 IMAGINARY PART OF THE DYNAMIC USE08400  
 000085 000 MODULUS IS TO BE CURVE-FIT. USE08500  
 000086 000  
 000087 000 2 21 - 25 I5 NIFOUT = NUMBER OF ACTUAL FREQUENCIES USE08700  
 000088 000 (NOT TEMPERATURE - REDUCED USE08800  
 000089 000 FREQUENCIES) FOR WHICH USE08900  
 000090 000 CALCULATIONS FOR THE IMAGINARY USE09000  
 000091 000 PART OF THE DYNAMIC MODULUS USE09100  
 000092 000 ARE DESIRED. USE09200  
 000093 000  
 000094 000 2 26 - 30 I5 NITEMP = NUMBER OF TEMPERATURES FOR USE09400  
 000095 000 WHICH CALCULATIONS OF THE USE09500  
 000096 000 IMAGINARY PART OF THE DYNAMIC USE09600  
 000097 000 MODULUS ARE DESIRED. USE09700  
 000098 000  
 000099 000 2 31 - 40 E10.0 TR = REFERENCE TEMPERATURE AT WHICH USE09900  
 000100 000 MASTER DYNAMIC MODULUS VERSUS USE10000  
 000101 000 TEMPERATURE - REDUCED FREQUENCY USE10100  
 000102 000 CURVE WAS GENERATED. (UNITS - USE10200  
 000103 000 DEGREES KELVIN) USE10300  
 000104 000  
 000105 000 2 41 - 50 E10.0 TA = EXPERIMENTALLY DETERMINED USE10500  
 000106 000 PARAMETER CHOSEN TO FIT EQ. (2) USE10600  
 000107 000 ABOVE TO EXPERIMENTAL TIME - USE10700  
 000108 000 TEMPERATURE SHIFT FUNCTION USE10800  
 000109 000 CURVE. (UNITS - DEGREES KELVIN) USE10900  
 000110 000  
 000111 000 2 51 - 60 E10.0 TM = EXPERIMENTALLY DETERMINED USE11100  
 000112 000 EXPONENT CHOSEN TO FIT EQ. (2) USE11200

REPRODUCIBILITY OF THE  
 ORIGINAL PAGE IS POOR

000113 000 ABOVE TO EXPERIMENTAL TIME - USE11300  
 000114 000 TEMPERATURE SHIFT FUNCTION USE11400  
 000115 000 CURVE. (UNITS - DIMENSIONLESS) USE11500  
 000116 000 USE11600  
 000117 000 5 1 - 80 8E10.0 RMOD(I) (I=1,NRFIN) = VALUES OF THE USE11700  
 000118 000 REAL PART OF THE DYNAMIC USE11800  
 000119 000 MODULUS TO BE CURVE-FIT. USE11900  
 000120 000 (UNITS - KILONEWTONS PER SQUARE USE12000  
 000121 000 METER) USE12100  
 000122 000 USE12200  
 000123 000 4 1 - 80 3E10.0 RFREQ(I) (I=1,NRFIN) = VALUES OF USE12300  
 000124 000 TEMPERATURE - REDUCED USE12400  
 000125 000 FREQUENCIES FOR WHICH THE REAL USE12500  
 000126 000 PART OF THE DYNAMIC MODULUS IS USE12600  
 000127 000 TO BE CURVE-FIT. (UNITS - USE12700  
 000128 000 HERTZ) USE12800  
 000129 000 USE12900  
 000130 000 5 1 - 80 8E10.0 IMOD(I) (I=1,NIFIN) = VALUES OF THE USE13000  
 000131 000 IMAGINARY PART OF THE DYNAMIC USE13100  
 000132 000 MODULUS TO BE CURVE-FIT. USE13200  
 000133 000 (UNITS - KILONEWTONS PER SQUARE USE13300  
 000134 000 METER) USE13400  
 000135 000 USE13500  
 000136 000 6 1 - 80 8E10.0 IFREQ(I) (I=1,NIFIN) = VALUES OF THE USE13600  
 000137 000 TEMPERATURE - REDUCED USE13700  
 000138 000 FREQUENCIES FOR WHICH THE USE13800  
 000139 000 IMAGINARY PART OF THE DYNAMIC USE13900  
 000140 000 MODULUS IS TO BE CURVE-FIT. USE14000  
 000141 000 (UNITS - HERTZ) USE14100  
 000142 000 USE14200  
 000143 000 7 1 - 10 E10.0 ERZERO = COEFFICIENT IN POWER LAW FOR USE14300  
 000144 000 THE REAL PART OF THE DYNAMIC USE14400  
 000145 000 MODULUS, AS GIVEN BY EQ. (1) USE14500  
 000146 000 ABOVE. (UNITS - KILONEWTONS PER USE14600  
 000147 000 SQUARE METER) USE14700  
 000148 000 USE14800  
 000149 000 7 11 - 20 E10.0 NREXP = EXPONENT IN THE POWER LAW FOR USE14900  
 000150 000 THE REAL PART OF THE DYNAMIC USE15000  
 000151 000 MODULUS, AS GIVEN BY EQ. (1) USE15100  
 000152 000 ABOVE. (UNITS - DIMENSIONLESS) USE15200

REPRODUCIBILITY OF THE  
 ORIGINAL PAGE IS POOR

000153	000					USE15300
000154	000					USE15400
000155	000					USE15500
000156	000					USE15600
000157	000					USE15700
000158	000					USE15800
000159	000					USE15900
000160	000	7	21 - 30	E10.0	EIZERO = COEFFICIENT IN THE POWER LAW FOR THE IMAGINARY PART OF THE DYNAMIC MODULUS, AS GIVEN BY EQ. (1) ABOVE. (UNITS - KILO-NEWTONS PER SQUARE METER)	USE16000
000161	000					USE16100
000162	000					USE16200
000163	000					USE16300
000164	000					USE16400
000165	000					USE16500
000166	000	8	1 - 80	BE10.0	RTEMP(I) (I=1,NRTEMP) = VALUES OF TEMPERATURES AT WHICH CALCULATIONS OF THE REAL PART OF THE DYNAMIC MODULUS ARE DESIRED. (UNITS - DEGREES KELVIN)	USE16600
000167	000					USE16700
000168	000					USE16800
000169	000					USE16900
000170	000					USE17000
000171	000					USE17100
000172	000	9	1 - 80	BE10.0	RFREQO(I) (I=1,NRFOUT) = VALUES OF THE ACTUAL FREQUENCIES (NOT THE TEMPERATURE - REDUCED FREQUENCIES) FOR WHICH CALCULATIONS OF THE REAL PART OF THE DYNAMIC MODULUS ARE DESIRED. (UNITS - HERTZ)	USE17200
000173	000					USE17300
000174	000					USE17400
000175	000					USE17500
000176	000					USE17600
000177	000					USE17700
000178	000					USE17800
000179	000					USE17900
000180	000	10	1 - 80	BE10.0	ITEMP(I) (I=1,NITEMP) = VALUES OF THE TEMPERATURES AT WHICH CALCULATIONS OF THE IMAGINARY PART OF THE DYNAMIC MODULUS ARE DESIRED. (UNITS - DEGREES KELVIN)	USE18000
000181	000					USE18100
000182	000					USE18200
000183	000					USE18300
000184	000					USE18400
000185	000					USE18500
000186	000					USE18600
000187	000	11	1 - 80	BE10.0	IFREQO(I) (I=1,NIFOUT) = VALUES OF THE ACTUAL FREQUENCIES (NOT THE TEMPERATURE - REDUCED FREQUENCIES) FOR WHICH CALCULATIONS OF THE IMAGINARY	USE18700
000188	000					USE18800
000189	000					USE18900
000190	000					USE19000
000191	000					USE19100

REPRODUCIBILITY OF THE  
ORIGINAL PAGE IS POOR

000192 000 PART OF THE DYNAMIC MODULUS USE19200  
 000193 000 ARE DESIRED. (UNITS - HERTZ) USE19300  
 000194 000 USE19400  
 000195 000 LAST 1 - 4 A4 END USE19500  
 000196 000 USE19600  
 000197 000 USE19700  
 000198 000 C\*\*\* \*\*\*USE19800  
 000199 000 USE19900  
 000200 000 USE20000  
 000201 000 USE20100  
 000202 000 USE20200  
 000203 000 C\*\*\* \*\*\*USE20300  
 000204 000 USE20400  
 000205 000 1 THE JOB INFORMATION ON CARD NO. 1 IS PRINTED WITH OUTPUT. USE20500  
 000206 000 USE20600  
 000207 000 2 THE FOLLOWING ARRAYS HAVE BEEN DEFINED TO BE REAL: USE20700  
 000208 000 USE20800  
 000209 000 1FREQ IFREQO TTEMP USE20900  
 000210 000 1MOD NREXP NIEXP USE21000  
 000211 000 USE21100  
 000212 000 3 CARD(S) NO. 3 IS REPEATED UNTIL ALL VALUES HAVE BEEN READ. USE21200  
 000213 000 USE21300  
 000214 000 4 CARD(S) NO. 4 IS REPEATED UNTIL ALL VALUES HAVE BEEN READ. USE21400  
 000215 000 USE21500  
 000216 000 5 CARD(S) NO. 5 IS REPEATED UNTIL ALL VALUES HAVE BEEN READ. USE21600  
 000217 000 USE21700  
 000218 000 6 CARD(S) NO. 6 IS REPEATED UNTIL ALL VALUES HAVE BEEN READ. USE21800  
 000219 000 USE21900  
 000220 000 7 CARD(S) NO. 8 IS REPEATED UNTIL ALL VALUES HAVE BEEN READ. USE22000  
 000221 000 USE22100  
 000222 000 8 CARD(S) NO. 9 IS REPEATED UNTIL ALL VALUES HAVE BEEN READ. USE22200  
 000223 000 USE22300  
 000224 000 9 CARD(S) NO. 10 IS REPEATED UNTIL ALL VALUES HAVE BEEN READ. USE22400  
 000225 000 USE22500  
 000226 000 10 CARD(S) NO. 11 IS REPEATED UNTIL ALL VALUES HAVE BEEN READ. USE22600

REPRODUCIBILITY OF THE  
 ORIGINAL PAGE IS POOR

000227	000		USE22700
000228	000	11      CARDS NOS. 3 & 4 ARE NOT READ IF NRFIN = 0. ,	USE22800
000229	000		USE22900
000230	000	12      CARDS NOS. 5 & 6 ARE NOT READ IF NIFIN = 0.	USE23000
000231	000		USE23100
000232	000	13      CARDS NOS. 8 & 9 ARE NOT READ IF NRTEMP = 0.	USE23200
000233	000		USE23300
000234	000	14      CARDS NOS. 10 & 11 ARE NOT READ IF NITEMP = 0.	USE23400
000235	000		USE23500
000236	000	15      CARD(S) NO. 7 IS READ ONLY IF IT IS DESIRED TO CALCULATE . DYNAMIC MODULUS WITHOUT CURVE-FITTING, (I.E.,	USE23600
000237	000	ONLY IF NRFIN = 0 AND NIFIN = 0).	USE23700
000238	000		USE23800
000239	000		USE23900
000240	000	16      SEVERAL JOBS CAN BE STACKED; HOWEVER, THE LAST CARD OF THE DATA INPUT DECK MUST HAVE 'END ' IN THE FIRST FOUR COLUMNS OF THE CARD.	USE24000
000241	000		USE24100,
000242	000		USE24200
000243	000		USE24300
000244	000		USE24400
000245	000	C***	***USE24500
000246	000	C***	***USE24600
000247	000	C***	***USE24700
000248	000	C***	***USE24800
000249	000	C*** ***USE24900	***USE24900
000250	000	C*** ***USE25000	***USE25000

END ELT.

## REPRODUCIBILITY OF THE ORIGINAL PAGE IS POOR

B - 3

DYNVIS  
COMPUTER PROGRAM  
LISTING

DELT,L \*DYNVIS.DYNVIS

ELT017 RL1870 05/08-15:13:12-(1,)

000001 000 C\*\*\* \*\*\*DYN00100  
000002 000 C\*\*\* \*\*\*DYN00200  
000003 000 C\*\*\*  
000004 000 C\*\*\*  
000005 000 C\*\*\*  
000006 000 C\*\*\* SOLID PROPELLANT VISCOELASTIC DYNAMIC RESPONSE MODEL \*\*\*DYN00600  
000007 000 C\*\*\* \*\*\*DYN00700  
000008 000 C\*\*\* \*\*\*DYN00800  
000009 000 C\*\*\* \*\*\*DYN00900  
000010 000 C\*\*\* \*\*\*DYN01000  
000011 000 C\*\*\* \*\*\*DYN01100  
000012 000 C\*\*\* DEVELOPED BY \*\*\*DYN01200  
000013 000 C\*\*\* \*\*\*DYN01300  
000014 000 C\*\*\* W L HUFFORD \*\*\*DYN01400  
000015 000 C\*\*\* \*\*\*DYN01500  
000016 000 C\*\*\* \*\*\*DYN01600  
000017 000 C\*\*\* \*\*\*DYN01700  
000018 000 C\*\*\* J. E. FITZGERALD & ASSOCIATES \*\*\*DYN01800  
000019 000 C\*\*\* ATLANTA, GEORGIA \*\*\*DYN01900  
000020 000 C\*\*\* \*\*\*DYN02000  
000021 000 C\*\*\* \*\*\*DYN02100  
000022 000 C\*\*\* \*\*\*DYN02200  
000023 000 C\*\*\* THIS PROGRAM PERFORMS A LEAST-SQUARES CURVE-FIT TO DYNAMIC \*\*\*DYN02300  
000024 000 C\*\*\* LABORATORY TEST DATA TO DETERMINE THE COEFFICIENTS IN A \*\*\*DYN02400  
000025 000 C\*\*\* POWER LAW REPRESENTATION OF THE FORM: \*\*\*DYN02500  
000026 000 C\*\*\* \*\*\*DYN02600  
000027 000 C\*\*\* E = EZERO \* (OMEGA \* ASUBT) \*\* N (1) \*\*\*DYN02700  
000028 000 C\*\*\* \*\*\*DYN02800  
000029 000 C\*\*\* AND/OR MAKES PREDICTIONS OF THE REAL AND/OR IMAGINARY \*\*\*DYN02900  
000030 000 C\*\*\* COMPONENTS OF THE DYNAMIC MODULUS. THE PROGRAM IS VALID \*\*\*DYN03000  
000031 000 C\*\*\* FOR THE REAL AND/OR IMAGINARY COMPONENTS OF THE DYNAMIC \*\*\*DYN03100  
000032 000 C\*\*\* TENSILE OR SHEAR MODULI. \*\*\*DYN03200  
000033 000 C\*\*\* \*\*\*DYN03300  
000034 000 C\*\*\* TEMPERATURE IS ACCOUNTED FOR THROUGH THE USE OF A TIME - \*\*\*DYN03400  
000035 000 C\*\*\* TEMPERATURE SHIFT FUNCTION REPRESENTED IN THE FORM OF A \*\*\*DYN03500  
000036 000 C\*\*\* MODIFIED POWER LAW: \*\*\*DYN03600

REPRODUCIBILITY OF THE  
ORIGINAL PAGE IS POOR

000037 000 C\*\*\* \*\*\*DYN03700  
 000038 000 C\*\*\* \*\*\*DYN03800  
 000039 000 C\*\*\* \*\*\*DYN03900  
 000040 000 C\*\*\* WHERE \*\*\*DYN04000  
 000041 000 C\*\*\* TREF = REFERENCE TEMPERATURE (DEGREES KELVIN). (2) \*\*\*DYN04100  
 000042 000 C\*\*\* TA, TM = EXPERIMENTALLY DETERMINED PARAMETERS TO \*\*\*DYN04200  
 000043 000 C\*\*\* FIT EQ. (2) TO THE ASUBT SHIFT CURVE \*\*\*DYN04300  
 000044 000 C\*\*\* VERSUS TEMPERATURE. \*\*\*DYN04400  
 000045 000 C\*\*\* \*\*\*DYN04500  
 000046 000 C\*\*\* \*\*\*DYN04600  
 000047 000 C\*\*\* \*\*\*DYN04700  
 000048 000 C\*\*\* \*\*\*DYN04800  
 000049 000 C\*\*\* \*\*\*DYN04900  
 000050 000 C\*\*\* \*\*\*DYN05000  
 000051 000 C\*\*\* \*\*\*DYN05100  
 000052 000 C\*\*\* \*\*\*DYN05200  
 000053 000 C\*\*\* \*\*\*DYN05300  
 000054 000 C\*\*\* \*\*\*DYN05400  
 000055 000 C\*\*\* \*\*\*DYN05500  
 000056 000 C\*\*\* \*\*\*DYN05600  
 000057 000 C\*\*\* \*\*\*DYN05700  
 000058 000 C\*\*\* \*\*\*DYN05800  
 000059 000 C\*\*\* \*\*\*DYN05900  
 000060 000 C\*\*\* THE MAIN ROUTINE, ' D Y N V I S ', READS CONTROL \*\*\*DYN06000  
 000061 000 C\*\*\* INFORMATION, CALLS THE CURVE-FITTING SUBROUTINE, \*\*\*DYN06100  
 000062 000 C\*\*\* ' C U R V I T ', IF NECESSARY, AND MAKES REQUESTED \*\*\*DYN06200  
 000063 000 C\*\*\* CALCULATIONS OF DYNAMIC RESPONSE. \*\*\*DYN06300  
 000064 000 C\*\*\* \*\*\*DYN06400  
 000065 000 C\*\*\* \*\*\*DYN06500  
 000066 000 C\*\*\* \*\*\*DYN06600  
 000067 000 C\*\*\* \*\*\*DYN06700  
 000068 000 C\*\*\* \*\*\*DYN06800  
 000069 000 C\*\*\* \*\*\*DYN06900  
 000070 000 C\*\*\* DIMENSION ITITLE(20), TEMP(20), RTEMP(20), ITEMP(20), RMOD(20),  
 000071 000 1 IMOD(20), RFREQ(20), IFREQ(20), RFREQ0(20), IFREQ0(20) DYN07000  
 000072 000 C\*\*\* DYN07100  
 000073 000 C\*\*\* REAL IMOD, IFREQ, ITEMP, IFREQ0, NREXP, NIEXP \*\*\*DYN07200  
 000074 000 C\*\*\* DYN07300  
 \*\*\*DYN07400

REPRODUCIBILITY OF THE  
ORIGINAL PAGE IS POOR

000075 000 DATA NEND/4HEND / DYN07500  
 000076 000 C\*\*\* \*\*\*DYN07600  
 000077 000 C\*\*\* \*\*\*DYN07700  
 000078 000 C\*\*\* \*\*\*DYN07800  
 000079 000 C\*\*\* \*\*\*DYN07900  
 000080 000 10 FORMAT (20A4) DYN08000  
 000081 000 12 FORMAT (1H1,,5(4H\* \* ),2X,20A4,2X,5(4H\* \* ),//) DYN08100  
 000082 000 20 FORMAT (6I5,5E10.0) DYN08200  
 000083 000 30 FORMAT (8E10.0) DYN08300  
 000084 000 310 FORMAT (30X,35HTEMPERATURE SHIFT FACTOR PARAMETERS,/,27X, DYN08400  
 000085 000 1 24HREFERENCE TEMPERATURE = ,F4.0,15H DEGREES KELVIN,/46X, DYN08500  
 000086 000 2 SHTA = ,F10.6,/,40X,11HEXPOENT = ,F10.6,///) DYN08600  
 000087 000 320 FORMAT (50X,20HCURVE-FIT PARAMETERS,/,32X,20HREAL PART OF MODULUS DYN08700  
 000088 000 1 ,10X,25HIMAGINARY PART OF MODULUS,/,31X,14HCoeffICIENT = DYN08800  
 000089 000 2 ,F9.4,9X,14HCoeffICIENT = F9.4,/,34X,11HEXPOENT = ,F9.4, DYN08900  
 000090 000 3 12X,11HEXPOENT = ,F9.4,///) DYN09000  
 000091 000 330 FORMAT (36X,48HLABORATORY DATA COMPARED WITH CURVE-FIT RESULTS , DYN09100  
 000092 000 1 //,36X,24HREFERENCE TEMPERATURE = ,F4.0,9H DEGREES , DYN09200  
 000093 000 2 6HKELVIN,/,20X,20HREAL PART OF MODULUS,38X,9HIMAGINARY ,DYN09300  
 000094 001 3 16H PART OF MODULUS,/,6X,19HTEMPERATURE-REDUCED,7X DYN09400  
 000095 000 4 7HMODULUS,13X,7HMODULUS,7X,19HTEMPERATURE-REDUCED,7X, DYN09500  
 000096 000 5 7HMODULUS,13X,7HMODULUS,/,11X,9HFREQUENCY,14X,3HLAB,14X, DYN09600  
 000097 000 6 9HCURVE-FIT,11X,9HFREQUENCY,14X,3HLAB,14X,9HCURVE-FIT,/, DYN09700  
 000098 000 7 14A,4H(HZ),13X,9H(KN/M\*\*2),11X,9H(KN/M\*\*2),14A,4H(HZ),13X,DYN09800  
 000099 000 8 9H(KN/M\*\*2),11X,9H(KN/M\*\*2),//) DYN09900  
 000100 000 350 FORMAT (6(5X,E15.0)) DYN10000  
 000101 000 410 FORMAT (40X,40HCALCULATED VISCOELASTIC DYNAMIC RESPONSE,/,5X, DYN10100  
 000102 000 1 5X,11HTEMPERATURE,10X,9HFREQUENCY,6X,12HTEMPERATURE-, DYN10200  
 000103 000 2 7HREDUCED,8X,4HREAL,14X,9HIMAGINARY,13X,4HLOSS,/,51X, DYN10300  
 000104 000 3 9HFREQUENCY,12X,7HMODULUS,13X,7HMODULUS,13X,7HTANGENT,/, DYN10400  
 000105 000 4 7X,16H(DEGREES KELVIN),11X,4H(HZ),16X,4H(HZ),13X, DYN10500  
 000106 000 5 9H(KN/M\*\*2),11X,9H(KN/M\*\*2),//) DYN10600  
 000107 000 412 FORMAT (//) DYN10700  
 000108 000 C\*\*\* \*\*\*DYN10800  
 000109 000 C\*\*\* TIME - TEMPERATURE SHIFT FUNCTION \*\*\*DYN10900  
 000110 000 C\*\*\* \*\*\*DYN11000  
 000111 000 AT(J) = ((TR-TA)/(TEMP(J)-TA))\*\*TM DYN11100  
 000112 000 C\*\*\* \*\*\*DYN11200

REPRODUCIBILITY OF THE  
ORIGINAL PAGE IS POOR

B-20

000113 000 C\*\*\* DEFINE INPUT/OUTPUT UNITS \*\*\*DYN11300  
000114 000 C\*\*\* \*\*\*DYN11400  
000115 000 IREAD = 5 DYN11500  
000116 000 IWRITE = 6 DYN11600  
000117 000 C\*\*\* \*\*\*DYN11700  
000118 000 C\*\*\* READ JOB INFORMATION \*\*\*DYN11800  
000119 000 C\*\*\* \*\*\*DYN11900  
000120 000 1 READ (IREAD,10) (ITITLE(I), I=1,20) DYN12000  
000121 000 IF (ITITLE(1) .EQ. NEND) CALL EXIT DYN12100  
000122 000 WRITE (IWRITE,12) (ITITLE(I), I = 1,20) DYN12200  
000123 000 READ (IREAD,20) NRFIN,NRFOUT,NRTEMP,NIFIN,NIFOUT,NITEMP,TR,TA,TM DYN12300  
000124 000 C\*\*\* \*\*\*DYN12400  
000125 000 C\*\*\* INITIALIZE PARAMETERS \*\*\*DYN12500  
000126 000 C\*\*\* \*\*\*DYN12600  
000127 000 ERZERO = 0.0 DYN12700  
000128 000 EIZERO = 0.0 DYN12800  
000129 000 NREXP = 0.0 DYN12900  
000130 000 NIEXP = 0.0 DYN13000  
000131 000 IF (NRFIN .EQ. 0) GO TO 100 DYN13100  
000132 000 READ (IREAD,30) (RMOD(I), I=1,NRFIN) DYN13200  
000133 000 READ (IREAD,30) (RFREQ(I), I=1,NRFIN) DYN13300  
000134 000 C\*\*\* \*\*\*DYN13400  
000135 000 CALL CURVIT (RMOD,RFREQ,NRFIN,ERZERO,NREXP) DYN13500  
000136 000 C\*\*\* \*\*\*DYN13600  
000137 000 100 IF (NIFIN .EQ. 0) GO TO 200 DYN13700  
000138 000 READ (IREAD,30) (IMOD(I), I=1,NIFIN) DYN13800  
000139 000 READ (IREAD,30) (IFREQ(I) , I=1,NIFIN) DYN13900  
000140 000 C\*\*\* \*\*\*DYN14000  
000141 000 CALL CURVIT (IMOD,IFREQ,NIFIN,EIZERO,NIEXP) DYN14100  
000142 000 C\*\*\* \*\*\*DYN14200  
000143 000 200 IF (NRFIN .EQ. 0 .AND. NIFIN .EQ. 0) DYN14300  
000144 000 1 READ (IREAD,30) ERZERO,NREXP,EIZERO,NIEXP DYN14400  
000145 000 IF (NRTEMP .EQ. 0) GO TO 220 DYN14500  
000146 000 READ (IREAD,30) (RTEMP(I), I=1,NRTEMP) DYN14600  
000147 000 READ (IREAD,30) (RFREQ0(I), I=1,NRFOUT) DYN14700  
000148 000 220 IF (NITEMP .EQ. 0) GO TO 300 DYN14800  
000149 000 READ (IREAD,30) (ITEMP(I), I=1,NITEMP) DYN14900  
000150 000 READ (IREAD,30) (IFREQ0(I), I=1,NIFOUT) DYN15000

REPRODUCIBILITY OF THE  
ORIGINAL PAGE IS POOR

PRODUCIBILITY OF THE  
ORIGINAL PAGE IS POOR

```

000151      000  C***          ***DYN15100
000152      000  300 WRITE (IWRITE,310) TR,TA,TM   DYN15200
000153      000  WRITE (IWRITE,320) ERZERO,EZERO,NREXP,NIEXP   DYN15300
000154      000  IF (NRFIN .EQ. 0 .AND. NIFIN .EQ. 0) GO TO 400   DYN15400
000155      000  C***          ***DYN15500
000156      000  C***          ***DYN15600
000157      001  C***          ***DYN15100
000158      000  WRITE (IWRITE,330) TR   DYN15800
000159      000  NN = MAX0(NRFIN,NIFIN)   DYN15900
000160      000  N = NRFIN - NIFIN   DYN16000
000161      000  IF (N) 335,340,337   DYN16100
000162      000  333 DO 335 J=1,NIFIN   DYN16200
000163      000  K = J + NRFIN   DYN16300
000164      000  RFREQ(K) = 0.0   DYN16400
000165      000  335 RMOD(K) = 0.0   DYN16500
000166      000  GO TO 340   DYN16600
000167      000  337 DO 339 J=1,NRFIN   DYN16700
000168      000  K = J + NIFIN   DYN16800
000169      000  IFREQ(K) = 0.0   DYN16900
000170      000  339 IMOD(K) = 0.0   DYN17000
000171      000  340 DO 345 K=1,NN   DYN17100
000172      000  IF (RFREQ(K) .LE. .1E-8) GO TO 343   DYN17200
000173      000  IF (IFREQ(K) .LE. .1E-8) GO TO 343   DYN17300
000174      000  CALC1 = ERZERO*((RFREQ(K))**NREXP)   DYN17400
000175      000  CALC2 = EZERO*((IFREQ(K))**NIEXP)   DYN17500
000176      000  GO TO 345   DYN17600
000177      000  343 CALC1 = ERZERO   DYN17700
000178      000  CALC2 = EZERO   DYN17800
000179      000  345 WRITE (IWRITE,350) RFREQ(K),RMOD(K),CALC1,IFREQ(K),IMOD(K),CALC2   DYN17900
000180      000  C***          ***DYN18000
000181      000  C***          ***DYN18100
000182      000  C***          ***DYN18200
000183      000  400 WRITE (IWRITE,12) (ITITLE(I), I =1,20)   DYN18300
000184      000  WRITE (IWRITE,410)   DYN18400
000185      000  IF (NRTEMP .EQ. 0) GO TO 450   DYN18500
000186      000  DO 430 J =1,NRTEMP   DYN18600
000187      000  TEMP(J) = RTEMP(J)   DYN18700

```

000188	000	DO 420 K = 1,NRFOUT	DYN18800
000189	000	REDF = AT(J) * RFREQ0(K)	DYN18900
000190	000	IF (RFREQ0(K) .LE. .1E-8) GO TO 405	REPRODUCIBILITY OF THE ORIGINAL PAGE IS POOR
000191	000	CALC1 = ERZERO*(REDF**NREXP)	DYN19000
000192	000	CALC2 = EIZERO*(REDF**NIEXP)	DYN19100
000193	000	GO TO 415	DYN19200
000194	000	405 CALC1 = ERZERO	DYN19300
000195	000	CALC2 = EIZERO	DYN19400
000196	000	415 TAN = CALC2/CALC1	DYN19500
000197	000	420 WRITE (IWRITE,350) RTEMP(J),RFREQ0(K),REDF,CALC1,CALC2,TAN	DYN19600
000198	000	WRITE (IWRITE,412)	DYN19700
000199	000	430 CONTINUE	DYN19800
000200	000	450 IF (NITEMP .EQ. 0) GO TO 500	DYN19900
000201	000	DO 480 J=1,NITEMP	DYN20000
000202	000	TEMP(J) = ITEMP(J)	DYN20100
000203	000	DO 460 K=1,NIFOUT	DYN20200
000204	000	REDF = AT(J) *IFREQ0(K)	DYN20300
000205	000	IF (IFREQ0(K) .LE. .1E-8) GO TO 453	DYN20400
000206	000	CALC1 = ERZERO*(REDF**NREXP)	DYN20500
000207	000	CALC2 = EIZERO*(REDF**NIEXP)	DYN20600
000208	000	GO TO 457	DYN20700
000209	000	453 CALC1 = ERZERO	DYN20800
000210	000	CALC2 = EIZERO	DYN20900
000211	000	457 TAN = CALC2/CALC1	DYN21000
000212	000	460 WRITE (IWRITE,350) ITEMP(J),IFREQ0(K),REDF,CALC1,CALC2,TAN	DYN21100
000213	000	WRITE (IWRITE,412)	DYN21200
000214	000	480 CONTINUE	DYN21300
000215	000	C***	DYN21400
000216	000	500 GO TO 1	***DYN21500
000217	000	C***	DYN21600
000218	000	END	***DYN21700
			DYN21800

END ELT.

ELT,L \*DYNVIS.CURVIT

ELTUT7 RLID70 05/08-15:13:13-(0,)

000001 000 SUBROUTINE CURVIT (VALUE,TYME,NT,COF,DN)

000002 000 C CUR0200  
 000003 000 C\*\*\* \*\*\*CUR0300  
 000004 000 C\*\*\* \*\*\*CUR0400  
 000005 000 C\*\*\* THIS SUBROUTINE PERFORMS A LEAST-SQUARES CURVE-FIT OF \*\*\*CUR0500  
 000006 000 C\*\*\* LABORATORY DATA TO A TWO-PARAMETER POWER-LAW OF THE FORM: \*\*\*CUR0600

୧୩

END ELT.

B - 4

DYNVIS

SAMPLE PROBLEMS

REPRODUCIBILITY OF THE  
ORIGINAL PAGE IS POOR

ELT,L \*DYNVIS.DATA  
ELTOT7 RLIB70 05/08-15:13:14-(0,  
000001 000 DYNAMIC VISCOELASTIC RESPONSE MODEL CHECK PROBLEM - TP-H1123 PROPELLANT DATA -  
000002 000 3 6 1 3 6 1 298.  
000003 000 2366. 4937. 11860.  
000004 000 6. 20. 100.  
000005 000 643. 1875. 7928.  
000006 000 6. 20. 100.  
000007 000 298.  
000008 000 6. 10. 15. 20. 50. 100.  
000009 000 298.  
000010 000 6. 10. 15. 20. 50. 100.  
000011 000 DYNAMIC VISCOELASTIC RESPONSE MODEL CHECK PROBLEM - H-13 PROPELLANT DATA -  
000012 000 3 6 1 3 6 1 298.  
000013 000 1675. 3357. 8687.  
000014 000 6. 20. 100.  
000015 000 545. 1600. 6819.  
000016 000 6. 20. 100.  
000017 000 298.  
000018 000 6. 10. 15. 20. 50. 100.  
000019 000 298.  
000020 000 6. 10. 15. 20. 50. 100.  
000021 000 DYNAMIC VISCOELASTIC RESPONSE MODEL CHECK PROBLEM - UTI-610 PROPELLANT DATA -  
000022 000 4 8 4 298. 233. 15.  
000023 000 7940. 13800. 26300. 48980.  
000024 000 1. 10. 100. 1000.  
000025 000 255. 277. 298. 322.  
000026 000 1. 3.5 10. 11. 35. 100. 110. 1000.  
000027 000 END

REPRODUCIBILITY OF THE  
ORIGIN A PAGE IS POOR

\* \* \* \* \* \* \* \* \* DYNAMIC VISCOELASTIC RESPONSE MODEL CHECK PROBLEM - TP-H1123 PROPELLANT DATA \* \* \* \* \* \* \* \* \*

TEMPERATURE SHIFT FACTOR PARAMETERS

REFERENCE TEMPERATURE = 298. DEGREES KELVIN  
TA = .000000  
EXONENT = .000000

CURVE-FIT PARAMETERS

REAL PART OF MODULUS	IMAGINARY PART OF MODULUS
COEFFICIENT = 874.9008	COEFFICIENT = 129.5722
EXONENT = .5686	EXONENT = .8930

LABORATORY DATA COMPARED WITH CURVE-FIT RESULTS

REFERENCE TEMPERATURE = 298. DEGREES KELVIN

REAL PART OF MODULUS			IMAGINARY PART OF MODULUS		
TEMPERATURE-REDUCED FREQUENCY (HZ)	MODULUS LAB (KN/M**2)	MODULUS CURVE-FIT (KN/M**2)	TEMPERATURE-REDUCED FREQUENCY (HZ)	MODULUS LAB (KN/M**2)	MODULUS CURVE-FIT (KN/M**2)
.600000+01	.238000+04	.242326+04	.600000+01	.643000+03	.641839+03
.200000+02	.493700+04	.480506+04	.200000+02	.187500+04	.188093+04
.100000+03	.118600+05	.119983+05	.100000+03	.792800+04	.791729+04

REPRODUCIBILITY OF THE  
ORIGINAL PAGE IS POOR

\* \* \* \* \* DYNAMIC VISCOELASTIC RESPONSE MODEL CHECK PROBLEM - TP-H1123 PROPELLANT DATA \* \* \* \* \*

CALCULATED VISCOELASTIC DYNAMIC RESPONSE

TEMPERATURE (DEGREES KELVIN)	FREQUENCY (HZ)	TEMPERATURE-REDUCED FREQUENCY (HZ)	REAL MODULUS (KN/M**2)	IMAGINARY MODULUS (KN/M**2)	LOSS TANGENT
.298000+03	.600000+01	.600000+01	.242326+04	.641839+03	.264866+00
.298000+03	.100000+02	.100000+02	.323995+04	.101285+04	.312612+00
.298000+03	.150000+02	.150000+02	.408001+04	.145479+04	.356565+00
.298000+03	.200000+02	.200000+02	.480506+04	.188093+04	.391449+00
.298000+03	.500000+02	.500000+02	.809020+04	.426331+04	.526972+00
.298000+03	.100000+03	.100000+03	.119983+05	.791729+04	.659869+00
.298000+03	.600000+01	.600000+01	.242326+04	.641839+03	.264866+00
.298000+03	.100000+02	.100000+02	.323995+04	.101285+04	.312612+00
.298000+03	.150000+02	.150000+02	.408001+04	.145479+04	.356565+00
.298000+03	.200000+02	.200000+02	.480506+04	.188093+04	.391449+00
.298000+03	.500000+02	.500000+02	.809020+04	.426331+04	.526972+00
.298000+03	.100000+03	.100000+03	.119983+05	.791729+04	.659869+00

\* \* \* \* \* DYNAMIC VISCOELASTIC RESPONSE MODEL CHECK PROBLEM - H-13 PROPELLANT DATA - \* \* \* \* \*

TEMPERATURE SHIFT FACTOR PARAMETERS

REFERENCE TEMPERATURE = 298. DEGREES KELVIN  
TA = .000000  
EXPONENT = .000000

CURVE-FIT PARAMETERS

REAL PART OF MODULUS	IMAGINARY PART OF MODULUS
COEFFICIENT = 583.2573	COEFFICIENT = 108.8253
EXPOENT = .5856	EXPOENT = .8982

LABORATORY DATA COMPARED WITH CURVE-FIT RESULTS

REFERENCE TEMPERATURE = 298. DEGREES KELVIN

REAL PART OF MODULUS		IMAGINARY PART OF MODULUS			
TEMPERATURE-REDUCED FREQUENCY (HZ)	MODULUS LAB (KN/M**2)	MODULUS CURVE-FIT (KN/M**2)	TEMPERATURE-REDUCED FREQUENCY (HZ)	MODULUS LAB (KN/M**2)	MODULUS CURVE-FIT (KN/M**2)
.600000+01	.167500+04	.166542+04	.600000+01	.545000+03	.544114+03
.200000+02	.333700+04	.337061+04	.200000+02	.160000+04	.160456+04
.100000+03	.868700+04	.864982+04	.100000+03	.681900+04	.681071+04

REPRODUCIBILITY OF THE  
ORIGINAL PAGE IS POOR

\* \* \* \* \* DYNAMIC VISCOELASTIC RESPONSE MODEL CHECK PROBLEM - H-13 PROPELLANT DATA - \* \* \* \* \*

CALCULATED VISCOELASTIC DYNAMIC RESPONSE

TEMPERATURE (DEGREES KELVIN)	FREQUENCY (HZ)	TEMPERATURE-REDUCED FREQUENCY (HZ)	REAL MODULUS (KN/M**2)	IMAGINARY MODULUS (KN/M**2)	LOSS TANGENT
.298000+03	.600000+01	.600000+01	.166542+04	.544114+03	.326712+00
.298000+03	.100000+02	.100000+02	.224612+04	.860916+03	.383290+00
.298000+03	.150000+02	.150000+02	.284805+04	.123917+04	.435095+00
.298000+03	.200000+02	.200000+02	.337061+04	.160456+04	.476044+00
.298000+03	.500000+02	.500000+02	.576411+04	.365424+04	.633966+00
.298000+03	.100000+03	.100000+03	.864982+04	.681071+04	.787381+00
B-29					
.296000+03	.600000+01	.600000+01	.166542+04	.544114+03	.326712+00
.296000+03	.100000+02	.100000+02	.224612+04	.860916+03	.383290+00
.296000+03	.150000+02	.150000+02	.284805+04	.123917+04	.435095+00
.296000+03	.200000+02	.200000+02	.337061+04	.160456+04	.476044+00
.296000+03	.500000+02	.500000+02	.576411+04	.365424+04	.633966+00
.296000+03	.100000+03	.100000+03	.864982+04	.681071+04	.787381+00

REPRODUCIBILITY  
ORIGINAL PAGE IS POOR

REPRODUCIBILITY OF:  
ORIGINAL PAGE IS POOR

\* \* \* \* \* DYNAMIC VISCOELASTIC RESPONSE MODEL CHECK PROBLEM = UTI-610 PROPELLANT DATA \* \* \* \* \*

TEMPERATURE SHIFT FACTOR PARAMETERS

REFERENCE TEMPERATURE = 298. DEGREES KELVIN  
TA = 233.00000  
EXPONENT = 15.00000

CURVE-FIT PARAMETERS

REAL PART OF MODULUS	IMAGINARY PART OF MODULUS
COEFFICIENT = 7759.2130	COEFFICIENT = .0000
EXponent = .2651	EXponent = .0000

LABORATORY DATA COMPARED WITH CURVE-FIT RESULTS

REFERENCE TEMPERATURE = 298. DEGREES KELVIN

B-30

REAL PART OF MODULUS		IMAGINARY PART OF MODULUS			
TEMPERATURE-REDUCED FREQUENCY (HZ)	MODULUS LAB (KN/M**2)	MODULUS CURVE-FIT (KN/M**2)	TEMPERATURE-REDUCED FREQUENCY (HZ)	MODULUS LAB (KN/M**2)	MODULUS CURVE-FIT (KN/M**2)
.100000+01	.794000+04	.775921+04	.000000	.000000	.000000
.100000+02	.138000+05	.775921+04	.000000	.000000	.000000
.100000+03	.263000+05	.775921+04	.000000	.000000	.000000
.100000+04	.489800+05	.775921+04	.000000	.000000	.000000

\* \* \* \* \* DYNAMIC VISCOELASTIC RESPONSE MODEL CHECK PROBLEM - UTI-610 PROPELLANT DATA - \* \* \* \* \*

CALCULATED VISCOELASTIC DYNAMIC RESPONSE

TEMPERATURE (DEGREES KELVIN)	FREQUENCY (HZ)	TEMPERATURE-REDUCED FREQUENCY (HZ)	REAL MODULUS (KN/M**2)	IMAGINARY MODULUS (KN/M**2)	LOSS TANGENT
.255000+03	.100000+01	.114120+08	.576092+06	.000000	.000000
.255000+03	.350000+01	.399418+08	.802983+06	.000000	.000000
.255000+03	.100000+02	.114120+09	.106062+07	.000000	.000000
.255000+03	.110000+02	.125532+09	.108775+07	.000000	.000000
.255000+03	.350000+02	.399418+09	.147834+07	.000000	.000000
.255000+03	.100000+03	.114120+10	.195266+07	.000000	.000000
.255000+03	.110000+03	.125532+10	.200262+07	.000000	.000000
.255000+03	.100000+04	.114120+11	.359495+07	.000000	.000000
.277000+03	.100000+01	.348265+03	.366096+05	.000000	.000000
.277000+03	.350000+01	.121893+04	.510281+05	.000000	.000000
.277000+03	.100000+02	.348265+04	.674003+05	.000000	.000000
.277000+03	.110000+02	.383092+04	.691247+05	.000000	.000000
.277000+03	.350000+02	.121893+05	.939455+05	.000000	.000000
.277000+03	.100000+03	.348265+05	.124088+06	.000000	.000000
.277000+03	.110000+03	.383092+05	.127263+06	.000000	.000000
.277000+03	.100000+04	.348265+06	.228452+06	.000000	.000000
.298000+03	.100000+01	.100000+01	.775921+04	.000000	.000000
.298000+03	.350000+01	.350000+01	.108151+05	.000000	.000000
.298000+03	.100000+02	.100000+02	.142851+05	.000000	.000000
.298000+03	.110000+02	.110000+02	.146506+05	.000000	.000000
.298000+03	.350000+02	.350000+02	.199113+05	.000000	.000000
.298000+03	.100000+03	.100000+03	.262998+05	.000000	.000000
.298000+03	.110000+03	.110000+03	.269727+05	.000000	.000000
.298000+03	.100000+04	.100000+04	.484194+05	.000000	.000000
.322000+03	.100000+01	.897119-02	.222426+04	.000000	.000000
.322000+03	.350000+01	.313992-01	.310027+04	.000000	.000000
.322000+03	.100000+02	.897119-01	.409499+04	.000000	.000000
.322000+03	.110000+02	.986831-01	.419976+04	.000000	.000000
.322000+03	.350000+02	.313992+00	.570778+04	.000000	.000000
.322000+03	.100000+03	.897119+00	.753911+04	.000000	.000000
.322000+03	.110000+03	.986831+00	.773200+04	.000000	.000000
.322000+03	.100000+04	.897119+01	.138799+05	.000000	.000000

B-31

ORIGINAL PAGE IS POOR  
REPRODUCIBILITY OF THE

APPENDIX C

DYNVIS  
COMPUTER PROGRAM  
CARD DECK

(Submitted Under Separate Cover)

Distribution List:

National Aeronautics and Space Administration  
George C. Marshall Space Flight Center  
Marshall Space Flight Center, Alabama 35812

Attention:

Code AS21-D	5 copies
Code AT	1 copy
ED 23	5 copies + repro.
EM 34-06	1 copy